INFORMATION TO USERS

This manuscript has been reproduced from the microfilm master. UMI films the text directly from the original or copy submitted. Thus, some thesis and dissertation copies are in typewriter face, while others may be from any type of computer printer.

The quality of this reproduction is dependent upon the quality of the copy submitted. Broken or indistinct print, colored or poor quality illustrations and photographs, print bleedthrough, substandard margins, and improper alignment can adversely affect reproduction.

In the unlikely event that the author did not send UMI a complete manuscript and there are missing pages, these will be noted. Also, if unauthorized copyright material had to be removed, a note will indicate the deletion.

Oversize materials (e.g., maps, drawings, charts) are reproduced by sectioning the original, beginning at the upper left-hand corner and continuing from left to right in equal sections with small overlaps.

Photographs included in the original manuscript have been reproduced xerographically in this copy. Higher quality 6" x 9" black and white photographic prints are available for any photographs or illustrations appearing in this copy for an additional charge. Contact UMI directly to order.

Bell & Howell Information and Learning
300 North Zeeb Road, Ann Arbor, MI 48106-1346 USA
800-521-0600

AN INVESTIGATION INTO THE MECHANISM RESPONSIBLE FOR CLOMETHIAZOLE-INDUCED NEUROPROTECTION IN A RAT MODEL OF SEVERE GLOBAL ISCHEMIA

by

Krista Lynn Gilby

Submitted in partial fulfillment of the requirements
for the degree of Doctor of Philosophy

at

Department of Pharmacology
Dalhousie University
Halifax, Nova Scotia
April, 2000

DALHOUSIE UNIVERSITY

DEPARTMENT OF PHARMACOLOGY

The undersigned hereby certify that they have read, and recommend that the Faculty of Graduate Studies accept the thesis entitled "An investigation into the mechanism responsible for clomethiazole-induced neuroprotection in a rat model of severe global ischemia" by Krista Lynn Gilby, in partial fulfillment of the requirements for the degree of Doctor of Philosophy.

Dated: April 10, 2000

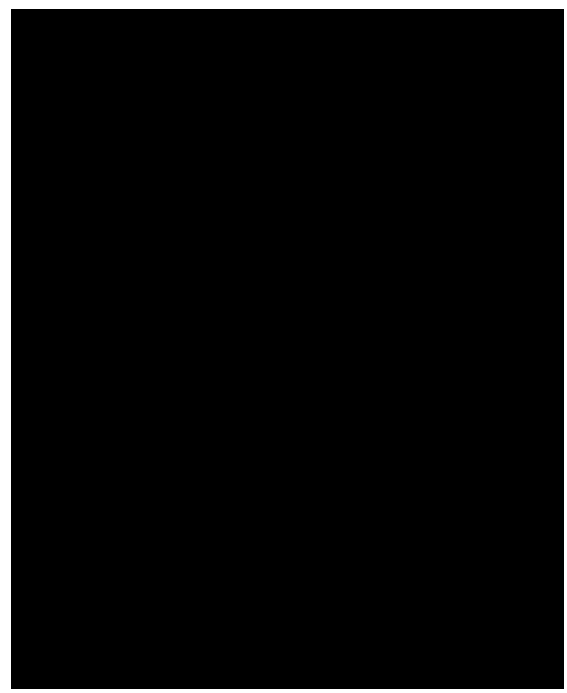

External Examiner: Dr. Alan Cross

Supervisor: Dr. Harold Robertson

Readers: Dr. Melanie Kelly

Dr. Teri Peterson

Dr. Susan Howlett

Dr. David Hopkins

Dalhousie University

Date: April, 2000

Author: Krista Lynn Gilby

Title: An investigation into the mechanism responsible for clomethiazole-induced neuroprotection in a rat model of severe global ischemia

Department: Pharmacology

Degree: Doctor of Philosophy. **Convocation**: Spring **Year**: 2000

Permission is hereby granted to Dalhousie University to circulate and to have copied, for non-commercial purposes, at its discretion, the above title upon request of individuals or institutions.

Krista L. Gilby (author)

The opposite of love is not hate, it's indifference...And
the opposite of life is not death, it's indifference

- Elie Wiesel

Table of Contents

List of Figures

Summary

Recent studies have shown that Clomethiazole (CMZ) may be neuroprotective in both global and focal animal models of ischemia. The primary objective of this thesis was to determine whether a single dose of CMZ could provide neuroprotection when administered following severe global ischemia. We used the Rice-Vannucci model of hypoxia-ischemia (H-I) to produce a large unilateral global ischemic injury in young (PND25) male rats. After testing several doses and timepoints of administration for CMZ, we were able to determine that doses of 100, 150 and 200 mg/kg administered at 1, 2 or 3 hours post-hypoxia provided significant neuroprotection in all brain regions normally susceptible to H-I injury. The ability of CMZ to potentiate GABAergic neurotransmission has generally been credited for its neuroprotective effects in animal models of ischemia. In order to determine whether the neuroprotective efficacy of CMZ was due to its $GABA_A$-potentiating properties, we examined the neuroprotective efficacy of known $GABA_A$-potentiating agents in the H-I model. Regardless of dosage, the highly specific $GABA_A$-agonist, muscimol, did not provide neuroprotection in any cell layer of H-I animals when administered at 3 hours post-hypoxia. However, high doses of the benzodiazepine, midazolam (150 and 200 mg/kg), provided significant neuroprotection in all cell layers of H-I animals when administered 3 hours post-hypoxia. Importantly, the neuroprotective efficacy of midazolam was substantially less than that of CMZ in this model. We, therefore, investigated whether an additive or alternate mechanism of action may be responsible for the profound neuroprotection provided by CMZ in the H-I model.

The effects of CMZ administration on normal patterns of gene expression following H-I were investigated using a number of molecular biological tools including RT-PCR, *in situ* hybridization, differential display and DNA sequencing. Results of these experiments demonstrated that CMZ administration altered the normal patterns of expression for several mRNAs following H-I including *hsp70*, *hsp25*, *hsp40*, *calmodulin*, *c-fos*, and *c-jun* and several proteins including Hsp70, Hsp25 and c-Fos. The effect of CMZ administration on subsequent gene expression in the H-I model was diverse but may indicate that a molecular mechanism of action exists for this compound.

In a parallel series of experiments, we investigated whether the apparent morphological neuroprotection provided by CMZ translated into functional sparing of neurons susceptible to H-I injury. Specifically, we wanted to determine whether the neuronal circuitry originating from cell regions normally susceptible to H-I was fully functional in CMZ-treated animals. Both vehicle-injected and CMZ-injected (200 mg/kg and 100 mg/kg) H-I animals were kindled approximately two months following H-I treatment in order to compare seizure susceptibility and seizure propagation characteristics in the ipsilateral hippocampus of animals from both treatment groups. CMZ-treated H-I animals exhibited a decreased susceptibility to seizures and a stronger resistance to initial seizure propagation than vehicle-injected H-I animals. Moreover, the seizure susceptibility of CMZ-treated H-I animals was decreased even when compared to naïve control animals. These results indicate that despite the apparent complete morphological neuroprotection observed following CMZ administration, permanent changes in neuronal circuitry may occur in CMZ treated H-I animals. It is unclear whether this alteration in neuronal circuitry would have clinical implications in stroke patients.

LIST OF ABBREVIATIONS

2-VO	two vessel occlusion
4-VO	four vessel occlusion
ABC	avidin-biotin complex
AD	after discharge
ADT	after discharge threshold
AMP	adenine monophosphate
ANOVA	Analysis of Variance
AONs	antisense oligonucleotides
AP-1	activating protein 1
ATP	adenine triphosphate
BDNF	brain-derived neurotrophic factor
BSA	bovine serum albumin
CA	*cornu ammonis*
cAMP	cyclic adenosine monophosphate
CBF	cerebral blood flow
CCA	common carotid artery
CED	*Caenorhabditis elegans* death gene
CMZ	clomethiazole
CNS	central nervous system
CRE	cAMP response element
CREB	cAMP response element binding protein
DAB	diaminobensidine-tetrachloride
DAG	diacylglycerol
DG	dentate gyrus
DNA	deoxyribonucleic acid
EAA	excitatory amino acid
ECD	excitotoxic cell death
ECL	electrogenerated chemiluminescence
EEG	electroencephalographic

GABA	γ-aminobutyric acid
GFAP	glial fibrillary amino acid protein
HES	hematoxylin-eosin-safran
H-I	hypoxia-ischemia
HSF	heat shock factor
hsp	heat shock gene
HSP	heat shock protein
i.p.	intraperitoneal
IBO	ibotenic acid
ICV	intracerebralventricular
IEG	immediate early gene
IEGP	immediate early gene protein
$InsP_3$	inositol 1,4,5-triphosphate
i.v.	intravenous
JNK	c-Jun N terminal kinase
KA	kainic acid
kD	kilodalton
MAP	mitogen activated protein
MCA	middle cerebral artery
MCAO	middle cerebral artery occlusion
MEKK1	MAPK/ERK kinase
MK-801	(+) –5-methyl–10, 11-dihydro-5H-dibenzo [a,d] cyclohepten-5,10-amine maleate
mRNA	messenger ribonucleic acid
NBQX	2,3 – dihydroxy– 6- nitro- 7- sulphamoyl-benzo (F) quinoxaline
NGF	nerve growth factor
NMDA	N-methyl-D-aspartate
NMDLA	N-methyl-DL-aspartate
OD	optical density
PAGE	polyacrylamide gel electrophoresis
PARP	poly (ADP-ribose) polymerase

PBS	phosphate buffered saline
PC12	pheochromocytoma cells
PCD	programmed cell death
PKA	protein kinase A
PKC	protein kinase C
pMCAO	permanent middle cerebral artery occlusion
PND	postnatal day
PTZ	pentylenetetrazol
RNA	ribonucleic acid
SDS	sodium dodecyl sulfate
SN_{pr}	substantia nigra pars reticulata
SRE	serum response element
SSC	sodium chloride citrate
TBPS	butyl-bicyclophosphothionate
tMCAO	transient middle cerebral artery occlusion
TNFα	tumor necrosis factor α
TUNEL	terminal deoxynucleotidyl transferase-mediated biotinylated UTP-nick end labeling

Acknowledgments

Someone once told me that each time you face a seemingly insurmountable challenge "God" sends you someone to ease the struggle and that person is not always whom you might expect. This statement has held through my entire PhD experience. To mention all those who have aided my academic, emotional and spiritual life would be impossible. However, I would like to give special thanks to Dr. Harold Robertson for the supervision he has given me in both the scientific and corporate facets of medical research. I also thank him for recognizing the importance of meeting other scientists from around the world which, I feel, has given me numerous opportunities that may otherwise have not been available. Thank you Harry.

I can honestly say that during my career as a PhD student I have met the most wonderful friends. I would like to give special mention to three "wise women" who were always bearing gifts. I thank "Pre-doctor" Anne Marie Krueger-Naug for her selflessness. Dr. Eileen-Denovan Wright for her perspective in all facets of life and Dr. Mary Ellen Kelly for her kindred spirit. During the past 6 years I have also found a special friend in Kay who was the one person I could turn to at any time and for any reason. I would also like to thank Brenda and Marc for their friendship and help in the lab. I would bet my life that no PhD thesis has been completed without a support system that provides new and interesting coping strategies. In this capacity, I cannot thank Lisa, John, Tim, Cindy, Erin, Karyn, Bill, Lyn, Grant, Eugene and all my other friends enough.

There are times when you realize that you are nothing more than a product of the love and support of your family and friends. I have been blessed with a loving mother, father and baby sister, Kara Lee. They have always encouraged me to achieve, have loved me when I have failed and have given me strength to stand on my own. I also want to thank Colin for his integrity, his intellect and his love during the past 6 years. While such qualities in another human being may appear peripheral to this thesis, I can assure you that without them this work would not have been attempted nor completed. I will end by dedicating this work to my Grandmother, Blanche Gilby, who passed away last year. She was a great advocate of any female achievement and I think this one may have her smiling.

General Introduction

'Stroke', as defined by the World Health Organization, is a term used to refer to rapidly developing clinical signs of a focal (or global) disturbance of cerebral function, with symptoms that last 24 hours or longer and have no apparent cause other than vascular origin (WHO MONICA Project, 1988 as sited in Green *et al.*, 1998a). Stroke typically arises from a lack of oxygen supply to brain cells and has a pathogenic origin related to a thrombotic or embolic clot in one or more of the arteries that supply blood to the brain. Oxygen starved brain cells eventually die, resulting in a variety of clinical symptoms. Depending upon the location and severity of the clot, symptoms of stroke in humans vary and may include paralysis, impaired cognition, communication difficulties, reduced co-ordination, visual disturbance, loss of sensation, depression or any combination of these effects (Shima *et al.*, 1994).

Historically, stroke has adopted such fatalistic terms as "a stroke of fate" or "a stroke of God's hands" because, clinically, stroke was believed to be both unpreventable and untreatable (Shima *et al.*, 1994). However, recent emergent stroke treatment strategies have led to unprecedented drug development activity in pre-clinical research laboratories. In general, "neuroprotective therapy" involves the use of a pharmacological agent that, when administered soon after a cerebrovascular accident, substantially decreases long term neuronal damage and does so by interfering with the cellular processes that result in cell death (Green *et al.*, 1998a). One of the more frustrating obstacles in the development of neuroprotective compounds for stroke has been that while stroke patients are rarely treated within the first few hours after onset of symptoms, most research into pharmacotherapy has focussed on agents that must be administered either prior to, during or immediately following the ischemic event. However, research has begun to focus on putative neuroprotective compounds that are able to minimize or prevent stroke-induced cell death by interfering with delayed molecular events that ultimately cause cells to die following ischemia.

Excitotoxic Injury

Investigations into the cause of stroke and the testing of potential neuroprotective agents is hampered by an inability to continuously follow the physical and chemical events that occur during ischemia and reperfusion *in vivo*. In the past decade, however, new advances in stroke research have given a better understanding of normal functioning in the brain and, as a consequence, a clearer understanding of the pathology of ischemia-induced cell death. Unfortunately, this research has indicated that there may be several interactive mechanisms ultimately responsible for ischemia-induced cell damage and/or death. As such, the probability of developing a single neuroprotective compound to combat stroke in humans is low.

Stroke-induced neuronal injury is currently believed to result from a phenomenon known as excitotoxicity, which involves excessive release of the primary excitatory neurotransmitter in the brain, glutamate. Under normal conditions, neuronal and glial uptake systems maintain the extracellular concentrations of glutamate at or below micromolar levels (Bouvier *et al.*, 1992). Excitotoxic insults, such as ischemia and seizure, cause an immediate release of excitatory amino acid (EAA) neurotransmitters (primarily glutamate) that is above the buffering capacity of neuronal and glial uptake systems. Accordingly, an approximate 30-fold increase in the extracellular concentration of EAAs has been reported in ischemic brain regions which ultimately leads to massive depolarizaton of postsynaptic membranes (Kanthan *et al.*, 1995). At the same time, the loss of adequate blood supply (and oxygen) to the brain results in reduced ATP synthesis which causes energy-requiring ionic pumps, that normally keep the membrane polarized, to fail and lead to additional depolarization of post-synaptic membranes (Hansen *et al.*, 1985). Excessive activation of calcium permeable N-methyl-D-aspartate (NMDA) receptors and voltage-gated calcium channels, in combination with the failure of ionic pumps, ultimately leads to an enormous increase in the intracellular concentration of calcium in ischemic neurons. It is believed that this increase in intracellular calcium concentration is pivotal to ischemia-induced cell death since increased intracellular calcium has been linked to the activation of several destructive enzymes including lipases, proteases and endonucleases (Choi *et al.*, 1990; Kristian and Siesj $\bar{}$, 1996). Phospholipid breakdown following lipase activation results in the formation of

arachidonic acid which, when metabolized, gives rise to highly reactive compounds known as oxygen free radicals that attack cell membranes through a process called lipid peroxidation (Meldrum, 1990a,b; 1992). Increased intracellular calcium concentrations have also been shown to alter the level of second messenger molecules in ischemic neurons and affect the transcription of numerous genes that may ultimately serve as part of a destructive molecular cascade leading to cell death (Choi, 1990).

Excitotoxic injury to cells within the ischemic infarct zone has been shown to ignite a secondary excitotoxic cascade in cells outside of the original infarct zone that have a residual although severely compromised blood supply. This larger surrounding area of compromised cells is known as the penumbra and, without restoration of the blood supply or protective intervention, these cells will also die following ischemic insult. In addition, the rapid pace of the excitotoxic cascade limits the window of opportunity for therapeutic intervention following ischemia, beyond which re-establishment of blood flow and/or administration of putative neuroprotective agents may be futile and could potentially cause further damage.

The search for universal therapeutic countermeasures to H-I injury has determined that both physiologic and pharmacologic strategies can be effective in reducing ischemia-induced cell death. Successful physiologic manipulations have included fasting hypoglycemia, mild hypothermia, mild hypercapnia and hypoxic preconditioning (Young *et al.*, 1983; Voorhies *et al.*, 1986; Vannucci and Mujsce, 1992; Yager *et al.*, 1992; Saeed *et al.*, 1993; Yager *et al.*, 1993; 1996; Gidday *et al.*, 1994; Vannucci *et al.*, 1995; Thoresen *et al.*, 1996; Trescher *et al.*, 1997; Williams *et al.*, 1997). Some pharmacologic interventions that have exhibited neuroprotective efficacy against H-I injury include glucocorticosteroids, glutamate receptor antagonists, calcium channel blockers, free radical scavengers, NO inhibitors, nerve growth factor and platelet-activating factor antagonists (Silverstein *et al.*, 1986; Trifiletti *et al.*, 1992; Palmer *et al.*, 1993; Thordstein *et al.* 1993; Hagberg *et al.*, 1994; Hamada *et al.*, 1994; Bagenholm *et al.*, 1996; Holtzman *et al.*, 1996; Liu *et al.*, 1996; Hudome *et al.*, 1997).

As might be expected, many studies have examined the neuroprotective effects of EAA receptor antagonists in animal models of ischemia. However, use of these compounds has produced varying degrees of neuroprotection that appears to be

dependent upon the ischemia model and species used, the receptor subtype targeted, the dosing regimen and the presence of hypothermia (Gill *et al.*, 1988; Buchan and Pulsinelli, 1990; Sheardown *et al.*, 1990; Gill and Lodge, 1997; McBurney, 1997; Small and Buchan, 1997). A study conducted by Hagberg *et al.*, (1994) demonstrated that post-hypoxic treatment with a non-competitive NMDA receptor antagonist, (+) –5-methyl–10, 11-dihydro-5H-dibenzo [a,d] cyclohepten-5,10-amine maleate (MK-801), at doses of 0.3 and 0.5 mg/kg reduced brain damage following H-I by 61 and 43% respectively while higher doses of MK 801 (0.75 mg/kg) provided no neuroprotection. One reason for the success of these compounds in animal models of ischemia may be the high correlation between the presence of glutamate receptors and the vulnerability of specific brain regions to ischemia. For instance, the CA1 pyramidal cell layer in the hippocampus is particularly rich in NMDA receptors and is also the most susceptible brain region in many animal models of ischemia (Monaghan *et al.*, 1983; Gilby *et al.*, 1997; Vannucci *et al.*, 1999). In spite of numerous studies that demonstrate a neuroprotective effect for NMDA antagonists in animal models of ischemia, there has been little interest in these compounds for stroke therapy in humans. Reasons for this discrepancy include the fact that administration of NMDA-antagonists has been shown to induce hypothermia in animals, a mechanism that is independently neuroprotective, and use of NMDA antagonists during human clinical trials has indicated that these agents are associated with adverse CNS side effects (hallucinations and sedation) and peripheral toxicity (Lipton *et al.*, 1993; Foutz *et al.*, 1994; Xue *et al.*, 1994; Grotta *et al.*, 1995; Gilland and Hagberg, 1997).

Renewed Interest in GABA

It is possible that ischemia-induced neuronal damage may be due to an imbalance between excitatory and inhibitory activation of post-synaptic neurons. γ-aminobutyric acid (GABA) is the most powerful inhibitory neurotransmitter in the CNS and one of the most important physiological regulators in neuronal cells (Dingledine and Gjerstad, 1979; Hill and Bowery, 1981). Approximately 30-50% of all synapses in the CNS are thought to be GABAergic (Vrbaski *et al.*, 1998). GABA dysfunction has been linked to numerous neurodegenerative disorders including epilepsy, ischemia, heptic

encephalopathy, Huntington's chorea, spinocerebellar degeneration, dementia and psychosis (Vrbaski *et al.*, 1998). Studies that have used microdialysis to determine extracellular concentrations of GABA in the brain of ischemic relative to control animals have reported an increase in the overall GABA concentration in the brains of rats that had been subjected to focal or global models of ischemia (Hagberg *et al.*, 1985; Baldwin *et al.*, 1993a; 1994; Mainprize *et al.*, 1995). Nuclear magnetic resonance studies have also shown that hippocampal GABA levels increase during and immediately after transient forebrain ischemia but decline significantly at 1 hour after reperfusion (Peeling *et al.*, 1989). Paradoxically, a near 70% inhibition of GABA synthesis has been observed in the cortex of rats immediately following premanent or reversible occlusion of the middle cerebral artery (Hagberg *et al.*, 1985; Baldwin *et al.*, 1994; Mainprize *et al.*, 1995; Green *et al.*, 1992a). Thus, overall GABAergic function may be reduced for a substantial period after ischemic insult, in spite of the fact that GABAergic neurons are remarkably resistant to ischemia-induced damage (Tecoma and Choi, 1989; Johansen *et al.*, 1991; Nitsch *et al.*, 1991; Kanai *et al.*, 1994). Similarly, an increase in extracellular GABA concentration has been observed in ischemic tissue of humans undergoing neurosurgery (Kanthan *et al.*, 1995). These data suggest that pharmacological compounds that amplify GABAergic neurotransmission may be of neuroprotective benefit in animal models of ischemia.

Three distinct types of GABA receptors have been identified in mammals ($GABA_A$, $GABA_B$ and $GABA_C$). In the late 1980's, the $GABA_A$ receptor was cloned and found to be a member of the broad class of multi-subunit proteins that form 'ligand-gated' ion channels (see review by Bowery and Brown, 1997). $GABA_A$ receptors have shown a large amount of molecular heterogeneity but are universally known to be GABA-gated pentomeric complexes consisting of at least 16 subunits ($\alpha_{1\text{-}6}$, $\beta_{1\text{-}3}$, $\gamma_{1\text{-}3}$, π, δ, ε, ϕ). When two molecules of GABA bind to the α_1-subunits of the ion-channel receptor the channel opens and there is a shift in membrane permeability to favor chloride ions. Influx of chloride ultimately causes hyperpolarization of the neuron and thereby produces a rapid cessation of the electrical discharge from the cell (Anderson *et al.*, 1993).

The $GABA_A$ receptor is part of a macromolecule that contains the GABA

receptor, chloride ionophore and several allosteric modulatory sites where benzodiazepines, barbiturates, various anesthetics and neurosteroids can bind in order to influence its activity (Sieghart, 1992; Green *et al.*, 1998a). It has traditionally been very difficult to determine the exact site of action for compounds that influence the $GABA_A$ receptor. Many GABAergic compounds can act at more than one binding site or, once bound to one site, can modulate the binding characteristics of other sites making it hard to determine their precise mechanism of action. For instance, Green *et al.* (1996) reported that neither of two compounds known to potentiate GABAergic effects, pentobarbitone nor clomethiazole (CMZ), appeared to interact directly with the GABA or benzodiazepine receptor binding sites yet both compounds indirectly influenced the characteristics of these binding sites.

It is also interesting that during the early stages of development, activation of $GABA_A$ receptors leads to depolarization of the post-synaptic membrane instead of hyperpolarization (Ben Ari *et al.*, 1989; LoTurco *et al.*, 1995; Serafini *et al.*, 1995; Chen *et al.*, 1996; Rohrbough and Spitzer, 1996). Thus, in several types of neonatal neurons activation of the $GABA_A$ receptor triggers action potentials and activates voltage-dependent calcium channels producing a rise in intracellular calcium concentrations (LoTurco *et al.*, 1995; Obrietan and van der Pol, 1995; Chen *et al.*, 1996). Around PND7 in rats, however, GABA begins to function as an inhibitory neurotransmitter, a characteristic that progressively increases in strength up to PND45 (Swann *et al.*, 1989; Kapur and MacDonald, 1998).

$GABA_B$ receptors are presynaptic and are present at lower concentrations than $GABA_A$ receptors (Sieghart, 1992). $GABA_B$ receptors are not linked to a chloride channel but instead are coupled to G_I proteins and are involved in synaptic transmission (neurotransmitter release). The $GABA_B$ receptor is a 7 helical transmembrane segment receptor that inhibits adenylate cyclase and modulates calcium and potassium channels (Sieghart, 1992; Pearson *et al.*, 1994). Reports have indicated that $GABA_B$ receptors may be involved in physiological conditions associated with absence epilepsy, cognitive disorders and nociception (Golovko *et al.* 1999). $GABA_C$ receptors are considered to be relatively simple ligand-gated chloride channels that function to stabilize the resting potential of the cell by increasing the conductivity of chloride (Sieghart, 1992; Pearson *et*

al., 1994). The pharmacology of $GABA_C$ receptors is distinct from $GABA_A$ receptors as they are not blocked by bicuculline and do not appear to be modulated by traditional GABA-potentiating compounds such as benzodiazepines, barbiturates or neuroactive steroids.

The search for GABA-potentiating compounds that may be neuroprotective in animal models of ischemia has generally focussed on $GABA_A$-agonists. Indeed, recent studies have shown that pharmacological agents that act directly on $GABA_A$ receptors or that modulate $GABA_A$, but not $GABA_B$, receptor activity can decrease the severity of brain injury following ischemia. For instance, Watanabe *et al.* (1999) demonstrated that while $GABA_A$-agonists provided neuroprotection against global ischemia in gerbils, $GABA_B$-agonists were not effective in the same protocol. A possible explanation for the ineffectiveness of $GABA_B$-agonists against ischemia-induced damage may be that $GABA_B$ receptors become dysfunctional under conditions of low energy that characteristically follow ischemia (Bowery *et al.*, 1993). Thus, an investigation into the ability of specific $GABA_A$-agonists to provide neuroprotection across a variety of animal models of ischemia may be important to the future treatment of stroke patients.

The Rice-Vannucci Model of H-I

In the past few years many drugs have been developed that provide powerful neuroprotection in animal models of ischemia but fail to improve ischemia-induced pathology in clinical trials (Grotta *et al.*, 1995). This failure is most likely due to an incompatibility between the design of experimental and clinical studies rather than a discrepancy in the pharmacological profile of the agent. More recent research has linked certain animal models to specific human stroke conditions with the most important selective criteria being the identification of the correct pathophysiology. In this way, therapeutic recommendations derived from animal studies can be restricted to a particular pathophysiological state in humans.

There are numerous animal models currently used to mimic ischemia-induced pathology in humans. These models are categorized as either focal or global insults. Animal models designed to mimic global ischemic injury in humans include those where permanent or transient occlusion of large blood vessels supplying the brain leads to a

widespread H-I episode. In contrast, focal animal models of ischemia involve transient or permanent occlusion of specific cerebral vessels and thus result in acute damage to localized brain regions. The differences between these animal models can specifically address different types of stroke injury in humans. For instance, global ischemic insults are most relevant to patients suffering from cardiac arrest, but are also used to address pathophysiology associated with perinatal asphyxia, strangulation, severe shock or intracranial hypertension (Hossmann *et al.*, 1998). Focal ischemic insults are pertinent to brain injury in humans that has been induced by thrombotic stroke, an embolic occlusion or lacunar infarction (Hossmann *et al.*, 1998).

The Rice-Vannucci model of hypoxia-ischemia (H-I) is a hemi-global model of ischemia and is based on the Levine preparation in the adult rat (Levine, 1960). In this model, ligation of one common carotid artery (CCA) combined with a transient period of systemic hypoxia (8% oxygen, balance nitrogen) produces progressive and permanent brain damage that is limited to the cerebral hemisphere ipsilateral to the carotid artery occlusion. Within the ipsilateral hemisphere, susceptible brain regions include the hippocampus, cerebral cortex and striatum (basal ganglia) (Gilby *et al.*, 1997; Martin *et al.*, 1997; Vannucci and Vannucci, 1999). The reason for the predilection of these regions to H-I is currently unknown. However, there is some evidence that metabolic factors such as regional cerebral glucose utilization, may play a dominant role (Vannucci and Vannucci, 1999). It is interesting that, in relation to control animals, there does not appear to be any change in blood flow to individual structures of the ipsilateral cerebral hemisphere following unilateral occlusion (Vannucci and Vannucci, 1999). Measurements of systemic physiologic variables in rats during the course of the hypoxic episode indicate that animals exhibit hypoxemia and hypocapnia that likely can be attributed to hyperventilation (Welsh *et al.*, 1982). Mean systemic blood pressure also decreases by 25% -30% in animals during the course of systemic hypoxia (Vannucci *et al.*, 1999). Neither the carotid artery ligation nor the hypoxic episode individually produce detectable neuronal damage in any brain region. Moreover, despite the profound cell loss produced in selective brain regions of the ipsilateral hemisphere following H-I, there have been no reports of cell loss in any structure of the contralateral hemisphere following H-I insult (Gilby *et al.*, 1997; Vannucci *et al.*, 1999).

Generally, the H-I model is considered to be clinically significant to many neurological disorders. Research has shown that H-I injury in humans can lead to the development of neurological impairments that are relatively minor such as learning disabilities and motor disturbances and to more debilitating impairments including mental retardation, cerebral palsy and epilepsy (Vannucci, 1990; Williams *et al.*, 1993; Volpe *et al.*, 1995). In the past 10 years, the H-I protocol has been adopted as a model for stroke-induced brain injury, with particular relevance to the pathology observed in the human brain following cardiac arrest (Hunter *et al.*, 1995). This immature rat model has also gained wide acceptance as the animal model of choice to study basic physiologic biochemical and molecular mechanisms of perinatal H-I-induced brain damage (Vannucci *et al.*, 1999).

There are several attributes of the H-I model that encourage researchers to utilize this model over other models of ischemia for stroke research. First, the severity of the resultant injury can be controlled in the H-I model. For instance, the surgical protocol (unilateral or bilateral occlusion) and/or the duration of the hypoxic interval have been manipulated by researchers in order to address specific pathophysiological questions related to stroke (Silverstein *et al.*, 1984; Ikonomidou *et al.*, 1989; Blumenfeld *et al.*, 1992; Munell *et al.*, 1994; Dragunow *et al.*, 1994). For instance, Rumpel *et al.* (1995) demonstrated that the extent of brain damage to the ipsilateral hemisphere could be titrated by varying the duration of the hypoxic episode. Second, the H-I model allows for prolonged loss of adequate blood flow (oxygenation) to the brain whereas in many other global ischemia paradigms animals are only able to withstand brief occlusion intervals. Rats used in the Rice-Vannucci model are capable of surviving in 8% oxygen for more than 3 hours before appreciable mortality occurs (Vannucci *et al.*, 1999). Third, the H-I model involves a relatively non-invasive surgical procedure. A small incision in the throat to enable occlusion of one CCA bears little threat to the animal and requires little time under anesthesia (approximately 5 minutes), thereby minimizing complications, such as hypothermia, that may arise from prolonged use of general anesthetic. Finally, while the H-I model is technically a permanent occlusion model, studies have shown that following the hypoxic episode there is, once again, adequate oxygenation of the ipsilateral hemisphere which suggests that this model does account for reperfusion injury

(Gilby *et al.*, 1997; Hunter *et al.*, 1995; Vannucci *et al*, 1999). Moreover, because the H-I model permits adequate perfusion of the compromised zone, in spite of the permanent occlusion, the true neuroprotective ability of potential compounds can be assessed. In many other permanent occlusion ischemia models, the permanent decrease in blood flow to the ischemic zone (8-10% of normal) limits the access of systemically administered compounds to the ischemic core and thereby may complicate and/or reduce the potential effects of the compound (Sydserff *et al.*, 1995a).

A major concern regarding the applicability of any animal model to stroke research is the age of the animals used in experimentation. Most human victims of stroke are affected in the later years of life yet most animals used in stroke experiments are relatively young. For example, rats used in the H-I model range between PND7 and PND25. Research has shown that while H-I injury produced using the Rice-Vannucci protocol is profound in young animals, no cell death has been observed in any brain region of adult animals that undergo the same procedure (Vannucci *et al.*, 1999). However, while important differences in pathophysiology may exist between PND7 and adult animals, few if any physiological differences have been observed between PND25 and adult rats (Towfighi *et al.*, 1991; Blumenfeld *et al.*, 1992; Hagberg *et al.*, 1997). Thus, any pathophysiological differences between PND25 rats and adults are likely more relevant to the predisposing factors of stroke and/or the ability of the animal to recover from the insult, rather than the etiology of ischemic insult once initiated.

Chapter 1: *Post-hypoxic Administration of Clomethiazole Provides Near Complete Neuronal Protection Against Severe Global Ischemia.*

Summary

The ability of CMZ to prevent neuronal death following hypoxia-ischemia (H-I) in young male rats was investigated. Experimental animals received an intraperitoneal (i.p.) injection of vehicle or 100, 150 or 200 mg/kg CMZ at 1, 2 or 3 hours post-hypoxia or 200 mg/kg CMZ at 4 hours post-hypoxia. Several control animal groups were used in this experiment including naïve animals, ligated controls, hypoxic controls and CMZ-injected naive animals. Analysis of cresyl violet stained sections revealed that CMZ administration at 3 hours post-hypoxia appeared to have a dose-dependent neuroprotective effect in H-I animals sacrificed at 7 days post-hypoxia. While 100 and 150 mg/kg CMZ did provide significant neuroprotection in susceptible cell layers when administered at 3 hours post-hypoxia, the mean percentage neuronal death was higher in these animals than in those that received 200 mg/kg at this timepoint. Significant neuroprotection was also observed in all susceptible cell layers of H-I animals when 200 mg/kg CMZ was administered at 1 or 2 hours post-hypoxia. However, if administration of CMZ (200 mg/kg) was delayed to four hours after the insult no neuroprotection was observed. This finding suggests that CMZ may exert its neuroprotective effect on an event that occurs within the acute phase (within 3 hours) of cell death. In order to ensure that CMZ did not merely delay cell death following H-I, separate groups of vehicle-injected and CMZ-injected H-I animals were sacrificed at 4 weeks post-hypoxia. In these animals, a significant neuroprotective effect was still evident in all susceptible cell layers of H-I animals that received 200 mg/kg CMZ at 3 hours post-hypoxia. Similarly, a significant level of neuroprotection was reached in the CA2 and CA3 cell layers of the hippocampus and in the parietal cortex of H-I animals that received 150 mg/kg at 3 hours post-hypoxia. However, a significant degree of neuroprotection was not evident in CA1 of these animals.

In order to exclude the possibility that any neuroprotective benefit provided by CMZ was attributable to hypothermia, a known neuroprotective physiological state, rectal body temperature was measured in all animals following H-I. Mean rectal temperatures did not fall below 37°C in either CMZ-injected or vehicle-injected H-I animals for at least 3 hours post-injection. In conclusion, the results of this experiment suggest that

irreversible neuronal damage does not occur for at least 3 hours following H-I injury and that administration of CMZ is capable of preventing irreversible cellular injury within this timeframe. Moreover, the fact that rectal temperatures of all animals remained at normothermic levels suggests that it is unlikely that CMZ-induced neuroprotection against H-I injury was attributable to the induction of hypothermia.

Introduction

Clomethiazole (CMZ) edisylate (INN: Clomethiazole; BAN: Chlormethiazole edisylate, Heminevrin, Distraneurin, Hemineurin, Distraneurine, Zendra) is derived from the thiazole moiety of thiamine (Charonnat *et al.*, 1957; Lechat, 1960, 1966 as sited in Green *et al.*, 1998a). See Figure 1-1. For over 25 years, CMZ has been used clinically as a sedative, anxiolytic and hypnotic agent and to treat patients suffering from alcohol withdrawal (Evans *et al.*, 1986; Green *et al.*, 1998a). CMZ has also been used successfully as an anticonvulsant in humans and has been shown to inhibit chemoconvulsions induced by bicuculline, picrotoxin, isoniazid and pentylenetetrazol (PTZ) in animal models (Ogren, 1986; Green and Murray, 1989). The anticonvulsant properties of CMZ have been demonstrated at doses of 50 and 100 mg/kg in an animal model of N-methyl-DL-aspartate (NMDLA)-induced tonic seizures (Cross *et al.*, 1993). Toxicological tests in animals, associated with CMZ administration, have revealed that while CMZ is sedative in high doses, there are no problems of clinical relevance other than a risk of respiratory depression (personal communication; Astra Inc.).

In addition to anticonvulsant, sedative, anxiolytic and hypnotic properties, it is now quite clear that CMZ has substantial neuroprotective efficacy in a variety of animal models of ischemia. Cross *et al.* (1991) observed near complete histological neuroprotection against hippocampal neuronal loss when CMZ (100 mg/kg, ip.) was administered 30 minutes prior to a global ischemic insult in the Mongolian gerbil. Neuroprotection was also observed in that study when the NMDA antagonists, MK 801 and ifenprodil, were substituted for CMZ. However, only CMZ (100 mg/kg) provided hippocampal neuroprotection (70-80%) when administered 3 hours after the global ischemic insult. Compounds that can be administered at delayed post-ischemic timepoints and still produce neuroprotection are of profound clinical relevance to stroke research. Thus, investigation into the neuroprotective benefits of CMZ in both focal and global animal models of ischemia may be beneficial to future neurotherapy.

Since the original finding, studies have shown a neuroprotective effect for CMZ in numerous animal models of ischemia. Using Lister hooded rats, Sydserff *et al.* (1995a) demonstrated that CMZ administration was neuroprotective in a model of

Figure 1-1

The chemical structure of Clomethiazole.

Clomethiazole (CMZ) edisylate (INN: Clomethiazole; BAN: Chlormethiazole edisylate, Heminevrin, Distraneurin, Hemineurin, Distraneurine, Zendra) is derived from the thiazole moiety of thiamine. This figure provides the structural formula for CMZ clomethiazole hemiethanedisulphonate.

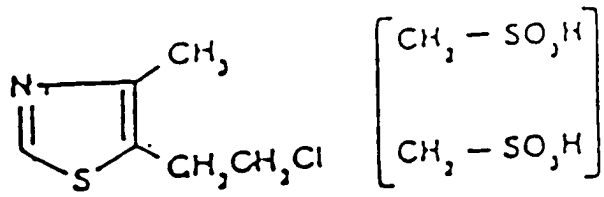

$C_6H_8ClNS \bullet 1/2C_2H_6O_6S_2$

5 - (2-Chloroethyl)-4-methylthiazole hemiethanedisulphonate

Figure 1-1

transient middle cerebral artery occlusion (tMCAO). In that study, pretreatment (60 minutes prior to MCAO) or post-treatment (10 minutes following the onset of reperfusion) with CMZ (1000 μmol kg^{-1}) produced an approximate 60% reduction in the volume of neuronal damage observed in both the cortex and striatum of CMZ-injected rats when compared to vehicle-injected rats. Similar neuroprotective effects were observed using Lister hooded rats in a model of permanent middle cerebral artery occlusion (pMCAO) where administration of CMZ (1000 μmol kg^{-1}) 1 hour following the ischemic event produced a near 60% reduction in the volume of ischemic damage (Sydserff *et al.*, 1995b). However, administration of the same dose of CMZ at 3 hours post-ischemia did not provide neuroprotection in that model of focal cerebral ischemia. On the other hand, a subcutaneous injection of CMZ (100 mg/kg) administered to gerbils up to 4 hours following two vessel occlusion (2-VO) produced substantial neuroprotection in that model of global ischemia (Shuaib *et al.*, 1995). In the photochemically-induced lesion model of ischemia (Rose Bengal), CMZ administration (200 mg/kg) 5 minutes following focal cerebral ischemia was shown to decrease infarct size by approximately 30-50% in treated versus control rats (Snape *et al.*, 1993; Baldwin *et al.*, 1994). Interestingly, replacement of CMZ with the calcium antagonist nimodipine (0.5 mg/kg) in that study did not provide neuroprotection in susceptible cell layers (Snape *et al.*, 1993). Moreover, neither MK801 nor the AMPA antagonist, 2,3 – dihydroxy– 6-nitro- 7- sulphamoyl-benzo (F) quinoxaline (NBQX), provided any neuroprotection in the Rose Bengal ischemia paradigm (Baldwin *et al.*, 1993c). Control experiments have indicated that the neuroprotective effect of CMZ observed in the Rose-Bengal model of ischemia was the result of neuroprotection rather than an effect on anion transport or glutamate release (Green and Cross, 1994a). To date, there has been one study published that failed to demonstrate a neuroprotective effect for CMZ against ischemia-induced cell death. Thaminy *et al.*, (1997) investigated whether CMZ (100 mg/kg) treatment 60 minutes following four vessel occlusion (4-VO), a global model of ischemia, was of any neuroprotective benefit. The findings of that study demonstrated that while there was consistently less cell death in CMZ-treated animals than in control animals statistical significance was not obtained. Thus, the authors of that study concluded that CMZ was not neuroprotective against ischemic injury induced by 4-VO. Collectively, these studies

have demonstrated that CMZ provides clear histological neuroprotection against ischemic injury. However, the exact mechanism through which CMZ achieved these neuroprotective effects is currently unknown.

The Pharmacology of Clomethiazole

Several active metabolites of CMZ have been identified in humans, however, it is generally believed that the neuroprotective ability of CMZ resides in the activity of the parent compound (Witts *et al.*, 1983; Green *et al.*, 1998a). In gerbils, CMZ is metabolized into at least three known metabolites (5-(1-hydroxy-2-chloroethyl)-4 methylthiazole [Company code: NLA-715], 5-(1-hydroxyethyl)–4 methylthiazole [NLA–272] and 5 acetyl–4 methylthiazole [NLA – 511]). Unlike CMZ, injection of the individual metabolites at a dose of 600 μmol/kg did not provide any neuroprotection in a gerbil model of global ischemia (Cross *et al.*, 1998 as sited in Green *et al.*, 1998a). In general, CMZ has a very short half-life (20-25 minutes in gerbils; 6.6 hours in humans) and a rapid clearance rate (103ml/kg/min in gerbils; 15 ml/kg/min in humans) (Pentikainin *et al.*, 1980; Cross *et al.*, 1995; Green *et al.*, 1998a).

The first indication that CMZ selectively modulated GABAergic activity was documented in a study conducted by Leeb-Lundberg *et al.* (1981) that demonstrated CMZ could potentiate [^{3}H]-muscimol binding. Since then, several studies have indicated that CMZ selectively modulates the $GABA_A$ receptor through potentiation of $GABA_A$-evoked responses and through direct activation of the receptor itself (Harrison and Simmonds, 1983; Cross *et al*, 1989; Moody and Skolnick, 1989; Vincens *et al.*, 1989; Hales and Lambert, 1992). There is presently no evidence to suggest that CMZ activates or modulates the activity of presynaptic $GABA_B$ receptors (Cross *et al.*, 1989; Vincens *et al.*, 1989). Thus, the GABAergic effects of this compound are generally ascribed to $GABA_A$-receptor mediated events.

The pharmacologic activity of CMZ at the $GABA_A$ receptor appears to have some barbiturate-like properties, however, biochemical studies suggest the interaction is not identical (Green *et al.*, 1998a). There is evidence that CMZ, like barbiturates, prolongs the GABA channel burst duration and enhances [^{3}H]-muscimol binding (Cross *et al.*, 1989; Hales and Lambert, 1992). Unlike barbiturates, CMZ is able to modulate the

strychnine-sensitive glycine receptor and does not potentiate specific [^{3}H]-flunitrazepam binding (Harrison and Simmonds, 1983; Cross *et al.*, 1989; Hales and Lambert, 1992; Green *et al.*, 1996; Zhong and Simmonds, 1997). Moreover, CMZ actually inhibits the stimulation of [^{3}H]–flunitrazepam binding that is normally induced by pentobarbitone (Cross *et al.*, 1989; Green *et al.*, 1996). While CMZ does have weak binding activity at benzodiazepine (BZD) receptors, the kinetic properties of CMZ are different from benzodiazepines (BZDs). For instance, the BZD receptor antagonist Ro 15-1788 had no effect on potentiation of GABA-evoked currents by CMZ but it did block the potentiation normally generated by the benzodiazepine, diazepam (Hales and Lambert, 1992). Thus, it is unlikely that CMZ interacts directly with the GABA or benzodiazepine receptor binding sites, although it does appear to influence the characteristics of these binding sites.

There is currently no evidence suggesting that CMZ alters the concentration of GABA in the brain, increases the rate of GABA synthesis (GAD activity) or increases GABA uptake into cerebral tissue (Ogren *et al.*, 1986; Cross *et al.*, 1989; Vincens *et al.*, 1989; Green *et al.*, 1998a). The GABA-potentiating effects of CMZ are, therefore, likely to be the result of an interaction with the $GABA_A$ receptor. There is evidence suggesting that CMZ can modulate $GABA_A$ chloride channel activity and thereby potentiate the GABAergic response in the absence of endogenous GABA (see review in Green *et al.*, 1998a). CMZ has been shown to increase the rate of dissociation of [^{35}S] butyl-bicyclophosphothionate (TBPS) from a binding site associated with the chloride channel (Cross *et al.*, 1989; Moody and Skolnick, 1989; Vincens *et al.*, 1989; Green *et al.*, 1996). Further studies are required in order to determine the exact site of action for CMZ on the $GABA_A$ receptor complex and to identify whether there is a specific subunit configuration of the receptor that permits CMZ interaction.

Studies have been conducted in order to determine whether the neuroprotective efficacy of CMZ in animal models of ischemia can be attributed to an interaction between CMZ and non-GABAergic systems. To date, there is no evidence to suggest that CMZ interacts at any site on the NMDA receptor, however, it has been shown to indirectly inhibit NMDA-receptor-mediated function, possibly by decreasing cellular levels of cGMP (Cross *et al.*, 1993a,b; Thoren and Sjolander, 1993; Green *et al.*, 1998b).

Similarly, CMZ does not appear to interact with the AMPA/kainate or metabotropic glutamate receptors at pharmacologically relevant doses but it has been shown to inhibit the downstream effects of AMPA/kainate receptor activation (Addae and Stone, 1988; Ogren, 1986; MacGregor *et al.*, 1997; Green *et al.*, 1998b). The effect of CMZ on adenosine function, monoamine levels (noradrenalin, dopamine and serotonin), histamine function and sodium, potassium and calcium channel activation has also been investigated and the results of these studies cannot account for the neuroprotective effects of CMZ in ischemic animal models (reviewed in Green *et al.*, 1998a).

Due to the number of experiments that have reported a neuroprotective efficacy for CMZ in animal models of ischemia, CMZ is now in clinical development for the treatment of acute ischemic stroke. A large clinical trial demonstrated that CMZ did, indeed, have a neuroprotective effect in a particular subpopulation of patients that exhibited clinical symptoms indicative of a large infarct volume or total anterior circulation syndrome (TACS) (Wahlgren *et al.*, 1999). In that study, patients with acute ischemic stroke received an intravenous infusion of CMZ (75 mg/kg) over 24 hours which produced a mean plasma concentration of approximately 13 μmol/L by the end of the infusion. Study inclusion criteria required that treatment be initiated within 12 hours of onset of symptoms. Functional outcome was assessed using the Barthel Index 3 months following treatment with CMZ or vehicle. The reason for the injury-dependent success of CMZ in human patients is currently unknown, however, it may indicate a relationship between the severity and/or type of ischemic insult and the efficacy of CMZ administration. In this way, use of a severe hemi-global animal model of ischemia, such as the Rice-Vannucci model, may be a clinically relevant method to address the mechanism underlying the neuroprotective efficacy of CMZ in TACS patients.

CMZ and Hypothermia

Several studies have reported that even mild hypothermia can provide histological and functional neuroprotection in various animal models of ischemia (Busto *et al.*, 1987; Buchan and Pulsinelli, 1990; Corbett *et al.*, 1990; Globus *et al.*, 1995; Nurse and Corbett, 1996; Colburne *et al.*, 1998). It is generally believed that hypothermia may exert a protective effect by causing a decrease in the cellular demand for energy that ultimately

decreases the impact of oxygen deprivation during an ischemic event. Alternatively, it has been suggested that hypothermia may cause a reduction in cerebrocortical production and release of nitric oxide (NO) and excitotoxins and thereby minimizes the deleterious cellular response to ischemia (Thoresen *et al.*, 1997). Hypothermia has also been shown to decrease glutamate efflux during ischemia and prevent subcellular redistribution and down regulation of both protein kinase C (PKC) and calcium/calmodulin protein kinase II (Busto *et al.*, 1987; Churn *et al.*, 1990; Cardell *et al.*, 1991). In rodents, the neuroprotective efficacy of post-ischemic hypothermia depends on the duration of hypothermia. A series of investigations into the neuroprotective effect of hypothermia reported that if hypothermia was maintained for 24 hours after ischemia in gerbils, neuronal protection was evident in the hippocampus up to 6 months post-ischemia (Colburne and Corbett, 1995). Similarly, hypothermia has proven to be an effective treatment against stroke in humans (Swain *et al.*, 1991). It is generally believed, however, that compounds that achieve their neuroprotective effect through the induction of hypothermia are not "truly neuroprotective" since hypothermia must be initiated during the ischemic event and maintained after the insult in order to produce neuroprotection (Swain *et al.*, 1991). As in other animal models of ischemia, hypothermia-induced neuroprotection has been reported in the H-I model. Bona *et al.* (1998) demonstrated an approximate 25% reduction in neuronal damage in the cerebral cortex, hippocampus, basal ganglia and thalamus of PND7 rats, histologically assessed at 1 and 6 weeks post-hypoxia, when measured rectal temperature was maintained at 32°C for 6 hours post-hypoxia. In view of this finding, the effect of CMZ on rectal temperature following H-I was investigated in this study.

Methods

Animals

Male Sprague-Dawley rats were purchased from Charles River Canada (Lasalle, Quebec). The animals were treated in accordance with the guidelines set by the Canadian Council on Animal Care. Animals were housed in groups of 3-11 in the Dalhousie Animal Care Facility and maintained on a 12:12 h dark-light cycle with *ad libitum* access to both food (Purina rat chow) and water. On post-natal day (PND) 25, rats (50-60 g) were randomly assigned to treatment groups.

H-I Animals

PND 25 animals were anesthetized by inhalation of a 2% halothane/oxygen mixture. A small longitudinal incision was made in the throat to expose the left CCA, which was then ligated with a sterile 3.0 silk non-absorbable surgical suture (Ethicon Inc.). The incision was sutured using sterile 4-0 absorbable surgical sutures (Dexon 11). Following surgery, the rats were monitored for any overt signs of impaired motor activity. After a 2 hour recovery period, the animals were placed into an air-tight plexiglass cylinder with controlled air flow. The cylinder, containing the rats, was placed in a 34°C circulating water bath. Preliminary experiments have indicated that holding water temperature at 34°C maintains the rectal temperature of the animals at normothermic levels (unpublished data). Compressed medical air (17% oxygen) was released into the cylinder and maintained at a constant flow rate for 30 minutes to allow the animal to habituate to the novel environment. The animals were then exposed to hypoxic air (8% oxygen, balance nitrogen) at the same flow rate for 60 minutes. Following the hypoxic episode, rats were removed from the cylinder and returned to their original housing conditions for recovery beneath a warming lamp intended to maintain rectal temperatures at normothermic levels for 4-10 hours. During this time, each animal was observed for any overt signs of seizure activity such as mastication, barrel rolling or limb tonus and clonus. Animals that exhibited such behavior were excluded from the study. Following the recovery/observation period all animals were returned to the Dalhousie Animal Care Facility until sacrificed.

Some H-I animals received an i.p. injection of either vehicle (distilled water), 100mg/kg, 150mg/kg or 200mg/kg CMZ (dichlormethiazole ethanedisulphonate; Astra Arcus, S dert≡lje, Sweden) at 3 hours post-hypoxia. Additional groups of H-I animals received an injection (i.p.) of either vehicle or 200 mg/kg CMZ at 1, 2 or 4 hours post-hypoxia. In order to determine whether hypothermia was induced in H-I animals by CMZ administration, rectal temperature was monitored in vehicle- and CMZ-injected H-I animals every 10 minutes for at least 180 minutes post-injection (6 hours post-hypoxia).

Control Animals

Animals in that served as ligated controls in this study were anesthetized using a 2% halothane/oxygen mixture. A small incision was made in the throat and the left CCA was ligated using sterile 3.0 non-absorbable silk surgical suture (Ethicon Inc.). The incision was then sutured using sterile 4-0 absorbable surgical sutures (Dexon 11) and the animals were returned to their original housing to recover from surgery beneath a warming lamp. Hypoxic control animals did not undergo surgery but were placed directly into the plexiglass cylinder. The cylinder containing the rat pups was placed in a 34°C circulating water bath (Canlab) and the rats were exposed to medical air followed by a 60 minute hypoxic episode in the exact manner detailed for H-I animals. Each rat pup was then returned to the original housing conditions to recover beneath a warming lamp. Animals that served as CMZ-injected controls did not undergo surgery or the H-I event but received an i.p. injection of either 100, 150 or 200 mg/kg CMZ in order to evaluate the effects of CMZ-administration alone. Finally, animals in the naïve control group received no experimental manipulation of any kind.

Adult H-I Animals

Fifteen male rats, each weighing approximately 400 grams, were subjected to surgical ligation of the left CCA in a manner identical to that outlined for the PND25 rats. Two hours following surgery, each rat was placed in a glass chamber and subjected to 30 minutes of medical air followed by 60 minutes of hypoxic air (8% oxygen, balance nitrogen) at room temperature. Following the hypoxic episode, each animal was removed from the chamber and placed beneath a warming lamp for at least 6 hours post-hypoxia.

During this time, animals were observed for any overt signs of seizure activity such as mastication, barrel rolling or limb tonus and clonus. Animals that exhibited such behavior were excluded from the study. Following the recovery/observation period all animals were returned to the Dalhousie Animal Care Facility until sacrificed.

Perfusion and Tissue Fixation

Animals were sacrificed 1 or 4 weeks following their various treatments. Each rat pup was deeply anaesthetized with 65 mg/kg of sodium pentobarbitol and was then perfused through the ascending aorta with 0.9% saline (60 ml) followed by cold 100 mM phosphate buffer containing 4 % paraformaldehyde (60 mls). Brains were removed and post-fixed in 100 mM phosphate buffer containing 4% paraformaldehyde at 4°C for at least 24 hours. Adult rats were perfused in the same manner, however, 120 mls of each perfusion solution was used.

Cresyl Violet Analysis

Fixed brains from all animals were sectioned coronally (40 μm) through the entire hippocampus on a Series 1000 Vibratome. Cresyl violet nissl stain was used to establish the profile of degenerating neurons in H-I animals and, thereby, evaluate the neuroprotective effect of CMZ in H-I animals sacrificed at 1 and 4 weeks post-hypoxia. For each rat pup, a series of representative 40 μm sections spanning the hippocampus was mounted directly onto chrom-alum, gelatin-coated slides and air-dried overnight. Sections were then dehydrated in a series of ethanols, defatted with xylene, rehydrated and stained with 1.0% cresyl violet acetate for visualization of nissl substance. The slides were then washed in water, dehydrated in a series of ethanols and put back into xylene. Slides were coverslipped with Entellan (E. Merck, Darmstadt, Germany).

Quantification of Cell Death

The extent of neuronal death in CMZ- and vehicle-injected animals was analyzed in both the ipsilateral hippocampus and parietal cortex using Jandel Scientific Digitization Hardware and was conducted by an examiner that was blinded to group assignments. For each animal, 4 to 6 cresyl-violet stained sections cut through the hippocampus (40 μm) were examined under the light microscope for evidence of ischemic neuronal death (pyknosis). Following cresyl violet stain, damaged neurons characteristically exhibit a shrunken densely stained appearance and are pyknotic (no nucleus). The amount of ischemic damage was calculated using a representative section from each animal that was equidistant from Bregma and the interaural plane. Regions of ischemia were delineated onto pre-matched stereotaxic maps adapted from The Rat Brain in Stereotactic Coordinates (Paxinos and Watson, 3rd Edition) and the area of cortical injury on each map determined by digitizing the image (Jandel Sigmascan Pro 4 Software; Summagraphics Summasketch III hardware). Similarly, the degree of hippocampal injury was determined by tracing the cumulative length of the injured cell regions (CA1, CA2 and CA3). Percentage neuronal death in the cortex was expressed as the area of dead cells in the cortex/total area of the cortex and the percentage length of damage to the hippocampus was expressed as length of dead cells/total length of cell layer. Mean group differences were statistically analyzed using a non-parametric test (Kruskall-Wallis ANOVA with Dunn's post-hoc analysis, Jandel Sigmastat 4.0 software).

Anatomical Terminology

Anatomical terminology used in this study conforms mainly to that of Amaral and Witter (1995). Refer to Figure 1-2.

Figure 1-2

Basic anatomy of the hippocampus.

Photomicrograph of a coronal section of the rat hippocampus. *Cornu ammonis 1 (regio superiore)* denoted as CA1 refers to a layer of small pyramidal cells and their associated interneurons. *Cornu ammonis 2 (regio inferiore)* denoted as CA2 refers to a small region of large pyramidal cells located between CA1 and CA3. *Cornu ammonis 3 (regio inferiore)* is denoted as CA3 and includes the remaining layers of large pyramidal cells that extend from CA2 to the region between the two blades of dentate gyrus. CA3 can be further divided into CA3a which refers to the curved layer of CA3 adjacent to CA2, CA3b which is located in the middle of CA3 and CA3c which refers to the large pyramidal cells adjacent to the dentate hilus. The cells that comprise the hilus (h) are located in the region between CA3c and the blades of the dentate gyrus. The upper and lower blades of the dentate gyrus are densely packed with granule cells (GC). The cortex and corpus callosum are labeled Ctx and cc respectively. The terminology used in this figure conforms mainly to that of Amaral and Witter (1995). (Scale bar = 200 μm)

Figure 1-2

Results

General Behaviour

Approximately 10% of PND25 animals subjected to H-I exhibited some form of overt seizure activity following removal from the hypoxic chamber. Six of 15 adult animals subjected to H-I died during the hypoxic episode. Two of 15 adult animals exhibited motor seizure activity within 1 hour following the hypoxic episode. Any animal exhibiting motor seizure activity was excluded from the study. CMZ administration produced sedation in all PND25 animals in an apparent dose-dependent manner, with the 200 mg/kg dose rendering the animals completely immobile for a minimum of 2 hours following the injection. Six of 42 animals that received 200 mg/kg CMZ died approximately 15 minutes following injection, presumably from respiratory depression.

Histology

In PND25 rats, ligation of the left CCA in combination with 60 minutes of systemic hypoxia resulted in profound degeneration of cell layers in the ipsilateral hippocampus and ipsilateral parietal cortex by 7 days post-hypoxia. The pyramidal neurons in the hippocampal CA1 sector were the most vulnerable to H-I, becoming pyknotic between 12-24 hours post-hypoxia. However, by 7 days post-hypoxia only the dentate granule cell layer of the ipsilateral hippocampus was spared in these brain regions. As in previous studies, neocortical damage following H-I was laminar in distribution, with layers 3, 5 and 6 containing the highest number of injured neurons (Gilby *et al.*, 1997; Vannucci *et al.*, 1999). Specifically, H-I animals that received a vehicle injection at 3 hours post-hypoxia (N = 10) exhibited a high mean percentage of neuronal death in CA1 (80.16%), CA2 (80.72%) and CA3 (54.31%) of the ipsilateral hippocampus and parietal cortex (42.29%) by 7 days post-hypoxia. Differences in mean percentage neuronal death in either the parietal cortex or any cell layer of the hippocampus were not statistically significant between H-I animals that received a vehicle-injection at 1 (N = 11), 2 (N = 7), 3 (N = 10) or 4 hours (N = 8) post-hypoxia. No neuronal degeneration was evident in any region of the contralateral hemisphere in H-I

animals or in any brain region of the hypoxic or ligated control animals sacrificed at any post-hypoxic timepoints (see also Gilby *et al.*, 1997). See Figure 1-3.

Hippocampus

Statistical analysis, using the Kruskall-Wallis ANOVA on Ranks test detected significant differences between all susceptible hippocampal cell layers of vehicle-injected H-I animals relative to CMZ-injected control animals (N = 15) (CA1 Q = 5.036; CA2 Q = 5.418; CA3 Q = 5.514; $P<0.05$). Relative to vehicle-injected H-I animals, a significant level of neuroprotection was observed in all susceptible cell layers of the ipsilateral hippocampus (CA1, CA2, CA3) of various groups of CMZ-injected H-I animals sacrificed at 7 days post-hypoxia (H = 61.789; DF = 9; $P<0.001$). See Figure 1-3. Specifically, significant sparing of CA1 pyramidal cells was observed in H-I animals that received 200 mg/kg CMZ at 1 (N = 10), 2 (N = 10) or 3 hours (N = 17) post-hypoxia (Q = 3.473; Q = 3.602; Q = 5.232 respectively; $P<0.05$). However, 200 mg/kg of CMZ did not provide a significant level of neuroprotection in CA1 when administration was delayed to 4 hours post-hypoxia (N = 14). The 100 mg/kg dose of CMZ (N = 10) also provided significant (Q = 3.625; $P<0.05$) neuroprotection in CA1 when injected at 3 hours post-hypoxia. However, the neuroprotection produced in CA1 by 150 mg/kg (N = 10) CMZ administered at 3 hours post-hypoxia did not reach statistical significance.

H-I animals that received 200 mg/kg CMZ at 1, 2 and 3, but not 4, hours post-hypoxia demonstrated significantly (H = 82.058; DF = 9; $P<0.001$) less neuronal damage in CA2 than vehicle-injected animals (Q = 3.863; Q = 5.016; Q = 5.629 respectively; $P<0.05$). Similarly, H-I animals that received lower doses of CMZ (150 and 100 mg/kg) at 3 hours post-hypoxia exhibited significant neuroprotection in CA2 relative to vehicle-injected animals (Q = 4.610; Q = 3.666 respectively; $P<0.05$). All animals that received 200 mg/kg CMZ at 1, 2 or 3 hours post-hypoxia exhibited a significant (H = 84.159; DF = 9; $P<0.001$) level of neuroprotection in CA3 relative to vehicle-injected H-I animals (Q = 4.273; Q = 5.105; Q = 5.592 respectively; $P<0.05$). However, a delay in the administration of 200 mg/kg CMZ to 4 hours post-hypoxia provided no protection against H-I-induced cell death in the CA3 cell layer. Animals that received lower doses of CMZ

Figure 1-3

Cresyl violet stained sections from vehicle- and CMZ-injected H-I animals sacrificed at 7 days post-hypoxia.

H-I animals received an ip injection of vehicle or 200 mg/kg CMZ 3 hours following H-I and were sacrificed 7 days following the H-I event. Cresyl violet analysis was used to detect pyknotic cells in susceptible brain regions of H-I animals. Panel A) a representative hippocampal section from a vehicle-injected H-I animal, Panel B) a representative cortical section from a vehicle-injected H-I animal, Panel C) a representative hippocampal section from a CMZ-injected (200 mg/kg) H-I animal, Panel D) a representative cortical section from a CMZ (200 mg/kg)-injected H-I animal. (Scale bar = 50 μm). The inserts in Panel B and D contain a higher magnification of the cortical section shown in that panel. (Scale bar = 50 μm).

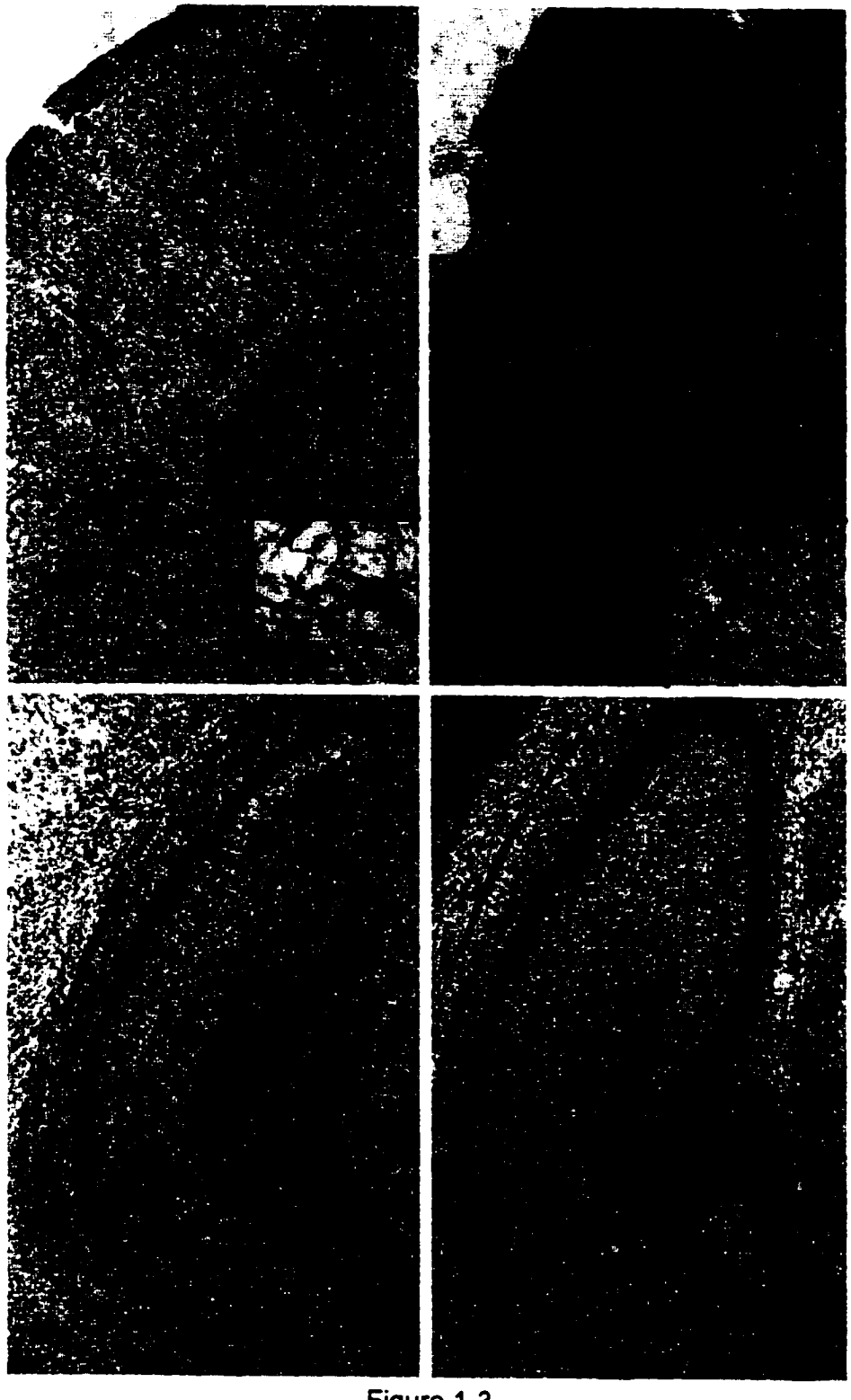

Figure 1-3

(150 and 100 mg/kg) also demonstrated significant neuroprotection in CA3 relative to vehicle-injected animals ($Q = 5.105$; $Q = 3.883$ respectively; $P<0.05$). See Figure 1-4.

In order to ensure that neuroprotection provided by CMZ administration was not the result of a delay in the neurodegenerative process, the mean percentage neuronal death was calculated for H-I animals sacrificed at 4 weeks post-hypoxia. Analysis of cresyl violet stained sections from H-I animals that received 200 mg/kg CMZ 3 hours post-hypoxia ($N = 7$) demonstrated that neuroprotection was evident in CA1 ($Q = 2.887$; $P<0.05$), CA2 ($Q = 4.552$; $P<0.05$) and CA3 ($Q = 4.632$; $P<0.05$) of animals sacrificed at 4 weeks post-hypoxia. Similarly, by 4 weeks post-hypoxia, neuroprotection was evident in CA2 ($Q = 4.408$; $P<0.05$) and CA3 ($Q = 4.017$; $P<0.05$) of H-I animals that received 150 mg/kg CMZ at 3 hours post-hypoxia ($N = 7$). However, by 4 weeks post-hypoxia a significant level of neuroprotection was not evident in CA1 of H-I animals that received 150 mg/kg CMZ at 3 hours post-hypoxia. See Figure 1-5.

Parietal Cortex

The area of cell death in the parietal cortices of CMZ-injected control animals (no H-I) was significantly ($H = 79.552$; $DF = 9$; $P<0.001$) different from vehicle-injected animals ($Q=4.999$; $P<0.05$). In fact, no cell death was detected in CMZ-injected H-I animals. When animals were sacrificed at 7 days post-hypoxia, significant neuroprotection was evident in the parietal cortices of H-I animals that received 200 mg/kg CMZ at 1, 2 or 3 hours post-hypoxia when compared to vehicle-injected animals ($Q = 4.308$; $Q = 4.628$; $Q = 5.193$ respectively; $P<0.05$). Similarly, substantial neuroprotection was produced in the parietal cortex when lower doses of CMZ, such as 150 mg/kg ($Q = 3.870$; $P<0.05$) and 100 mg/kg ($Q = 2.898$; $P<0.05$) were administered at 3 hours post-hypoxia. A statistically significant difference in percentage area of cortical damage was not detected between animals that received 200 mg/kg CMZ at 4 hours post-hypoxia and vehicle-injected animals. When H-I animals were sacrificed at 4 weeks post-hypoxia, significant neuroprotection remained evident in the parietal cortices of H-I animals that received 200 mg/kg CMZ ($Q = 3.048$; $p<0.05$), but not 150 mg/kg, at 3 hours post-hypoxia.

Figure 1-4

Quantitative analysis of the neuroprotective effect of CMZ in the H-I model.

Graphic illustration of mean percentage neuronal death in all susceptible cell layers (CA1, CA2, CA3 and parietal cortex) of vehicle-injected H-I animals and H-I animals that received various doses of CMZ (100, 150, 200 mg/kg) at 3 hours post-hypoxia. In addition, mean percentage neuronal death is provided for all cell layers of H-I animals that received 200 mg/kg CMZ at 1, 2 and 4 hours post-hypoxia. All animals were sacrificed at 7 days post-hypoxia. A P value of < 0.05 was considered statistically significant. The data are presented as means ± S.E.M. (* = significantly different from the same cell layer in vehicle-injected H-I animals).

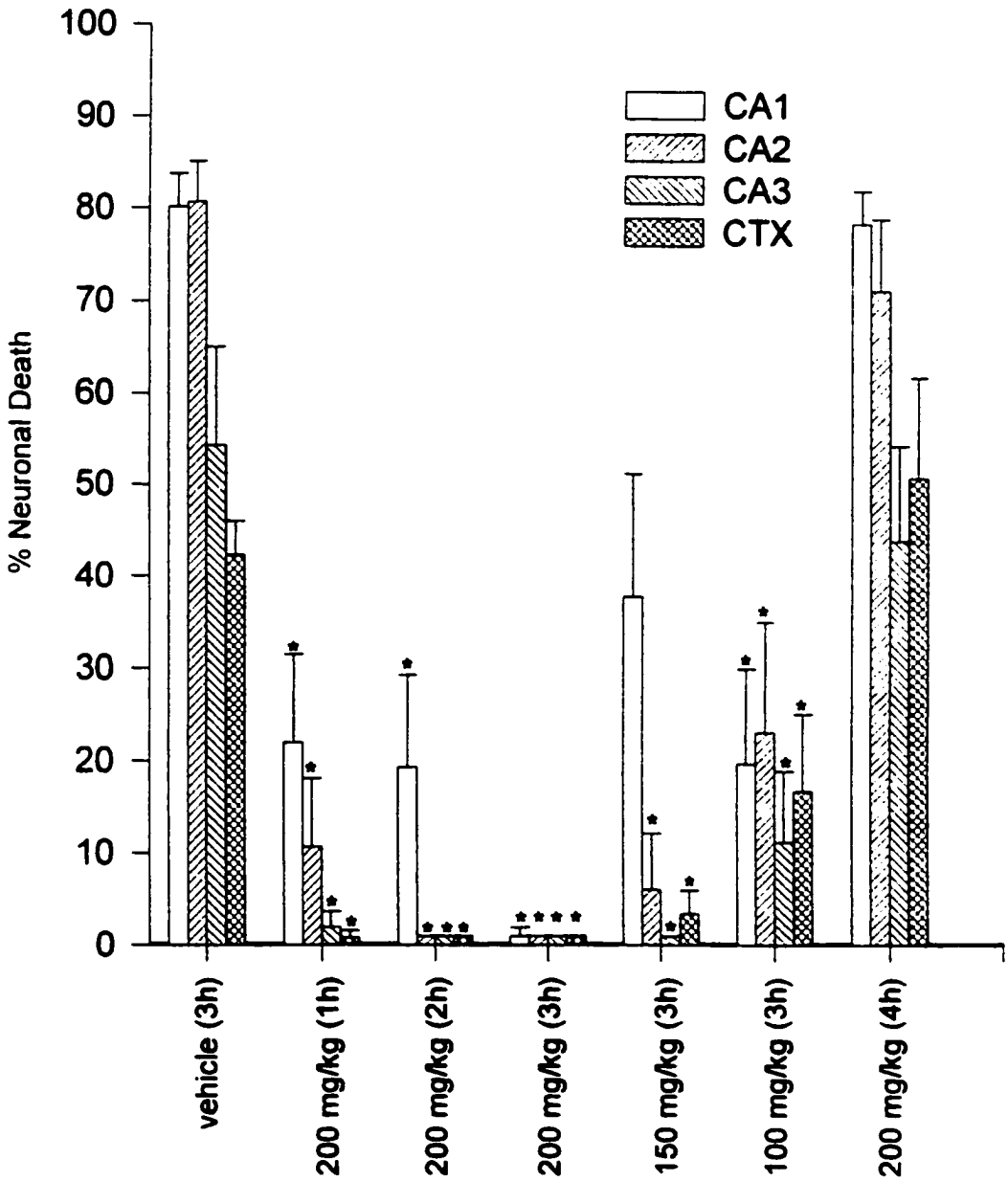
100
90
80
70
60
50
40
30
20
10
0
% Neuronal Death
CA1
CA2
CA3
CTX
vehicle (3h)
200 mg/kg (1h)
200 mg/kg (2h)
200 mg/kg (3h)
150 mg/kg (3h)
100 mg/kg (3h)
200 mg/kg (4h)

Figure 1-4

Figure 1-5

Quantitative analysis of the neuroprotective effect of CMZ in H-I animals sacrificed at 4 weeks post-hypoxia.

Graphic illustration of mean percentage neuronal death in all susceptible cell layers (CA1, CA2, CA3 and parietal cortex) of vehicle-injected H-I animals and H-I animals that received either 150 or 200 mg/kg CMZ at 3 hours post-hypoxia. All animals were sacrificed at 4 weeks post-hypoxia. A P value of < 0.05 was considered statistically significant. The data are presented as means ± S.E.M. (* = significantly different from the same cell layer in vehicle-injected H-I animals).

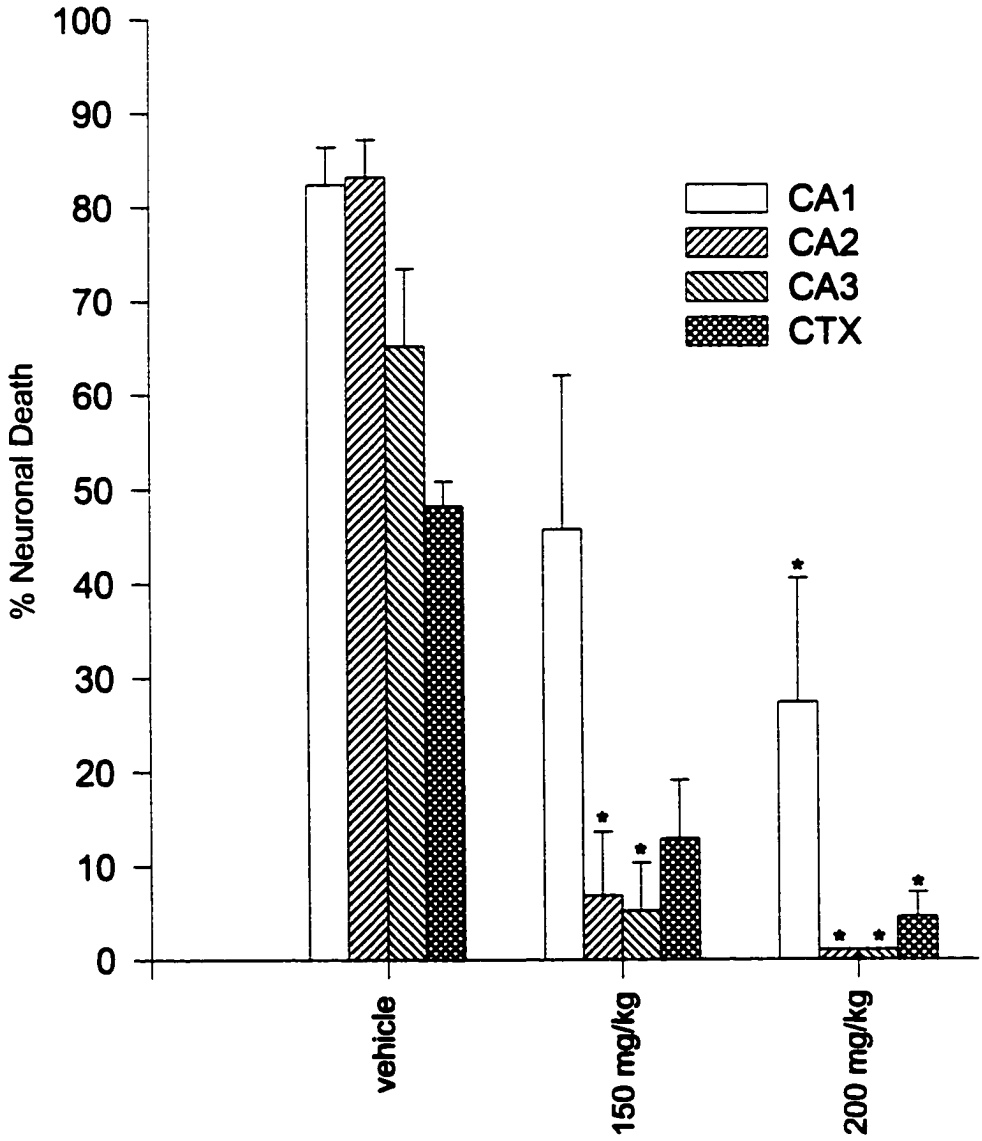
100
90
80
70
60
50
40
30
20
10
0
% Neuronal Death
CA1
CA2
CA3
CTX
vehicle
150 mg/kg
200 mg/kg

Figure 1-5

Rectal Temperatures

At no time did mean rectal temperatures of either vehicle-injected H-I animals or CMZ-injected (200 mg/kg) H-I animals fall below normothermic levels (37°C). However, a slight decrease in rectal temperature (0.3–0.5°C) was observed in CMZ-injected H-I animals relative to vehicle-injected H-I animals following injection. See Figure 1-6.

Adult Animals and H-I Injury

No cell death was evident in any brain region of 5 out of 7 adult male rats that survived the H-I event. However, discrete patches of pyknosis were observed in the medial CA1 region of the ipsilateral hippocampus in 2 of these animals by 7 days post-hypoxia. See Figure 1-7.

Figure 1-6

Graphic illustration of mean rectal temperatures in vehicle-injected and CMZ-injected H-I animals.

Rectal temperatures were monitored every ten minutes following the hypoxic event in both vehicle- and CMZ- (200 mg/kg) injected H-I animals for at least 3 hours post-injection (6 hours post-hypoxia). Mean rectal temperatures of animals in these treatment groups are illustrated graphically for all post-hypoxic timepoints examined. The data are presented as means ± S.E.M.

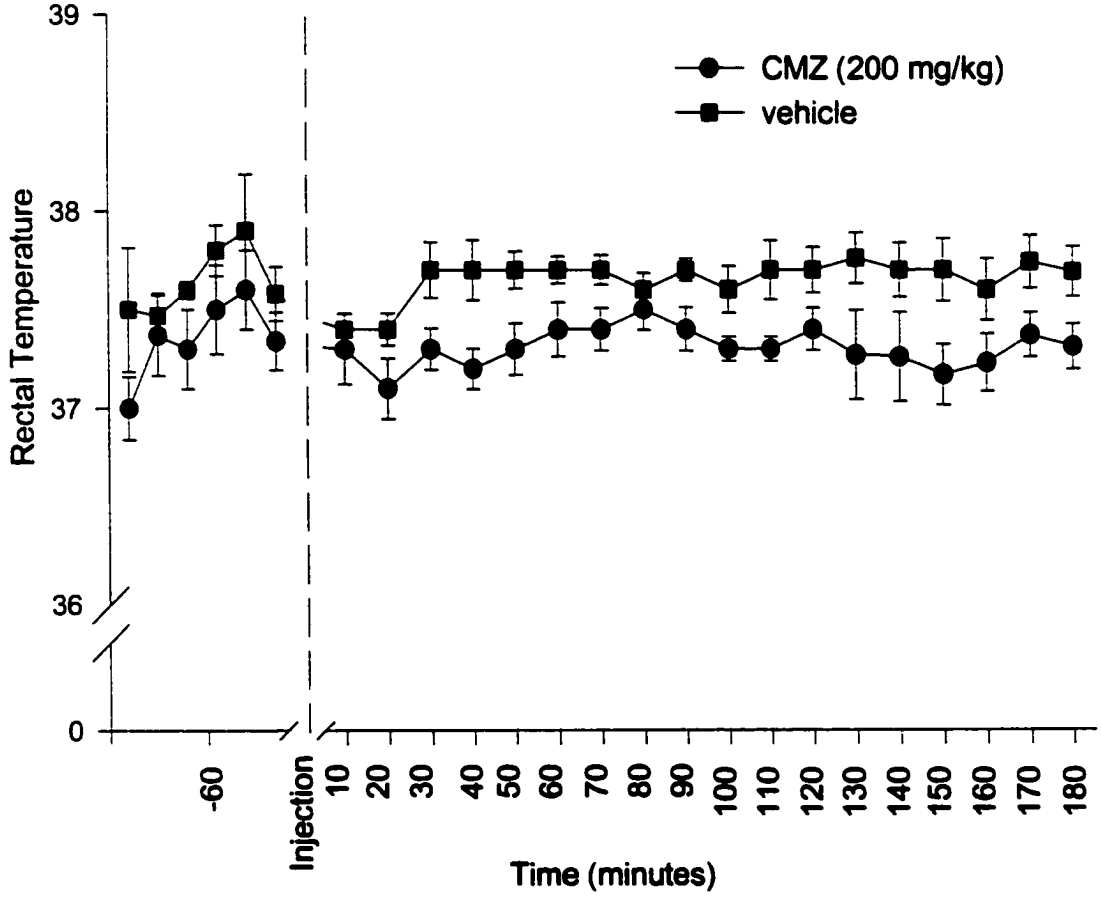
39
38
37
36
0
Rectal Temperature
CMZ (200 mg/kg)
vehicle
-60
Injection
10
20
30
40
50
60
70
80
90
100
110
120
130
140
150
160
170
180
Time (minutes)

Figure 1-6

Figure 1-7

Cresyl violet stained sections from adult rats sacrificed 7 days following H-I.

Cresyl violet analysis was used to detect pyknotic cells in the ipsilateral hippocampus and cortex of adult H-I animals sacrificed 7 days following H-I. Panel A) a representative section from the medial CA1 region of a naive adult rat, Panel B) a representative section from the medial CA1 region of an adult H-I rat, Panel C) a representative section from the parietal cortex of a naïve adult animal, Panel D) a representative section from the parietal cortex of an H-I animal. Areas of pyknosis in H-I animals are indicated by the arrows in Panel B. (Scale bar = 100 μm).

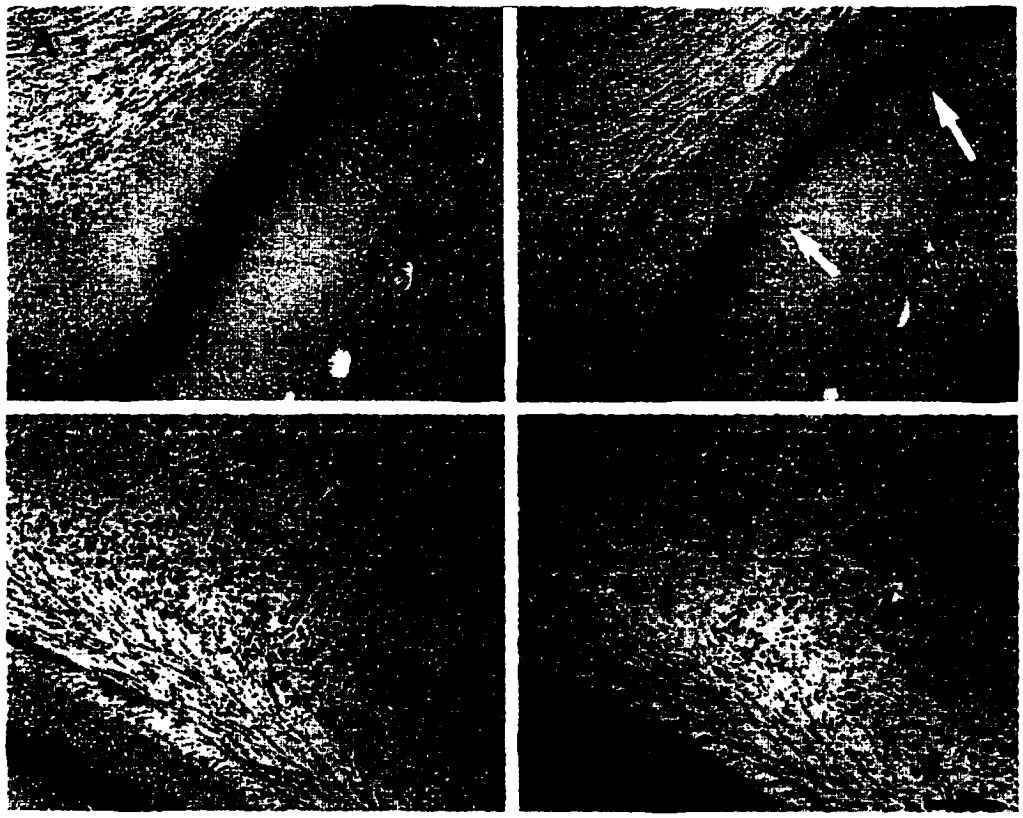

Figure 1-7

Discussion

Analysis of cresyl violet stained sections from PND25 male rats, sacrificed at 1 and 4 weeks post-hypoxia, demonstrated that various doses of CMZ provided substantial neuroprotection against a previous H-I injury. Specifically, significant neuroprotection was observed in H-I animals, sacrificed at 1 week post-hypoxia, when 200 mg/kg was administered at 1, 2 or 3 hours post-hypoxia and when 100 or 150 mg/kg were administered at 3 hours post-hypoxia. Similar results have been reported in a gerbil model of global ischemia where administration of 100 mg/kg CMZ, up to 3 hours post-ischemia, produced a 70% reduction in resultant cell death (Cross *et al.*, 1991). In the present study, administration of 200 mg/kg CMZ at 3 hours post-hypoxia provided almost 100% neuroprotection in all cell layers of the ipsilateral hippocampus and parietal cortex. This profound neuroprotective effect was observed in CMZ-injected H-I animals sacrificed at 1 and 4 weeks post-hypoxia. Thus, the findings of this study strongly suggest that irreversible cellular damage does not occur before 3 hours post-hypoxia in the H-I model of global ischemia.

It is interesting that the therapeutic window for CMZ was limited in this model such that, if the injection of CMZ was delayed to 4 hours post-hypoxia no neuroprotection was evident in any cell layer of animals sacrificed at 7 days post-hypoxia. A similar therapeutic window has been reported for in the gerbil model of global ischemia used by Cross *et al.* (1991) where, despite its efficacy at 3 hours post-ischemia, CMZ (100 mg/kg) did not provide neuroprotection when administered at post-ischemic time-points beyond 3 hours (Cross *et al.*, 1991). Seemingly contradictory findings have been reported by Shuaib *et al.* (1995) where subcutaneous administration of CMZ (100 mg/kg) produced substantial neuroprotection against global ischemia (2-VO) in the gerbil when administered at 4 hours post-ischemia. The discrepancy in the "apparent therapeutic window" for CMZ reported in the present study and by Shuaib *et al.* (1995) may be due to differences in the severity of the initial insult inflicted by the two animal models of ischemia. As judged by histology profiles, the Rice-Vannucci model of H-I appears to produce a more severe injury than does the 2-VO model of ischemia which may permit the delay in the administration of CMZ to be effective in the

2-VO model. Differences in the length of the therapeutic window for any neuroprotecitve compound across various animal models of ischemia may help to define which cellular processes are important to the subsequent development of neuronal death.

In the present study, mean percentage neuronal damage was higher in CA1 when the 200 mg/kg dose of CMZ was administered at 1 or 2 hours post-hypoxia than when the same dose was administered at 3 hours post-hypoxia. This result appears paradoxical since CMZ is thought to behave as a $GABA_A$-modulator which have generally been shown to have superior neuroprotective efficacy when administered prior to or during the ischemic event rather than at delayed post-hypoxic timepoints. However, this finding is in accordance with Shuaib *et al* (1995) who demonstrated that following global ischemia (2-VO) in mongolian gerbils, a superior neuroprotective effect was observed when CMZ (100 mg/kg) was administered at 4 hours rather than 1 hour post-ischemia. The reason for the increased efficacy of CMZ at delayed post-hypoxic time-points in global animal models of ischemia is unclear. One possible explanation may be derived from a study conducted by Grondahl *et al.* (1998) that demonstrated a possible role for chloride in cellular injury during energy deprivation in hippocampal slices. Specifically, Grondahl *et al.* (1998) suggested that while glutamate release is chloride-independent at late-post-hypoxic timepoints, there may be an early chloride-dependent glutamate release immediately following cerebral ischemia. Thus, CMZ-induced potentiation of GABAergic activity at early post-hypoxic timepoints may produce a chloride-dependent increase in glutamate release that partially counteracts is inhibitory effects. Alternatively, the apparent time-dependent effect of CMZ may point to an interaction with a delayed molecular event that is not fully active within the early post-hypoxic timepoints.

It is noteworthy that the time-dependent effects of CMZ reported in the present study and in Shuaib *et al.* (1995) contradict the neuroprotective profile for CMZ reported in focal animal models of ischemia. Specifically, using the pMCAO model of ischemia, CMZ (100 mg/kg) was shown to be neuroprotective when administered at 1, but not 3, hours post-ischemia in Lister rats (Sydserff *et al.*, 1995b). The apparent contradiction in the efficacy of CMZ in these studies is likely the result of differences in the pathophysiology produced by focal versus global animal models of ischemia. In permanent focal ischemia models, cellular changes are almost immediate and ischemic

cells are evident within a few hours after the insult (Sydserff *et al.*, 1995b). Permanent focal ischemia models also involve complete cessation of blood flow to a brain region thus, without the use of vasoactive compounds, an infarct zone is inevitable. This is not true in global ischemia models where there is a severe reduction, but not complete blockage, of blood flow that does not produce obvious cell death until 12 to 24 hours post-hypoxia. This delayed progression in cell death elicited by global ischemia may alter the timepoint at which CMZ administration would be effective in global ischemia models relative to focal ischemia models. Regardless, differences between the neuroprotective profile of CMZ in these models may indicate that there is a critical post-ischemic timepoint at which CMZ is effective and may, therefore, add to the evidence that suggests CMZ interferes with a particular event in the ischemic cascade.

Neuroprotection studies using CMZ have indicated that there may be a critical drug concentration required to produce a neuroprotective effect (Cross *et al.*, 1995; Liang *et al.*, 1997; Thaminy *et al.*, 1997). The results of the present study demonstrate that CMZ, at bolus doses ranging between 100 mg/kg and 200 mg/kg, has a potent neuroprotective effect in the H-I model. This finding is in accordance with several other studies that have reported neuroprotection in a variety of ischemia models using a bolus dose of CMZ, 100 mg/kg (ip) or higher (Cross *et al.*, 1991; Cross *et al.*, 1995; Shuaib *et al.*, 1995; Liang *et al.*, 1997). Since dosages of CMZ below 100 mg/kg were not used in the present study, it remains unclear whether lower doses of CMZ would have provided a significant degree of neuroprotection. A previous study has indicated that intravenous (iv) infusion of CMZ, reaching a constant non-sedative plasma concentration of approximately 10 μM (nmol/ml) for 24 hours, provided complete neuroprotection in Mongolian gerbils following global ischemia (Cross *et al.*, 1995). This finding may indicate that the presence of CMZ at a critical post-ischemic timepoint is more important to its neuroprotective efficacy than the plasma concentration achieved. Further research into the efficacy of a prolonged i.v. infusion of low doses of CMZ is of substantial clinical relevance. Despite the fact that very high plasma concentrations of CMZ are well-tolerated in humans, they are highly sedative and are, therefore, not ideal for use in stroke patients (Scott *et al.*, 1980).

Several different therapeutic interventions have been shown to reduce brain injury

after H-I in the short-term (7 days or less), however, in most neuroprotection studies long-term histological evaluation has not been conducted. In order to rule out the possibility that CMZ merely delayed H-I-induced neurodegeneration in the present study, we conducted long term histological analysis of cell death in CMZ-injected H-I animals. Animals sacrificed at 4 weeks post-hypoxia clearly demonstrated that 200 mg/kg CMZ administered at 3 hours post-hypoxia provided significant neuroprotection in all susceptible cell layers. Following global ischemia, equivalent histological neuroprotection has been observed in Mongolian gerbils sacrificed at 5, 14 and 21 days following ischemia when CMZ (100 mg/kg, ip) was administered at 1 hour post-ischemia (Cross *et al.*, 1995). It is important to note that in the present study, when animals were sacrificed at 4 weeks post-hypoxia, a significant degree of neuroprotection was not evident in CA1 or the parietal cortex of H-I animals that received 150 mg/kg CMZ at 3 hours post-hypoxia. Nevertheless, both 150 and 200 mg/kg of CMZ did produce highly significant neuroprotection in the H-I model when administered at 3 hours post-hypoxia.

Collectively, the results of this study demonstrate that regardless of cell type, location or mode of cell death, an injection of CMZ as late as 3 hours post-hypoxia provided near complete neuroprotection in the H-I model. Originally, CMZ was not developed as a neuroprotective compound to combat ischemia-induced neurodegeneration but as a sedative hypnotic agent for Alzheimer's patients (Green *et al.*, 1998a). Thus, the neuroprotective efficacy of CMZ can not be readily associated with any known pharmacological target for which CMZ was specifically designed (Green *et al.*, 1998a). To date, the exact mechanism through which this agent confers neuroprotection is unknown. In light of experimentation indicating that changes in body temperature can directly affect the degree of neuronal damage in the CNS after ischemic injury, rectal temperatures of H-I animals following CMZ administration were investigated in the present study. Cerebral temperatures were not assessed in this experiment, however, a study conducted by Cross *et al.* (1991) has shown that following CMZ administration in ischemia models, rectal temperatures corresponded with cerebral temperatures measured using a thermocouple probe implanted above the hippocampus (Cross *et al.*, 1991; Schwartz-Bloom *et al.*, 1998). Many studies have reported no change in rectal temperature following CMZ administration in ischemia models (Cross *et al.*,

1991; MacGregor *et al.*, 1997). In this study, continuous monitoring of rectal temperatures for up to 6 hours post-hypoxia (3 hours post-injection) indicated that mean rectal temperatures of CMZ-injected H-I animals did not fall below normothermic levels (37°C) and did not differ from vehicle-injected H-I animals by more than 0.3-0.5°C at any time-point examined. It is unlikely that this slight decrease in rectal temperature was responsible for the profound neuroprotective effects of CMZ observed in this study and likely reflects a difference in activity levels of sedated versus non-sedated animals rather than an effect of the drug. Moreover, a slight decrease in mean rectal temperature was noted in CMZ-injected versus vehicle-injected H-I animals prior to injection. In general, hypothermia studies have indicated that there must be a prolonged drop in body temperature of at least 2°C in order to produce a neuroprotective effect following ischemia (Widmann *et al.*, 1993). Furthermore, studies conducted in rats and gerbils have shown that the neuroprotection produced by 3-12 hours of post-ischemic hypothermia was either reduced or lost by 1-2 months post-ischemia (Colburne and Corbett, 1995; Shuaib *et al.*, 1995). Thus, the findings of the present study extend the evidence demonstrating that the neuroprotective efficacy of CMZ in animal models of ischemia is not attributable to uncontrolled hypothermia (Snape *et al.*, 1993; Green and Cross, 1994b; Shuaib *et al.*, 1995).

CMZ is one of ten classes of neuroprotective agents that have reached Phase III efficacy trials in stroke patients. Other than CMZ, compounds tested include calcium channel antagonists, NMDA antagonists, lubeluzole, CDP choline, the free radical scavenger tirilizad, antiintracellular adhesion molecule-1 (ICAM-1) antibody, GM-1 ganglioside, the sodium channel antagonist fosphenytoin and piricetam (Hickenbottom and Grotta, 1998). Results pertaining to the neuroprotective efficacy of these compounds in the treatment of human stroke patients are mixed. However, results generated using CMZ in human stroke patients have been quite promising. Thus, a better understanding of the mechanism responsible for the profound neuroprotective effects of CMZ in the H-I model may provide important insight into the pathophysiology and treatment of stroke. Moreover, verification of the existence of such a mechanism would increase our understanding of the cell death cascade induced by ischemia and may have important clinical implications in a number of neurological disorders.

A particularly novel finding of this study was the fact that the H-I model produced cell death in the hippocampus of adult rats. One of the most criticized characteristics of the Rice-Vannucci model of H-I for use in stroke research has been that it does not produce cell death in adult animals. Previous studies have reported that the high level of collateral blood flow in adult rats prevents ischemia-induced cell death in the ipsilateral side of the brain following H-I (Vannucci *et al.*, 1999; Vannucci and Vannucci, 1999). While the deleterious effects of H-I in the present study were neither consistent nor of great magnitude, these findings indicate that the H-I animal model may not be limited for use in neonatal or perinatal rats. Further manipulation of the Rice-Vannucci protocol is required in order to determine whether an equivalent amount of cell death can be produced in adult and perinatal rats using the H-I model.

Chapter 2: *An Investigation into the Neuroprotective Effects of a Post-hypoxic Injection of Midazolam or Muscimol*

Summary

There is substantial evidence indicating that CMZ has GABA-potentiating properties at the $GABA_A$ receptor, however, it is not known whether these properties are responsible for its neuroprotective efficacy in animal models of ischemia. In order to address this issue, the present study was conducted to determine whether a post-hypoxic injection of a known $GABA_A$-agonist or modulator, muscimol and midazolam, could provide neuroprotection similar to that observed using CMZ in the H-I model. In previous experiments, CMZ was shown to be highly effective against H-I injury when administered 3 hours following H-I. In the present study, the neuroprotective efficacy of various doses of muscimol and midazolam were, therefore, examined when these compounds were administered (ip) at 3 hours post-hypoxia. PND25 H-I animals received an injection of a vehicle (dH_2O), muscimol (1, 1.5, 2, 2.5, 3, 3.5 or 4 mg/kg) or midazolam (50, 100, 150 or 200 mg/kg) at 3 hours post-hypoxia and were sacrificed 7 days later for histological evaluation. Mean percentage cell death in both the ipsilateral hippocampus and parietal cortex of midazolam and muscimol-injected H-I animals was evaluated through light microscopic analysis of cresyl violet-stained sections and was compared to percentage cell death in CMZ- and vehicle- injected H-I animals. Histological analysis revealed that, regardless of dose, administration of muscimol at 3 hours post-hypoxia did not provide significant neuroprotection in any cell layers known to be susceptible to H-I injury. However, high doses of midazolam (150 or 200 mg/kg) administered at 3 hours post-hypoxia did provide significant protection throughout the ipsilateral hippocampus (CA1, CA2, CA3) and parietal cortex when compared to vehicle-injected H-I animals. It is noteworthy, however, that collective statistical analysis conducted to compare percentage cell death in CMZ-, vehicle and midazolam-injected animals, indicated that the neuroprotective efficacy of midazolam was less than that of CMZ regardless of the dose of CMZ used or whether CMZ was administered at 1, 2 or 3 hours post-hypoxia. The inability of midazolam and muscimol to provide equivalent neuroprotection to that provided by CMZ in this model strongly suggests that the neuroprotective effects of CMZ can not solely be attributed to $GABA_A$-potentiation.

Introduction

Stimulation of GABA receptors has been shown to cause membrane hyperpolarization via increased chloride influx, inhibit cytosolic free radical formation via phospholipase A_2 activation and suppress excessive activity of excitatory neurons (O'Regan *et al.*, 1995; Kahn *et al.*, 1997a; 1997b; Schwartz *et al.*, 1997). As such, it is conceivable that any loss in GABAergic influence following a neurological insult, such as ischemia, may be detrimental to cell viability. While GABAergic neurons appear to be relatively resistant to ischemic damage, a transient decrease in GABAergic neurotransmission has been documented following both focal and global ischemia (Tecoma and Choi, 1989; Johansen *et al.*, 1991; Nitsh *et al.*, 1991; Inglefield *et al.*, 1997). The exact mechanism responsible for the ischemia-induced reduction in GABAergic neurotransmission is presently unclear. However, using ischemic hippocampal slice preparations, Inglefield and Swartz-Bloom (1998) have shown a reduction in the ability of muscimol, a $GABA_A$-agonist, to increase intracellular concentrations of chloride after 20 minutes of reoxygenation which may indicate a decrease in $GABA_A$ receptor sensitivity following ischemia. Thus, it is conceivable that restoration of inhibitory neurotransmission following ischemia, by administration of compounds that potentiate the GABA response, may protect susceptible cells from ischemia-induced neurodegeneration until endogenous inhibitory mechanisms can resume function.

Several cited reports have indicated that administration of positive GABAergic modulators or agonists can have a neuroprotective effect in both focal and global animal models of ischemia (Hallmayer *et al.*, 1985; Araki *et al.*, 1990; Shuaib *et al.*, 1992; 1996; Kanai *et al.*, 1994; Green *et al.*, 1998a). Most studies that have reported a neuroprotective effect for these agents have involved pre-ischemic administration of such compounds as pentobarbitol, diazepam, muscimol and γ-vinyl GABA (Hallmayer *et al.*, 1985; Araki *et al.*, 1990; Shuaib *et al.*, 1992; 1996; Kanai *et al.*, 1994; Green *et al.*, 1998a). There have, however, been a few reported studies that have claimed that post-ischemic administration of certain $GABA_A$-agonists or modulators can be neuroprotective in ischemia models (Lynden and Lonzo, 1994; Marie *et al.*, 1994; Lynden *et al.*, 1997).

When an iv infusion of muscimol was administered to rats and rabbits within 5 minutes after focal cerebral ischemia, histological neuroprotection and functional sparing of susceptible cell layers was evident up to 18 days following the insult (Lyden and Lonzo, 1994). A study that investigated the neuroprotective efficacy of BZDs against transient cerebral ischemia showed neuroprotection when administration of these agents was delayed up to 90 minutes post-ischemia in gerbils (Swartz-Bloom *et al.*, 1998). In addition, Shuaib *et al.* (1996) demonstrated that administration of γ-vinyl GABA, 60 minutes following transient global ischemia in gerbils, produced histological protection that was evident up to 7 days post-ischemia. However, in that study it was also reported that the histological neuroprotection provided by γ-vinyl GABA in that study did not translate into functional sparing of neurons when these animals were subjected to Morris water maze testing. As with any potentially neuroprotective compound used in stroke models, neuroprotective efficacy at delayed post-ischemic timepoints is important to clinical relevance. Thus, further research is needed in order to establish a therapeutic window for $GABA_A$-potentiating compounds in the treatment of stroke and to determine whether these agents are "truly neuroprotective" when administered at delayed post-ischemic time-points.

Since there are several allosteric modulatory sites on the $GABA_A$ receptor, potentiation of $GABA_A$-mediated neurotransmission can be achieved through various pharmacologically distinct mechanisms (Vicini, 1991). For instance, clinically sedative $GABA_A$-modulators, such as benzodiazepines (BZDs) and barbiturates, both act as positive allosteric modulators of $GABA_A$ receptors, yet the manner in which these agents facilitate GABAergic neurotransmission is unique. BZDs bind to specific high affinity sites on the cell membrane, which are separate from but adjacent to the $GABA_A$ receptor. Once bound, BZDs enhance the affinity of $GABA_A$ receptors for GABA and thereby increase the opening frequency of the chloride channel (Study and Barker, 1981; Vincini, 1991). Alternatively, barbiturates bind to a separate site on the $GABA_A$ receptor macromolecule and potentiate GABA-evoked currents by increasing the amount of time the chloride channel remains in its open conformation (Twyman *et al.*, 1989; Vincini, 1991). Nonetheless, compounds from both of these families of $GABA_A$-modulators ultimately hyperpolarize the post-synaptic cell and thereby decrease its excitability. It

has been shown that CMZ is also a positive allosteric modulator of the $GABA_A$ receptor and acts to potentiate the actions of GABA and prolong the opening of the $GABA_A$ receptor associated ion channel (Harrison and Simmonds, 1983; Cross *et al.*, 1989; Moody and Skolnick, 1989). However, neither the exact binding site for CMZ nor the specific receptor subunit configurations with which CMZ interacts are currently known (Green *et al.*, 1998a).

It is conceivable that differences in the pharmacology of specific $GABA_A$-potentiating compounds may affect their neuroprotective profile in animal models of ischemia. Accordingly, Watanabe *et al.* (1999) demonstrated that administration of the highly selective $GABA_A$-agonist, muscimol (2 mg/kg), or the benzodiazepine (BZD), midazolam, 15 minutes prior to two vessel occlusion (2-VO) in gerbils provided significant neuroprotection in both the hippocampus (CA1) and the parietal cortex of these animals. However, in the same study, administration of a barbiturate, pentobarbitol, 15 minutes prior to forebrain ischemia did not provide neuroprotection to susceptible brain regions. In addition, using a model of transient forebrain ischemia in gerbils, Swartz-Bloom *et al.* (1998) demonstrated that administration of the full BZD agonist, diazepam (10 mg/kg; ip), at both 30 and 90 minutes post-ischemia provided protection (70% ± 30%) in the CA1 cell layer of the hippocampus that was evident at 7 and 35 days post-ischemia. Functional analysis of neuroprotection, using an eight arm radial maze, revealed that diazepam administration up to 90 minutes after ischemia also prevented the increase in working memory error normally associated with ischemia in gerbils. In the same study, however, administration of the partial $GABA_A$-agonist, imidazenil (3 mg/kg; ip), provided a similar level of neuroprotection to that provided by diazepam when examined histologically at 7, but not 35, days post-ischemia. In addition, unlike diazepam, administration of imidazenil did not provide functional sparing of CA1 neurons. Similarly, Cross *et al.* (1991) showed that CMZ (100 mg/kg) injection 3 hours following transient forebrain ischemia in gerbils provided substantial protection to susceptible cell layers, however, administration of other GABA-potentiating compounds, including saffan, phenobarbitol (100 mg/kg) and pentobarbitol (30 mg/kg) did not provide significant levels of protection in this paradigm. Such differences, even between compounds that ultimately elicit the same physiological response from cells, illustrate the

difficulty in establishing the exact mechanism of action for a particular drug and suggest that seemingly minor pharmacological differences can result in broad alterations in the neuroprotective profile of an agent. Thus, it may be the manner in which a compound interacts at the $GABA_A$ receptor that is critical to its neuroprotective profile in ischemia models.

Muscimol and Midazolam

Attempts to determine whether a specific receptor interaction is responsible for the physiological effects of a compound has led researchers to strategically compare the effects of known modulators of that receptor to the physiological effects produced by the compound of interest (Cross *et al.*, 1993a; Swartz-Bloom *et al.*, 1998; Watanabe *et al.*, 1999). Thus, the primary objective of the present study was to compare the neuroprotective efficacy of CMZ in the H-I model to that of known $GABA_A$-potentiators, muscimol and midazolam. In this way, the role of GABA-potentiation in the profound neuroprotective effects of CMZ in the H-I model could be determined.

Muscimol, an alkaloid derived from mushrooms, is well studied as an anticonvulsant and is highly specific to bicuculline-sensitive, strychnine-insensitive post-synaptic receptors in the mammalian nervous system (Hill *et al.*, 1981). Muscimol is unusually potent at the $GABA_A$ receptor, having an affinity 10 times that of GABA for the same receptor and a site of action that is likely distinct from other sedative and hypnotic GABAergic compounds. One of the first indications that muscimol may be of some neuroprotective benefit against an excitotoxic insult, such as ischemia, was the finding that muscimol could depress spontaneous firing of pyramidal cells in rabbit hippocampus (Defrance *et al.*, 1979). Since that publication, studies have reported some degree of neuroprotection using muscimol in a variety of excitotoxic animal models. Long term intracerebralventricular (ICV) infusion of muscimol (10 ng/μl), initiated within 1-2 hours and lasting 15 days after an injection of the excitotoxin ibotenic acid (IBO) into the substantia nigra pars reticulata (SNpr), provided complete protection against the delayed neuronal death normally seen in control rats (Saji and Reis, 1987). Shuaib *et al* (1993) demonstrated that ICV infusion of muscimol (20 ng/μl) over a 7 day period, beginning just prior to repetitive 2 minute periods of ischemia, provided

neuroprotection to all cell layers in rat brain susceptible to excitotoxic injury (CA1, CA3, substantia nigra, striatum and thalamus). Interest in muscimol for use in the present study was ignited by evidence that suggested muscimol may have a similar neuroprotective profile to CMZ. Co-administration of muscimol and MK 801 has been shown to provide a higher degree of neuroprotection in susceptible cell layers following focal cerebral ischemia than monotherapy with either drug (Lyden and Lonzo, 1994). Similarly, co-administration of CMZ and MK 801 proved to be more neuroprotective in a model of kainate-induced neurotoxicity than monotherapy with either drug (MacGregor *et al.*, 1997). In addition, neither muscimol nor CMZ require the presence of endogenous GABA in order to provide neuroprotection in animal models of ischemia (Harrison and Simmonds, 1983; Hales and Lambert, 1992; Anderson *et al.*, 1993). This is not true for other families of $GABA_A$-modulators such as BZDs and barbiturates (Green *et al.*, 1998a).

Since 1965, BZDs have been used to terminate seizure activity in animals and humans (Gastaut *et al.*, 1965; Davidson, 1983; Deshmukh *et al.*, 1986). In general, BZDs have a reasonably rapid onset of action that has traditionally made them an attractive alternative to barbiturates and anesthetic agents in the control of excessive excitatory neurotransmission in the clinic. Information regarding the use of BZDs in ischemia models is limited, however, there is some evidence that administration of BZDs such as diazepam, imidazenil and midazolam, before and after an ischemic event, can provide neuroprotection in animal models of ischemia (Swartz-Bloom *et al.*, 1998; Watanabe *et al.*, 1999). There is also evidence that suggests BZDs may be a better alternative than barbiturates in the treatment of ischemia. Administration of midazolam (50 mg/kg) 15 minutes prior to 2-VO in gerbils provided neuroprotection in CA1, the parietal cortex and the lateral thalamus whereas administration of pentobarbitol (50 mg/kg) at the same timepoint did not provide any neuroprotection in the 2-VO model (Ito *et al.*, 1999).

CMZ administration has been shown to potentiate [^{3}H] muscimol but not [^{3}H] diazepam binding (Leeb-Lundberg *et al.*, 1981; Harrison and Simmonds, 1983; Cross *et al.*, 1989). This finding suggests that while CMZ and muscimol are likely to have different pharmacological profiles, the pharmacology of CMZ and BZDs may be similar at the $GABA_A$ receptor. Midazolam is a water-soluble 1,4, benzodiazepine and exhibits

numerous properties that are characteristic of BZDs, *ie*, it is hypnotic and has both anti-anxiety and muscle-relaxant properties (Jaimovich *et al.*, 1990). In addition, like CMZ, midazolam has a very short half-life (approximately 1.3-2.2 hours) in relation to other benzodiazepines such as diazepam ($t_{1/2}$ = 30) (Cross *et al.*, 1995; Green *et al.*, 1998a). Also, like CMZ, midazolam has a large margin of safety compared to other benzodiazepines and has demonstrated a similar solubility profile to CMZ (Jaimovich *et al.*, 1990). Thus, the neuroprotective effect of midazolam against H-I injury was investigated in this study.

Methods

Animals

Male Sprague-Dawley rats were purchased from Charles River Canada (Lasalle, Quebec). The animals were treated in accordance with the guidelines set by the Canadian Council on Animal Care. Animals were housed in groups of 3-11 in the Dalhousie Animal Care Facility and maintained on a 12:12 h dark-light cycle with *ad libitum* access to both food (Purina rat chow) and water. On PND25, rats (50-60 g) were randomly assigned to treatment groups.

H-I animals

The H-I protocol used in this study was identical to the protocol outlined in Chapter 1. Following the hypoxic event, one group of H-I animals received an ip injection of either vehicle (dH_2O) or one of varying doses of muscimol (1, 1.5, 2, 2.5, 3, 3.5 and 4 mg/kg) at 3 hours post-hypoxia. A second group of animals received either a vehicle injection (ip) or one of many doses of midazolam (50, 100, 150 or 200 mg/kg) at 3 hours post-hypoxia. Due to excessive sedation, the maximal dose of midazolam used in this study was 200 mg/kg. Some animals served as drug-injected controls and received between 2-4 mg/kg muscimol or between 100-200 mg/kg midazolam but did not undergo H-I. While animals that exhibited post-hypoxic seizure activity were generally removed from the study, animals that seized as a result of a high dose of muscimol (3-4 mg/kg) at 3 hours post-hypoxia were not excluded from the study. In order to determine whether hypothermia was induced in H-I animals by high doses of muscimol or midazolam, rectal temperature was monitored in H-I animals that received either 200 mg/kg midazolam or 2 mg/kg muscimol every 10 minutes for at least 90 minutes post-injection (4.5 hours post-hypoxia).

Drugs

Muscimol hydrobromide ($C_4H_6N_2O_2 \bullet HBr$) was obtained from Research Biochemicals International (RBI). Midazolam maleate (8-chloro-6- (2-flurophenyl)-1-methyl–4H–imidazol [1,5-α] [1,4] benzodiazepine) was obtained from Roche (Lot # 0403004).

Assessment of Neuroprotection

Animals were sacrificed 7 days following their various treatments. Each rat was deeply anesthetized with 65 mg/kg of sodium pentobarbitol and was then perfused through the ascending aorta with 0.9% saline (60 ml) followed by cold 100 mM phosphate buffer containing 4 % paraformaldehyde (60 ml). Brains were removed and post-fixed in 100 mM phosphate buffer containing 4% paraformaldehyde at 4°C for at least 24 hours prior to sectioning and staining with cresyl violet. The protocol used for histology is outlined in Chapter 1. The method of quantitation of cell death and statistical analysis used in this study was identical to the protocol outlined in Chapter 1.

Results

General Behavior

Both muscimol and midazolam produced sedation in H-I and naïve rats, however, muscimol appeared to be less sedative than either midazolam or CMZ. High doses of muscimol (3.5- 4 mg/kg) induced tonic seizures in both H-I and naïve rats within 30 minutes of injection. Seventy percent of H-I animals injected with 3.5 or 4 mg/kg of muscimol died within 1 hour of the injection.

Muscimol

Statistical analysis, using the Kruskall-Wallis ANOVA on Ranks ($H=59.726$; $DF=12$; $P< 0.001$) revealed that regardless of dosage, 1 ($N = 8$), 1.5 ($N = 7$), 2 ($N = 8$), 2.5 ($N = 6$), 3 ($N = 6$), 3.5 ($N = 5$) or 4 mg/kg ($N = 3$), muscimol administration at 3 hours post-hypoxia did not provide significant neuroprotection in susceptible hippocampal cell layers (CA1, CA2, CA3) of H-I animals when compared to vehicle-injected H-I animals. See Figure 2-1 and Figure 2-2. Similarly, no neuroprotection was evident in the ipsilateral parietal cortex of H-I animals regardless of the dosage of muscimol injected. A significant difference ($H = 31.146$; $DF = 6$; $P<0.001$) was observed between the mean percentage neuronal damage in CA1 ($Q = 4.645$; $P<0.05$), CA2 ($Q = 3.062$; $P<0.05$), CA3 ($Q = 4.067$; $P<0.05$) and the parietal cortex ($Q = 3.247$; $P<0.05$) of muscimol-injected naïve animals (no H-I) when compared to vehicle-injected H-I animals. However, the mean percent neuronal damage in the parietal cortex of muscimol-injected naïve animals was 5.6%, not zero as it was in midazolam and CMZ-injected naïve animals.

Midazolam

As in CMZ-injected naïve animals, no cell death was evident in midazolam-injected naïve animals. When compared to vehicle-injected H-I animals, statistical analysis ($H=31.146$; $DF = 4$; $P<0.001$) revealed significant neuroprotection in CA1 cells of H-I animals that received 100 ($Q = 3.308$; $P<0.05$; $N = 7$), 150 ($Q = 3.008$; $P<0.05$; $N = 8$) or 200 mg/kg ($Q = 3.157$; $P<0.05$; $N = 9$) midazolam at 3 hours post-hypoxia.

Figure 2-1

Cresyl violet analysis of H-I animals that received an injection of muscimol at 3 hours post-hypoxia.

This figure contains photomicrographic representation of cresyl violet-stained hippocampal sections from H-I animals that received a vehicle injection (B) or 1.0 mg/kg (C), 1.5 mg/kg (D), 2.0 mg/kg (E) or 2.5 mg/kg (F) muscimol at 3 hours post-hypoxia. Panel A contains a photomicrograph of a cresyl violet-stained hippocampal section from the contralateral hippocampus of an H-I animal that received 2 mg/kg muscimol. All animals were sacrificed at 7 days post-hypoxia. (Scale bar = 400 μm).

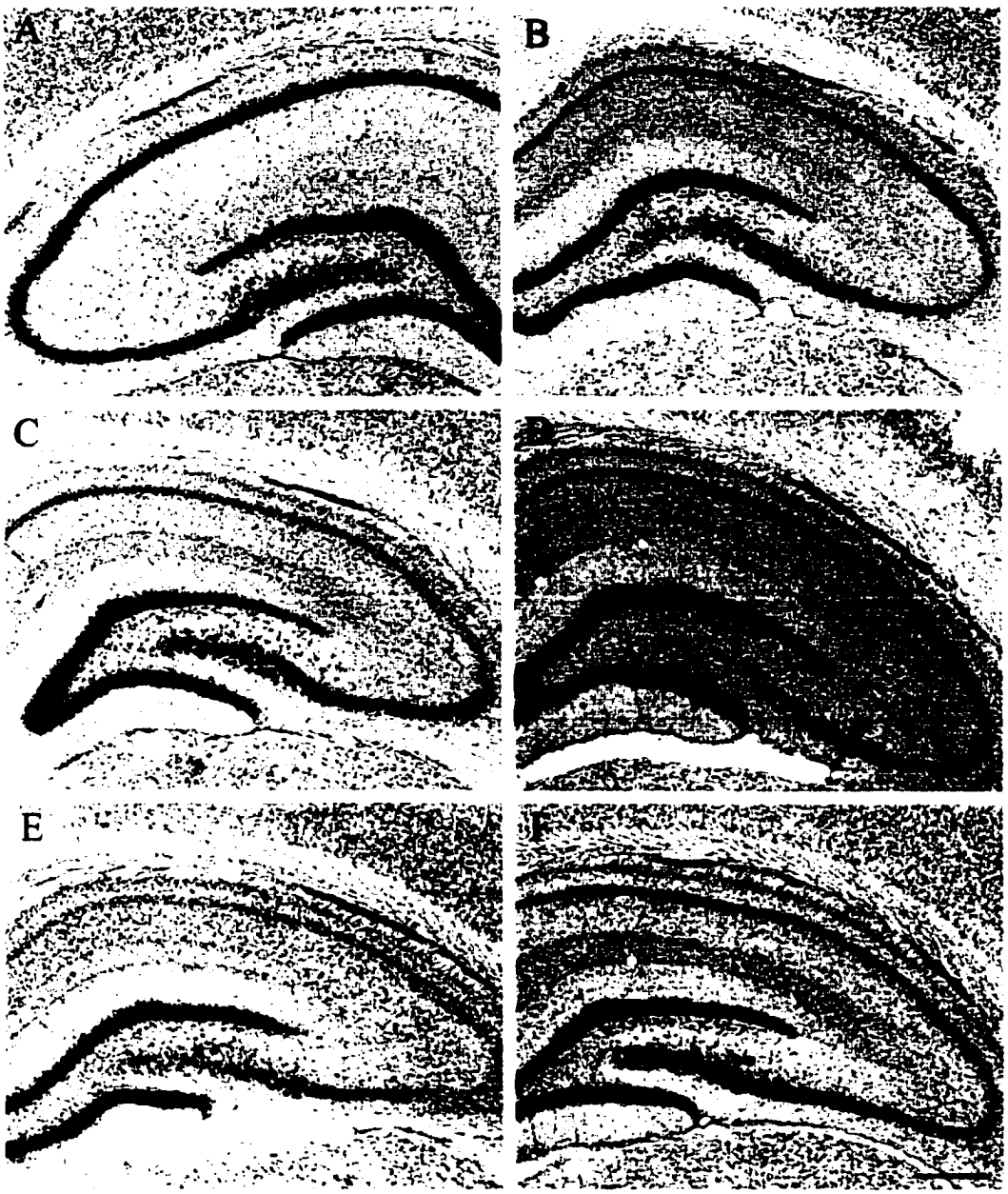

Figure 2-1

Figure 2-2

Graphic illustration of the neuroprotective effect of muscimol in the H-I model.

Mean percentage neuronal death is provided from all susceptible cell layers (CA1, CA2, CA3 and parietal cortex) of vehicle-injected, CMZ (200 mg/kg)-injected and muscimol (1, 1.5, 2, 2.5 and 3 mg/kg)-injected H-I animals. All animals were injected with one of the compounds at 3 hours post-hypoxia and were sacrificed at 7 days post-hypoxia. A P value of <0.05 was considered to be statistically significant. The data are presented as means ± S.E.M. (* = significantly different from the same cell layer in vehicle-injected H-I animals).

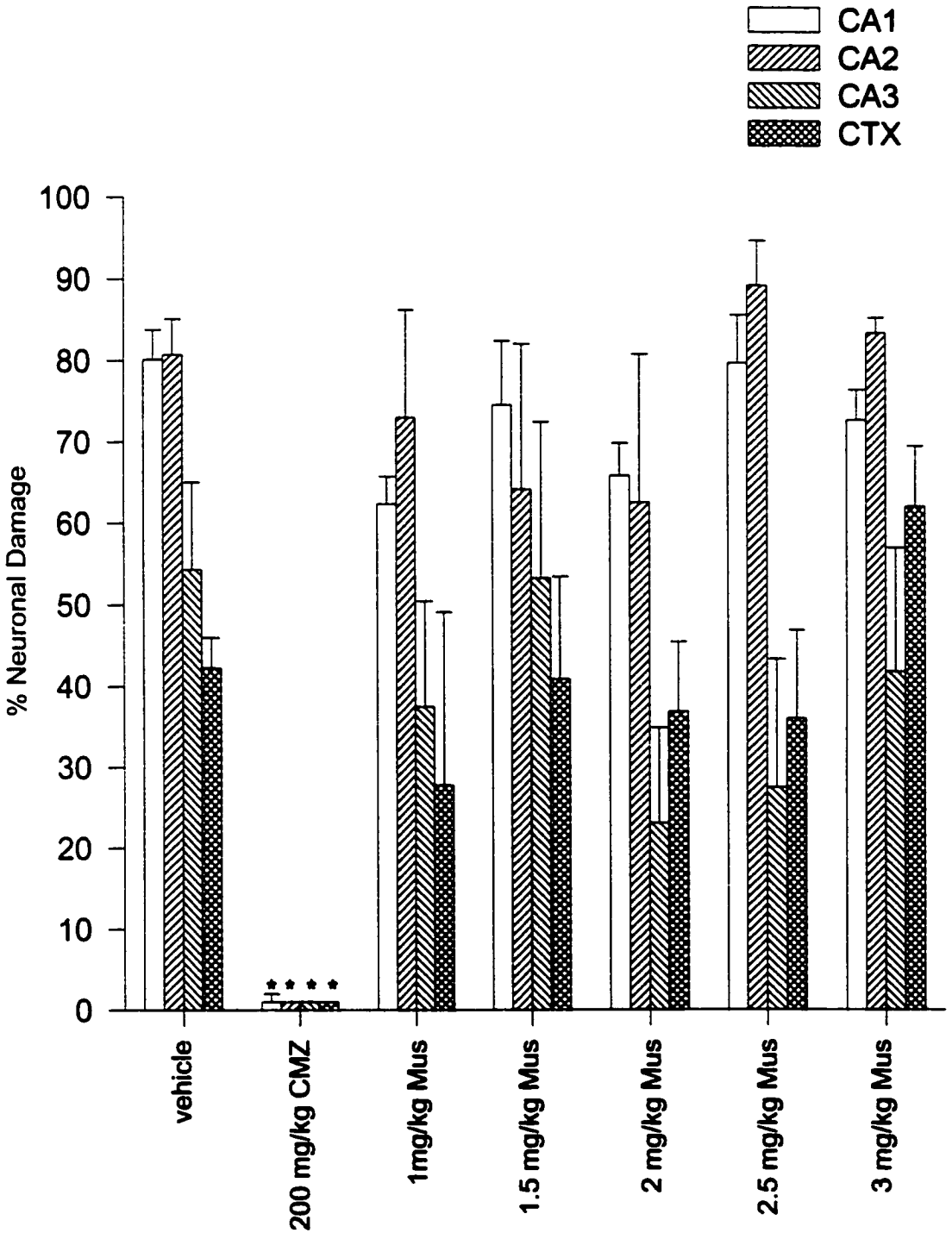
CA1
CA2
CA3
CTX
% Neuronal Damage
100
90
80
70
60
50
40
30
20
10
0
vehicle
200 mg/kg CMZ
1mg/kg Mus
1.5 mg/kg Mus
2 mg/kg Mus
2.5 mg/kg Mus
3 mg/kg Mus

Figure 2-2

Significant ($H = 20.842$; $DF = 4$; $P<0.001$) neuroprotection was also evident in the CA2 cell layer of H-I animals that received post-hypoxic injections (3 hours) of 150 ($Q = 3.457$; $P<0.05$) and 200 mg/kg ($Q = 3.185$; $P<0.05$) midazolam when compared to vehicle-injected H-I animals. Similarly, a statistically significant ($H = 18.665$; $DF = 4$; $P<0.001$) degree of neuroprotection was evident in CA3 of H-I animals that received either 150 ($Q = 3.245$; $P<0.05$) or 200 mg/kg ($Q = 3.726$; $P<0.05$) midazolam at 3 hours post-hypoxia. Finally, statistical analysis ($H = 19.557$; $DF = 4$; $P<0.001$) revealed that both 150 ($Q = 3.474$; $P<0.05$) and 200 mg/kg ($Q = 3.992$; $P<0.05$) midazolam provided neuroprotection in the parietal cortex of H-I animals when compared to vehicle-injected H-I animals. Neuroprotection was not evident in any cell layer of H-I animals that received 50 mg/kg midazolam at 3 hours post-hypoxia. See Figure 2-3.

In order to compare the neuroprotective effect of CMZ and midazolam in this model, collective statistical analysis was conducted on vehicle-injected, CMZ-injected (100, 150 and 200 mg/kg at 1, 2, 3 and 4 hours post-hypoxia) and midazolam-injected (50, 100, 150 and 200 mg/kg at 3 hours post-hypoxia) H-I animals. When ranked against CMZ-injected H-I animals the neuroprotection provided by 150 and 200 mg/kg midazolam was no longer significant in CA1 or CA2 of the ipsilateral hippocampus. However, the neuroprotective effect of 200 mg/kg midazolam remained significant ($Q = 3.154$; $P<0.05$) in CA3 when compared to CMZ-injected H-I animals ($H = 116.743$; $DF = 19$; $P<0.001$). Similarly, statistical significance ($H = 118.126$; $DF = 19$; $P<0.001$) was still evident in the parietal cortex of H-I animals that received 150 ($Q = 2.744$; $P<0.05$) and 200 ($Q = 3.263$; $P<0.05$) mg/kg of midazolam at 3 hours post-hypoxia.

Rectal Temperatures

At no timepoint examined did mean rectal temperatures of either midazolam (200 mg/kg) or muscimol-injected (2 mg/kg) H-I animals fall below 36°C. However, a slight decrease in rectal temperature was observed in both midazolam- and muscimol-injected animals relative to either CMZ-injected or vehicle-injected H-I animals by 10 minutes following the injections. By 80 minutes post-injection, rectal temperatures in both muscimol- and midazolam-injected animals had returned to normothermic levels. See Figure 2-4.

Figure 2-3

Graphic illustration of the neuroprotective effect of midazolam in the H-I model.

Mean percentage neuronal death is provided for all susceptible cell layers (CA1, CA2, CA3 and parietal cortex) of vehicle-injected, CMZ (200 mg/kg)-injected and midazolam (50, 100, 150 and 200 mg/kg)-injected H-I animals. All animals received an injection of one of these agents at 3 hours post-hypoxia and were sacrificed at 7 days post-hypoxia. A P value of <0.05 was considered to be statistically significant. The data are presented as means ± S.E.M. (* = significantly different from the same cell layer in vehicle-injected H-I animals).

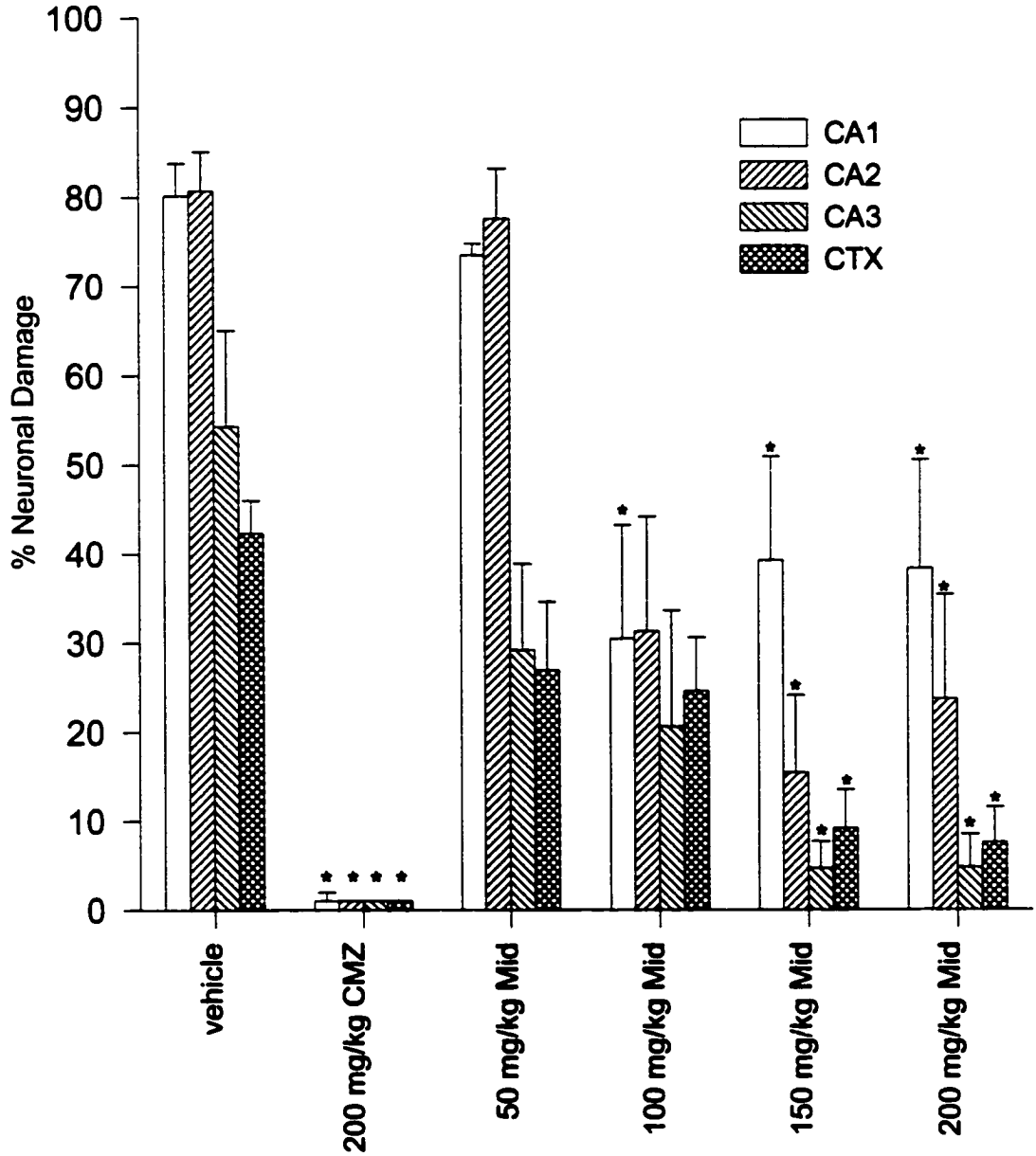
100
90
80
70
60
50
40
30
20
10
0
% Neuronal Damage
CA1
CA2
CA3
CTX
vehicle
200 mg/kg CMZ
50 mg/kg Mid
100 mg/kg Mid
150 mg/kg Mid
200 mg/kg Mid

Figure 2-3

Figure 2-4

Graphic illustration of mean rectal temperatures following midazolam or muscimol injection in H-I animals.

Mean rectal temperatures are provided for vehicle-injected, CMZ-injected (200 mg/kg), midazolam (200 mg/kg)-injected and muscimol (2 mg/kg)-injected H-I animals. Rectal temperature readings for all animal treatment groups were recorded every 10 minutes following injection of the various compounds up to 1.5 hours post-injection. The data are presented as means ± S.E.M.

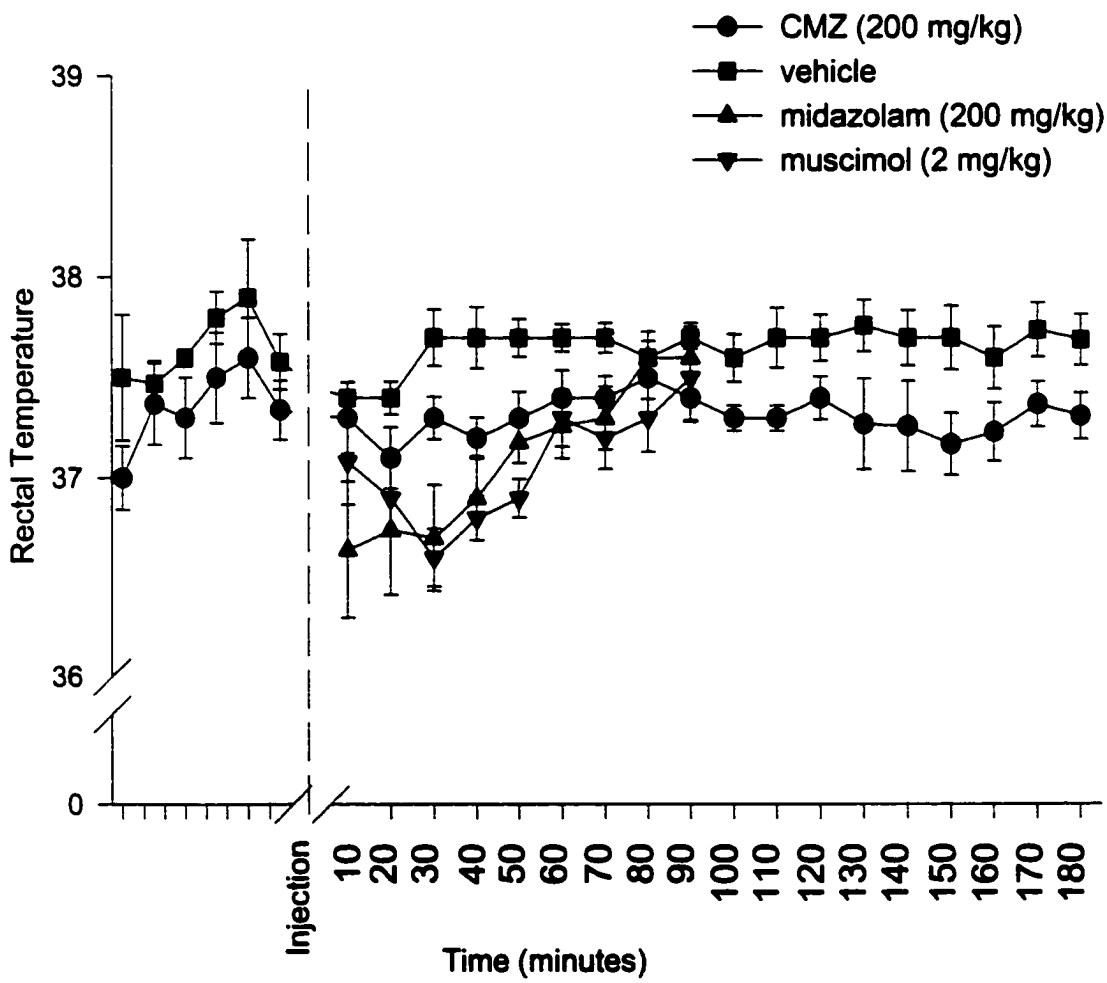
CMZ (200 mg/kg)
vehicle
midazolam (200 mg/kg)
muscimol (2 mg/kg)
Rectal Temperature
39
38
37
36
0
Injection
10
20
30
40
50
60
70
80
90
100
110
120
130
140
150
160
170
180
Time (minutes)

Figure 2-4

Discussion

The results of this study have shown that neither midazolam nor muscimol provided neuroprotection in the H-I model that was comparable to that produced by CMZ when administered 3 hours post-hypoxia. Muscimol was unable to provide any significant reduction in neuronal damage when administered at 3 hours post-hypoxia. This finding is not surprising since previous studies that have reported muscimol-induced neuroprotection in ischemia models administered muscimol prior to the ischemic insult or through a constant iv infusion that lasted 7-15 days post-ischemia (Saji and Reis, 1987; Shuaib *et al.*, 1993; Lyden and Lonzo, 1994). Moreover, a study conducted by MacGregor *et al.* (1997) demonstrated that both CMZ and muscimol were able to attenuate kainate-induced neuronal death (MacGregor *et al.*, 1997). In that study, CMZ (3.6 mg/kg) administration also reduced mean [^{3}H]-PK11195 binding to glia, which serves as an indicator of gliosis, by 33% and muscimol (27 μg/kg) decreased mean [^{3}H]-PK11195 binding by 22% following kainic acid administration. Thus, muscimol and CMZ appeared to provide near equivalent neuroprotection in a model of kainate-induced excitotoxicity. It should be noted, however, that co-administration of these agents resulted in a 73% decrease in mean [^{3}H]-PK11195 binding which suggests that the neuroprotective effects of these compounds were additive in this model. Thus, even though CMZ and muscimol both potentiate $GABA_A$-mediated activity and produce a similar neuroprotective effect in the kainate model, these compounds appear to exhibit different pharmacological effects in excitotoxic animal models.

Administration of muscimol in the present study produced a seemingly paradoxical effect. High doses of muscimol induced tonic seizures in both H-I and naïve animals in spite of the fact that muscimol is a potent $GABA_A$-agonist. In addition, a small amount of pyknosis was observed in the parietal cortex of muscimol-injected control animals that received between 3-4 mg/kg. These findings are in accordance with studies that have shown that some $GABA_A$-agonists, including muscimol, actually potentiate epileptiform activity in the CNS (Scotti di Carolis and Massotti, 1978; King *et al.*, 1979; Pedley *et al.*, 1979; Vergnes *et al.*, 1984; Chesnut and Swann, 1989). While prolonged ICV infusion of muscimol (10 ng/μl), beginning 1-2 hours after an injection of

ibotenic acid (IBO) and lasting 15 days post-injection, has been shown to provide neuroprotection in the SNpr, infusion of high doses of muscimol (100 ng/μl) were neurotoxic in both IBO-injected and sham-operated animals (Saji and Reis, 1987). An increase in the development of epileptiform activity following administration of compounds that potentiate GABAergic activity has also been observed in the clinical setting where use of progabide, in children, has resulted in increased seizure activity (Viani and Romeo, 1984; Dulac *et al.*, 1985). Clearly, the seizure-inducing properties of muscimol may underlie the lack of neuroprotective efficacy for this compound in the H-I model.

An alternate explanation for the inability of muscimol to provide any neuroprotection in the H-I model, despite its success in other excitotoxic animal models, may be that animals used in this study were only 25 days old. It has been shown that GABAergic neurotransmission does not function at maximum capacity by PND25 in rodents (Swann *et al.*, 1987; Kapur and MacDonald, 1998). The kinetic properties of GABA-mediated inhibitory post-synaptic potentials (IPSPs) continue to develop up to PND60 in the dentate granule cells of the hippocampus (Kapur and MacDonald, 1998). While a substantial increase in the density of GABA receptors and maximal chloride current has been documented between PND10 and PND 28, an additional enhancement of the maximal chloride current has also been observed between PND 28 and PND 52 (Swann *et al.*, 1987; Kapur and MacDonald, 1998). Since the cytosolic chloride dynamic strongly interferes with the calcium cascade in neuronal systems, differences in maximal chloride currents existing between PND25 animals and adults may account for the inability of muscimol to provide neuroprotection in this particular model. However, if this explanation is valid then these studies would also imply that the neuroprotective efficacy of CMZ in this model can not be attributed to increased GABAergic neurotransmission.

Midazolam and The Rice-Vannucci Model of H-I

When administered at 3 hours post-hypoxia, high doses of midazolam (150 and 200 mg/kg) provided significant protection in all susceptible cell layers of the ipsilateral hippocampus and parietal cortex following H-I. This finding is in accordance with existing evidence that has reported a neuroprotective effect for midazolam, and other BZDs, in excitotoxic animal models (Jaimovich *et al.*, 1990; Kochhar *et al.*, 1991; Swartz-Bloom *et al.*, 1998; Watanabe *et al.*, 1999). As with muscimol, previous studies that have reported neuroprotective efficacy for BZDs in excitotoxic animal models have generally used a timepoint of administration that was either prior to or within 60 seconds of the insult. A study conducted by Swartz-Bloom *et al.* (1998), however, did show that administration of diazepam (10 mg/kg) up to 90 minutes following transient cerebral ischemia in gerbils provided neuroprotection (70% ± 30%) in the CA1 pyramidal cell layer of the hippocampus. Thus, our results using midazolam in the H-I model are in general agreement with those of Swartz-Bloom *et al.* (1998). It is also noteworthy that the neuroprotection provided by diazepam in the transient cerebral ischemia model was evident up to 35 days post-ischemia. However, in this study, cresyl violet analysis was not conducted on animals sacrificed beyond 1 week post-hypoxia, therefore, the possibility that high doses of midazolam may have only attenuated ischemia-induced cell death can not be ruled out.

While the doses of muscimol used in this study produced substantial sedation, the level of sedation appeared to be less than that produced by CMZ or midazolam. It is, therefore, possible that differences in levels of post-ischemic sedation may play a role in the different neuroprotective profiles of these compounds in the H-I model. However, a study conducted by Cross *et al.*, (1995) has shown that the neuroprotective effect of CMZ was not diminished when non-sedative doses of this compound were administered following global ischemia in gerbils.

In the present study, midazolam produced a slight decrease in rectal temperature, although rectal temperature never fell below 36°C and had returned to baseline levels by 80 minutes post-injection. Since midazolam and muscimol produced a similar drop in temperature it is unlikely that the neuroprotective effect of midazolam is due to a hypothermic effect. In addition, midazolam administration caused rectal temperatures to

drop below those observed in CMZ-injected animals and therefore demonstrate that the increased neuroprotective efficacy of CMZ can not be attributed to uncontrolled hypothermia.

Collective statistical analysis of mean percentage neuronal damage in CMZ, midazolam and vehicle-injected H-I animals masked the neuroprotective effect of midazolam in this model. This finding indicates that the neuroprotective efficacy of midazolam was marginally less than that of CMZ. A possible explanation for the fact that high doses of midazolam provided only partial neuroprotection relies on the assumption that there is a component of ischemia-induced cell death that is attributable to sub-convulsive epileptiform activity. Considerable evidence has indicated that midazolam has substantial anti-convulsant activity. Jaimovich *et al.* (1990) demonstrated that an iv infusion of midazolam (0.1 mg/kg) completely ablated ictal activity following administration of PTZ (100 mg/kg) in swine. Moreover, like other BZDs, midazolam has proven effective as an iv agent for seizure control in humans (Jawad *et al.*, 1986; Galvin and Jelinek, 1987). As such, the superior neuroprotective efficacy of CMZ relative to midazolam may be due to the ability of CMZ to both inhibit post-ischemic epileptiform activity and interfere with other ischemia-induced events whereas midazolam may only interfere with post-ischemic epileptiform activity. This explanation may also help to explain the superior efficacy of midazolam relative to muscimol in this model, since administration of muscimol appears to potentiate post-ischemic epileptiform activity. Substantial differences in the anti-convulsant profiles of $GABA_A$-agonists have been reported. For instance, Zhang *et al.* (1989) showed that microinjections of a wide dose-range of GABA and muscimol into the SN did not inhibit PTZ-induced seizure activity whereas microinjections of midazolam, and other BZDs, produced a clear, dose-dependent inhibition of PTZ-induced seizure activity when infused into the SN. An investigation into whether co-administration of CMZ and midazolam would produce an additive neuroprotective effect following H-I may help to determine whether these two compounds act through different mechanisms to produce neuroprotection in animal models of ischemia.

In conclusion, while there is clear evidence that CMZ does exhibit $GABA_A$-potentiating properties, behavioral and histological differences were observed between

H-I animals that received CMZ, midazolam and muscimol. The differences in the efficacy of these compounds following H-I may suggest that subtle differences in the way these compounds bind to the $GABA_A$ receptor macromolecule and in the specific subunit configurations with which they interact actually dictate the level of neuroprotection achieved in animal models of ischemia. An example of the diverse physiological effects of $GABA_A$-potentiators was observed in prepared membranes from rat cerebellum and in HEK cells transfected with α_1, β_3 and δ_2 subunits of the $GABA_A$ receptor wherein CMZ administration profoundly inhibited [^{3}H]-flunitrazepam binding (IC_{50} = 1.4 mM and 1.8 mM respectively). In contrast, even at low concentrations administration of pentobarbitone stimulated [^{3}H]-flunitrazepam binding in transfected HEK cells (Cross *et al.*, 1989; Green *et al.*, 1996; Zhong and Simmonds; 1997; Green *et al.*, 1998a).

There is, however, evidence that may indicate that the neuroprotective efficacy of CMZ in this model is not attributable to its $GABA_A$-potentiating properties. First, the fact that the highly specific and most potent $GABA_A$-agonist used in this study had no neuroprotective effect appears to suggest that a non-GABAergic mechanism is responsible for CMZ-induced neuroprotection. Interestingly, Delorey *et al.* (1993) demonstrated that combinations of BZDs (midazolam and diazepam) with barbiturates (phenobarbitone and pentobarbitone) produced synergistic hypnotic interactions in rodents. Yet, combinative administration of BZDs and barbiturates enhanced [^{3}H]-muscimol binding but did not enhance muscimol-stimulated chloride ion flux suggesting that non-GABAergic mechanisms were involved in the synergistic effects of these compounds. Second, several studies have shown a dramatic decrease in both the density of $GABA_A$ receptors and the mRNA for the α_1 subunit of the $GABA_A$ receptor between 1-4 hours following focal and global ischemia (Baldwin *et al.*, 1993; Li *et al.*, 1993; Qu *et al.*, 1998). Thus, administration of $GABA_A$-agonists during these post-ischemic timepoints may be futile and may also explain why muscimol is not neuroprotective when administered at delayed post-hypoxic time-points in animal models of ischemia. It should be noted that by 4 hours post-hypoxia, when $GABA_A$ receptor density is just beginning to return to normal, even the highest dose of CMZ did not have a neuroprotective effect in the H-I model. Finally, while numerous studies have shown CMZ to be a superior neuroprotective agent relative to other $GABA_A$-agonists in animal

models of excitotoxicity the reverse has not been documented. Collectively, these findings are highly indicative of an additive or alternate mechanism of action for CMZ that may account for its increased efficacy relative to other $GABA_A$-potentiating compounds in animal models of ischemia.

Part II

An investigation into mechanisms responsible for CMZ-induced neuroprotection in the H-I model

The response of the brain to ischemic insult appears to involve a balance between the activation of endogenous neuroprotective mechanisms and the initiation of a series of destructive changes that lead to cell death. The implementation of these opposing processes following cellular stressors is regulated through the activation of specific genetic programs. On the one hand, increased expression of some genes may limit cell loss and activate repair mechanisms to aid in cellular recovery. Alternatively, coordinated expression of "death-associated" genes may be ignited and play an active role in promoting neuronal demise.

CMZ has been shown to provide near 100% neuroprotection in the H-I model when administered at 3 hours post-hypoxia. It has also been demonstrated that these neuroprotective effects are probably not the result of the GABAergic properties of this compound or the induction of hypothermia. Thus, the exact mechanism through which CMZ provided neuroprotection in the H-I model, and in other animal models of ischemia, is currently unknown. The fact that CMZ was effective when administered after the ischemic injury suggests that the drug may interfere with delayed molecular events that ultimately determine cell fate following H-I. It is, therefore, important to determine whether CMZ facilitates constitutive neuroprotective mechanisms or actively interferes with "cell death-inducing" events following H-I. The following section details a number of molecular experiments designed to identify and characterize differences in gene expression between vehicle-injected H-I animals and H-I animals that have received a bolus dose of CMZ (200 mg/kg) at 3 hours post-hypoxia. While other doses and time-points of administration for this agent did provide substantial neuroprotection in the H-I model, the 200 mg/kg dose of CMZ administered at 3 hours post-hypoxia produced the most reliable and complete level of neuroprotection and was, therefore, used for molecular comparisons.

Chapter 3: *Suppression of Heat Shock Protein Expression by CMZ-Induced Neuroprotection in H-I Animals*

Summary

The objective of this study was to determine whether CMZ-induced neuroprotection in the H-I model could be attributed to potentiation of endogenous neuroprotective mechanisms. Numerous studies have shown that the induction of various heat shock proteins (Hsps) can enhance cellular survival in ischemically-injured cells. Thus, we wanted to determine whether Hsps are involved in the neuroprotection provided by CMZ in the H-I model. We used young male rats in the Rice-Vannucci model of unilateral global ischemia and examined the resultant expression patterns for *hsp70*, *40* and *27* mRNA and Hsp70 and 27 protein in CMZ-injected versus vehicle-injected H-I animals. Specifically, PND25 male H-I animals received a vehicle injection (ip) or an injection of 200 mg/kg CMZ at 3 hours post-hypoxia. *In situ* hybridization analysis of brain sections from these animals revealed that H-I produced high levels of *hsp27*, *40* and *70* mRNA in vehicle-injected animals sacrificed at 1, 2, 3, and 12 hours post-injection. However, a significant reduction in all *hsp* transcripts was observed in CMZ-injected (200 mg/kg) H-I animals, relative to vehicle-injected H-I animals, by 2 hours post-injection. Moreover, expression levels of these transcripts were at basal levels in CMZ-injected animals by 12 hours post-injection. Immunohistochemical analysis demonstrated that vehicle-injected H-I animals exhibited high levels of Hsp70 and 27 protein at 12, 24, 48 and 72 hours post-injection. However, H-I animals that received 200 mg/kg CMZ showed little to no expression of these proteins at any time point investigated. These results suggest that CMZ-induced neuroprotection is not achieved through an enhancement or prolongation of Hsp expression following H-I. In fact, a neuroprotective dose of CMZ (200 mg/kg) appeared to selectively prevent the translation of these allegedly protective proteins in all cell layers normally susceptible to H-I injury.

Introduction

One route through which CMZ might facilitate endogenous neuroprotective mechanisms is through the induction of heat shock proteins (Hsps). Throughout evolution, Hsps have been highly conserved in both prokaryotic and eukaryotic cells and are expressed under both normal and pathological conditions (Nowak *et al.*, 1985; 1990; Kiang and Tsokos, 1998). Such high conservation of these proteins may indicate that Hsps play a critical role in fundamental cellular processes. One of the most interesting characteristics of this family of proteins, with respect to neuroprotection, is their preferential induction in injured cells despite the fact that the synthesis of most other proteins is significantly reduced (Lindquist and Craig, 1988; Higashi *et al.*, 1994; Koroshetz and Bonventre, 1994). Hsp induction has been observed following a variety of stressful and benign cellular stimuli including exposure to amino acid analogues, glucose analogues, heavy metals, protein kinase C (PKC) stimulation, ischemia, sodium arsenite, microbial infections, nitric oxide, hormones, antibiotics, cellular development, growth, differentiation and aging (Zimmerman *et al.*, 1983; Lowenstein *et al.*, 1991; Kiang and Tsokos, 1998). Under these conditions, the duration and degree of Hsp induction appears to be directly related to the nature, severity and duration of cellular exposure to stress.

The mammalian genome contains six distinct families of Hsps, *hsp70*, *90*, *27*, *60*, *40* and *110*, some of which are constitutively expressed while others are highly inducible (Feige and Polla, 1994). Members of the Hsp family are reported to have different cellular functions and localizations (cytosol, mitochondria, endoplasmic reticulum (ER) and nucleus) which enable them to partake in protective or adaptive responses against cellular stress (Yost and Lindquist, 1986; Morimoto *et al.*, 1990; Kiang and Tsokos, 1998). Preferential induction of Hsps has been linked to the ability of individual cells to survive many endogenous and exogenous cellular stressors, including ischemia (Mailhos *et al.*, 1994; Plumier *et al.*, 1995; Yenari *et al.*, 1998). Little is known about the exact mechanism through which Hsps protect injured cells, particularly because it is not known which apoptotic or necrotic event is critical to cell death. For the most part, members of the Hsp family are thought to act

as molecular chaperones during intracellular processing of other proteins. Simply, Hsps transiently bind to unfolded proteins and ensure their correct synthesis, folding, assembly, transport and degradation (reviewed in Hartl, 1996). Under stressful conditions, this binding helps to stabilize the conformation of proteins and prevent their denaturation, misfolding or aggregation and also assists in the refolding or removal of damaged proteins. Once an Hsp binds to an irreparable protein that has been damaged by stress, the damaged protein is often delivered to the proteolytic machinery of the cell for degradation (Dice *et al.*, 1994).

Specific, transient expression of the highly inducible 70, 000 mol. wt. Hsp (Hsp71 in rats; Hsp72 in humans) has been observed in anatomic regions known to be susceptible to various cellular stressors and is thought to be a reliable indicator of cell stress or injury (Currie and White, 1981; Gubits *et al.*, 1993; Kiang and Tsokos, 1998). Immunohistochemical analysis targeting Hsp70 has revealed that Hsp70 induction, following numerous cellular stressors, is predominantly located in neurons (ischemia) but has occasionally been observed in glia (heat shock) and endothelial cells (Sharp *et al.*, 1991; Simon *et al.*, 1991; Nowak *et al.*, 1994; Armstrong *et al.*, 1996). As is characteristic of the Hsp family of proteins, neuroprotective benefits obtained from Hsp70 expression are thought to be due to its action as a molecular chaperone (Beckmann *et al.*, 1992; Palleros *et al.*, 1991). Specifically, Hsp70 appears to maintain the tertiary structure of normal and denatured proteins, which prevents their aggregation. Hsp70 has also been shown to remove denatured proteins from the cell, assist in new protein synthesis and facilitate protein transport across membranes of the mitochondria and endoplasmic reticulum (Deshaies *et al.*, 1988a; 1988b; Welch, 1993; Nowak *et al.*, 1994). The manner in which Hsp70 executes such a variety of functions has not been fully determined. However, it has been shown that removal of Hsp70 C-terminal amino acids, necessary for localization, abolished the neuroprotective effects of this protein whereas removal of the N-terminal amino acids, necessary for ATP binding, did not alter the function of this protein (Li *et al.*, 1992). In light of the functional heterogeneity, it is easy to see why control of the level of expression of Hsp70 in the brain has been proposed as a clinical strategy for neuroprotection against neurodegenerative disorders.

The 27, 000 mol. wt Hsp (Hsp27) is a small, highly conserved oligomeric protein related to the α-crystallin proteins (Kiang and Tsokos, 1998). In contrast to Hsp70, Hsp27 expression has primarily been localized in glial cells following injury to the brain (Kato *et al.*, 1994). Plumier *et al.* (1996) have shown that following kainic acid treatment, Hsp27-positive cells also stained positive for glial fibrillary amino acid protein (GFAP) indicating that these cells were likely reactive astrocytes. Cellular exposure to a variety of stressing stimuli has been shown to cause a rapid phosphorylation of Hsp27, transcriptional activation of the Hsp27 gene and accumulation of the protein (Arrigo and Landry, 1994). Like Hsp70, molecular chaperoning-like properties have been reported for Hsp27 (Jakob *et al.*, 1993). However, Hsp27 can also function as a phosphorylation-regulated F-actin capping protein that is capable of inhibiting actin polymerization (Miron *et al.*, 1991). There is also evidence that Hsp27 may be directly linked to the inhibition of cell proliferation (Knauf *et al.*, 1992).

The 40 000 mol. wt. protein Hsp40 is the mammalian homologue of the bacterial protein known as DnaJ (Yamane *et al.*, 1995). Hsp40 is constitutively expressed at a very low concentration but is highly inducible following cellular stress (Sugito *et al.*, 1995). Hsp40 protein functions as a collagen-specific molecular chaperone, thus, its expression always correlates with that of collagen in the endoplasmic reticulum (Nagata *et al.*, 1991). Specifically, Hsp40 may participate in the processing or secretion of procollagen in the ER (Nagata *et al.*, 1988; Nakai *et al.*, 1992). Hsp40 has also been shown to interact with Hsp70 in order to ensure the correct folding of newly synthesized proteins (Frydman *et al.*, 1994). In fact, the interaction of Hsp40 with Hsp70 has been shown to stimulate the ATPase activity of Hsp70 seven-fold (Hartl, 1996). In this way, it is believed that Hsp40 may play a distinct role in the recovery of susceptible tissues following various types of brain damage.

Hsps and Apoptosis

Delayed cell death following a variety of cellular stressors, including ischemia, often occurs through an ordered pathway of self-destruction termed apoptosis or programmed cell death (PCD) (Mosser *et al.* 1997). While the neuroprotective effects of Hsps have generally been ascribed to their ability to chaperone nascent and denatured proteins, recent reports have suggested that several members of the Hsp family may act as negative regulators of PCD (Ahn *et al.*, 1998; Chen *et al.*, 1999; Schett *et al.* 1999; Wang *et al.*, 1999; Yaglom *et al.*, 1999). PCD is an active, genetically controlled, cellular process that results in characteristic morphological changes to the cell that include condensed regions of nuclear material, internucleosomal DNA cleavage and membrane blebbing (Wyllie *et al.*, 1980).

Numerous experiments have shown that PCD-inducing stimuli trigger the activation of protein kinase cascades, such as the Ras-regulated mitogenic cascade SAPK/JNK (Stokeo *et al.*, 1992; Dubois and Bensuade, 1993). Thus, it has been proposed that inhibition of protein kinase signal transduction pathways may prevent the execution of PCD. Recent evidence has shown that elevated cellular levels of Hsp70 may inhibit the activation of specific protein kinases following heat shock, tumor necrosis factor α (TNFα) application or ceremide application (Mosser *et al.* 1997; Buzzard *et al.*, 1998). Specifically, it has been proposed that Hsp70 interferes with the stress-induced activation of c-Jun N-terminal kinase (JNK), an essential component in the heat-induced PCD pathway (Gabai *et al.*, 1997). Indeed, Mosser *et al.* (1997) demonstrated that in response to heat and ceremide-induced PCD *in vitro*, activation of JNK was strongly inhibited in cells that overexpressed Hsp70. It is possible that the suppression of JNK activation by Hsp70 may have been achieved through inhibition of the repression of JNK dephosphorylation that normally occurs following stressful treatments (Wei *et al.*, 1995; Dix *et al.*, 1996; Volloch *et al.*, 1998; Meriin *et al.*, 1999; Yaglom *et al.*, 1999). While these findings are interesting, they are made more complicated by *in vitro* studies that showed neuroprotection in stably transfected cells that chronically overexpress Hsp72, even when JNK activity was not inhibited (Gabai *et al.*, 1997). Moreover, Gabai *et al*, (1997) found protein aggregation itself to be an activator of JNK and p38 kinases indicating that the ability

of Hsp70 to interfere with the activation of these kinase pathways may, in fact, be due to its chaperoning ability. An overall hypothesis provided by Gabai *et al.* (1997) has suggested that, in unstressed cells, Hsp70 associates with an upstream component of the kinase cascade and holds it in its inactive form. Following cellular stress, depletion of free cellular Hsp70 by accumulated abnormal proteins may cause the bound Hsp70 to dissociate from the upstream component of the kinase cascade and thereby lead to downstream activation of kinases. See Figure 3-1. Furthermore, evidence provided by Buzzard *et al.* (1998) and Mosser *et al.*, (1997) has suggested that Hsp70 may also actively interfere with the PCD pathway at a site downstream from JNK activation. See Figure 3-2. Mosser *et al.* (1997) demonstrated a reduced processing of the *Caenorhabditis elegans* death gene (CED-3)-related proteases known as caspase-3 (CPP32/Yama/apopain) in Hsp70-overexpressing cells which caused a reduced cleavage of the common death substrate protein poly (ADP-ribose) polymerase (PARP). However, Hsp70-overexpression did not reduce the activity of the mature caspase-3 enzyme in that study.

Neuroprotection observed following Hsp27 induction has also been linked to an anti-PCD mechanism. Hsp27 expression has been reported to protect murine fibrosarcoma cells (L929) from damage following exposure to the protein kinase C (PKC) inhibitor, staurosporine, by blocking the activation of the cell surface receptor Fas/Apo1 which, in turn, inhibits the activation of the pro-PCD enzyme caspase-3 (Mehlen *et al.*, 1995; 1996). Collectively these studies indicate that control of Hsp expression in the brain may serve as an anti-PCD neuroprotective strategy in the clinical paradigm (Sato *et al.*, 1996).

Hsps and Ischemia

The first indication that Hsp expression might increase the likelihood of cell survival following various cellular stressors was a study conducted by Gerner and Schneider (1975). In that study, thermotolerance, a transient resistance to heat induced by prior exposure to high temperature, provided neuroprotection against mild hyperthermia-induced cell death. The level of cellular thermotolerance in that study was quantitatively related to the absolute levels of Hsps observed. Moreover, a study

Figure 3-1

Proposed role of Hsp70 in protein kinase activation following cellular stress.

Various cellular stressors lead to an intracellular accumulation of abnormal proteins that cause a depletion of unbound Hsp70. A decrease in free intracellular Hsp70 ultimately leads to the activation of stress kinases and subsequent PCD events. However, when Hsp70 is overexpressed in cells, stress kinase activation can be prevented and may thereby block the initiation of PCD-mediated events. (Adapted from Gabai *et al.*, 1997).

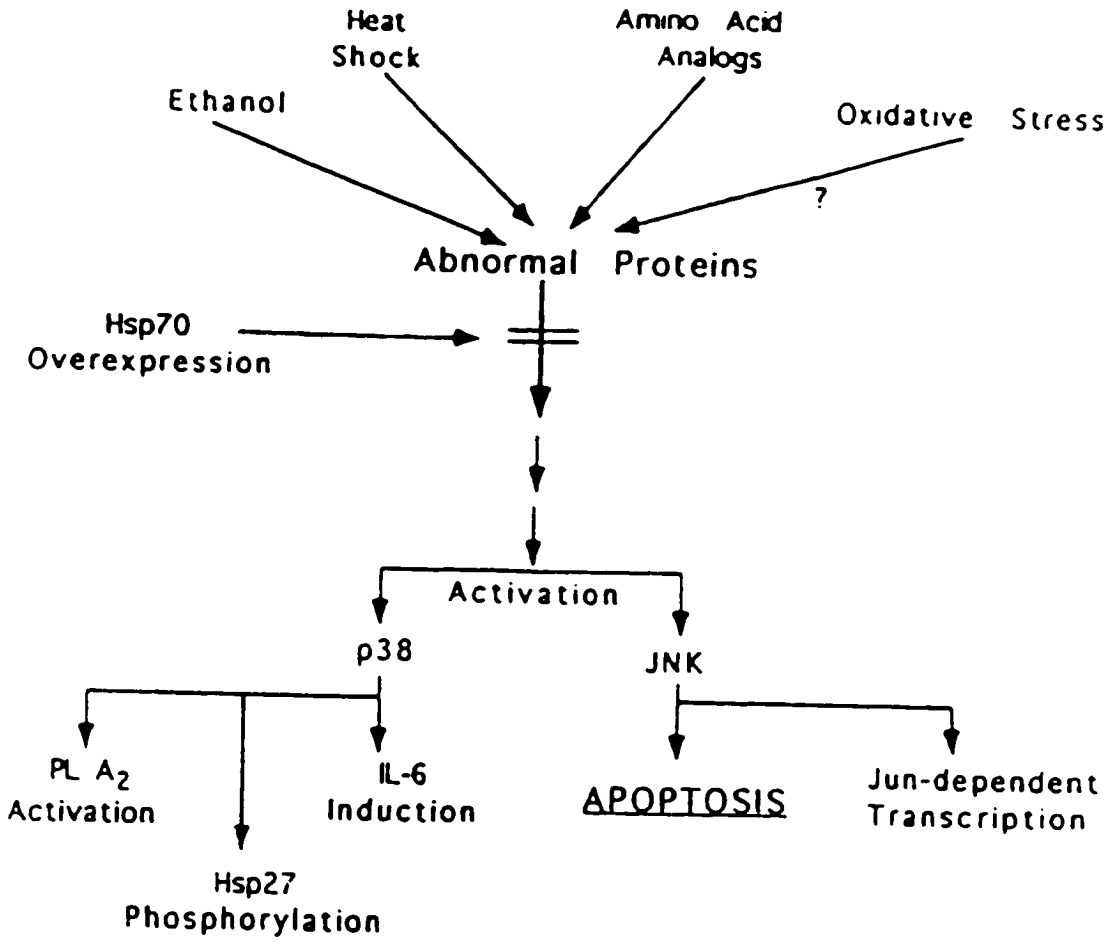
Heat
Shock
Amino Acid
Analogs
Ethanol
Oxidative Stress
?
Abnormal Proteins
Hsp70
Overexpression
Activation
p38
JNK
PL A2
Activation
IL-6
Induction
APOPTOSIS
Jun-dependent
Transcription
Hsp27
Phosphorylation

Figure 3-1

Figure 3-2

Hsp70 expression may inhibit caspase-3 activation following exposure to PCD-inducing stimuli.

A cellular stressor, such as heat shock, may activate the MEKK1 (MAPK/ERK kinase) pathway directly or indirectly by causing an increase in intracellular levels of ceremide and/or abnormal proteins. Elevated levels of MEKK1 ultimately lead to the activation of the pro-PCD protease cascade and caspase-3. Hsp70 overexpression may interfere with the progression of the MEKK1 pathway or it may bind to Bcl-2 and prevent the activation of caspase-3. Increased concentrations of abnormal proteins following cellular stressors also lead to an increase in p38 (a subgroup of MAP kinases) which phosphorylates Hsp27 protein. It has been postulated that the conformational state of Hsp27 determines its function. As a multimeric molecule, Hsp27 may function as a molecular chaperone whereas Hsp27 in a monomeric state it may be involved in the regulation of actin dynamics. (Adapted from Mosser *et al.*, 1997)

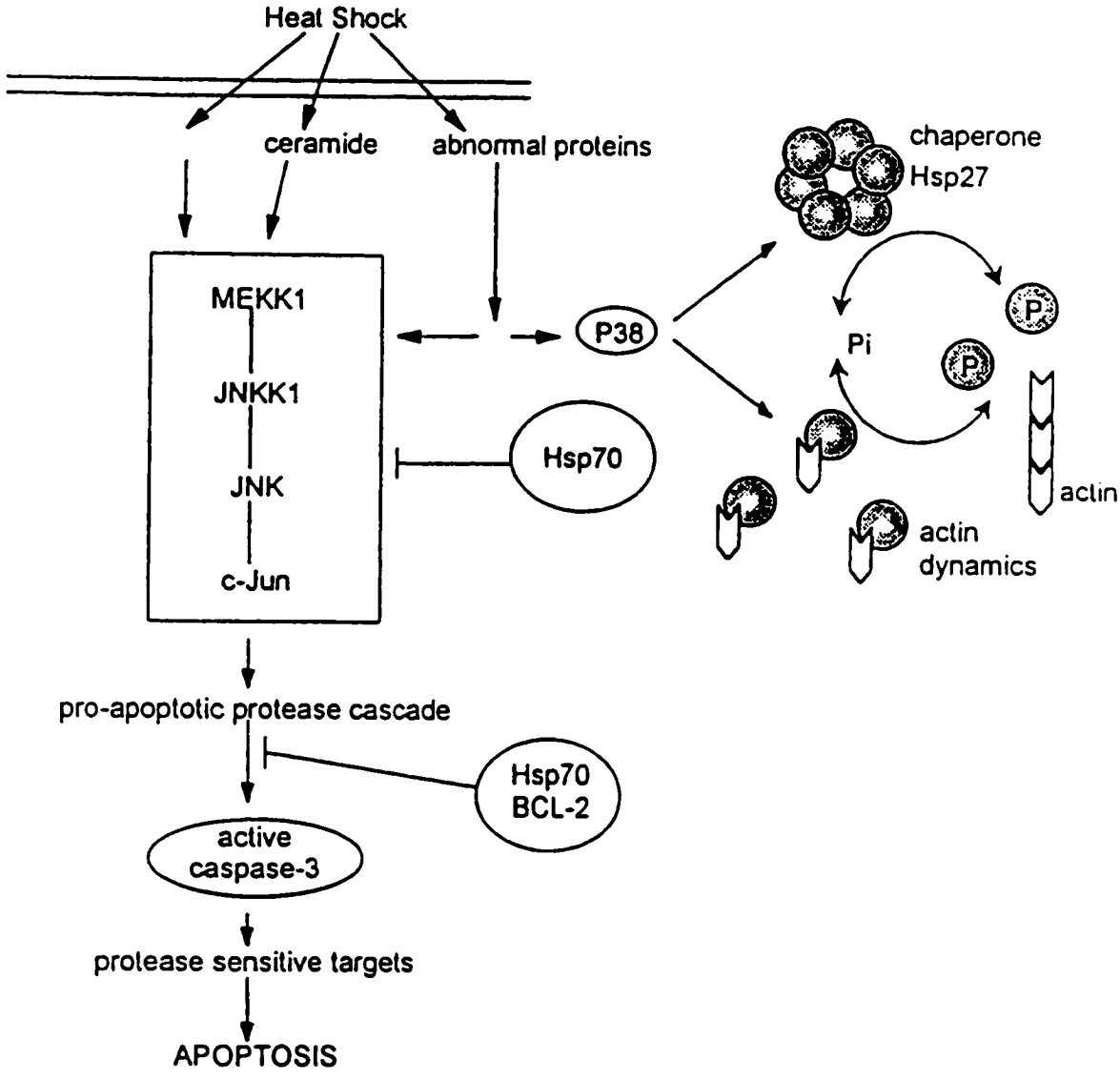
Heat Shock
ceramide
abnormal proteins
chaperone
Hsp27
MEKK1
JNKK1
JNK
c-Jun
P38
Hsp70
Pi
P
actin
actin
dynamics
pro-apoptotic protease cascade
Hsp70
BCL-2
active
caspase-3
protease sensitive targets
APOPTOSIS

Figure 3-2

of proteins that were newly synthesized after focal cerebral ischemia in rats demonstrated that two polypeptides (27 kDa and 70 kDa) dominated residual protein synthesis following severe ischemia (Jacewicz *et al.*, 1986). Subsequently, both direct and indirect evidence has suggested that the induction of some members of the Hsp family may play a pivotal role in the fate of ischemic cells (Nowak *et al.*, 1990; Kirino *et al.*, 1991; Kitigawa *et al.*, 1991; Mailhos *et al.*, 1994; Yellon and Marber, 1994; Plumier *et al.*, 1995; 1997).

Several efforts have been made to determine whether the highly inducible Hsp70 is neuroprotective in animal models of ischemia. Somewhat of a controversy has evolved regarding the significance of Hsp70 expression to ischemic cells. Some research has shown that Hsp70 is expressed only in cell populations that will ultimately recover from cerebral ischemia (Gonzalez *et al.*, 1991; Kinouchi *et al.*, 1993). Conversely, other studies have found Hsp70 expression in cell populations destined to die following excitotoxic injury (Chopp *et al.*, 1991 Simon *et al.* 1991). The question of whether Hsp70 is only expressed in dying cell populations is important, but correlational studies can not directly address the function of Hsp70 in ischemic cells. However, there has been some direct evidence indicative of a neuroprotective role for Hsp70 in ischemic cells. First, overexpression of Hsp72, established using a retrovirus vector, was shown to be neuroprotective against ischemic stress in cultured peripheral neurons (Amin *et al.*, 1996; Papadopoulos *et al.*, 1996). Second, Sato *et al.* (1996) used antisense oligonucleotides (AONs) to determine whether Hsp70 was essential to the neuroprotective effect of heat shock pre-conditioning. In brief, that study first demonstrated that heat shock (42°C for 30 minutes), which results in an elevation of Hsp70 for approximately 6 hours, significantly increased the number of surviving neurons in primary culture following a change to serum-free medium. However, when Hsp70 was "knocked down" in neurons using AONs the neuroprotective effect of heat shock against the serum change was abolished. Third, Yenari *et al.* (1998) demonstrated that gene transfer therapy with defective herpes simplex virus vectors that overexpress *hsp70* improved neuronal survival against subsequent focal cerebral ischemia or kainic acid administration. In that study, bilateral vector implantation 12 hours before a 60

minute MCAO or kainic acid administration was neuroprotective in dentate granule cells (64.4%) and striatal neurons (95.4%). Finally, studies using transgenic animals that overexpress Hsp72 have demonstrated increased cellular survival in susceptible tissues following ischemia and other cellular stressors (Marber *et al.*, 1995; Plumier *et al.*, 1995; Radford *et al.*, 1996; Plumier *et al.*, 1997). It is interesting, however, that GABAergic neurons do not express Hsp70 following transient forebrain ischemia in the gerbil but they are the most resistant cells to ischemic insult (Ferrer *et al.*,1995).

Gene transfection studies have indicated that overexpression of Hsp27 may also confer resistance against heat shock and oxidative stress (Landry *et al.*, 1989; Huot *et al.*, 1991; Lavoie *et al.*, 1993; Mehlen *et al*, 1995 and Huot *et al.*, 1996). Following MCAO, Hsp27 was expressed primarily in microglia approximately 4 hours after the insult and was then expressed in reactive astrocytes (Kato *et al.*, 1995). In that study, expression of Hsp27 was also noted in neurons 1 day following MCAO (Kato *et al.*, 1995). The wide distribution of Hsp25 in glial cells following ischemia suggests that this protein may be involved in post-ischemic repair and restorative processes (Kato *et al.*, 1995). Interestingly, studies have shown that there is far less expression of Hsp27 following focal cerebral ischemia than global ischemia (Siesjö, 1992a, b). At present, it is still uncertain which Hsp, if any, is responsible for neuroprotection observed in animal models of ischemia. In fact, there is some speculation that protective effects observed in various ischemia models were not due to one Hsp but may have required the co-ordinate synthesis of all the Hsps (Mailhos *et al.*, 1994).

As in other animal models of ischemia, high levels of Hsp70 expression have been observed following H-I injury (Dwyer *et al.*, 1989; Ferriero *et al.*, 1990; Blumenfeld *et al.*, 1992; Gilby *et al.*, 1997). Thus, the primary objective of this series of experiments was to determine whether CMZ-induced neuroprotection disrupted the normal expression patterns for *hsp70*, *27* or *40* mRNA and/or proteins following H-I in PND25 male rats. Examination of the expression patterns of Hsps may enable us to determine whether amplification or manipulation of an endogenous neuroprotective mechanism (Hsps) is responsible for the neuroprotective effects of CMZ in this model.

Methods

Animals

Animal procedures used in this experiment were identical to those outlined in Chapter 1. Three hours post-hypoxia, H-I animals received an i.p. injection of either vehicle (distilled water), 100mg/kg or 200mg/kg CMZ. Naive animals and ligated and hypoxic control animal groups were included in this study. Drug-injected control animals received an i.p. injection of either 100 mg/kg or 200 mg/kg CMZ but did not experience the H-I event. Following treatment, each animal was observed for any overt signs of seizure activity such as mastication, barrel rolling or limb tonus and clonus. Animals that exhibited such behavior were excluded from the study.

Perfusion and Tissue Fixation

Animals were sacrificed at varying timepoints following their repective treatments. Each rat was deeply anesthetized with 65 mg/kg of sodium pentobarbitol and was then perfused through the ascending aorta with 0.9% saline (60 mls) followed by cold 100 mM phosphate buffer containing 4 % paraformaldehyde (60 mls). Brains were removed and post-fixed in 100 mM phosphate buffer containing 4% paraformaldehyde at 4°C for at least 24 hours.

In situ hybridization

Fixed brains were sectioned at 40 μm on a Series 1000 vibratome, mounted onto SuperFrost™ (Fisher Scientific) slides and permitted to dry overnight before further processing. Once dry, fixed sections were dehydrated in a series of increasing ethanol concentrations (50% - 100%), defatted in xylene and rehydrated in decreasing concentrations of ethanol (100% - 50%). Slides containing the fixed sections were rinsed in 1X phosphate buffered saline (PBS) (3 x 5 minutes), and put into 2X sodium chloride citrate (SSC) for 20 minutes and left to air dry for at least 1 hour.

Oligonucleotides designed to target specific mRNAs were 3' end-labeled with [α^{33}P] - dATP for 90 minutes at 37°C using terminal deoxynucleotidyl transferase (Amersham). Unincorporated radionucleotides were removed from the labeled

probes using a Sephadex G-25 spin column (Pharmacia). The labeled probes were added to hybridization buffer (50% formamide, 5X SSC, 10% dextran sulfate, 1X Denhardt's reagent, 20 mM sodium phosphate, pH 6.8, 0.2% SDS, 5mM EDTA, 10 µg/ml poly A, 50 µg/ml sheared salmon sperm DNA, 50 µg/ml yeast RNA) in such a proportion that 1ml of hybridization buffer contained 5 x 10^6 cpm of radio-labeled probe. 200 µl of the hybridization mixture was added to each slide containing the brain sections and a piece of parafilm was placed on top to contain the hybridization mixture. Sections were then incubated overnight at 42°C in a humidified chamber. The next day parafilm coverslips were removed in 1X SSC and the slides were washed in 1X SSC (4 x 30 minutes) at 55°C, 0.5 x SSC (4 x 30 minutes) at 55°C and finally in 0.25 x SSC (1 x 30 minutes) at room temperature. Following the washes, sections were dipped in DEPC water and air dried overnight. When dry, the slides were exposed to Kodak Biomax MS film (Intersciences, Markham, ON) for 2-4 days in order to visualize the hybridizing oligonucleotide probe.

An *hsp70* oligonucleotide probe, specific for the inducible *hsp70* mRNA (*hsp$_i$*), was synthesized commercially (Marine Gene Probe Lab, Dalhousie University, Halifax, Nova Scotia) with the following sequence: 5' CGA TCT CCT TCA TCT TGG TCA GCA CCA TGG –3'. This sequence is complimentary to nucleotides 568-539 of the rat *hsp70* mRNA (Genbank Assession Number: L16764). The *hsp27* oligonucleotide probe used to target *hsp27* mRNA had the following sequence: 5' GAA TGG TGA TCT CCG CTG ATT GTG TGA CTG CTT TG-3' which was complimentary to nucleotides 1653-1687 of the rat *hsp27* cDNA (GenBank Assession Number: S6775). The oligonucleotide probe synthesized by Genosys Inc. designed to target *hsp40* mRNA had the following sequence: 5' CCT GGC TCC AGT CCT GGTTCT TGG TCT CCT TCA CC 3' and was complimentary to nucletides 797-831 of the rat DnaJ-like protein mRNA (Genbank Assession Number: U53922).

Immunohistochemistry

Hsp70

Coronal sections (40 μm) cut through the hippocampus were washed in 100 mM Tris buffer (pH = 7.6; 3 x 5 minutes) and incubated with 1% hydrogen peroxide in Tris buffer for 30 minutes with gentle agitation. Sections were then washed in Tris buffer for 5 minutes, then 0.1% Triton X in Tris buffer (Tris A) for 15 minutes followed by a 15 minute wash in 0.1% Triton X plus 0.005% bovine serum albumin (BSA) in Tris (Tris B). Sections were incubated for 1 hour at room temperature in Tris B containing 10% normal horse serum (Vector Laboratories, Burlingame, CA, USA) and then washed in Tris A for 15 minutes followed by 15 minutes in Tris B. Following washing, sections were incubated for 48 hours at 4°C in primary mouse monoclonal antibody raised against human Hsp70 (StressGen Biotechnologies Corp, Victoria, BC, Canada) at a dilution of 1:5000 in Tris B. Following the incubation period, the sections were washed 15 minutes in Tris A, 15 minutes in Tris B followed by 60 minutes in Tris B containing a rat absorbed biotinylated horse antibody raised against mouse (1:400; Vector Laboratories Inc.). Subsequent to the incubation, the sections were washed in Tris A for 15 minutes, then in 0.1% Triton X in 55 mM Tris Buffer (Tris D) for another 15 minutes. Sections were then incubated for 1 hour in avidin-biotin-horseradish peroxidase complex (ABC Elite; Vector Laboratories) at a dilution of 1:1000 made up in Tris D followed by 3 x 5 minutes in 100 mM Tris buffer. Sections were then treated with 0.05% diaminobensidine-tetrachloride (DAB) (Sigma Chemical Co.) made up in Tris buffer containing 0.1 mg/100 ml glucose oxidase, 40 mg/100 ml ammonium chloride and 200 mg/100 ml b-D(+) glucose (Sigma Chemical Co.) for approximately 15 minutes. Stained sections were then washed 3 x 5 minutes in Tris buffer and mounted on gelatinized slides. Once air-dried (overnight), the slides were dehydrated in a series of ethanols (50-100%), defatted with xylene and then coverslipped using Entellan (E. Merck, Darmstadt).

Hsp27

Similar procedures to those of Hsp70 immunohistochemistry were used for detection of Hsp27 protein with some exceptions. Sections were first washed in PBS

(3 x 10 minutes) and incubated in 3% hydrogen peroxide in PBS for 30 minutes. Sections were again washed in PBS (3 x 10 minutes) and put directly into a rabbit anti-mouse Hsp27 polyclonal primary antibody (1:5000; StressGen Biotechnologies Corp.) made in PBS containing 2% goat serum and incubated overnight at 4°C. The next day sections were washed in PBS (3 x 10 minutes) and then incubated in a biotinylated goat anti-rabbit secondary antibody (1:400; Vector Laboratories Inc.) for 60 minutes. Following incubation sections were washed in PBS (3 x 10 minutes) and then incubated for 1 hour in avidin-biotin-horseradish peroxidase complex (ABC Elite; Vector Laboratories) at a dilution of 1:1000 in PBS followed by 3 x 10 minutes in PBS. Sections were then treated with 0.05% diaminobensidine-tetrachloride (Sigma Chemical Co.) in PBS containing 0.1 mg/100 ml glucose oxidase, 40mg/100ml ammonium chloride and 200mg/100ml b-D(+) glucose (Sigma Chemical Co.) for approximately 15 minutes. Subsequently, stained sections were washed 3 x 10 minutes in PBS, mounted on gelatinized slides and coverslipped. Previous unpublished work in our laboratory, using this antibody, has demonstrated that this polyclonal antibody selectively recognizes rat Hsp27, the homologous protein to mouse Hsp25.

Western Blot Analysis

Extracted hippocampal tissue was homogenized in 0.32 M sucrose and the total protein concentration in was determined in each sample. Homogenate samples containing 20 μg of protein were solubilized in SDS sample buffer [10% glycerol, 5% β-mercaptoethanol, 3% SDS in upper Tris buffer (0.125 M Tris-HCl pH = 8.8/0.1% SDS), boiled for 10 minutes and then loaded into a polyacrylamide gel (2.5% upper gel, 7.5% running gel). Proteins within the samples were fractionated electrophoretically (75V for one hour then 125V for 2 hours) and electroblotted onto an Immobilon-P membrane (Millipore, Mississauga, ON) at 40 volts for 18 hours and then air dried.

In preparation of immunohistochemical detection, membranes were first saturated in methanol, rinsed with 1X PBS and then incubated in 5% skim milk/1% bovine serum albumin (BSA) in 1X PBS for 1 hour at 37°C to block non-specific

antibody binding. Primary mouse monoclonal antibody specific for the inducible form of Hsp70 (StressGen Biotechnologies, Victoria, BC, Canada) was diluted 1:1000 in 5% skim milk/1% (BSA). Membranes were incubated with primary antibody at 4°C for 18 hours with gentle agitation. To remove excess primary antibody, membranes were washed 3 x 20 minutes in 1X PBS/0.2%Tween 80 at 37°C then incubated 1 hour at 37°C with peroxidase-labeled horse anti-mouse IgG (Vectors Laboratories Inc., Burlingame, CA) at a 1:5000 dilution in PBS skim milk 1% BSA. To remove any unbound secondary antibody, blots were washed 1 x 15 minutes and 4 x 15 minutes in 1X PBS/0.2%Tween 80 at 37°C. Immunolabeled proteins were detected using the electrogenerated chemiluminescence (ECL) Western Blot Detection Kit (Amresham, Arlington Height, IL). In order to ensure that the relative concentrations of protein loaded in each lane were approximately equal the membrane was counter-stained with Amido Black.

Densitometric Analysis

Densitometric analysis of mRNA expression on *in situ* autoradiograms was performed using the Optical Density-Model GS0290 Imaging Densitometer and Molecular Analyst (Biorad) software to determine the optical density (OD) of the radio-labeled brain regions. Animals from all control groups were analyzed as one group for statistical and graphical analysis. Any differences in mean transcript expression were statistically analyzed using a 1-way Analysis of Variance (ANOVA) followed by Tukey's post-hoc analysis.

Results

In situ Hybridization

Densitometric analysis of *hsp70*, *hsp40* and *hsp27* mRNA expression was conducted on CA1, CA3 and the dentate gyrus in the ipsilateral hippocampus and on parietal cortex of vehicle-injected and CMZ (200 mg/kg)-injected H-I animals. At no time were any of these transcripts expressed in any cell layer of naïve, ligated, hypoxic or drug-injected control animals used in this study.

hsp70

In order to compare relative patterns of *hsp70* expression across treatment groups, vehicle- and CMZ-injected H-I animals were sacrificed at 1 (N = 8; N = 10 respectively), 2 (N = 6; N = 6 respectively), 3 (N = 6; N = 5 respectively), 12 (N = 7; N = 7 respectively) and 24 (N = 7; N = 7 respectively) hours post-injection. Mean *hsp70* expression was found to be significantly higher in the CA1 pyramidal cell layers of both CMZ-injected and vehicle-injected H-I animals than it was in control animals (N = 16) at 1 ($q = 12.47$; $q = 13.809$ respectively; $P<0.05$), 2 ($q = 14.979$; $q = 8.219$ respectively; $P<0.05$) and 3 ($q = 16.687$; $q = 9.98$ respectively; $P<0.05$) hours post-injection. Mean *hsp70* expression in CA1 of vehicle-injected animals was also found to be significantly higher than in control animals at 12 hours post-injection ($q = 8.308$; $P<0.05$). However, mean expression of this transcript in the CA1 cell layer of CMZ-injected H-I animals was not significantly different from control animals at this time-point. In animals sacrificed at 24 hours post-injection, the reverse was true where mean *hsp70* expression in CA1 of vehicle-injected animals was not significantly different from control animals but was significantly elevated in CA1 of CMZ-injected H-I animals ($q = 5.276$; $P<0.05$) at this time-point. In a pairwise comparison between CMZ-injected and vehicle-injected H-I animals only, no significant difference in mean CA1 *hsp70* expression was evident at 1 hour post-injection between these treatment groups. However, mean *hsp70* expression was found to be significantly higher in CA1 of vehicle-injected animals than it was in CMZ-injected animals at 2 ($q = 6.005$; $P<0.05$), 3 ($q = 4.832$; $P<0.05$) and 12 ($q =$

7.017; P<0.05) hours post-injection.

Mean *hsp70* expression in the CA3 cell layer of the hippocampus was significantly higher in both vehicle- and CMZ-injected H-I animals than it was in control animals at 1 (q = 15.207; q = 19.786 respectively; P<0.05), 2 (q = 16.79; q = 11.55 respectively; P<0.05) and 3 (q = 19.183; q = 10.210 respectively; P<0.05) hours post-injection. Significantly higher mean *hsp70* expression was also observed in CA3 of vehicle-injected H-I animals, relative to control animals, at 12 hours post-injection (q = 9.510; P<0.05) whereas CMZ-injected H-I animals did not show an elevation of this transcript at this time-point. Mean *hsp70* expression in the CA3 cell layer of both treatment groups was near baseline level by 24 hours post-injection. An investigation into differences in mean *hsp70* expression in CA3 between CMZ- and vehicle-injected H-I animals revealed a significantly higher expression of this transcript in vehicle-injected H-I animals at 3 (q = 6.527; P<0.05) and 12 (q = 8.541; P<0.05) hours post-injection.

Mean *hsp70* expression in both vehicle- and CMZ- injected H-I animals was significantly higher in the granule cells of the dentate gyrus (DG) than it was in control animals when sacrificed at 1 (q = 18.616; q = 24.443 respectively; P<0.05), 2 (q = 22.034; q = 12.81 respectively; P<0.05) and 3 (q = 23.91; q = 13.301 respectively; P<0.05) hours post-injection. However, this elevation in transcript expression was only detected in vehicle-injected animals at 12 hours post-injection (q = 12.08; P<0.05). Mean *hsp70* expression in the DG of both treatment groups was no longer significantly higher than control animals by 24 hours post-injection. At 2 (q = 7.646 P<0.05), 3 (q = 7.648; P<0.05) and 12 (q = 10.434; P<0.05) hours post-injection, mean *hsp70* expression was significantly higher in the dentate granule cells of vehicle-injected H-I animals than in CMZ- injected H-I animals.

Mean *hsp70* expression in the parietal cortex was found to be significantly higher than control animals in both vehicle- and CMZ-injected H-I animals at 1 (q = 19.602; q = 22.35 respectively; P<0.05), 2 (q = 26.684; q = 19.2 respectively; P<0.05) and 3 (q = 25.848; q = 14.832 respectively; P<0.05) hours post-injection. By 12 hours post-injection a significant elevation in mean *hsp70* expression was observed in the parietal cortex of vehicle-injected H-I animals (q = 21.434; P<0.05) relative to

controls, but was not evident in the parietal cortex of CMZ-injected animals at the same time-point. By 24 hours post-injection, mean *hsp70* expression in CA3 of both treatment groups had returned to control levels. Mean *hsp70* expression in the parietal cortex of vehicle-injected animals were found to be significantly higher than CMZ-injected animals at 2 ($q = 6.206$; $P<0.05$), 3 ($q = 7.884$; $P<0.05$) and 12 ($q = 18.343$; $P<0.05$) hours, but not at 1 or 24 hours post-injection. See Figure 3-3.

hsp40

Vehicle- and CMZ-injected animals were sacrificed at 1 ($N = 11$; $N = 7$ respectively), 2 ($N = 5$; $N = 7$ respectively), 3 ($N = 6$; $N = 11$ respectively), 12 ($N = 15$; $N = 12$ respectively) and 24 ($N = 6$; $N = 7$ respectively) following injection of vehicle or CMZ. A significant elevation in mean *hsp40* expression was observed in CA1 of vehicle-injected animals relative to control animals ($N = 13$) at 1 ($q = 5.410$; $P<0.05$), 2 ($q = 6.894$; $P<0.05$), 3 ($q = 6.97$; $P<0.05$) and 12 ($q = 7.961$; $P<0.05$) hours post-injection, but had returned to control levels in this cell layer by 24 hours post-injection. In contrast, the only time-point at which mean *hsp40* expression was significantly higher in CA1 of CMZ-injected H-I animals than in control animals was at 2 hours post-injection ($q = 6.551$; $P<0.05$). Regardless, in pairwise comparisons between CMZ- and vehicle-injected animals, differences between these treatment groups only reached statistical significance at 12 hours ($q = 4.704$; $P<0.05$) post-injection.

In the CA3 pyramidal cell layer, a significant elevation in mean *hsp40* expression was observed between vehicle-injected animals relative to control animals at 1 ($q = 5.773$; $P<0.05$) and 2 ($q = 9.59$; $P<0.05$) hours post-injection. Mean *hsp40* expression in CA3 of CMZ-injected animals, however, did not differ from that in control animals at any time-point examined. A significant difference in mean *hsp40* expression in CA3 between vehicle-injected and CMZ-injected animals was not evident at any time-point examined.

Mean *hsp40* expression in the dentate gyrus of vehicle-injected H-I animals was significantly higher than in control animals at 1 ($q = 6.216$; $P<0.05$), 2 ($q = 8.115$; $P<0.05$), 3 ($q = 5.492$; $P<0.05$) and 12 ($q = 4.757$; $P<0.05$) hours post-injection but had returned to basal levels by 24 hours post-injection. However, a significant elevation in

Figure 3-3

Expression of hsp70 mRNA in vehicle- and CMZ-injected H-I animals.

Mean density of *hsp70* mRNA expression in all hippocampal and cortical cell layers of control, CMZ-injected and vehicle-injected H-I animals across various post-injection timepoints. A) Mean density of *hsp70* expression in CA1 of animals from treatment groups. B) Mean density of *hsp70* expression in CA3 of animals from both treatment groups. C) Mean density of *hsp70* expression in DG of animals from both treatment groups. D) Mean density of *hsp70* expression in the cortex of animals from both treatment groups. A P value of <0.05 was considered to be statistically significant. The data are presented as means ± S.E.M. (* = significantly different from transcript density in control animals; ■ = significantly different from transcript density in vehicle-injected H-I animals sacrificed at the same timepoint).

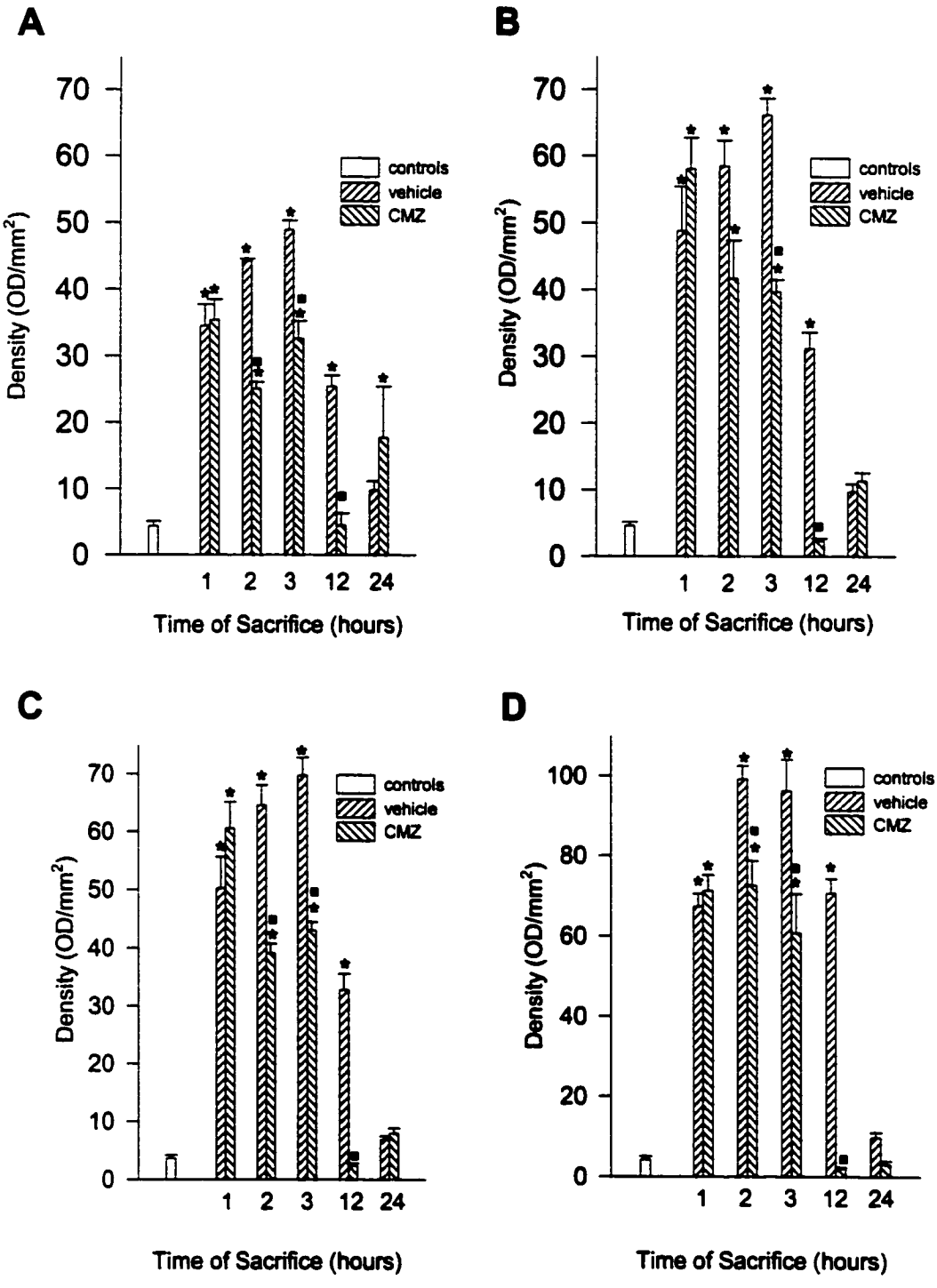
A
B
C
D
Density (OD/mm²)
Time of Sacrifice (hours)
controls
vehicle
CMZ
1
2
3
12
24
0
10
20
30
40
50
60
70
80
100

Figure 3-3

mean *hsp40* expression in the dentate gyrus of CMZ-injected animals was only evident at 3 hours post-injection ($q = 4.863$; $P<0.05$) when compared to control animals. A significant difference in mean *hsp40* expression in the dentate gyrus was evident between vehicle- and CMZ-injected animals at 2 hours post-injection only ($q = 6.83$; $P<0.05$)

Finally, mean *hsp40* expression in the parietal cortex of vehicle-injected animals was found to be significantly higher than control animals at 1 ($q = 6.25$; $P<0.05$), 2 ($q = 7.77$; $P<0.05$), 3 ($q = 5.38$; $P<0.05$) and 12 ($q = 7.99$; $P<0.05$) hours post-injection. In contrast, elevation of this transcript did not attain statistical significance in the parietal cortex of CMZ-injected animals when compared to control animals at any time-point examined. A significant difference in mean *hsp40* expression was evident only at 2 ($q = 5.405$; $P<0.05$) and 12 ($q = 6.271$; $P<0.05$) hours post-injection. See Figure 3-4.

hsp25

Vehicle- and CMZ-injected H-I animals were sacrificed at 1 ($N = 6$; $N = 6$ respectively), 2 ($N = 7$; $N = 6$ respectively), 3 ($N = 7$; $N = 6$ respectively), 12 ($N = 6$; $N = 5$ respectively) and 24 ($N = 5$; $N = 6$ respectively) hours post-injection. Statistical analysis revealed that a significant elevation in mean *hsp25* expression was evident only in CA1 of vehicle-injected animals relative to control animals when sacrificed at 2 ($q = 7.665$; $P<0.05$) and 3 ($q = 6.037$; $P<0.05$) hours post-injection. Similarly, mean *hsp25* expression was not significantly different from control animals in CA1 of CMZ-injected H-I animals at any time-point examined. A significant difference in mean *hsp25* expression was not evident between CMZ- and vehicle-injected animals at any time-point examined.

In CA3, mean *hsp25* expression in vehicle-injected H-I animals was significantly higher than in control animals at 1 ($q = 6.01$; $P<0.05$), 2 ($q = 7.232$; $P<0.05$), 3 ($q = 5.609$; $P<0.05$) and 12 ($q = 7.189$; $P<0.05$) hours post-injection. However, a significant elevation of this transcript in CA3 of CMZ-injected animals was only evident at 2 hours post-injection ($q = 5.78$; $P<0.05$). Mean *hsp25* expression was significantly higher in CA3 of vehicle-injected animals than in CMZ-injected animals sacrificed at 12 hours post-injection ($q = 5.44$; $P<0.05$).

Figure 3-4

Expression of hsp40 mRNA in vehicle- and CMZ-injected H-I animals.

Mean density of *hsp40* expression in all hippocampal and cortical cell layers of control, CMZ- and vehicle-injected H-I animals. A) Mean density of *hsp40* expression in CA1 of animals from both treatment groups. B) Mean density of *hsp40* expression in CA3 of animals from both treatment groups. C) Mean density of *hsp40* expression in DG of animals from both treatment groups. D) Mean density of *hsp40* expression in the cortex of animals from both treatment groups. A P value of <0.05 was considered to be statistically significant. The data are presented as means ± S.E.M. (* = significantly different from transcript density in control animals; ■ = significantly different from transcript density in vehicle-injected H-I animals sacrificed at the same timepoint).

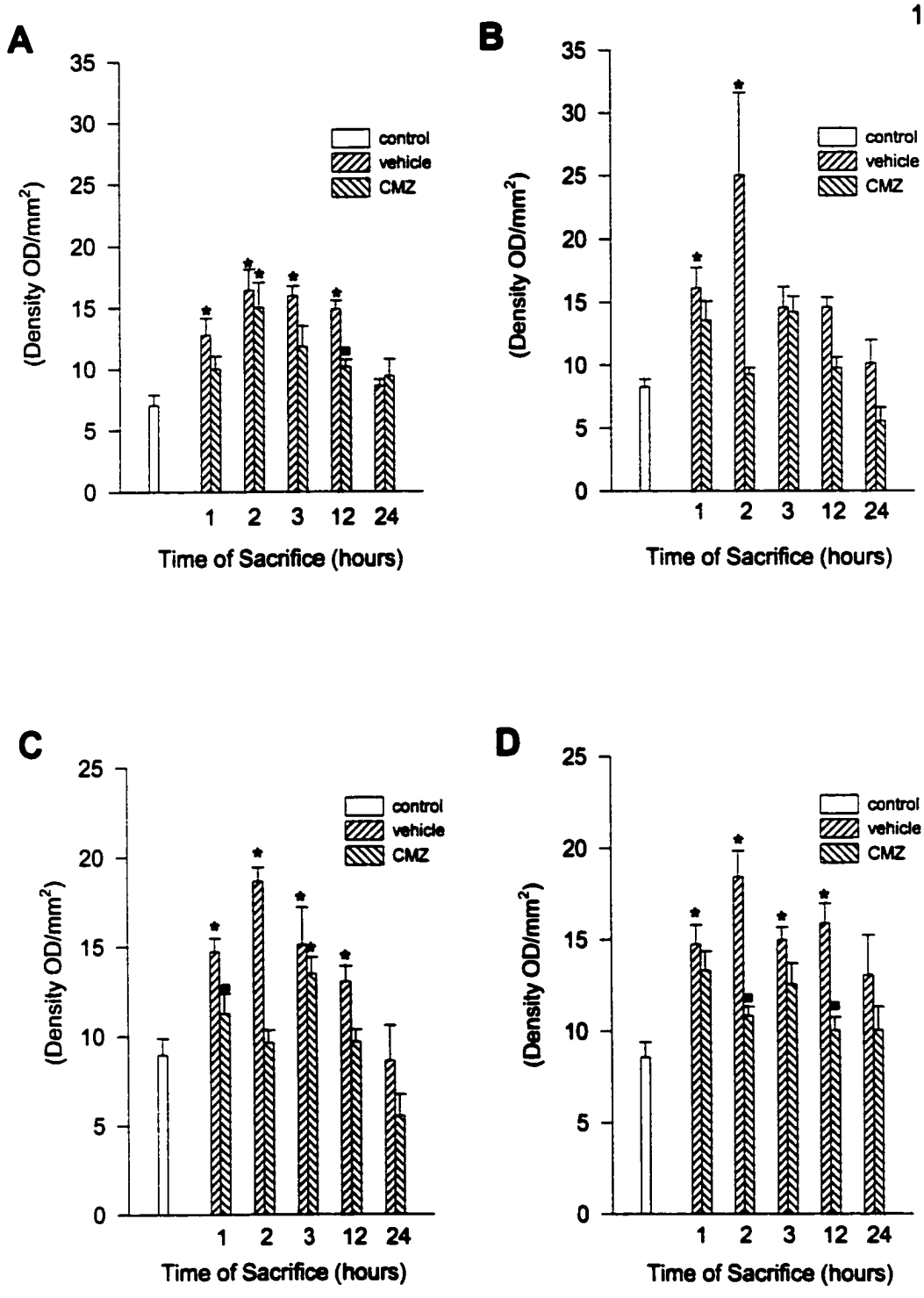
A
B
C
D
(Density OD/mm²)
control
vehicle
CMZ
1 2 3 12 24
Time of Sacrifice (hours)

Figure 3-4

No significant difference in mean *hsp25* expression was observed in the dentate gyrus of either vehicle- or CMZ-injected animals relative to control animals, or relative to each other, at any time-point examined.

Mean cortical *hsp25* expression was found to be significantly higher in vehicle-injected H-I animals than in control animals at 2 ($q = 7.759$; $P<0.05$), 3 ($q = 7.035$; $P<0.05$) and 12 ($q = 5.495$; $P<0.05$) hours post-injection. Similarly, CMZ-injected animals exhibited significantly higher levels of *hsp25* expression in the parietal cortex than did control animals at 2 ($q = 6.983$; $P<0.05$) and 3 ($q = 5.295$; $P<0.05$) hours post-injection. A significant difference in mean *hsp25* expression was noted between CMZ- and vehicle-injected animals at 12 hours post-injection ($q = 4.930$; $P<0.05$). See Figure 3-5.

Immunohistochemistry

Immunohistochemical analysis of vehicle-injected H-I animals revealed that Hsp70 protein was expressed in the dentate granule cells and in some hilar cells of these animals at 1 (N=13), 2 (N=5), 3 (N = 4) and 6 (N =4) hours post-injection. By 12 hours post-injection Hsp70 staining was observed in patches of the DG and throughout CA3c and layer 3 of the parietal cortex. Staining was also evident in CA1 at this time-point (N = 5). Nearly identical staining patterns for Hsp70 were observed in vehicle-injected H-I animals at 24 hours post-hypoxia (N = 5). However, animals sacrificed beyond the 24 hour post-injection time point exhibited a variable pattern of Hsp70 expression. At 48 hours post-injection one animal showed basal levels of Hsp70 expression (1/4) whereas in some animals Hsp70 expression was observed in all hippocampal pyramidal cells, in patches of the DG and in throughout the parietal cortex (3/4). Similarly, by 72 hours post-hypoxia some animals demonstrated basal levels of Hsp70 expression (3/5) while some showed expression in the hilus, CA3, and in layer 3 of the parietal cortex (2/5).

The expression pattern for Hsp70 in CMZ-injected H-I animals exhibited dramatic differences when compared to the expression profile for Hsp70 in vehicle-injected animals. CMZ-injected H-I animals sacrificed at early post-injection time points such as 1 (N=7), 2 (N=6) and 3 (N=5) hours post-injection did show faint

Figure 3-5

Expression of hsp27 mRNA in vehicle- and CMZ-injected H-I animals.

Mean density of *hsp27* expression in all hippocampal and cortical cell layers of CMZ- and vehicle-injected H-I animals. A) Mean density of *hsp27* expression in CA1 of animals from both treatment groups. B) Mean density of *hsp27* expression in CA3 of animals from both treatment groups. C) Mean density of *hsp27* expression in DG of animals from both treatment groups. D) Mean density of *hsp27* expression in the cortex of animals from both treatment groups. A P value of <0.05 was considered to be statistically significant. The data are presented as means ± S.E.M. (* = significantly different from transcript density in control animals; ■ = significantly different from transcript density in vehicle-injected H-I animals sacrificed at the same timepoint).

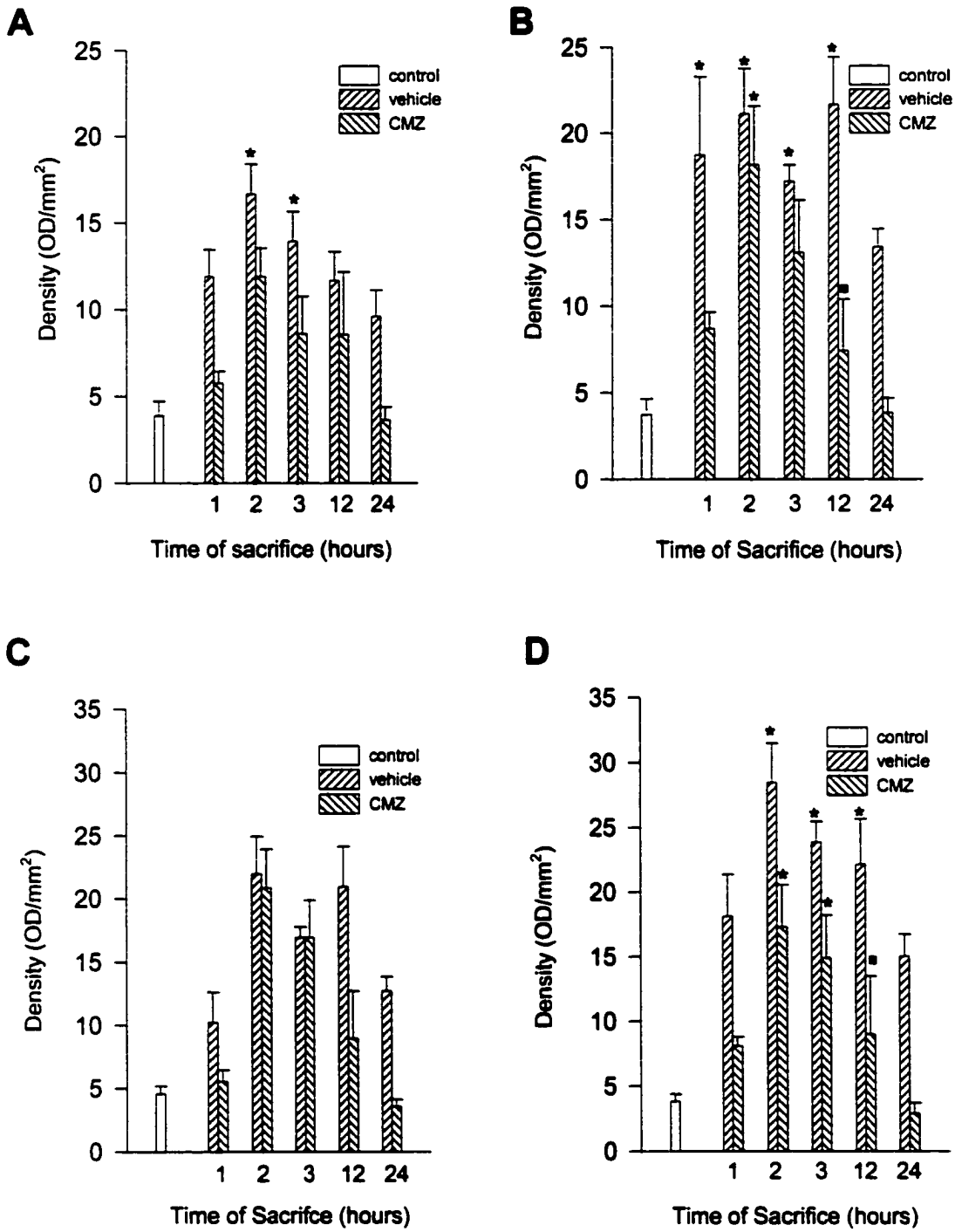
A
B
C
D
control
vehicle
CMZ
Density (OD/mm²)
Time of sacrifice (hours)
Time of Sacrifice (hours)
Time of Sacrifce (hours)
1
2
3
12
24

Figure 3-5

staining in DG cells. However, animals sacrificed at 6 (N=8), 12 (N=8), 24 (N=4), 48 (N=6) and 72 (N=6) hours post-injection expressed basal levels of this protein in all brain regions. See Figures 3-6 and 3-7.

H-I animals that received 100 mg/kg CMZ at 3 hours post-hypoxia demonstrated variable expression patterns for this protein. Some animals sacrificed at 12 hours post-injection showed basal levels of expression (2/4) while others demonstrated staining in the DG, hilus, hippocampal pyramidal cell layers and in layer 3 of the parietal cortex (2/4). At 24 hours post-injection, basal levels of expression were observed in 4/6 animals that received 100 mg/kg CMZ at 3 hours post-hypoxia, while 2/6 animals demonstrated expression patterns similar to that seen in vehicle-injected animals. However, all animals that received 100 mg/kg CMZ that were sacrificed at 48 (N=5) and 72 hours (N=3) post-injection demonstrated basal levels of expression.

Immunohistochemical detection of Hsp27 protein revealed that all vehicle-injected H-I animals that were sacrificed at 1 (N=11), 2 (N=4), 3 (N=5) or 6 (N=4) hours post-injection exhibited basal levels of Hsp27 expression. However, by 12 hours post-injection, 4/5 vehicle-injected animals exhibited high levels of Hsp27 expression in basket cells of the DG and in the hilus. Sporadic glial expression was observed around all hippocampal pyramidal cell layers and in the infarct zone of the parietal cortex. Basal levels of Hsp27 expression were observed in 1/5 vehicle-injected animals sacrificed at this time point. By 24 hours post-hypoxia 4/4 animals exhibited very high glial expression around all hippocampal pyramidal cell layers, expression in the cell bodies and processes of CA3 neurons and basket cells and intensive neuronal and glial expression in the infarct zone in the parietal cortex. By 48 hours post-injection, 4/4 vehicle-injected animals demonstrated Hsp25 expression in all remaining viable pyramidal neurons and in glia throughout the hippocampus and parietal cortex. By 72 hours post-injection, expression patterns were variable in vehicle-injected animals with 3/5 animals exhibiting basal levels of Hsp27 expression in all susceptible brain regions and 2/5 animals exhibiting both glial and neuronal expression in remaining pyramidal cell layers of the hippocampus and in the infarct zone of the parietal cortex. Neuronal expression of Hsp27 is shown in Figure 3-8.

Figure 3-6

Hsp70 expression in the hippocampus of vehicle- and CMZ-injected H-I animals at varying post-hypoxic timepoints.

Photomicrographic representation of Hsp70 expression in the ipsilateral hippocampus of vehicle-injected (A, C, E, G) and CMZ-injected (B, D, F, H) H-I animals. Animals were sacrificed 6 (A, B), 12 (C, D), 24 (E, F) and 48 (G, H) hours post-injection. (Scale bar = 400 μm).

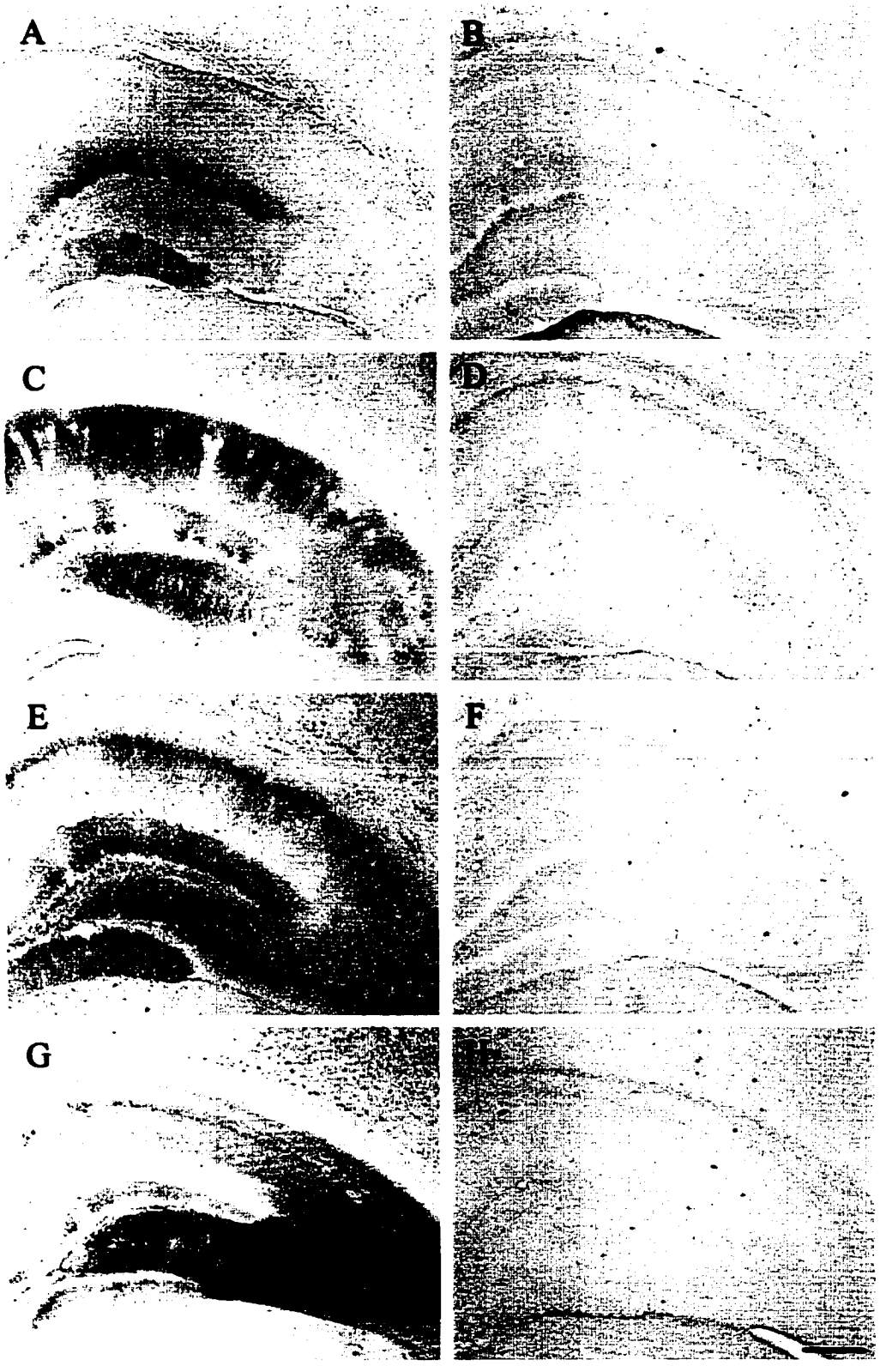

Figure 3-6

Figure 3-7

Hsp70 expression in the parietal cortex of vehicle- and CMZ-injected H-I animals at varying post-hypoxic timepoints.

Photomicrographic representation of Hsp70 expression in the ipsilateral parietal cortex of vehicle-injected (A, C, E, G) and CMZ-injected (B, D, F, H) H-I animals. Animals were sacrificed 6 (A, B), 12 (C, D), 24 (E, F) and 48 (G, H) hours post-injection. (Scale bar = 400 μm).

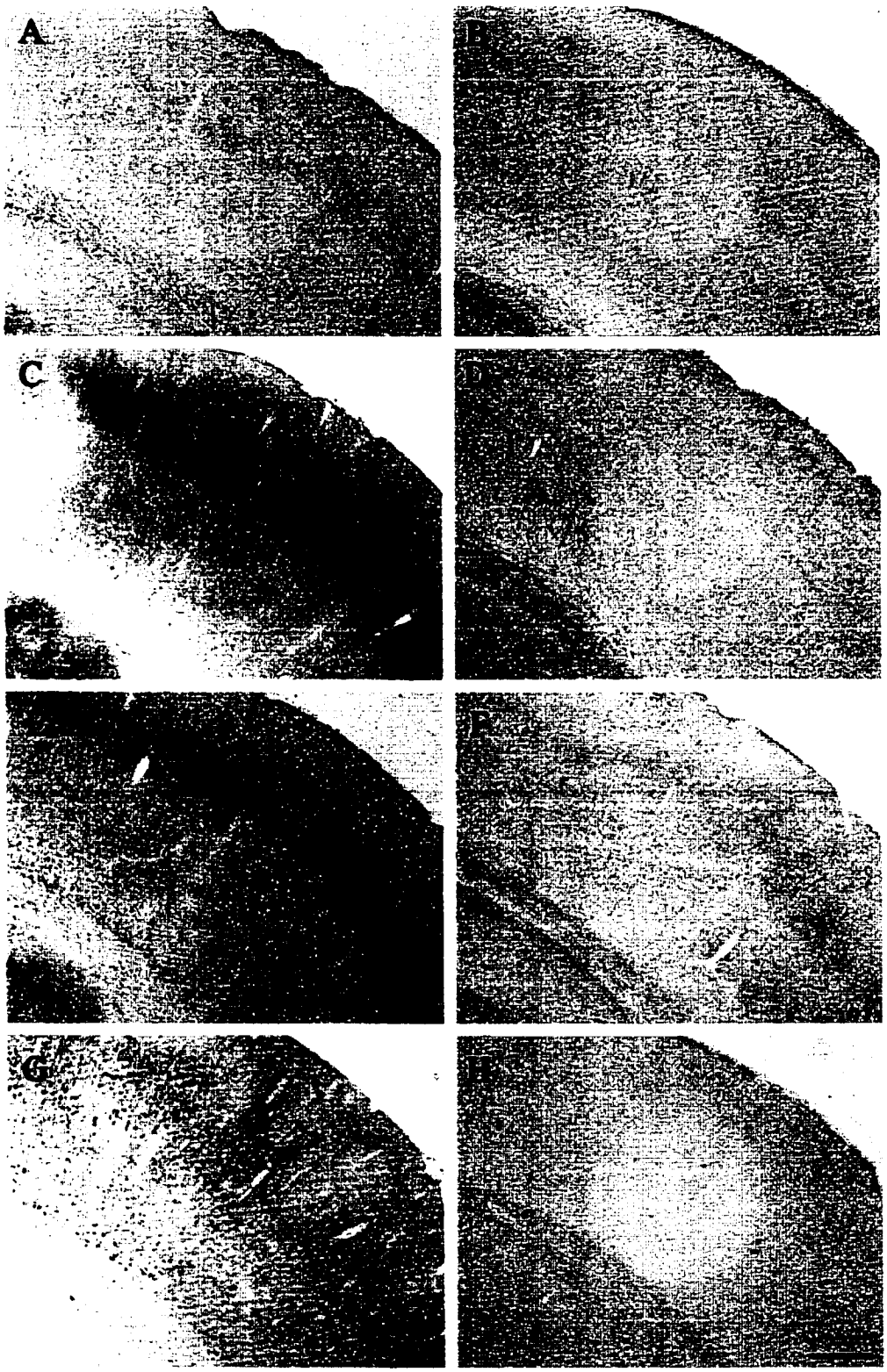

Figure 3-7

Figure 3-8

Neuronal expression of Hsp27 protein.

Hsp27 protein expression was detected in hippocampal neurons (A) and cortical neurons (B) of vehicle-injected H-I animals at various post-hypoxic timepoints. Specific neuronal staining in the hippocampus and cortex is indicated by arrows. (Scale bar =50 μm)

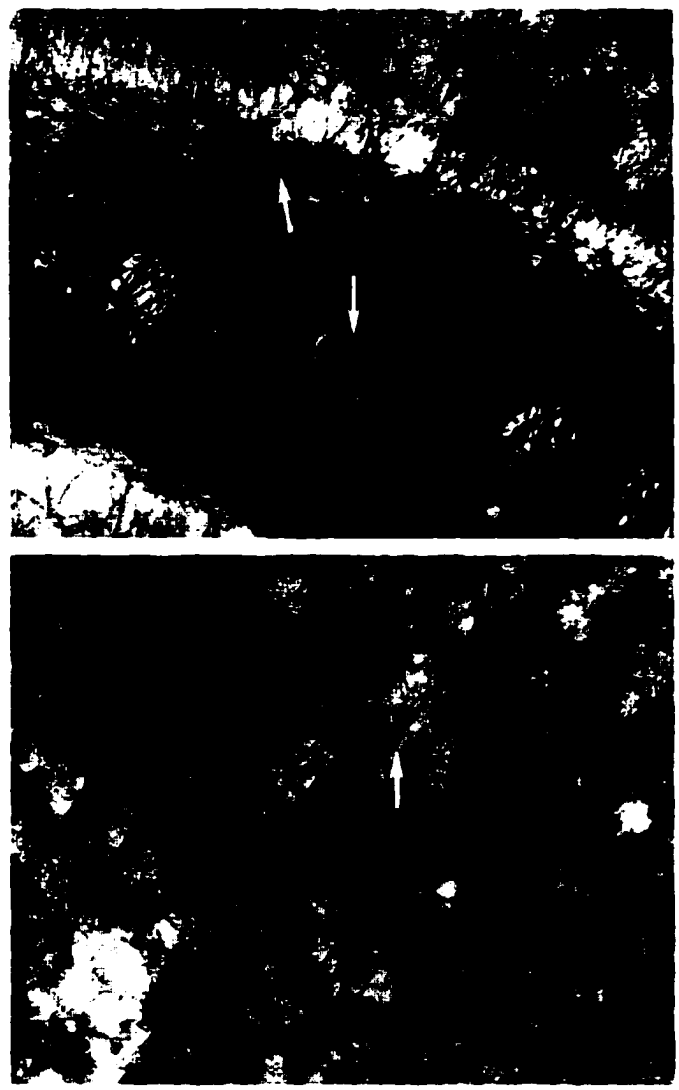

Figure 3-8

H-I animals that received the fully protective dose of CMZ at 3 hours post-hypoxia exhibited basal levels of Hsp27 expression in all animals sacrificed at 1 (N=4), 2 (N=5), 3 (N=3), 6, (N=6), 12 (N=12), 24 (N=4), 48 (N=5) and 72 (N=8) hours post-injection. Similar to the results produced using Hsp70 immunohistochemical analysis, H-I animals that had received 100 mg/kg at 3 hours post-hypoxia exhibited varying profiles of Hsp27 expression at 12 (N=4) and 24 (N=6) hours post-injection but were at basal levels by 48 (N=5) and 72 (N=4) hours post-injection. See Figures 3-9 and 3-10.

Western Analysis

Specificity of the anti-Hsp70 mouse monoclonal antibody was confirmed by immunohistochemical analysis of total protein that had been electrophoretically-fractionated by one-dimensional polyacrylamide gel electrophoresis (PAGE). The anti-Hsp70 antibody recognized one band of approximately 70 kDa in the hippocampal homogenate derived from the ipsilateral hippocampus of 4/4 vehicle-injected H-I animals. Faint expression of Hsp70 was noted at both 12 and 24 hours post-injection in the ipsilateral hippocampus of 3/7 CMZ-injected animals while 4/7 of these animals exhibited basal levels of this protein. No expression of Hsp70 was detected in any control animals examined using this antibody.

Figure 3-9

Hsp27 expression in the hippocampus of vehicle- and CMZ-injected H-I animals at varying post-hypoxic timepoints.

Photomicrographic representation of Hsp27 expression in the ipsilateral hippocampus of vehicle-injected (A, C, E, G) and CMZ-injected (B, D, F, H) H-I animals. Animals were sacrificed 12 (A, B), 24 (C, D), 48 (E, F) and 72 (G, H) hours post-injection. (Scale bar = 400 μm)

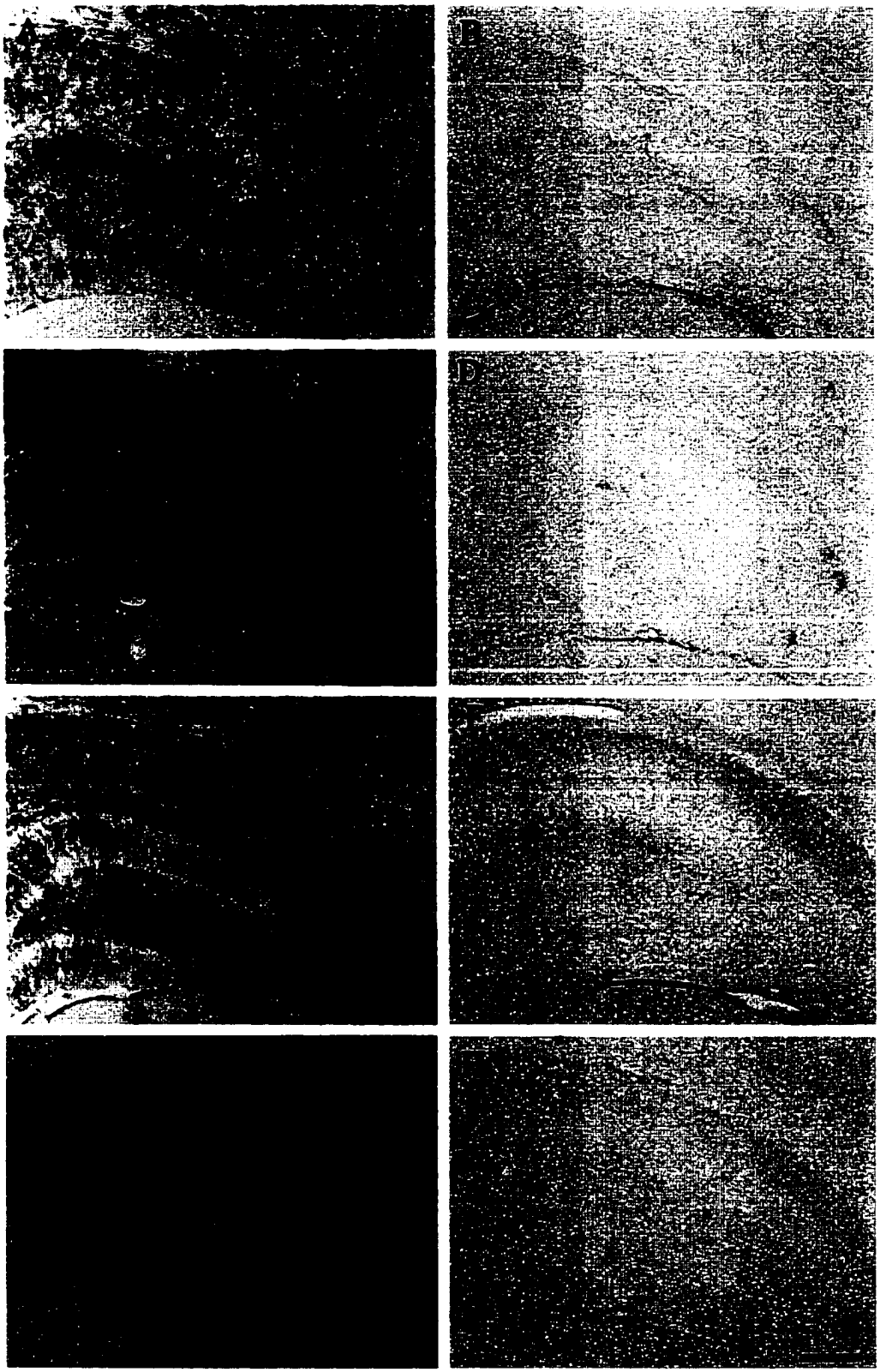

Figure 3-9

Figure 3-10

Hsp27 expression in the parietal cortex of vehicle- and CMZ-injected H-I animals at varying post-hypoxic timepoints.

Photomicrographic representation of Hsp27 expression in the ipsilateral parietal cortex of vehicle-injected (A, C, E, G) and CMZ-injected (B, D, F, H) H-I animals. Animals were sacrificed 12 (A, B), 24 (C, D), 48 (E, F) and 72 (G, H) hours post-injection. (Scale bar = 400 μm).

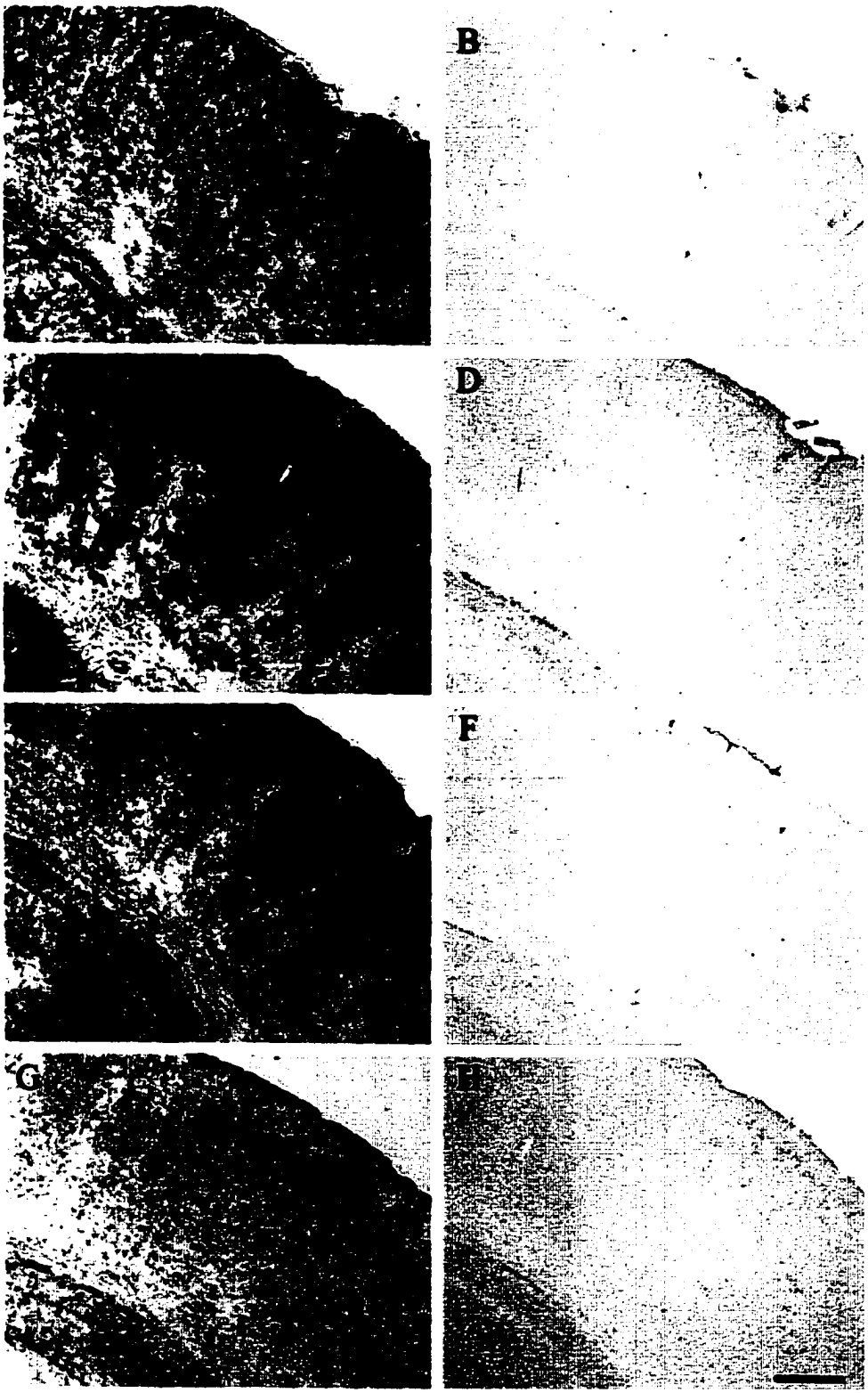

Figure 3-10

Discussion

In spite of evidence that has indicated that both CMZ and Hsps provide neuroprotection in animal models of ischemia, this study was the first to investigate putative interactive effects between CMZ and the endogenous stress response. The results of this study, however, did not support an involvement of Hsps in CMZ-induced neuroprotection against H-I injury. In fact, CMZ administration at 3 hours post-hypoxia had a negative effect on the levels of *hsp* mRNA induced by H-I that was detectable by 2 hours post-injection. Moreover, CMZ administration at 3 hours post-hypoxia appeared to selectively prevent the translation of these transcripts in protected cell layers. These findings may indicate that CMZ administration interrupts the ischemic cascade upstream of Hsp activation in order to achieve its neuroprotective effect.

As in other ischemia studies, neuronal expression of *hsp70* mRNA and protein was up-regulated in a temporal and graded fashion in vehicle-injected H-I animals used in this study (Gonzalez *et al.*, 1991; Simon *et al.*, 1991; Kobayashi *et al.*, 1995). Specifically, a profound induction of *hsp70* mRNA was observed throughout the ipsilateral hippocampus and cortex of H-I animals for at least 12 hours following a vehicle injection (15 hours post-hypoxia). This timeline of expression for *hsp70* mRNA is in accordance with timelines reported using other animal models of ischemia (Kobayashi *et al.*, 1995; Wagstaff *et al.*, 1996). In contrast, H-I animals that received a CMZ (200 mg/kg) injection at 3 hours post-hypoxia showed high levels of *hsp70* mRNA expression for up to 3 hours post-injection in the ipsilateral hippocampus and cortex, however, expression of this transcript was at basal levels in all cell layers of these animals by 12 hours post-injection. When pairwise comparisons were made between *hsp70* mRNA expression in CMZ-injected and vehicle-injected H-I animals, mean density of *hsp70* expression was found to be significantly higher in susceptible cell layers of vehicle-injected H-I animals at 2, 3 and 12 hours post-injection. Thus by 2 hours post-injection the, seemingly synchronous, negative effects of CMZ administration on *hsp70* expression were evident. However, at 24 hours post-injection a secondary increase in *hsp70* mRNA

expression, specific to the CA1 pyramidal cell layer, was observed. This delayed elevation may be indicative of delayed neuronal death and may correspond to the slight increase in mean neuronal death observed in some CMZ-injected (200 mg/kg) H-I animals sacrificed at 4 weeks, relative to 1 week, post-hypoxia (see Chapter 1). Thus, while early *hsp70* expression may not predict subsequent cell death, a secondary induction of this transcript may signify impending cell death. This finding may also explain the neuroprotective success of a prolonged infusion of low dose CMZ against ischemic injury, reported by Cross *et al.* (1995), as the presence of CMZ at delayed post-hypoxic timepoints may interfere with events responsible for the secondary increase in *hsp70* mRNA expression.

One explanation for the CMZ-induced reduction in *hsp70* mRNA levels may be that, once administered, CMZ interrupted additional transcription of this mRNA. Alternatively, since *hsp70* mRNA has been shown to have a relatively long half-life (12-24 hours), the rate of reduction in the level of this transcript observed in this study may indicate that CMZ administration increased the degradation of *hsp70* mRNA (Mizzen *et al.*, 1988; Kirino *et al.*, 1991). A finding reported by Yenari *et al.*, (1998) is particularly relevant to this hypothesis. Yenari *et al.*, (1998) infected striatal neurons of rats with a viral vector containing sequences for both *hsp70* and *β-galactosidase (β-gal)*, under two separate promoters, 12 hours prior to focal cerebral ischemia (MCAO). Gene transfer therapy with the *hsp70* overexpressing vector improved neuronal survival following MCAO, whereas infection with control vectors was of no neuroprotective benefit. Infected neurons exposed to cerebral ischemia *in vivo* exhibited co-expression of Hsp70 protein and β-gal up to 18 hours post-injection (6 hours post-ischemia). However, by 36 hours post-injection immunohistochemical analysis no longer detected Hsp70 expression, yet the levels of β-gal staining remained high in infected neurons up to 60 hours post-injection. The authors determined that the discrepancy in expression patterns of these proteins was not likely due to differences in the duration of expression of the two promoters, as both promoters (α4 and α22) were immediate early promotors of the herpes simplex virus (HSV) and would, therefore, be expected to show similar kinetics of expression (Ho *et al.*, 1995). Considering the striatal neurons infected with the *hsp70*-containing

vector were protected against subsequent ischemic insult (12 hours later), these findings may indicate an active suppression of *hsp70* expression following ischemia in protected cells. It is not known whether the effects observed in that study were due to a decrease in *hsp70* transcription, an increased degradation of *hsp70* mRNA and/or a block in the translation of Hsp70 protein. However, it is interesting that the neuroprotective effect of CMZ, observed in the present study, caused a rapid decrease in *hsp70* mRNA expression and prevented the translation of Hsp70 in all protected cell layers following H-I.

It is conceivable that CMZ administration reduced *hsp70* mRNA expression following H-I by causing a premature translation of this transcript into its functional protein. Thus, immunohistochemical analysis was conducted to determine whether CMZ altered Hsp70 protein expression patterns following H-I. Hsp70 expression was first detected in the dentate gyrus (DG) and in the cortical infarct zone at 1-2 hours post-injection in vehicle-injected animals. By 12 hours post-hypoxia, Hsp70 expression was evident in all susceptible cell layers and remained at detectable levels for at least 48 hours post-injection. This finding is in agreement with other reports documenting Hsp70 expression following an excitotoxic injury (Welsh *et al.*, 1992; Kinouchi *et al.*, 1993; Armstrong *et al.*, 1996; Zhang *et al.*, 1996). In contrast, immunohistochemical analysis of sections from CMZ-injected H-I animals, sacrificed between 1 hour and 7 days post-injection, demonstrated that Hsp70 protein was not expressed in any brain region. Thus, CMZ administration did not induce a premature translation of *hsp70* mRNA in susceptible cell layers in this model. In fact, CMZ administration appeared to prevent translation of Hsp70 in all cell layers that would normally have died following H-I, but not in cell layers known to be highly resistant to H-I injury, such as the DG.

Differential induction patterns were noted for *hsp27* mRNA expression across susceptible cell layers following H-I. In vehicle-injected H-I animals, significant detection of *hsp27* was first evident in CA3 at 1 hour post-injection. At 2 and 3 hours post-injection, *hsp27* expression was significantly elevated in CA1, CA3 and in the cortex of these animals. At 12 hours post-injection, significant expression of *hsp27* remained in CA3 and in the cortex but had diminished in CA1. An injection of CMZ

(200 mg/kg) in H-I animals at 3 hours post-hypoxia reduced *hsp27* mRNA expression in both CA3 and the cortex and prevented significant induction of *hsp27* in CA1 cells. It is also noteworthy that *hsp27* mRNA was never expressed above control levels in the DG of vehicle- or CMZ-injected H-I animals, which is the one cell layer in the hippocampus that is resistant to H-I injury. Immunohistochemical analysis of sections from vehicle-injected H-I animals indicated that Hsp27 protein expression remained at control levels in all cell layers for up to 6 hours post-injection. However, by 12 hours post-injection Hsp27 protein was detected in the basket cells of the DG and was sporadically expressed in glia around pyramidal cell layers in the hippocampus and in the penumbral region of the cortex. High levels of Hsp27 expression remained up to 3-4 days post-hypoxia in vehicle-injected H-I animals. Hsp27-positive cells in these animals appeared to be predominantly glial in origin. Previous studies have indicated that, following kainic acid administration, Hsp27-positive cells are likely reactive astrocytes and/or microglia (Plumier *et al.*, 1996). However, in the present study, Hsp27 was also detected in neurons of the ipsilateral hippocampus and cortex of vehicle-injected H-I animals approximately 24-72 hours post-injection. Hsp27-postive cells were not detected in any cell layers of CMZ-injected H-I animals at any post-hypoxic timepoint examined. Thus, regardless of cell type, administration of a neuroprotective dose of CMZ (200 mg/kg) at 3 hours post-hypoxia completely prevented the expression of Hsp25 in H-I animals. This finding strongly suggests that Hsp27 is not involved in CMZ-induced neuroprotection. Reports have indicated that Hsp27 expression is also prevented in a preconditioning paradigm of neuroprotection. Kato *et al.* (1994) demonstrated that preconditioning the rat brain with sublethal cerebral ischemia produced tolerance to a subsequent lethal period of ischemia. In contrast to non-preconditioned animals, no expression of Hsp27 was evident in brain regions of preconditioned animals following ischemia. Furthermore, any Hsp27 expression that had been induced by exposure to the sublethal preconditioning ischemic event in that study was predominantly detected in glial cells which indicates that Hsp25 expression was not directly involved in the neuronal protection provided by ischemic preconditioning.

Significantly elevated levels of *hsp40* transcript were observed in CA1, the

DG and the cortex of vehicle-injected H-I animals at 1, 2, 3 and 12 hours post-injection. High levels of *hsp40* were also detected in CA3 of these animals, however, statistical significance was only attained at 1 and 2 hours post-injection. As with the other *hsp* transcripts, CMZ (200 mg/kg) administration altered the expression patterns for this transcript such that the expression of *hsp40* mRNA did not reach significant levels in CA3, the DG or in the cortex of CMZ-injected H-I animals at any time point examined. Moreover, significant *hsp40* expression was only detected in the CA1 layer of CMZ-injected H-I animals at 2 hours post-injection. Cell layers that demonstrated an elevation of *hsp40* mRNA in vehicle- or CMZ-injected H-I animals did not exhibit any correlation with ultimate cell fate.

To date, studies that have suggested a neuroprotective role for Hsps have shown that overexpression of these proteins either prior to or during a cellular stress is neuroprotective (Marber *et al.*, 1995; Chen *et al.*, 1996b; Mosser *et al.*, 1997). Sato *et al.* (1996) demonstrated that prior heat shock (42°C for 30 minutes), which causes increased *hsp70* expression, significantly increased the number of surviving rat hippocampal neurons in primary culture upon addition of serum free media. However, treatment with an *hsp70* antisense oligonucleotide (AON) suppressed the neuroprotective effect of heat shock to control levels indicating that Hsp70 expression was essential to the neuroprotective effect of prior heat shock. However, pre-induction of these proteins in ischemia models is associated with a host of changes in protein expression and metabolism which makes it difficult to ensure that Hsps play a pivotal role in mediating neuroprotection in these models. Indeed, protection in ischemic tolerance studies has been reported even when Hsp synthesis has been blocked (Smith and Yaffe, 1991). Furthermore, Buzzard *et al.* (1998) demonstrated that activation of SAPK/JNK following a lethal stressor was strongly inhibited in thermotolerant cells that exhibited high levels of Hsps. However, cells that constitutively over-expressed Hsp70, but were not made thermotolerant, did not demonstrate decreased SAPK/JNK activation following exposure to lethal stressors. Thus factors, other than Hsp70 expression, induced by the thermotolerant state may have reduced the activation of the PCD cascade in that study. As such, it is presently not known whether an increase in Hsp expression at post-ischemic timepoints is of

any neuroprotective value. Certainly, studies have shown that even very high cellular levels of *hsp70* mRNA and protein following a severe excitotoxic insult is not sufficient to prevent neurodegeneration (Armstrong *et al.*, 1996; Gilby *et al.*, 1997).

In conclusion, we have shown that CMZ does not augment the endogenous stress response in order to provide neuroprotection in the H-I model. In fact, the decreased expression of *hsp* transcripts in CMZ-injected, relative to vehicle-injected H-I animals, at 2, 3 and 12 hours post-injection may suggest that CMZ administration actively terminates the transcription or promotes the degradation of these mRNAs. Such an active reduction of all *hsp* mRNAs and proteins following administration of this compound may indicate that CMZ interferes with H-I induced events upstream of Hsp activation. A clear understanding of the induction mechanisms for Hsps may, therefore, implicate a route through which CMZ administration interferes with the expression of these transcripts and selectively blocks their translation in protected tissues. It has been reported that increased intracellular levels of calcium induce *hsp70* mRNA and protein (Kiang *et al.*, 1994). In addition, the activation of many Hsp genes in yeast is caused by reduced intracellular cAMP levels (Fuhr *et al.*, 1976; 1977; Kiang and Tsokos, 1998). Increased activation of inositol 1,4,5-triphosphate ($InsP_3$) and PKC has also been shown to increase Hsp70 production whereas a decrease in $InsP_3$ reduced Hsp70 expression (Kiang *et al.*, 1994; Kiang and Tsokos, 1998). Several studies have also indicated that protein unfolding is required to elicit stress-induced expression of *hsps* (Ananthan *et al.*, 1986; Morimoto *et al.*, 1994). Finally, the induction of Hsp70 has been observed in response to increased levels of ceremide, a second messenger in the apoptotic cascade (Ahn *et al.*, 1999). Clearly, the results of this study can not determine whether CMZ directly or indirectly intereferes with any one of these events in order decrease *hsp* mRNA expression or to halt Hsp70 translation. However, future studies directed towards the determination of the mechanism through which CMZ reduces the expression of Hsps may provide information applicable to the neuroprotective actions of CMZ in ischemia models.

Chapter 4: An Investigation into Putative mRNAs Linked to CMZ-Induced Neuroprotection in the H-I model

Summary

In this series of experiments, the predictive validity of the differential display protocol was first examined in the H-I model using *c-fos* mRNA as a positive control. A *c-fos*-targeted primer set was used during PCR amplification of cDNA derived from RNA samples extracted from the ipsilateral hippocampus of control animals and the ipsilateral and contralateral hippocampii of vehicle-injected H-I animals. When the resultant PCR products were electrophoretically fractionated, increased expression of a fragment that corresponded to rat *c-fos* mRNA was observed in the ipsilateral hippocampus of H-I animals at 3 and 6 hours post-hypoxia on a differential display autoradiogram. However, expression of this fragment was not detected in control tissues at these timepoints. An identical pattern of *c-fos* mRNA expression was observed on a northern blot when the isolated fragment or a manufactured *c-fos* oligonucleotide was used as a hybridization probe. Thus, the expression pattern of *c-fos* mRNA produced on a differential display autoradiogram following PCR amplification was identical to that observed in the original RNA populations contained on a northern blot.

Once the predictive validity of the differential display protocol was established in the H-I model, this technique was used to examine differential gene expression in susceptible cell layers of vehicle-injected and CMZ-injected H-I animals sacrificed at 12 and 24 hours post-injection. A putative neuroprotection-related fragment was isolated using differential display that corresponded to sequence from rat *calmodulin* mRNA. On the differential display autoradiogram, the *calmodulin* fragment was expressed in all cDNA populations examined except those derived from the ipsilateral hippocampus of CMZ-injected H-I animals sacrificed at 12 and 24 hours post-injection. This expression pattern was replicated using northern blot analysis where *calmodulin* mRNA was significantly increased relative to control animals in the ipsilateral hippocampus of vehicle-injected, but not CMZ-injected, H-I animals sacrificed at 12 and 24 hours post-injection. The results of this study indicate that PCR-amplified cDNA samples used in differential display can accurately reflect relative transcript expression in template mRNA populations. In addition, the reduced expression of *calmodulin* mRNA in the hippocampus of CMZ-injected H-I animals sacrificed at 12 and 24 hours post-hypoxia

may indicate that CMZ-induced neuroprotection is achieved through direct or indirect antagonism of *calmodulin* mRNA expression.

Introduction

There are approximately 50 000-100 000 genes in the human genome, however, both the identity and number of genes expressed in a given cell may vary with time, physiological conditions and disease states (Wang *et al.*, 1996). As such, the ability to detect and characterize differences in gene expression is central to the understanding of molecular mechanisms involved in both normal and pathological states. Determination of factors that control the activation and/or suppression of these molecular mechanisms may provide some insight toward the discovery of new molecular targets for pharmacological manipulation and drug development (Wang *et al.*, 1996). Within the last decade, the emergence of molecular biological tools, such as differential display, has enabled scientists to examine changes in gene expression induced by a variety of pathological states including ischemia, heart disease, diabetes and certain cancers (Liang and Pardee, 1992, 1995; Mok *et al.*, 1994; Nishio *et al.*, 1994; Utans *et al.*, 1994).

Differential display is a powerful, PCR-based, molecular technique that permits the simultaneous screening of large numbers of transcripts and can be used, in combination with DNA sequencing, to detect mRNAs that are unique to a particular cell type, tissue or developmental stage (Liang and Pardee, 1992). Briefly, the methodology used in differential display involves the use of 3'-anchored primers to reverse transcribe cellular mRNA to single-stranded cDNA, which is then used as a substrate for a series of polymerase chain reactions (PCR). Specific PCR cycling parameters and primer sets (an arbitrary upstream primer and an anchored downstream primer) are used to generate a subpoplation of cDNA fragments that correspond to the 3' ends of the mRNAs present in the original total RNA population. Following electrophoretic fractionation of the radio-labeled PCR products, potentially interesting fragments (cDNAs) can be excised from the dried gel, cloned and sequenced in order to determine their identity. Several molecular techniques have been used to confirm the differential expression of specific mRNAs that correspond to fragments isolated from the differential display gel. These techniques include quantitative reverse transcription-polymerase chain reaction (RT-PCR), RNase protection assays and use of the excised fragment as a hybridization probe in northern blot or dot blot analyses (Callard *et al.*, 1994).

Although the utility and power of differential display as a molecular tool is well established, a few technical difficulties remain (Callard *et al.*, 1994; Bertioll *et al.*, 1995). The detection of differential gene expression from fractionated cDNA relies on differences in PCR product abundance between samples. However, the kinetic parameters governing the amplification of products via PCR are complex. This is especially true in reactions, such as those used in differential display, where many products are generated in the same tube. For instance, it has been shown that, in the late cycles of PCR, the amplification rate of abundant PCR products generally declines faster than the amplification rate of less abundant products in the same tube (Mathieu-Daudé *et al.*, 1996). This effect is due to the high concentration of PCR products at late cycling stages in the PCR reaction which increases the probability that the PCR product strands will re-anneal during the low temperature phase of each PCR cycle (Gilliland *et al.*, 1990). Therefore, differences in initial product abundance may diminish as the number of PCR cycles increase and result in an underestimate of the "true differences" in starting template concentrations. This phenomenon is known as the "C_0t effect" (Mathieu-Daudé *et al.*, 1996). Furthermore, Callard *et al.* (1994) demonstrated that cDNAs isolated from the differential display gel may be contaminated with unrelated cDNA sequences of a similar size that are actually not differentially expressed. Such contamination may lead to the artificial isolation of "false positive" fragments, as detected by autoradiography, from electrophoretically fractionated cDNA. Thus, even in experiments where samples are processed in parallel using identical buffers, polymerase concentration and cycling parameters, it is not always possible to amplify all products such that their final concentration accurately reflects their relative starting concentrations. These inherent difficulties are further amplified when differential display is used to examine changes in gene expression within specific brain regions that have a complex mRNA population and/or a heterogeneous cell population (Sutcliff *et al.*, 1983). In view of these difficulties, it is important to design differential display experiments that include controls for as many sources of experimental variability as possible. Previous attempts to circumvent these problems have focussed on such variables as RNA preparation, primer length variation and better experimental design (Liang and Pardee, 1995).

It is also conceivable that inclusion of a paradigm-specific positive control in the

initial differential display of any series of experiments would be useful. Specifically, the initial differential display for a set of PCR-generated samples should be carried out using a primer set that has been designed to amplify a cDNA fragment that corresponds to a mRNA with a known pattern of expression within that paradigm. For instance, if the induction pattern of a specific mRNA has been established by northern blot or *in situ* hybridization analysis in an experimental paradigm, then use of a primer set designed to target that gene in the same RNA population should produce a banding pattern on a differential display autoradiogram that is identical to the banding pattern on a northern blot. In this way, it can be determined whether the PCR-amplified samples accurately reflect known changes in gene expression within an experimental paradigm. However, choosing a positive control mRNA that would be applicable to any experimental paradigm has proven difficult. Ideally, selection criteria would include genes that have a robust expression and are induced by a number of cellular events.

c-fos, an immediate-early gene (IEG), is rapidly but transiently activated in the brain following many endogenous and exogenous stimuli and is considered to be a marker for neuronal activation (Herrera and Robertson, 1996). While the cascade of intracellular events that lead to the expression of *c-fos* has yet to be fully mapped, *c-fos* induction appears to occur through multiple signaling pathways that involve different second messenger systems (Sheng and Greenberg, 1990; Morgan and Curran, 1991; Hisanga *et al.*, 1992). Generally, the activation of any intracellular messenger that can bind to the Ca/CRE and SRE elements in the *c-fos* promotor can initiate its transcription (Herrera and Robertson, 1996). In pheochromocytoma cells (PC12), there are at least three different second messenger systems that can activate *c-fos* transcription, those being: diacylglycerol (DAG)-protein kinase C, cAMP and calcium-calmodulin (Greenberg *et al.*, 1985; Greenberg *et al.*, 1986a; Morgan and Curran, 1986). Consequently, *c-fos* induction has been reported in a multitude of experimental paradigms ranging from the endogenous circadian rhythm to neurodegenerative diseases (Hughes *et al.*, 1992; Herdegen *et al.*, 1995; Guido *et al.*, 1999). In this way, *c-fos* mRNA may be an ideal candidate for use as a paradigm-specific positive control in the initial differential display experiment used in a number of experimental paradigms.

The first objective of this series of experiments was to determine the predictive

validity of the differential display protocol in the H-I model by comparing *c-fos* expression, as detected on a northern blot by a manufactured oligonucleotide probe, to *c-fos* expression on a differential display autoradiogram generated using *c-fos*-targeted primers. The second objective of this experiment was to use differential display to identify changes in gene expression that may be related to H-I induced delayed cell death or to CMZ-induced neuroprotection in H-I tissue. Molecular screening of mRNA populations generated from ischemic and control tissue may identify important changes in gene expression, of known or unknown sequence, linked to ischemia-induced delayed cell death. In the H-I animal model, delayed neuronal death (12-24 hours post-hypoxia) is observed in the pyramidal and hilar regions of the ipsilateral hippocampus and in layers 1-6 of the ipsilateral parietal cortex, however, all cell layers in the contralateral hemisphere remain completely intact (Gilby *et al.*, 1997). Thus, differences in gene expression that may be responsible for ischemia-induced cell death can be identified in a single animal through comparison of gene expression in the ipsilateral versus contralateral brain structures following H-I. In this way, the contralateral brain structures can serve as an internal hypoxic control. Furthermore, comparison of differential gene expression in susceptible ipsilateral brain structures between vehicle and CMZ (200 mg/kg)-injected H-I animals may reveal the identity of genes that are relevant to the neuroprotection provided by CMZ in H-I animals.

Methods

The animals used in this experiment were treated in an identical manner to the protocol outlined in Chapter 1. All animals were decapitated at 3, 6, 12 or 24 hours post-hypoxia, or, when appropriate, at 12 or 24 hours post-injection. The differential display method used in this set of experiments was similar to the methodology described in Denovan-Wright *et al.* (1999) and was based on the commercially available Clontech Delta RNA fingerprinting™ protocol (The Delta Fingerprinting Kit; CLONTECHniques, X, 5). Disposable sterile plasticware was used wherever possible to avoid RNase contamination of samples.

RNA extraction

Brains were removed from control, vehicle-injected H-I and CMZ-injected H-I animals and the ipsilateral and contralateral hippocampii and corticies were extracted. These tissues were immediately frozen in liquid nitrogen and put into cryovials for long-term storage in liquid nitrogen. Tissue samples from some animals were pooled (3 animals) while some samples only contained tissue from a single animal. Total RNA was isolated from these samples using TRIzol™ reagent (Gibco BRL). First, frozen tissue was added to a centrifuge tube containing 1.0 ml of TRIzol per 50 mg of tissue and homogenized using a polytron until the sample was uniformly dissociated. 200 µl of chloroform per 1 ml of Trizol used for homogenization was then added and the tubes were shaken vigorously and incubated for 3 minutes at room temperature. The homogenate was centrifuged at 12,000 g for 15 minutes at 4°C. A colorless upper aqueous phase formed that contained the RNA. The aqueous phase was removed, placed in a sterile microfuge tube and mixed with 0.5 ml isopropanol per 1.0 ml Trizol used in the initial extraction. The solution was then permitted to precipitate at room temperature for 15 minutes and centrifuged at 12, 000 g for 15 minutes at 4°C. The supernatant was, once again, removed and the RNA pellet was washed using 75% ethanol. Following the ethanol wash, all remaining ethanol was removed and the RNA pellet was permitted to dry at room temperature before resuspension in 30 µl of dH_20. The sample was then heated to 65°C for 10 minutes. The concentration of the RNA in each sample was

determined using a spectrophotometer.

Reverse Transcription

Following RNA extraction, 10 μg of RNA from each sample was added to 5 μl of 10X One-Phor-All Plus buffer (Pharmacia), 1μl of RNAsin™ (Promega) 20 U/μl, 1 μl of RQ1 RNase-free DNase (Promega) 1 U/μl and dH_20 to a final volume of 50 μl. Samples were then incubated at 37°C for 30 minutes. The DNase-free RNA sample was extracted using 100 μl of Trizol reagent in a manner identical to the protocol used in the initial total RNA extraction procedure. The resultant RNA pellet was resuspended in 9 μl of DEPC-treated H_20.

In order to reverse-transcribe the DNase-treated RNA into single-stranded cDNA, 2μg of each RNA sample (4 μl of the 500 ng/μl DNase-treated sample) was added to 1 μl of 1 μM oligo dT (12-18mer), heat-denatured at 70°C for 3 minutes and put on ice for 3 minutes. Once denatured, 5 μl of first-strand cDNA master mix [2 μl of 5X first strand cDNA buffer (250 mM Tris-HCl, pH 8.3, 375 mM KCl, 15 mM $MgCl_2$, 50 mM dithiothreitol), 2 μl 5mM dNTP and 1 μl of M-MLV reverse transcriptase (Gibco BRL) for each reverse transcriptase reaction to be performed)] was added to the chilled RNA/oligodT mixture and incubated at 42°C for 60 minutes. Following incubation, mixtures were heated to 80°C for 5 minutes in order to heat-inactivate the reverse transcriptase. The single-stranded cDNA mixtures were then diluted to a final volume of 100 μl using dH_20 and stored at -20°C.

PCR Amplification

The differential display master mix included the following reagents: 6.6 μl of dH_20, 1 μl of 10X KlenTaq Buffer (ClonTech), 0.1 μl of 5 mM dNTP, 0.1 μl [α^{33}P]dATP (2000Ci/mmol), 0.5 μl of 5' (P) primer (20 μM), 0.5 μl of 3' (T) primer (20 μM) and 0.2 μl of 50X Advantage™ KlenTaq polymerase mix (Clontech). After mixing, 9 μl of the differential display master mix was added to 1 μl of each cDNA reaction. The resultant mixture was subject to the following PCR conditions: 1) 94°C for 5 min, 2) 40°C for 5 min, 3) 68°C for 5 min 4) 94°C for 2 min 5) 40°C for 5 min 6) 68°C for 5 min 7) Repeat

steps 4-6, 1 time 8) 94°C for 1 min 9) 60°C for 1 min 10) 68°C for 2 min + 4 sec/cycle 11) Repeat steps 8-10, 26 times 12) 68°C for 7 min 13) 0°C soak.

Primers used in Differential Display

The 5' primers (P1-P10) used in these experiments consisted of 16 nucleotides that correspond to the T3 polymerase recognition site. The 5' primers also contain a 9 nucleotide sequence that is involved in the initial priming of the cDNA during the first few low temperature annealing reactions (Denovan-Wright *et al.*, 1999). The 3' primers (T1-T9) contain the recognition site for T7 polymerase and nine T residues followed by two nucleotides that are either A, C or G. The nine T residues enable the 3' primer to anneal to all cDNA that contains a poly A sequence (Denovan-Wright *et al.*, 1999).

A specific primer set was designed to selectively amplify *c-fos* cDNA during the PCR amplification reactions. The 5' primer (5' ATT-AAC-CCT-CAC-TAA-AGG-TTC-CTG-G 3') has the T7 polymerase recognition sequence followed by 8 nucleotides that would anneal with single-stranded *c-fos* cDNA. The 8 3' terminal nucleotides of this oligonucleotide primer correspond to nucleotides 1734-1741 of the *c-fos* cDNA (Genbank Accession number X06769). The last two nucleotides of the 3' primer (5' CAT-TAT-GCT-GAC-TCA-TAT-CTT-TTT-TTT-TGC 3') used to target *c-fos* could anneal with the two nucleotides that precede the poly A tail of *c-fos* transcripts in addition to a large number of other transcripts.

Gel Electrophoresis

Following the PCR amplification, 10 µl of standard denaturing loading dye (deionized formamide, 10mM Na_2EDTA; pH 8.0, 0.1% w/v xylene cyanol, 0.1% w/v bromophenol blue) was added to each sample and then heated at 92°C for 3 min and chilled on ice. Samples (4 µl) were then loaded on a standard sequencing gel in a Genomyx machine (6% polyacrylamide, 8 M urea gel). Electrophoretic fractionation of the PCR products occurred under the following conditions: 50°C, 3000V, 100 W. Once the gel had run for approximately 4 hours (until xylene cyanol ran off the bottom of the gel) it was dried until urea crystalization was visable on the surface of the gel. The urea was then rinsed from the gel with dH_2O. The rehydrated gel was transferred to Whatman

3 MM paper and returned to the Genomyx machine until completely dried. The dried gel was exposed to Biomax MR film (Kodak) overnight at room temperature and then re-aligned with the dried gel. Fragments that appeared to be differentially expressed in a banding pattern of interest were excised from the dried gel/3MM paper using a razor blade.

PCR Reamplification Protocol

Once isolated, putative cDNA bands of interest (gel/3MM paper) were rehydrated in 40 µl of dH_20 and incubated at room temperature for 10 minutes. Samples were then heated to 95°C for 5 minutes to dissolve the gel and cooled on ice. Once cooled, 8.5 µl of the solution was added to 10.75 µl of dH_20, 1.25 µl of the 3' and of the 5' primer (20 µM) that had been used to generate the cDNA, 2.5 µl of 10X rTaq buffer (Pharmacia), 0.5 µl of 5 mM dNTP and 0.25 µl of rTaq polymerase (5 U/µl). The cDNA band was then reamplified using the following PCR conditions. 1) 94°C for 1 minute 2) 94°C for 30 seconds 3) 58°C for 30 seconds 4) 68°C for 2 minutes + 4 seconds/ cycle 5) Repeat steps 2, 3 and 4, nineteen times 6) 68°C for 7 minutes 7) 0°C. An aliquot of the resultant mixture was electrophoretically separated on a 1% agarose gel/EtBr (5 µl/ml) in order to visualize the reamplified PCR products. The PCR products cut from the agarose gel were gel-purified using QIAquick Gel Extraction Kit (Qiagen) and cloned using pGem-T cloning vector (Promega) according to the manufacturers' recommended protocol. Electrocompetent Inv cells (Invitrogen) were transformed using one-tenth of the ligation mixture (fragment + vector). DNA was extracted from recombinant bacterial colonies using the Qiagen mini-prep kit and several clones were subjected to dideoxy DNA sequencing using the T7 sequencing kit (Pharmacia) and the M13 Universal forward and reverse sequencing primers. The sequencing reactions were fractionated on a 6% acrylamide denaturing sequencing gel using the standard methodology (Sambrook *et al.*, 1989). DNA sequence obtained using this technique was analyzed using BlastN (Altshul *et al.*, 1990).

Northern Hybridization Protocol

Aliquots (10 µl) of total RNA samples isolated from hippocampal and cortical

cell layers of control, H-I and CMZ-injected H-I animals were fractionated on a 1% formaldehyde agarose gel and transferred to a Zetaprobe nylon membrane (Biorad) using standard methodology (Sambrook *et al.*, 1989). Once the RNA transfer was complete, the membrane was stained with methylene blue in order to visualize the relative concentrations of 28S and 18S ribosomal RNA in each lane. The membrane containing fractionated RNA was first pre-hybridized overnight in 50% formamide, 5X SSC, 1X Denhardt's reagent, 20 mM sodium phosphate, pH 6.8, 0.2% SDS, 5mM EDTA, 10 μg/ml poly A, 50 μg/ml sheared salmon sperm DNA and 50 μg/ml yeast RNA at 42°C. In order to use cDNA clones as probes for Northern analysis, the reamplified PCR fragment was radiolabeled by random hexamer priming using [α-^{32}P] dCTP (3000Ci/mmol) and a Ready-to-Go DNA labeling bead (Amersham Pharmacia Biotech Inc.). This mixture was incubated at 37°C for at least 15 minutes and run through a Sephadex G-25 spin column (Pharmacia) to remove unincorporated radionucleotides. Once labeled, the probe was denatured at 95°C for 5 minutes, put on ice for 3 minutes and then added to hybridization buffer to a final concentration of 2 x 10^6 cpm/ml. Hybridization buffer consisted of 50% formamide, 5X SSC, 10% dextran sulphate, 1X Denhardt's reagent, 20 mm sodium phosphate, pH 6.8, 0.2% SDS, 5mM EDTA, 10 μg/ml polyA, 50 μg/ml sheared salmon sperm DNA and 50 μg/ml yeast RNA. The hybridization mixture was added to the membrane and held at 42°C overnight. The next day, hybridization buffer and non-specific labeling was washed away from the blot using 2X SSC, 0.1% SDS (1 x 20 minutes) at 42°C; 2X SSC, 0.1% SDS (2 x 15 minutes) at 55°C; 1X SSC, 0.1% SDS (2 x 15 minutes) at 55°C and 0.5X SSC, 0.1% SDS (2 x 15 minutes) at 55°C and exposed to Biomax MS (Kodak) autoradiography film at –70°C for 2 or more days. An oligonucleotide probe designed to target *c-fos* mRNA was 3'-end labeled with [α-^{32}P] dATP (3000Ci/mmol) for 90 minutes at 37°C using terminal deoxynucleotidyl transferase (Amersham).

Densitometry

Densitometric analysis of mRNA expression in each lane on a northern blot autoradiogram was performed using the Optical Density-Model GS0290 Imaging Densitometer and Molecular Analyst (Biorad) software to determine the optical density

(OD/mm^2) of transcript hybridization in specific brain regions. The relative density of labeling was compared to the density of 18S and 28S ribosomal RNA (rRNA) visible on the northern blot membrane once stained with methylene blue and on the spectrophotometric determination of the concentration of RNA in each sample. Animals from all control groups were analyzed as one group for statistical and graphical analysis. Any differences in mean transcript expression were statistically analyzed using a 1-way ANOVA followed by Tukey's post-hoc analysis.

Results

A total of 35 primer sets were used to PCR-amplify cDNA derived from total RNA extracted from the ipsilateral hippocampii and corticies of control animals, vehicle-injected and CMZ-injected H-I animals. These primer sets were also used to PCR-amplify cDNA populations derived from the contralateral hippocampus of vehicle-injected H-I animals which was used as an internal hypoxic control. These primer sets generated numerous fragments that conformed to an expression pattern of interest. Once sequenced some of these fragments were identified to share a very high sequence similarity to genes such as calmodulin, transferrin, B1SINE, acyl CoA oxidase, *c-fos* and thymidylate synthase. However, some of these fragments did not share sequence with any known genes recorded in GenBank.

Predictive Validity of the Differential Display Protocol

A *c-fos*-targeted 5' primer and an oligodT 3' primer (T6) were used to amplify reverse transcribed template mRNA isolated from the ipsilateral hippocampus of ligated control animals and the ipsilateral and contralateral hippocampii of H-I animals. The resultant PCR products were then fractionated on a denaturing acrylamide gel. The majority of co-migrating bands on the differential display autoradiogram were present in all lanes of the autoradiogram. Only one fragment on the autoradiogram conformed to the banding pattern of interest. Specifically, the fragment was present in the ipsilateral hippocampus of H-I animals sacrificed at 3 and 6 hours post-hypoxia. It is noteworthy that a faint band was also noted in the lane that corresponded to the contralateral hippocampus of H-I animals sacrificed at 6 hours post-hypoxia. See Figure 4-1A. As judged by the relative mobility of this PCR fragment in relation to a DNA sequencing ladder, the fragment was estimated to be approximately 420 base pairs (bp) in length. When the 420 bp fragment was used as a hybridization probe for northern blot analysis a single, 2.5 kB band was observed in RNA samples from the ipsilateral hippocampus of H-I animals at 3 and 6 hours post-hypoxia and in the contralateral hippocampus of H-I animals at 6 hours post-hypoxia. See Figure 4-1B.

Figure 4-1

Selective amplification of c-fos mRNA using c-fos targeted primers in a differential display experiment.

c-fos targeted primers were designed to selectively amplify *c-fos* mRNA during PCR. Panel A) a portion of a differential display autoradiogram depicting a fragment that is expressed in the ipsilateral hippocampus of H-I animals sacrificed at 3 (Lane 3) and 6 (Lane 6) hours post-hypoxia. Elevated levels of this fragment were also noted in the contralateral hippocampus of H-I animals sacrificed at 6 hours (Lane 5) post-hypoxia. This fragment was not present in the ipsilateral hippocampus of ligated control animals (Lanes 1 and 4) nor in any tissue samples from ligated control or H-I animals sacrificed at 12 hours post-hypoxia (Lanes 7, 8 and 9). Lanes 10-18 represent a duplicate experiment. Panel B) northern blot probed with the isolated fragment; Lanes 1 and 4 contain total RNA isolated from the contralateral hippocampus of H-I animals sacrificed at 3 and 6 hours post-hypoxia respectively. Lanes 2 and 5 contain total RNA extracted from the ipsilateral hippocampus of H-I animals sacrificed at 3 and 6 hours post-hypoxia respectively. Lane 3 contains total RNA isolated from the ipsilateral hippocampus of ligated control animals sacrificed at 6 hours post-hypoxia. Lanes 6-11 contain total RNA extracted from the same tissues from the same animal groups sacrificed at 12 and 24 hours post-hypoxia. The lower blot in Panel B contains a scan of the same membrane probed with β-actin to control for lane loading. Panel C) northern blot probed using a manufactured *c-fos* oligonucleotide probe; Lanes 1 and 4 contain total RNA isolated from the ipsilateral hippocampus of ligated control animals sacrificed at 3 and 6 hours post-hypoxia respectively. Lanes 2 and 5 contain total RNA isolated from the contralateral hippocampus of H-I animals sacrificed at 3 and 6 hours post-hypoxia respectively. Lanes 3 and 6 contain total RNA extracted from the ipsilateral hippocampus of H-I animals sacrificed at 3 and 6 hours post-hypoxia respectively. Lanes 6-11 contain total RNA extracted from the same tissues from the same animal groups sacrificed at 12 and 24 hours post-hypoxia. The lower blot in Panel C contains a scan of the same membrane stained with methylene blue for detection of rRNA to control for lane loading.

A

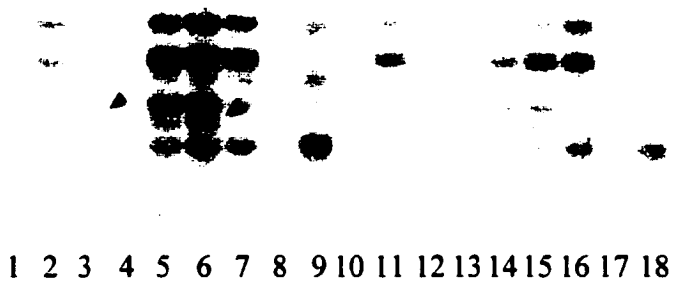

B

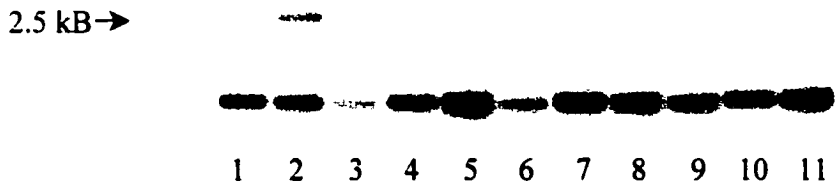

C

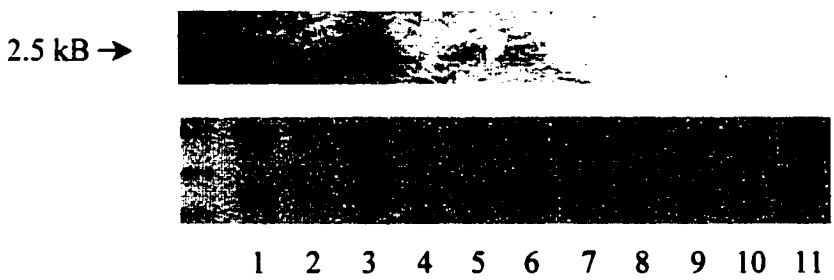

Figure 4-1

DNA sequencing of recombinant plasmids containing the differentially displayed fragment demonstrated that the fragment was derived from rat *c-fos* mRNA. Specifically, the estimated 420 bp fragment exhibited 98% nucleotide identity (E value = e^{-125}) with the 3' end of the rat *c-fos* cDNA (nts 1732-1981; Genbank Accession number X06769). A synthetic oligonucleotide probe was then used to confirm the pattern of *c-fos* mRNA expression following H-I. The oligonucleotide probe also annealed to a 2.5 kB band on a northern blot in lanes that contained RNA samples isolated from the ipsilateral hippocampus of H-I animals sacrificed at 3 and 6 hours post-hypoxia and from the contralateral hippocampus of H-I animals sacrificed at 6 hours post-hypoxia. See Figure 4-1C.

Calmodulin

The primer set P9, T4 was used to amplify cDNA populations produced from the ipsilateral hippocampus of ligated control animals, the contralateral and ipsilateral hippocampus of vehicle-injected H-I animals and the ipsilateral hippocampus of CMZ-treated H-I animals. A parallel set of cDNA samples was also amplified from the parietal cortex of these animal groups. Visual analysis of the differential display autoradiogram revealed a fragment that was expressed in all cDNA populations, except those derived from the ipsilateral hippocampus of CMZ-injected (200 mg/kg) H-I animals sacrificed at 12 and 24 hours post-hypoxia. See Figure 4-2A. DNA sequencing of recombinant plasmids containing this fragment revealed that the fragment shared a 93% sequence identity with mRNA for the rat calcium binding protein, *calmodulin* (E = $1e^{-29}$), and corresponded to nucleotides 4378-4284 (Genbank Accession number X05117).

The isolated cDNA fragment was used as a hybridization probe on northern blots containing total RNA isolated from the ipsilateral hippocampus and cortex of naïve and ligated control animals, the contralateral and ipsilateral hippocampus and cortex of vehicle-injected H-I animals and the ipsilateral hippocampus and cortex of CMZ-injected H-I animals. It is noteworthy that two of the northern blots probed using this cDNA fragment contained pooled RNA samples in each lane (3 animals/lane) while others contained RNA samples generated from 1 animal in each lane. Regardless, each lane was counted as a single sample. The cDNA probe detected a single hybridization signal in all

Figure 4-2

Decreased expression of calmodulin mRNA may be linked to CMZ-induced neuroprotection in the H-I model.

The primer set P9, T4 amplified a fragment that corresponded to rat *calmodulin* mRNA. Panel A contains a portion of a differential display autoradiogram containing PCR products generated from the ipsilateral hippocampus and cortex of ligated control animals (Lanes 1and 5 respectively), the contralateral hippocampus and cortex of vehicle-injected H-I animals (Lanes 2 and 6 respsectively), the ipsilateral hippocampus and cortex of vehicle-injected H-I animals (Lanes 3 and 7 respectively) and the ipsilateral hippocampus of CMZ-injected H-I animals (Lane 4) sacrificed at 12 hours post-injection. Lanes 8-11 contain PCR products from the ipsilateral hippocampus of ligated control animals, the contralateral and ipsilateral hippocampus of vehicle-injected H-I animals and the ipsilateral hippocampus of CMZ-injected H-I animals sacrificed at 24 hours post-hypoxia respectively. The fragment of interest (arrowhead) was expressed in all lanes except those that correspond to the ipsilateral hippocampus of CMZ-injected H-I animals sacrificed at 12 (Lane 4) and 24 (Lane 11) hours post-hypoxia. Panel B) Northern blot containing total RNA isolated from the ipsilateral hippocampus of ligated control animals at 12 hours post-hypoxia (Lane 1), the ipsilateral hippocampus of vehicle-injected H-I animals at 12 (Lanes 2 and 3) and 24 hours (Lanes 6, 7 and 8) and from the ipsilateral hippocampus of CMZ-injected H-I animals sacrificed at 12 (Lanes 4 and 5) and 24 hours (Lanes 9 and 10) post-injection. The lower blot in Panel B is the same membrane stained with methylene blue for detection of rRNA to control for lane loading.

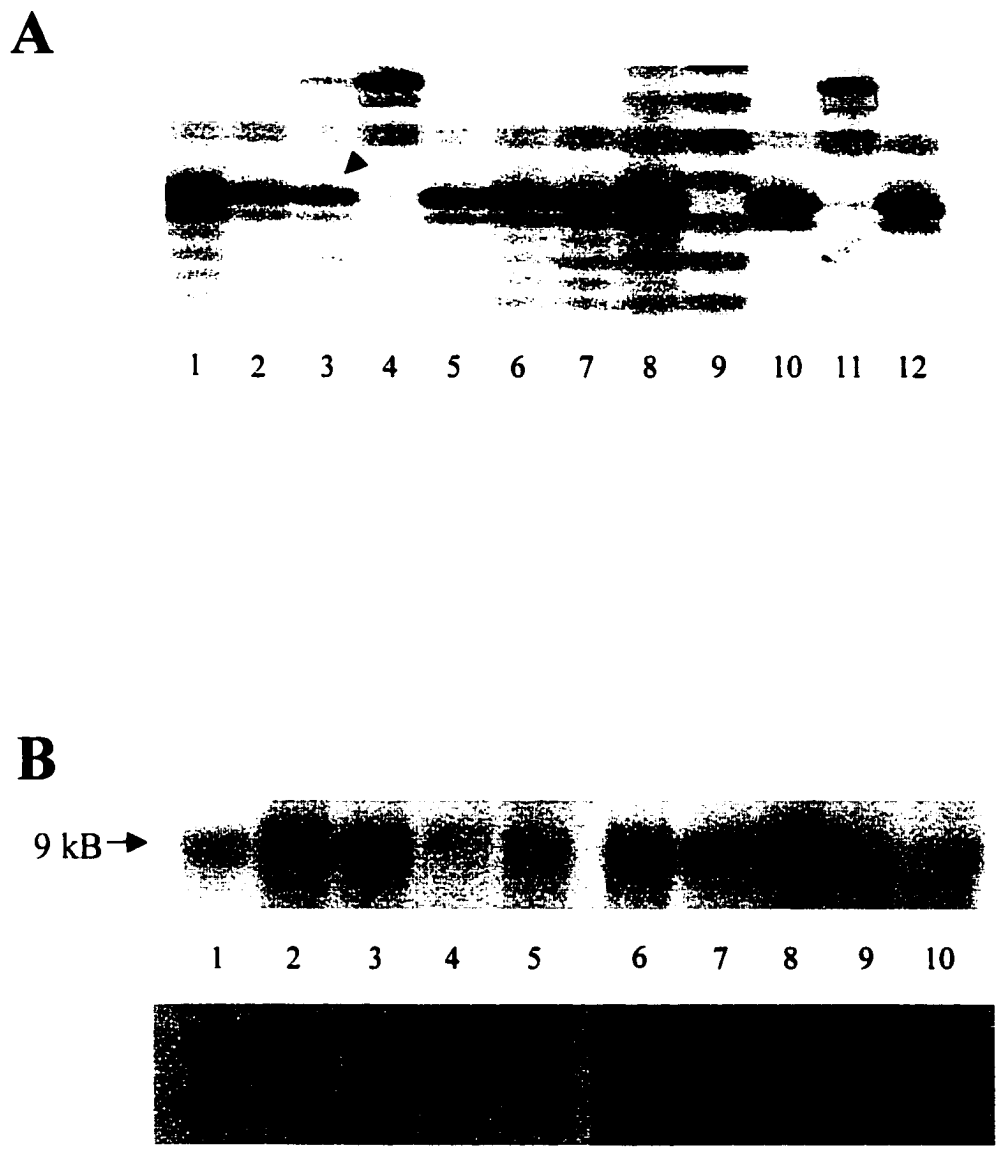

Figure 4-2

RNA populations examined. However, the density of the band in lanes that corresponded to the ipsilateral hippocampus of vehicle-injected H-I animals sacrificed at 12 and 24 hours post-injection was substantially higher than the density of bands detected in RNA populations isolated from the ipsilateral hippocampus of control (N = 6) or CMZ-induced H-I animals sacrificed at 12 and 24 hours post-injection. See Figure 4-2B (All data points are not shown in figure). Statistical analysis of relative differences in the density of bands across animal groups indicated a significant difference between mean density (OD/mm^2) of bands corresponding to the ipsilateral hippocampus of vehicle-injected H-I animals (N = 5) and CMZ-treated H-I animals (N = 3) sacrificed at 24 hours post-injection ($q = 5.425$; $P<0.05$). See Figure 4-3. The mean density of *calmodulin* mRNA in the ipsilateral hippocampus of vehicle-injected H-I animals was significantly different from control animals (N = 3) at 12 ($q = 5.143$; $P<0.05$; N = 3) and 24 hours ($q = 5.681$; $P<0.05$; N = 4) post-injection. However, the mean density of *calmodulin* mRNA expression in the ipsilateral hippocampus of CMZ-injected H-I animals was not significantly different from control animals at 12 (N = 4) or 24 (N = 3) hours post-injection. Significant differences in mean density *calmodulin* expression were not observed in any RNA samples extracted from the cortices of these animal groups.

Acyl-coA oxidase mRNA

The primer set P6, T6 generated a fragment that was expressed in the ipsilateral hippocampus of CMZ-injected H-I animals at 12 and 24 hours and in vehicle-injected H-I animals sacrificed at 12 hours post-injection but was not present in any other cDNA populations examined. See Figure 4-4A. DNA sequencing revealed that this fragment shared a 95% sequence identity with nucleotides 3344-3551 of the rat *acyl-coA oxidase* mRNA ($E = 5e^{-89}$; Genbank Accession number J02752). When the fragment was used as a cDNA probe for northern blot analysis, two hybridization signals depicting bands of different sizes were were detected on an autoradiogram. See Figure 4-4B. The hybridization signal from the lower molecular weight band (low band in the figure) appeared to have a higher density in tissue isolated from the ipsilateral hippocampus of

Figure 4-3

Densitometric analysis of calmodulin expression in vehicle- and CMZ-injected H-I - animals at 12 and 24 hours post-hypoxia.

Graphical illustration of the mean density of the hybridization signal (*calmodulin* mRNA expression) detected across animal groups examined using northern blot analysis. All animals were sacrificed at 12 or 24 hours post-injection. RNA populations used for quantitation included RNA from the hippocampii of control animals (C), the ipsilateral hippocampus of vehicle-injected H-I animals (VIH), the ipsilateral hippocampus of CMZ-injected H-I animals (CIH), the ipsilateral cortex of vehicle-injected H-I animals (VIC) and the ipsilateral cortex of CMZ-injected H-I animals (CIC). For quantitative and graphical analysis, the control group used was a collective representation of the density of hybridization signal in the ipsilateral hippocampus of ligated and naïve control animals and from the contralateral hippocampus of vehicle-injected H-I animals. A P value of <0.05 was considered to be significant. The data are presented as means ± S.E.M. (* = significantly different from control animals; ■ = significantly different from CMZ-injected H-I animals sacrificed at the same timepoint).

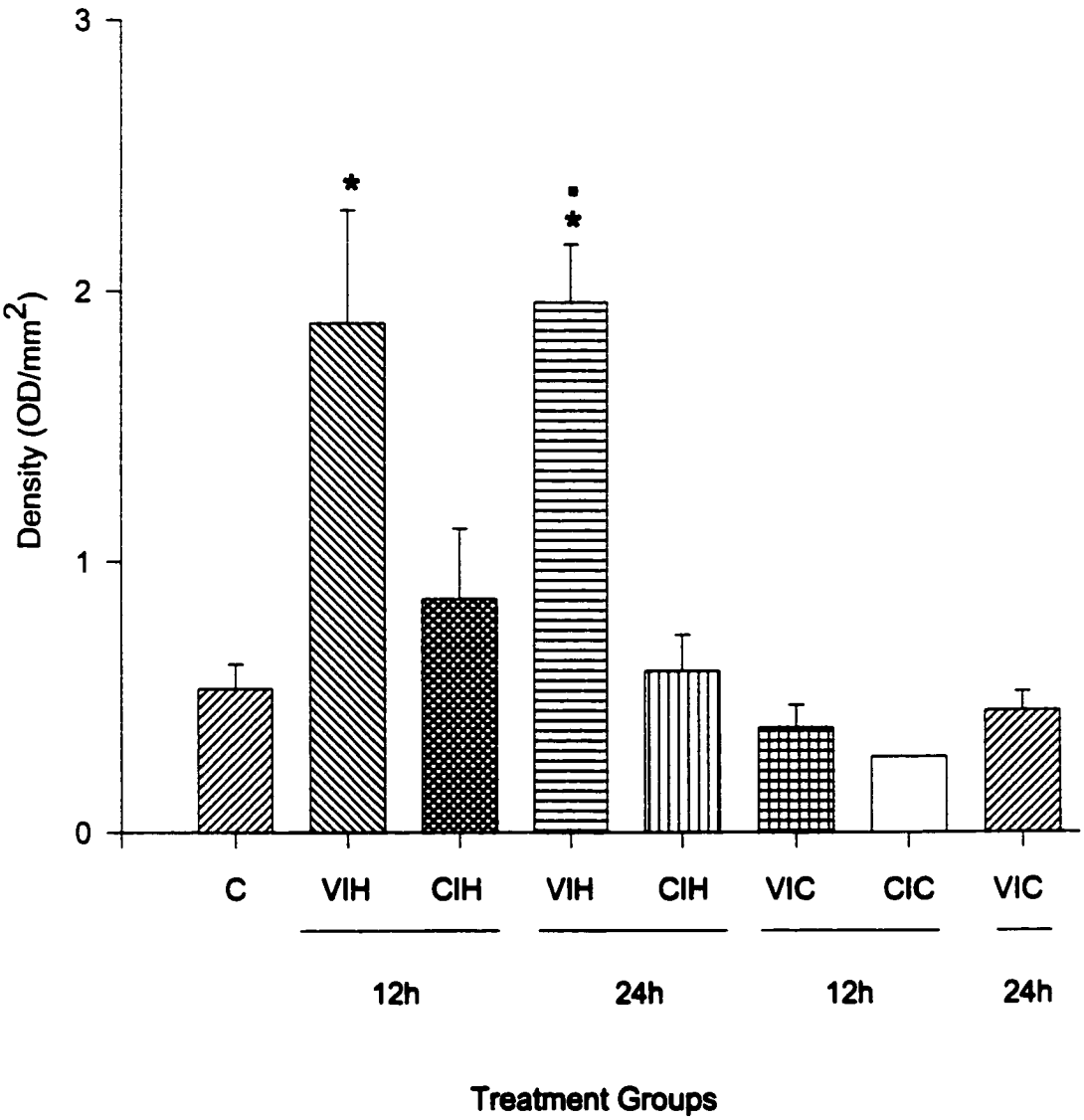
3
2
1
0
Density (OD/mm2)
*
*
C
VIH
CIH
VIH
CIH
VIC
CIC
VIC
12h
24h
12h
24h
Treatment Groups

Figure 4-3

Figure 4-4

Increased expression of Acyl CoA oxidase mRNA may be linked to CMZ-induced neuroprotection in the H-I model.

The primer set P6, T6 amplified a fragment that corresponded to rat *Acyl CoA oxidase* mRNA. Panel A) portion of a differential display autoradiogram containing PCR products generated from the ipsilateral hippocampus and cortex of ligated control animals (Lanes 1and 5 respectively), the contralateral hippocampus and cortex of vehicle-injected H-I animals (Lanes 2 and 6 respsectively), the ipsilateral hippocampus and cortex of vehicle-injected H-I animals (Lanes 3 and 7 respectively) and the ipsilateral hippocampus of CMZ-injected H-I animals (Lane 4) sacrificed at 12 hours post-injection. Lanes 8-11 contain PCR products from the ipsilateral hippocampus of ligated control animals, the contralateral and ipsilateral hippocampus of vehicle-injected H-I animals and the ipsilateral hippocampus of CMZ-injected H-I animals sacrificed at 24 hours post-hypoxia respectively. The fragment of interest (arrowhead) was expressed in lanes 3, 4 and 11 which correspond to the ipsilateral hippocampus of vehicle and CMZ-injected H-I animals sacrificed at 12 hours and the ipsilateral hippocampus of CMZ-injected H-I animals sacrificed at 24 hours post-hypoxia respectively. Panel B) northern blot containing total RNA isolated from the ipsilateral hippocampus of naïve animals (Lane 1), the contralateral and ipsilateral hippocampus of vehicle-injected H-I animals sacrificed at 12 (Lanes 2 and 3 respectively) and 24 hours (Lanes 5 and 6 respectively) and from the ipsilateral hippocampus of CMZ-injected H-I animals sacrificed at 12 (Lane 4) and 24 hours (Lane 7) post-injection. The lower blot in Panel B contains a scan of the same membrane stained with methylene blue for detection of rRNA to control for lane loading.

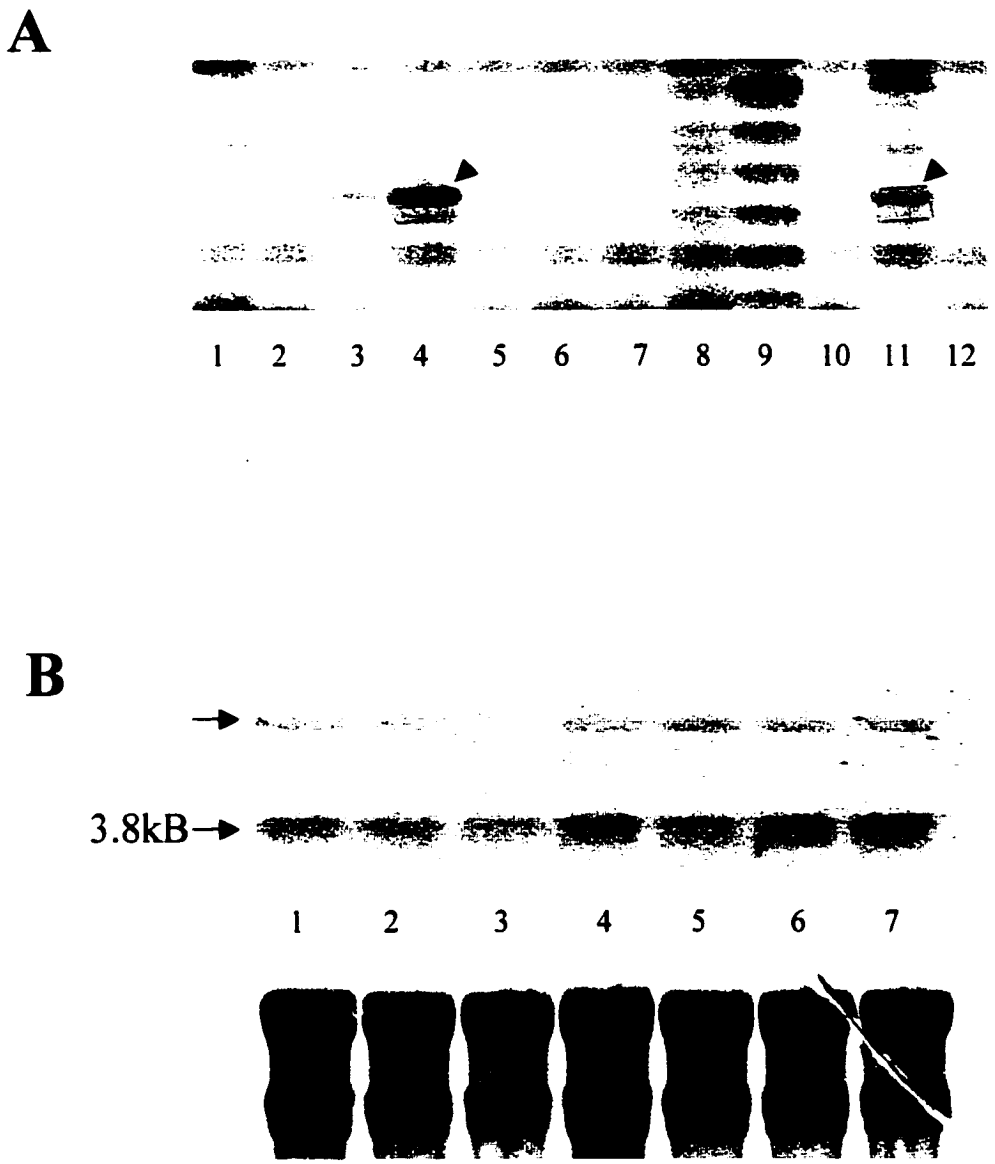

Figure 4-4

CMZ-injected H-I animals sacrificed at 12 (N= 3) and 24 (N = 4) hours post-hypoxia than in any other tissue examined. However, statistical analysis of the densitometry indicated that the mean density of these bands were not significantly different in any tissues examined. See Figure 4-5.

Figure 4-5

Densitometric analysis of Acyl CoA oxidase expression in vehicle- and CMZ-injected H-I -animals at 12 and 24 hours post-hypoxia.

Graphical illustration of the mean density of hybridization signal (*Acyl CoA oxidase* mRNA expression) detected across animal groups examined using northern blot analysis. All animals examined were sacrificed at 12 or 24 hours post-injection. Animal groups used for quantitation included the control animals (C), the ipsilateral hippocampus of vehicle-injected H-I animals (VIH), the ipsilateral hippocampus of CMZ-injected H-I animals (CIH), the ipsilateral cortex of vehicle-injected H-I animals (VIC) and the ipsilateral cortex of CMZ-injected H-I animals (CIC). For quantitative and graphical analysis, the control group used was a collective representation of the density of the hybridization signal detected in the ipsilateral hippocampus of ligated and naïve control animals and from the contralateral hippocampus of vehicle-injected H-I animals. A P value of <0.05 was considered to be significant. The data are presented as means ± S.E.M.

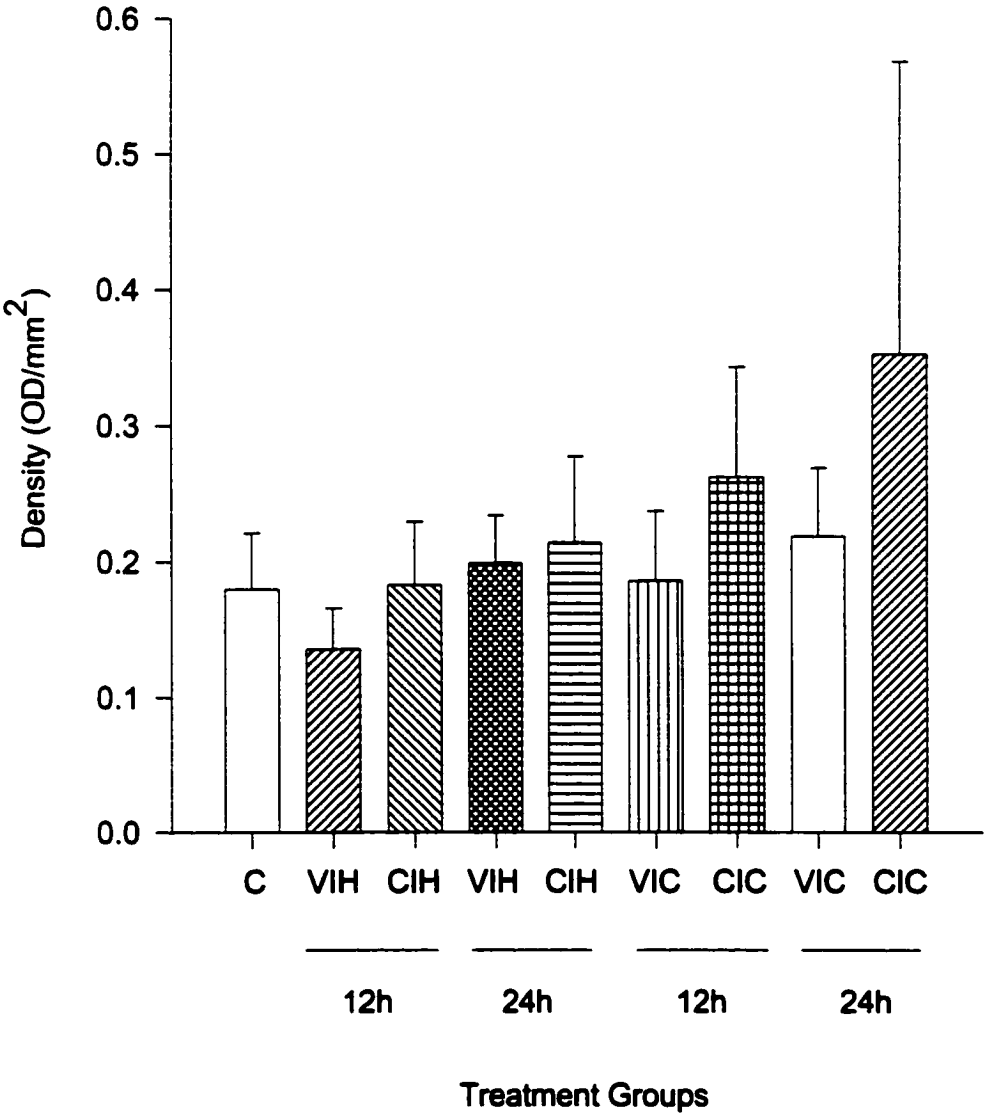
0.6
0.5
0.4
0.3
0.2
0.1
0.0
Density (OD/mm2)
C
VIH
CIH
VIH
CIH
VIC
CIC
VIC
CIC
12h
24h
12h
24h
Treatment Groups

Figure 4-5

Discussion

The results of this experiment demonstrate that the differential display protocol exhibited predictive validity in the H-I paradigm. The *c-fos*-targeted primer set annealed with the complementary nucleotides of the *c-fos* single-stranded cDNA and amplified a fragment that was expressed in H-I tissue at 3 hours post-hypoxia and corresponded to the 3' end of rat *c-fos* mRNA. When the cDNA fragment was used as a hybridization probe in northern blot analysis, a single transcript, of the size previously reported for rat *c-fos* mRNA (2.5 kB), was detected in tissues known to express *c-fos* mRNA at 3 hours following H-I injury (Blumenfeld *et al.*, 1992; Gubits *et al.*, 1993; Aden *et al.*, 1994; Dragunow *et al.*, 1994; Munell *et al.*, 1994). These results clearly demonstrate that PCR primer sets can be selected to anneal with specific cDNAs that have a known pattern of expression in a particular paradigm and can replicate that pattern of expression on a differential display autoradiogram. Paradigm-specific positive controls can, therefore, confirm the integrity of the original RNA samples and ensure that differentially expressed PCR-amplified cDNAs accurately reflect differentially expressed mRNAs in the total RNA population. The success of targeted PCR primer sets may also increase the utility of the differential display protocol. For instance, differential display has generally been conducted such that random primer sets generate differentially expressed bands on autoradiograms that are subsequently substantiated using northern blot analysis or *in situ* hybridization. Although this method has obvious merit, it does not demonstrate that differential display can reliably be used for more than a random search for differentially expressed mRNAs. On the other hand, use of PCR primer sets that are targeted for highly conserved regions of genes may enable a search for relative expression patterns of mRNAs from a particular family of genes that can be simultaneously examined on a differential display autoradiogram.

Once the integrity of the differential display protocol had been established, a number of RT-PCR differential display experiments were conducted to identify mRNAs that may be differentially expressed in the ipsilateral hippocampus or cortex of vehicle-injected or CMZ-injected H-I animals in relation to each other or to control cDNA populations. Differentially displayed fragments specific to the ipsilateral structures of

vehicle-injected H-I animals may identify genes involved in ischemia-induced cell death. Differentially displayed fragments that are specific to the ipsilateral structure of CMZ-injected H-I animals may be relevant to the mechanism through which CMZ provides neuroprotection in the H-I model.

Calmodulin

In this study, a fragment that corresponded to rat *calmodulin* mRNA was detected in all PCR-amplified cDNA populations with the exception of the cDNA populations derived from the ipsilateral hippocampii of CMZ-injected H-I animals sacrificed at 12 and 24 hours post-injection. Calmodulin is a major calcium binding protein within the CNS and has been implicated in a number of cellular functions through the activation of calmodulin-dependent enzymes including phosphodiesterase, protein kinase and protein phosphatase (Zhou *et al.*, 1985; James *et al.*, 1995). When bound to calcium, calmodulin appears to contribute to cellular pathology by activating calcium-dependent enzymes such as phospholipases, proteases, endonucleases and nitric oxide (NO) synthase (Hajimohammadreza *et al.*, 1995; Kuroda *et al.*, 1997). Thus, calcium influx and its subsequent binding to calmodulin, have been implicated in the initiation of cellular events that culminate in ischemic cell death (Picone *et al.*, 1989; Sun *et al.*, 1997). A number of studies have shown that calmodulin antagonists reduce ischemia-induced cell death in both heart and CNS tissue (Beresewicz, 1989; Gabaeur *et al.*, 1991; Kimura *et al.*, 1992; Otani *et al.*, 1992; Sargent *et al.*, 1992). Kuroda *et al* (1997) demonstrated that the calmodulin antagonist, Trifluoperazine, was neuroprotective in Wistar rats when administered (ip) 5 minutes following a 2 hour MCAO and then re-administered 24 hours later. However, an ip injection of Trifluperazine administered at 1 or 2 hours following MCAO was not neuroprotective. Furthermore, Sato *et al.* (1999) recently demonstrated that an iv infusion (0.25, 0.50 or 1.00 mg/kg/hr) of 3-[2–[4–(3-chloro-2-methylphenyl)–1–piperazinyl] ethyl]–5,6-dimethyl-1-(4-imidazolylmethyl)-1 *H*-indazole dihydrochloride 3.5 hydrate (DY-9760) for 6 hours, starting 1 hour after transient MCAO, reduced cerebral infarct volume by 30, 42 and 60% respectively. It is difficult to interpret the function of a gene based on its temporal and spatial expression after an ischemic insult because a variety of cellular and extracellular events occur during the interval between

ischemic insult and final neuronal death that have an unclear pathophysiological meaning. However, cells appear to have developed specific cellular processes that respond to the frequency and longevity of calcium signals within the cell, such as calmodulin-dependent protein kinases, which may actively affect cell fate. Thus, while there is no concrete link between the mechanism of action for CMZ and either of these calmodulin antagonists in ischemic injury, the results of this experiment may imply that CMZ directly or indirectly antagonizes the expression level of *calmodulin* mRNA following H-I insult in order to exert its neuroprotective effects.

Acyl coA oxidase

A fragment that corresponded to the mRNA for rat *Acyl CoA oxidase* was detected in the ipsilateral hippocampus of CMZ-injected H-I animals sacrificed at 12 and 24 hours post-injection and the the ipsilateral hippocampus of vehicle-injected H-I - animals sacrificed at 12 hours post-injection. However, this fragment was not expressed in any control tissues or in the ipsilateral hippocampus of vehicle-injected H-I animals sacrificed at 24 hours post-injection. While hybridization analysis on a northern blot appeared to demonstrate an elevation of *Acyl CoA oxidase* mRNA on a northern blot in CMZ-injected animals relative to control animals, statistical significance was not obtained. In addition, the results of this study also demonstrated that use of the fragment isolated from the differential display gel as a hybridization probe produced two bands of different molecular weight on the northern blot indicating that the isolated fragment was contaminated with a second cDNA sequence. The Acyl CoA oxidase protein is an enzyme involved in the peroxisomal beta oxidation system (Fan *et al.*, 1996). Interestingly, a study has been conducted by Gulati *et al.* (1993) reporting that ischemia leads to a decrease Acyl coA oxidase activity in the kidney. Thus, it seemed plausible that CMZ-induced neuroprotection could lead to an increase in this transcript. However, the results of this experiment can not ensure that CMZ administration in H-I animals caused an increase in the expression of this transcript.

Difficulties in the Differential Display Protocol used in this Experiment

Investigation of cell death pathways ignited by ischemic injury *in vivo* is

technically extremely difficult. Interpretation of the results must consider the heterogeneity of cell types, the diversity of cell death paradigms and exacerbation of tissue damage caused by the immigration of leukocytes during inflammation (Saikumar *et al.*, 1998). Despite the demonstration of predictive validity for the differential display technique in the H-I model, confirmation of differentially displayed fragments isolated from differential display gels using northern blot analysis was inconsistent. The most likely explanation for this discrepancy was the procedure used for cellular isolation from susceptible brain regions. Specifically, the RNA populations used for reverse transcription and PCR amplification were extracted from a homogenate of the entire hippocampus or parietal cortex and, therefore, contained RNA from all cell layers within those regions. Following H-I, dentate granule cells in the hippocampus ultimately survive the injury while the pyramidal cell layers undergo delayed cell death (Gilby *et al.*, 1997). However, tissue homogenization precludes the ability to evaluate gene expression on a cell by cell basis. Thus, the presence of cells that survive the H-I injury and those that die within the same RNA sample is clearly problematic and may confound the interpretation of gene expression in these samples. At the cellular level, the heterogeneity of the brain from even a small collection of cells may average out any minor differences in genetic phenotying between cells. This flaw in the extraction procedure used in this study may also explain why the correct pattern of expression for *c-fos* mRNA was produced using this extraction method while replicating data generated using other fragments was difficult. Numerous studies have documented a robust expression of *c-fos* mRNA at early timepoints following H-I (within 3-6 hours) that is present in all ipsilateral hippocampal cell layers, including the dentate granule cells (Blumenfeld *et al.*, 1992; Munell *et al.*, 1994; Dragunow *et al.*, 1994). Thus, in this case, inclusion of all cell layers in a tissue homogenate would not mask the overall effect. However, examination of differential gene expression in cell layers at delayed post-hypoxic timepoints in search of genes related to only the protected or dying cell populations, as was done in this study, is very difficult and may only detect gene changes that are very robust. In light of this difficulty, future experiments using this protocol should use extracted RNA from discrete cell layers from a brain region of interest (eg CA1 from the hippocampus).

***Chapter 5**: An Investigation into the Effect of CMZ-Induced Neuroprotection on PCD-related Gene Expression Following H-I*

Summary

In this study, various molecular biological tools were used in order to determine whether the normal pattern of expression for genes, believed to be involved in PCD, was altered by the administration of a neuroprotective dose of CMZ 3 hours following H-I injury. Specifically, northern blot analysis and *in situ* hybridization were used to investigate the effects of CMZ administration on normal patterns of *c-fos* and *c-jun* mRNA expression following H-I. Targeted PCR primers were used to selectively amplify and compare the pattern of expression for *c-myc*, *bcl-2*, *p53* and *caspase-3* mRNA in CMZ versus vehicle-injected H-I animals sacrificed at 12 and 24 hours post-hypoxia. Finally, immunohistochemical techniques were used to examine differences in the expression pattern of c-Fos protein in CMZ-injected versus vehicle-injected H-I animals. The results of these experiments demonstrate that CMZ administration in H-I animals prolonged the expression of *c-fos* mRNA and protein, in relation to vehicle-injected H-I animals, by approximately 10-16 hours in ipsilateral structures normally susceptible to H-I insult. However, a significant prolongation of *c-fos* mRNA expression was only detected in the ipsilateral cortex of CMZ-injected H-I animals sacrificed at 12 hours post-hypoxia. Moreover, CMZ administration caused a significant reduction in the density of *c-jun* mRNA expression in all cell layers of the ipsilateral hippocampus and cortex of H-I animals sacrificed at 12 hours post-hypoxia. Finally, CMZ administration appeared to cause a protracted expression of *bcl-2* mRNA in the ipsilateral hippocampus of CMZ-injected H-I animals, relative to vehicle-injected animals, that was evident at 24 hours post-hypoxia. The fact that CMZ administration caused a reduction of *c-jun* mRNA at 12 hours post-hypoxia and affected the expression pattern for c Fos mRNA and protein and possibly *bcl-2* mRNA may indicate that CMZ has an affect on PCD-related mechanisms. However, the functional implications of these alterations are difficult to interpret due to technical limitations.

Introduction

The concept of pharmacological neuroprotection in animal models of ischemia, and in human stroke victims, relies on the assumption that there is delayed neuronal death following ischemic injury. Indeed, selective delayed neuronal death has been observed in many animal models of ischemia (Gillardon *et al.*, 1996; Siesj ¯and Siesj ¯, 1996; Pulera *et al.*, 1998). For instance, a 24 to 72 hour delay in the death of CA1 neurons has been reported following transient forebrain ischemia (Colburne *et al.*, 1999). A previous study in our laboratory reported a similar time-line of neuronal death in PND25 male rats following H-I. Neuronal death was delayed for at least 12-24 hours post-hypoxia in the most susceptible cell layer (CA1) of the ipsilateral hippocampus and progressed for up to 4 days post-hypoxia in the more resistant cell layers (CA3b and c) of this brain region (Gilby *et al.*, 1997). Interestingly, delayed neuronal death has also been reported in the brain of human cardiac arrest victims that have been resuscitated 8-10 minutes following the insult (Petito *et al.*, 1997).

The cellular events that take place several hours following an ischemic event and culminate in cell death are currently unknown. One mechanism that may be responsible for ischemia-induced delayed cell death is the activation of a genetically controlled cellular suicide program known as apoptosis or programmed cell death (PCD). PCD was first defined as a cell death process that had characteristic morphologic features and occurred in a variety of different circumstances, all having to do with controlled cell deletion (Kerr *et al.*, 1972). Under homeostatic conditions, PCD is an efficient mechanism through which an organism can remove superfluous, aged or damaged cells from the CNS without provoking an inflammatory response (Evan and Littlewood, 1998). However, deregulation of the PCD process is thought to underlie a number of human pathologies. Cellular resistance to PCD has been linked to autoimmune diseases and cancer while uncontrolled deletion of cells by PCD has been linked to chronic pathologies including neurodegenerative diseases and delayed cell death following stroke (Cotman and Anderson, 1995; Chopp *et al.*, 1996; Du *et al.*, 1996; Zamzami *et al.*, 1997). Neuroscientists have, therefore, become interested in the role of PCD-linked processes (signaling mechanisms, effector molecules and essential targets) in basic CNS function

(Mosser *et al.* 1997). For obvious reasons, research interests have also focussed on the development of pharmacological agents that may interfere with the delayed events of PCD. In contrast, there are several lines of evidence that suggest that an excitotoxic cell death (ECD) process may underlie ischemia-induced delayed cell death (Kirino and Sano, 1984; Yamamoto *et al.*, 1990).

Programmed Cell Death (PCD) versus Excitotoxic Cell Death (ECD)

Experimentation in the last decade has confirmed that both physiological and pathological triggers can ignite the PCD cascade but once initiated this cascade generally has a common temporospatial patterned sequence (Mosser *et al.*, 1997; Pulera *et al.*, 1998; Yang *et al.*, 1998). The initial morphological changes that characterize PCD include nuclear chromatin clumping and mild cellular condensation. Subsequently, the nuclear envelope becomes fragmented into flocculent densities that are diffusely distributed throughout the cell just before the cell divides into "apoptotic bodies" for biological degradation (Nunez *et al.*, 1998; Pulera *et al.*, 1998; Colburne *et al.*, 1999). It is important to note that the presence of apoptotic bodies within the CNS does not evoke a phagocytic inflammatory response (Ishimaru *et al.*, 1999).

Although the critical cellular mechanisms that underlie the initiation and execution of PCD are poorly understood, it is clear that PCD is the result of a complex set of molecular interactions between several proteins and that it requires both energy and synthesis of new proteins (Eguchi *et al.*, 1997). As such, PCD is dependent upon coordinated gene expression (Mosser *et al.*, 1997; Saikumar *et al.*, 1998). Genetic studies in the nemotode, *Caenorhabolitis elegans (C. elegans),* identified 3 genes that were essential for the control and execution of PCD in developing worms, *C. elegans* death associated protein-3 (CED-3), CED-4 and CED-9 (Hengartner and Horvitz, 1994; Dragovich *et al.*, 1998). Mammalian homologues of these genes have been discovered and have been designated caspases, Apaf-1 and Bcl-2-related proteins respectively (Yuan *et al.*, 1993). Members of the Bcl-2 family of proteins are considered to be among the most prominent families of PCD regulators and include such proteins as Bid, Bax, Bik, Bim, Blk and Bcl-2 (Dragovich *et al.*, 1998). Although these proteins all share domains of structural homology, some Bcl-2 related proteins promote PCD while others exhibit an

anti-PCD function (Dragovich *et al.*, 1998). Permutations in protein dimerization among Bcl-2 family members have a major influence on cell fate and have, therefore, been deemed "gate-keepers" of the PCD machinery. For instance, dimers formed between BAD and Bcl-2 have been shown to promote cell death whereas dimers formed between BAX and Bcl-2 promote cellular survival (reviewed in Reed, 1998). Several lines of evidence have indicated that members of the Bcl-2 family function upstream of caspase activation and thereby can exert an overriding protective role within the cell (Yuan *et al.*, 1993; Saikumar *et al.*, 1998). It has been postulated that Bcl-2 provides cellular protection through the inhibition of mitochondrial permeability transitions and the release of apogenic factors such as cytochrome c and apoptosis-inducing factor (AIF) from the mitochondria to the cytoplasm (Reed, 1998).

The pro-PCD family of proteins known as caspases are a conserved group of constitutively expressed cysteine proteases. Caspases undergo proteolytic cleavage and subunit rearrangement in order to produce active enzymes that cleave nuclear proteins (poly ADP-ribose polymerase, DNA-dependent protein kinases, heteronuclear ribonuclear proteins or lamins), cytoskeletal proteins (actin, fodrin), or inflammatory mediators (prointerleukin-1β). The systematic cleavage of such a diverse array of proteins is thought to be pivotal to the progression of the PCD process. Recently, the link between PCD, cell growth and cell cycle-related genes has generated research interest. The tumor-suppressor transcription factor known as p53 is currently believed to possess pro-apoptotic properties. P53 is a DNA-binding protein that is thought to be important in the regulation of cell proliferation following DNA damage (Bates and Vousden, 1996). P53 is normally maintained at low cellular levels but increased levels of p53 expression have been shown to halt cell cycle progression (in cell cycle stages G_1 and G_2) and in some circumstances induce PCD (Hughes *et al.*, 1996; Evan and Littlewood, 1998). The cellular oncogene *c-myc* is a potent inducer of cellular proliferation, however, substantial evidence suggests that *c-myc* also has pro-PCD abilities (Evan *et al.*, 1992; Sakamuro *et al.*, 1995; Evan and Littlewood, 1998). For the most part, however, PCD is characterized by the activation of specific proteins, including catabolic enzymes (caspases) that systematically degrade cellular constituents, that actively contribute to the removal of the cell within the limits of an intact plasma membrane (Zamzami *et al.*, 1997).

On the other hand, delayed ischemic cell death may be the result of an ECD process. In the 1970's, excitotoxicity was first used to refer to an acute process by which glutamate or its various excitatory structural analogs trigger neuronal cell death in the CNS of either rodents or primates (Olney *et al.*, 1971; 1974). The profound increase in extracellular glutamate that characteristically occurs following ischemic insult has caused researchers to link ischemia-induced cell death to the excitotoxic/necrotic phenomenon. Morphological changes evident in cells dying from an ECD process are quite different from those observed in cells undergoing PCD. The first morphological changes associated with ECD include a massive dilation of dendritic, but not axonal, processes in the neuropil, cellular swelling and the breakdown of cellular membranes. These events are quickly followed by vacuolation of the endoplasmic reticulum (ER) and condensation of the mitochondria. Subsequently, the mitochondria begin to swell and become progressively more edematous, swollen and vacuous. Following these cytoplasmic events, the nuclear chromatin begins to clump and migrate to the nuclear envelope. Within hours of the initial morphological events, phagocytic cells engulf and biologically degrade the degenerated cell (Ishimaru *et al.*, 1999). Thus, in contrast to PCD, ECD is a primarily cytoplasmic event that is initiated only by exogenous stimuli and ultimately provokes an inflammatory response in the brain.

At present, there is a wealth of conflicting data, from both *in vivo* and *in vitro* models of ischemia, that address whether delayed ischemia-induced neuronal degeneration is the result of a PCD or an ECD phenomenon. Numerous reports in the literature support an ECD theory for delayed ischemic cell death (Kirino and Sano, 1984; Yamamoto *et al.*, 1990; Deshpande *et al.*, 1992; Tomimoto *et al.*, 1993). In fact, delayed cell death induced by 5 minutes of global ischemia in gerbils has been shown to exhibit features of necrotic, but not apoptotic, neuronal death even in cells that died 2 months after the ischemic event (Colbourne *et al.*, 1999). Furthermore, Ishimaru *et al.*, (1999) conducted a detailed electron microscopic evaluation of the ultrastructural appearance of neurons undergoing delayed degeneration in the cingulate cortex following glutamate application and reported that the degenerative reaction was identical to the ECD process and exhibited no resemblance to PCD-induced neuronal degeneration. In contrast, multiple lines of evidence exist suggesting that ischemia-induced delayed cell death

occurs via PCD mechanisms (Kure *et al.*, 1991; Tominaga *et al.*, 1993; Filipkowski *et al.* 1994; Sei *et al.*, 1994; Beilharz *et al.*, 1995; Bonfoco *et al.*, 1995; Ferrer *et al.*, 1995). Studies have shown both DNA fragmentation and synthesis of new mRNA/protein in ischemic cells and have reported that protein synthesis, endonuclease and caspase inhibitors provide neuroprotection in animal models of ischemia (Goto *et al.*, 1990; Charriaut-Marlangue *et al.*, 1992; Heron *et al.*, 1993; Nitatori *et al.*, 1995; Loddick *et al.*, 1996).

Interestingly, a number of studies have suggested that PCD and ECD occur simultaneously in susceptible brain regions following ischemia (Lieberthal and Levine, 1996; Kato *et al.*, 1997; Kajstura *et al.*, 1998; Li *et al.*, 1998; Noda *et al.*, 1998). For instance, Martin *et al.* (1998) demonstrated that degeneration of selectively vulnerable neurons after global ischemia was morphologically non-apoptotic and was indistinguishable from NMDA-mediated excitotoxic cell death. However, prominent apoptotic cell death was evident in neuronal clusters that were interconnected with the selectively vulnerable neurons and in non-neuronal cells following the ischemic event. To add to the confusion, studies have even suggested that the mode of cell death following ischemic injury is actually a hybrid form of cell death that falls along a PCD-ECD continuum (Martin *et al.*, 1998). Thus, the triggering event may be common for both types of cell death and, as a consequence, cells undergoing either mode of cell death may initially demonstrate some of the same pathogenic responses. In support of this hypothesis, it has been shown that severe, irreversible, changes in mitochondrial structure and function are present in cells undergoing either ECD or PCD (Zamzami *et al.*, 1997). It is also conceivable that a downstream molecular event may be required to direct cells towards the organized execution of PCD, therefore, even if the PCD program was aborted before this control point cell death may still result through ECD if the initiating stimulus was severe (Leist *et al.*, 1997).

It is important to note that many of these conflicting studies relied heavily on non-ultrastructural methods, primarily DNA fragmentation analysis, to diagnose PCD. This may be problematic since one of the most popular methods for distinguishing PCD from ECD, the terminal deoxynucleotidyl transferase-mediated biotinylated UTP-nick end labeling (TUNEL) technique, has recently been shown to label cells undergoing both

PCD and ECD (Ishimaru *et al.*, 1999). Clearly, a more rigorous methodology is required to provide unquestionable identification of PCD and ECD processes following ischemia.

H-I and PCD

Traditionally, H-I injury has been attributed to an ECD process. However, as in other animal models of ischemia, the delayed cell death observed following H-I insult has recently been linked to PCD and delayed activation of "cell-death related" proteins. Using PND7 male rats in the bilateral carotid occlusion version of the H-I model, Pulera *et al.*, (1998) demonstrated that cells undergoing H-I-induced cell death exhibited numerous features of PCD including caspase-related cleavage of actin, DNA fragmentation and morphological markers of PCD such as chromatin condensation and "apoptotic bodies". Further support for the induction of PCD following H-I insult include several reports of neuroprotection in H-I susceptible cell layers following the administration of caspase inhibitors and in caspase-deficient mice (Shimaru *et al.*, 1996; Grotten *et al.*, 1997; Hara *et al.*, 1997; Schielke *et al.*, 1997; Cheng *et al.*, 1998). Interestingly, clinical studies have indicated that delayed cell death observed in human stroke patients also exhibit hallmark characteristics of PCD including increased Bcl-2 expression, cleavage of caspase-1, upregulation and cleavage of caspase-3, and DNA fragmentation (Clark *et al.*, 1999).

As mentioned previously, specific molecules may be responsible for the detection and execution of PCD processes. Aside from caspase activation, the identity of genes critically involved in the PCD process is highly controversial. The involvement of a class of genes known as immediate early genes (IEGs), specifically *c-fos* and *c-jun*, in PCD has been extensively studied. Rapid and transient transcriptional activation of IEGs can be elicited by relatively short periods of excessive excitation arising from a multitude of endogenous and/or exogenous events (Hughes *et al.*, 1992; Herdegen *et al.*, 1995). IEGs, such as *c-fos* and *c-jun*, encode nuclear proteins, c-Fos and c-Jun respectively, that act as transcription factors to invoke the transcription of downstream genes (Morgan and Curran, 1989). C-Jun and c-Fos may dimerize with each other or with other members of the c-Fos and c-Jun protein families in order to form the activating transcription factor protein 1 (AP-1). The AP-1 complex can bind with high affinity to the DNA consensus sequence TGAC/GTCA in promoter regions of various genes, however, the subunit

composition of the dimer formed affects both the binding affinity for the AP1 consensus site and whether the target gene is turned on or off. In this way, IEGs can alter the transcription of a number of genes and, thereby, re-program the expression patterns of cellular proteins to affect cellular phenotype. The activation of inducible transcription factors is, therefore, considered to be one of the most important steps linking rapid cellular events with long-lasting adaptive cellular responses. As such, IEGs may play a pivotal role in the activation or suppression of critical pathways involved in neuronal function, plasticity and cellular survival and/or death.

One of the first cellular responses upon exposure to PCD-inducing stimuli is the induction of *c-fos* mRNA (Kaina *et al.*, 1997). While the expression of both *c-fos* and *c-jun* is increased following H-I injury, the function associated with this increased expression is unclear. Recent studies, conducted both *in vivo* and *in vitro*, have suggested that *c-fos* expression following cellular injury may serve an anti-PCD function (Kaina *et al.*, 1997, Yoneda *et al.*, 1997; He *et al.*, 1998). In contrast, reports have indicated that *c-fos* expression contributes to the PCD process (Smeyne *et al.*, 1993; Hafezi *et al.*, 1997). A similar controversy exists with respect to the function of c-Jun expression following cellular stressors. c-Jun was first described as the oncogene of the avian sarcoma virus 17, a retrovirus capable of causing fibrosarcomas in chickens (Morgan and Curran, 1989). Several reports have suggested that both c-Jun N terminal kinase (JNK; SEK1) and its substrate, c-Jun, function as positive regulators of the PCD process (Chen *et al.*, 1995; Verheij *et al.*, 1996). Ishikawa *et al.* (1997) have shown that down regulation of c-Jun/AP-1 using a dominant negative mutant of c-Jun, an antisense *c-jun* or pharmacological inhibitors of c-Jun attenuated hydrogen peroxide-induced apoptosis. Moreover, when PCD was induced in an *in vitro* preparation of rat sympathetic neurons by the removal of nerve growth factor (NGF), administration of c-Jun (8.0 mg/kg) and c-Fos (5.0 mg/kg) antibodies provided neuroprotection against apoptotic cell death (Estus *et al.*, 1994). However, a number of studies have also reported that c-Jun expression serves an anti-PCD function. For instance, the induction of c-Jun has been linked to axonal regeneration and neuronal survival (Jenkins and Hunt 1991; Leah *et al.*, 1991; Schaden *et al.*, 1994; Sommer *et al.*, 1995). The conflicting data presented in these studies has prevented a clear understanding of IEG function in the PCD process.

Thus, it remains unclear whether H-I induced delayed cell death is due to an ECD or PCD process, however, H-I injury has been shown to consistently induce a robust and extensive IEG response in the brains of neonatal as well as perinatal animals (Blumenfeld *et al.*, 1992; Dragunow *et al.* 1994; Munell *et al.*, 1994; Gilby *et al.*, 1997). In addition, elevated levels of PCD-related genes/proteins such as caspase-3 and bcl-2 have been reported following H-I injury (Shimizu *et al.*, 1996; Cheng *et al.*, 1998; Kaushal *et al.*, 1998; Yaoita *et al.*, 1998;). Therefore, regardless of the exact mode of cell death, H-I injury leads to an increased expression of genes/proteins that are believed to be involved in the PCD process. In order to determine whether CMZ-induced neuroprotection in the H-I model may involve an anti-PCD mechanism, we examined the effects of CMZ treatment on the normal patterns of PCD-linked gene and protein expression following H-I.

Methods

Animals

Animal treatments in this experiment were identical to those outlined in Chapter 1. Three hours post-hypoxia, H-I animals received an i.p. injection of either vehicle (distilled water) or 200mg/kg CMZ. Naïve, ligated and hypoxic control animal groups were included in this study. Drug-injected control animals received an i.p. injection of 200 mg/kg CMZ but were not subjected to the H-I event. Following treatment, each animal was observed for any overt signs of seizure activity such as mastication, barrel rolling or limb tonus and clonus. Animals that exhibited such behavior were excluded from the study.

RNA Isolation

Animals used for RNA isolation were decapitated at 3, 6, 12 or 24 hours post-injection and their brains were removed and stored in liquid nitrogen. The RNA isolation procedure was identical to that outlined in Chapter 4. Similarly, the methodology for Northern blot analysis used in this experiment is detailed in Chapter 4. The hybridization probe used in this experiment to detect *c-fos* expression was generated from the cDNA fragment that corresponded to rat *c-fos* mRNA isolated from the differential display in Chapter 4.

In situ hybridization

The *in situ* hybridization protocol used to detect expression patterns of *c-fos* and *c-jun* mRNA was identical to the methodology outlined in Chapter 3. Oligonucleotide probes designed to hybridize to nts 140-184 of the rat *c-fos* mRNA (Genbank Assession number: X06769) had the following sequence; 5'- CAG CGG GAG GAT GAC GCC TCG TAG TCC GCG TTG AAA CCC GAG AAC– 3'. The oligonucleotide probe designed to target nts 1287-1346 of rat *c-jun* mRNA (Genbank Assession Number X17163) had the following sequence 5'-GCA ACT GCT GCG TTA GCA TGA CTT GGC ACC CAC TGT TAA CGT GGT TCA TGA CTT TCT GTT-3'.

Immunohistochemistry

Fixed tissue sections (40 μm) were washed in 0.1M phosphate-buffered saline (PBS) containing 0.1% Triton-X (PBS-TX) (3 x 5 minutes) and incubated with 1% hydrogen peroxide in PBS buffer for 15 minutes to inactivate endogenous peroxidase activity. Sections were then washed in PBS-TX (3 x 5 minutes) at room temperature and incubated in 10 normal horse serum (Dimension Laboratories Inc) diluted in PBS-TX. Following the blocking procedure, sections were washed in PBS-TX (3 x 5 minutes) and then incubated in a sheep polyclonal c-Fos antibody at a dilution of 1:5000 (Genosys) for 48 hours at 4°C. Following incubation with the primary antibody, sections were again washed in PBS-TX (3 x 10 minutes) and then incubated in a rat absorbed biotinylated secondary antibody (1:400; Vector Laboratories) for 1 hour. Excess antibody was removed by washing 3 x 10 minutes in PBS-TX and sections were stained using the ABC/DAB protocol outlined in the immunohistochemistry section of Chapter 3.

The immunohistochemical protocol used to detect the expression of c-Jun protein was similar to that for c-Fos with the exception of the primary antibody used. The primary antibody for c-Jun was raised in rabbit and was diluted to a concentration of 1:5000 in PBS-TX.

rAPO1

The protocol for this procedure involved the use of reverse-transcribed cDNA populations generated according to the methodology outlined in Chapter 4. The remainder of the protocol was conducted according to the manufacturer's recommended protocol in the Rat Apoptosis Genes-1 MPCR Amplification/Detection Kit. This protocol is designed to selectively amplify the mRNAs for *c-myc*, *bcl-2*, *caspase-3* and *P53* from cDNA populations for visualization on an agarose gel. Following reverse transcription, 5 μl of 10X rAPO1 MPCR buffer, 5 μl each of 10X rAPO1 MPCR primers; 0.5 μl Taq DNA polymerase (U/μl); 5 μl of sample cDNA, 4 μl dNTPs (3.125 mM) and 30 μl of dH_20 were combined in a sterile PCR tube per sample. PCR cycling parameters were as follows: 1) 96°C for 1 minute, 2) 60 °C for 4 minutes, 3) 96°C for 1 minute, 4) 60°C for 4 minutes 5) 98°C for 1 minute 6) 60°C for 2.5 minutes 7) repeat previous 2 steps between 28-35 times, 8) 70°C for 10 minutes and 9) 25°C soak. Upon completion

of the PCR cycles, samples were removed from the PCR machine and placed on ice. PCR products were electrophoretically separated on an agarose/EtBr (5 μg/ml) and the relative density of bands expressed in the lanes was examined under ultra-violet light using the Geldoc Molecular Analyst software.

Densitometry

Densitometric analysis of specific brain regions on *in situ* hybridization autoradiograms was performed using the Optical Density-Model GS0290 Imaging Densitometer and Molecular Analyst (Biorad) software to determine the optical density (OD/mm^2) of the radiolabeled brain regions on an *in situ* hybridization autoradiogram. The relative density of labeling was compared to the density of the same brain regions in naïve, ligated and hypoxic control animals. Animals from all control groups, regardless of timepoint sacrificed were analyzed as one group for statistical and graphical analysis. Any differences in mean transcript expression were statistically analyzed using a 1-way ANOVA followed by Tukey's post-hoc analysis.

Results

Northern Blot Analysis

Visualization of northern blot analysis revealed that RNA extracted from the ipsilateral hippocampus of CMZ-injected H-I animals exhibited an increased expression of *c-fos* mRNA at 12 (N = 5) and 24 (N = 4) hours post-injection relative to control (N = 4; N = 3 respectively) or H-I hippocampal tissue (N = 3; N = 4 respectively) at these time points. However, statistical analysis of the mean density of these bands, using a 1-way ANOVA, did not detect a significant difference in *c-fos* mRNA expression between these tissues. An increase in *c-fos* transcript level was also observed in tissue isolated from the ipsilateral parietal cortex of CMZ-injected H-I (N=4) animals sacrificed at 12 hours post-injection that was not present in control (N = 4) or H-I cortical tissue (N = 3) at this timepoint. Statistical analysis of the mean density of these bands demonstrated that the level of *c-fos* expression in the ipsilateral cortex of CMZ-injected H-I animals was significantly higher than in vehicle-injected H-I animals sacrificed at 12 hours post-injection ($q = 4.773$; $P<0.05$). Relative to the mobility of molecular weight standards (RNA ladder 0.24-9.5 kb, Gibco), the size of the hybridizing band was calculated to be approximately 2.3 kb as would be expected for the *c-fos* transcript. In order to ensure that each lane contained approximately the same amount of RNA, densitometric analysis was conducted on both the 28S and 18S ribosomal RNA. See Figures 5-1 and 5-2.

In situ Hybridization

Densitometric analysis of the pattern of expression for *c-fos* mRNA in control (N = 15), vehicle-injected (N = 9) and CMZ-injected H-I animals (N = 11) sacrificed at 12 hours post-injection did not demonstrate any significant differences in the level of this transcript within the ipsilateral hippocampus or cortex of vehicle-injected or CMZ-injected H-I animals relative to control animals. See Figure 5-3. However, in 7/11 CMZ-injected H-I animals sacrificed at 12 hours post-injection, specific and robust expression of *c-fos* mRNA was detected in the alveus, which surrounds the hippocampus, of the ipsilateral hemisphere. See Figure 5-4.

In order to compare relative expression patterns for *c-jun* mRNA across animal

Figure 5-1

Determination of the pattern of expression of c-fos mRNA in rat brain following hypoxia-ischemia.

Northern blot analysis of rat hippocampal total RNA using a cDNA probe complimentary to *c-fos* mRNA. Lanes 1 and 8 represent electrophoretically fractionated total RNA isolated from the ipsilateral hippocampus of naive control animals. Lanes 2 and 5 represent total RNA isolated from the contralateral hippocampus of vehicle-injected H-I animals. Lanes 3 and 6 contain total RNA isolated from the ipsilateral hippocampus of vehicle-injected H-I animals. Lanes 4 and 7 contain RNA samples isolated from the ipsilateral hippocampus of CMZ-injected H-I animals. Lanes 8, 9, 10 and 11 contain RNA isolated from the ipsilateral cortex of ligated control animals, the contralateral and ipsilateral cortex of vehicle-injected H-I animals and the ipsilateral hippocampus of CMZ-injected H-I animals respectively. The post-hypoxic time points for RNA isolation were as follows: 12 hours (lanes 1, 2, 3, 4, 8, 9, 10 and 11); 24 hours (Lanes 5, 6 and 7) post-hypoxia. The hybridization probe used in this experiment was generated from the cDNA fragment isolated from the differential display in Chapter 4 that corresponded to rat *c-fos* mRNA.

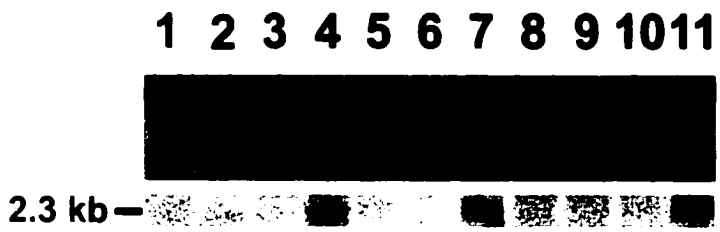

Figure 5-1

Figure 5-2

Densitometric analysis of c-fos expression in vehicle- and CMZ-injected H-I animals observed using northern blot analysis.

Graphical illustration of the mean density of the hybridization signal (*c-fos* mRNA expression) detected across animal groups examined using northern blot analysis. All animals were sacrificed at 12 or 24 hours post-injection. RNA populations used for quantitation included RNA from the hippocampii of control animals (C), the ipsilateral hippocampus of vehicle-injected H-I animals (VIH), the ipsilateral hippocampus of CMZ-injected H-I animals (CIH), the ipsilateral cortex of vehicle-injected H-I animals (VIC) and the ipsilateral cortex of CMZ-injected H-I animals (CIC). For quantitative and graphical analysis, the control group used was a collective representation of the density of hybridization signal in the ipsilateral hippocampus of ligated and naïve control animals and from the contralateral hippocampus of vehicle-injected H-I animals. A P value of <0.05 was considered to be significant. The data are presented as means ± S.E.M. (* = significantly different from control animals).

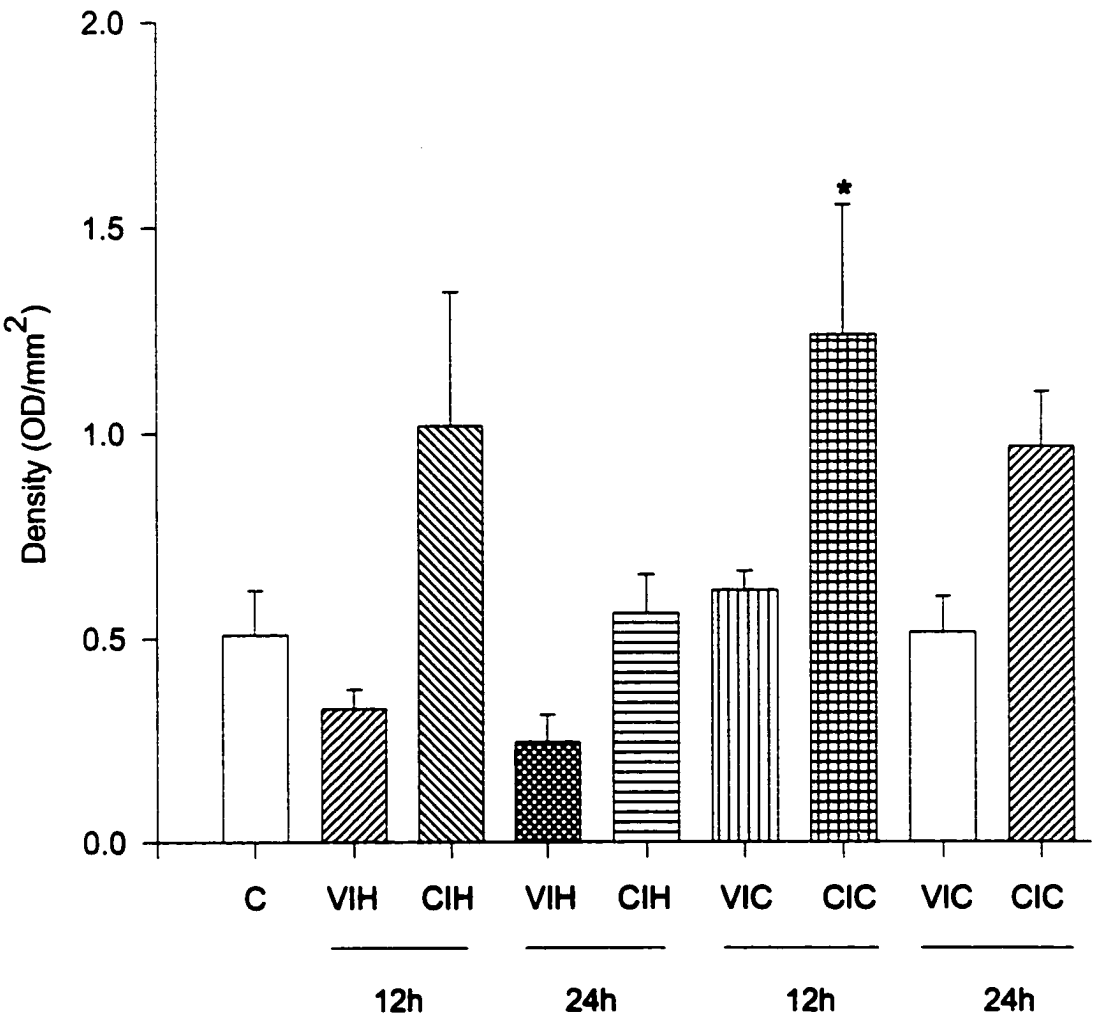
2.0
1.5
1.0
0.5
0.0
Density (OD/mm2)
*
C
VIH
CIH
VIH
CIH
VIC
CIC
VIC
CIC
12h
24h
12h
24h
Treatment Groups

Figure 5-2

Figure 5-3

Densitometric analysis of c-fos expression in vehicle- and CMZ-injected H-I animals observed using in situ hybridization.

Graphical illustration of the mean density of the hybridization signal (*c-fos* mRNA expression) detected across animal groups using *in situ* hybridization techniques. All animals were sacrificed at 12 hours post-injection. For quantitative and graphical analysis, the control group used was a collective representation of the density of hybridization signal in the ipsilateral hippocampus of ligated and naïve control animals and from the contralateral hippocampus of vehicle-injected H-I animals. A P value of <0.05 was considered to be significant. The data are presented as means ± S.E.M.

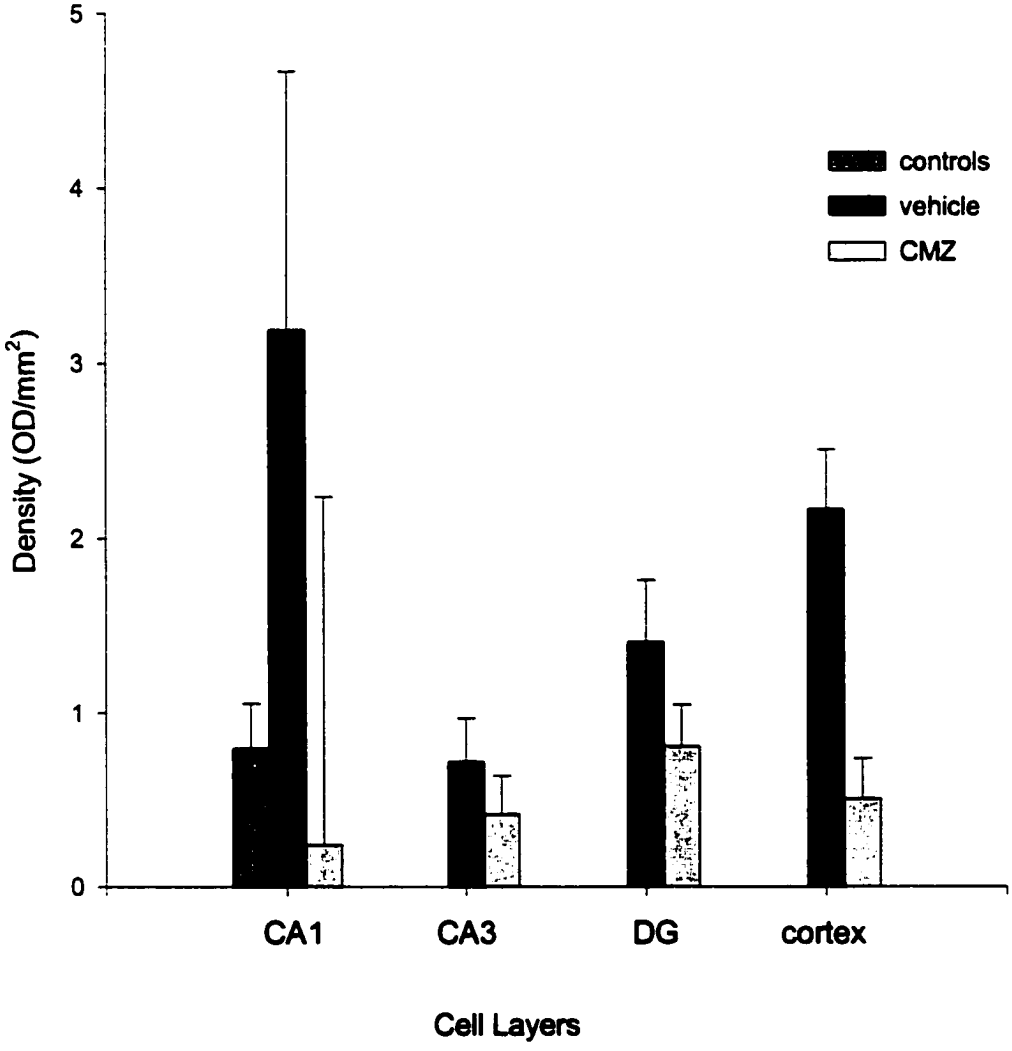
5
4
3
2
1
0
Density (OD/mm²)
controls
vehicle
CMZ
CA1
CA3
DG
cortex
Cell Layers

Figure 5-3

Figure 5-4

Localization of c-fos mRNA expression in CMZ-injected H-I animals.

Panel A) representative coronal section of a CMZ-injected H-I animal sacrificed at 12 hours post-injection. An oligonucleotide probe targeted for *c-fos* mRNA detection was used for *in situ* hybridization analysis. Arrow indicates positive hybridization signal in the alveus. Panel B) representative coronal section of a vehicle-injected H-I animal sacrificed at 12 hours post-injection.

A

B

Figure 5-4

treatment groups, control (N = 12), vehicle-injected (N = 9) and CMZ-injected (N = 11) H-I animals were sacrificed at 12 hours post-injection. The mean density of *c-jun* mRNA expression was found to be significantly higher in CA1 of the ipsilateral hippocampus in vehicle-injected H-I animals than in the CA1 layer of CMZ ($q = 4.985$; $P<0.05$) or control animals ($q = 5.988$; $P<0.05$). Moreover, the mean density of *c-jun* expression in CA1 of the ipsilateral hippocampus of CMZ-injected H-I animals was not significantly different from control animals. The mean density of *c-jun* mRNA was also significantly increased in the CA3 cell layer of the ipsilateral hippocampus of vehicle-injected H-I animals relative to control animals ($q = 5.345$; $P<0.05$) sacrificed at this time-point. However, the mean density of *c-jun* expression in CA3 of CMZ-injected H-I animals was not significantly different from control animals. The mean density of *c-jun* mRNA expression was increased significantly in the dentate gyrus of vehicle-injected ($q = 11.58$; $P<0.05$) and CMZ-injected ($q = 7.184$; $P<0.05$) H-I animals when compared to control animals. However, the mean density of expression for this transcript was still significantly higher in the DG of vehicle-injected H-I animals than in CMZ-injected H-I animals ($q = 4.677$; $P<0.05$). The mean density of *c-jun* expression was significantly elevated in the cortex of vehicle-injected ($q = 5.185$; $P<0.05$) and CMZ-injected ($q = 4.528$; $P<0.05$) H-I animals when compared to controls. It is also noteworthy that *c-jun* expression was significantly higher in the DG of vehicle-injected H-I animals than in the CA1 ($q = 5.22$; $P<0.05$), CA3 ($q = 5.821$; $P<0.05$) or the cortex ($q = 5.971$; $P<0.05$) of these animals at 12 hours post-hypoxia. See Figure 5-5.

Immunohistochemistry

c-fos

Immunohistochemical analysis demonstrated a very low constitutive expression of c-Fos immunoreactivity in the hippocampus of naïve animals (N = 6). Briefly, sporadic expression of Fos was observed in the upper blade of the dentate gyrus and in the CA3 subregion of the hippocampii. An identical pattern of c-Fos expression to that of naïve animals was observed in animals exposed to hypoxia alone (N = 20), ligation alone (N = 27) or varying doses of CMZ (N = 20).

c-Fos was observed in CA3, the hilus and the DG of the ipsilateral hippocampus

Figure 5-5

Densitometric analysis of c-jun expression in vehicle- and CMZ-injected H-I animals observed using in situ hybridization.

Graphical illustration of the mean density of the hybridization signals (*c-jun* mRNA expression) detected across animal groups examined using *in situ* hybridization techniques. All animals were sacrificed at 12 hours post-injection. For quantitative and graphical analysis, the control group used was a collective representation of the density of hybridization signal in the ipsilateral hippocampus of ligated and naïve control animals and from the contralateral hippocampus of vehicle-injected H-I animals. A P value of <0.05 was considered to be significant. The data are presented as means ± S.E.M. (* = significantly different from control animals; ■ = significantly different from CMZ-injected H-I animals).

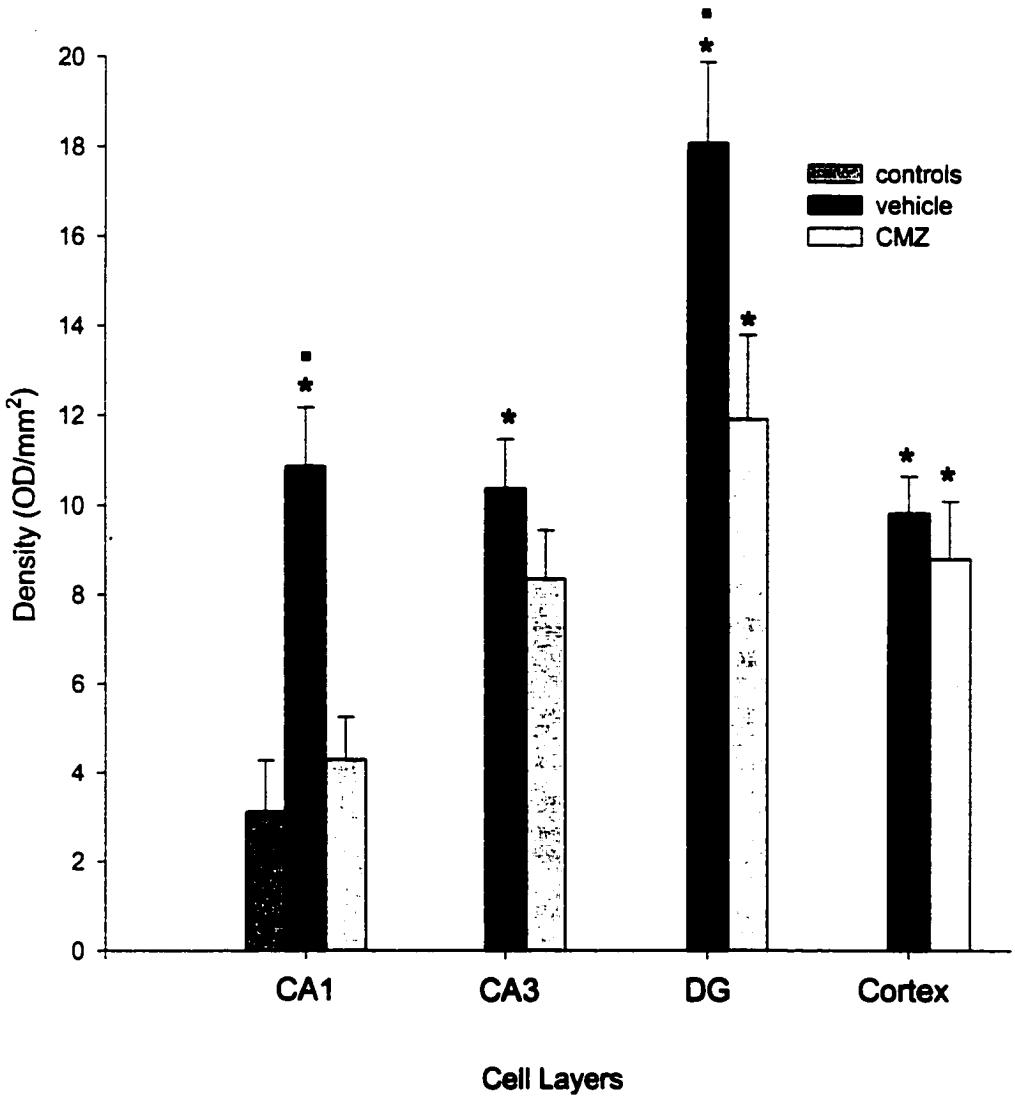
20
18
16
14
12
10
8
6
4
2
0
Density (OD/mm^2)
controls
vehicle
CMZ
CA1
CA3
DG
Cortex
Cell Layers

Figure 5-5

and in layers 3-6 of the ipsilateral parietal cortex of 3/4 vehicle-injected H-I animals sacrificed at 2 hours post-injection, however, 1/4 of those animals exhibited basal levels of this protein. All 3 vehicle-injected H-I animals sacrificed at 3 hours post-injection exhibited c-Fos in all cell layers of the ipsilateral hippocampus and parietal cortex. Similarly, c-Fos was present throughout the ipsilateral hippocampus and parietal cortex of 4/4 vehicle-injected H-I animals sacrificed at 6 hours post-injection. By 12 hours post-injection 3/4 vehicle-injected H-I animals exhibited basal levels of c-Fos in the ipsilateral hippocampus, but c-Fos expression was still detectable in the parietal cortex of these animals. Moreover, c-Fos remained in all cell layers of the ipsilateral hippocampus and parietal cortex of one vehicle-injected H-I animal. Finally, all 4 vehicle-injected H-I animals sacrificed at 24 hours post-injection exhibited basal levels of this protein in all brain regions.

A similar, but not identical, pattern of expression for c-Fos protein was observed in H-I animals that received an injection of 200 mg/kg CMZ at 3 hours post-hypoxia. In 5/7 CMZ-injected H-I animals sacrificed at 2 hours post-injection, c-Fos was noted throughout the CA3 cell layer and in patches of the DG in the ipsilateral hippocampus and in the ipsilateral parietal cortex. It is interesting that one of these 7 animals exhibited increased c-Fos in the pyramidal cell layers and hilus of the contralateral hippocampus. In addition, one of 7 H-I animals sacrificed at 2 hours post-injection exhibited basal levels of c-Fos in all cell layers. When CMZ-injected H-I animals were sacrificed at 3 hours post-injection, c-Fos was noted in all cell layers of the ipsilateral hippocampus of 5/5 animals, however, little expression was noted in the parietal cortex of these animals. A similar pattern of expression for c-Fos was observed in all 5 CMZ-injected H-I animals sacrificed at 6 hours post-injection. However, the cortical expression of c-Fos appeared to be more abundant in animals sacrificed at this timepoint. In contrast to vehicle-injected H-I animals, all 4 CMZ-injected H-I animals sacrificed 12 hours post-injection exhibited c-Fos-IR in CA3 and the DG of the ipsilateral hippocampus and parietal cortex. Moreover, in 4/4 CMZ-injected H-I animals sacrificed at 24 hours post-injection, c-Fos-IR was noted in CA1, CA3 and the hilus of the ipsilateral hippocampus and exhibited a patchy expression in the parietal cortex. See Figures 5-6 and 5-7.

Figure 5-6

C Fos expression in the hippocampus of vehicle- and CMZ-injected H-I animals at varying post-hypoxic timepoints.

Photomicrographic representation of c Fos expression in the ipsilateral hippocampus of vehicle-injected (A, C, E, G) and CMZ-injected (B, D, F, H) H-I animals. Animals were sacrificed 2 (A, B), 3 (C, D), 6 (E, F) and 12 (G, H) hours post-injection. (Scale bar = 400 μm).

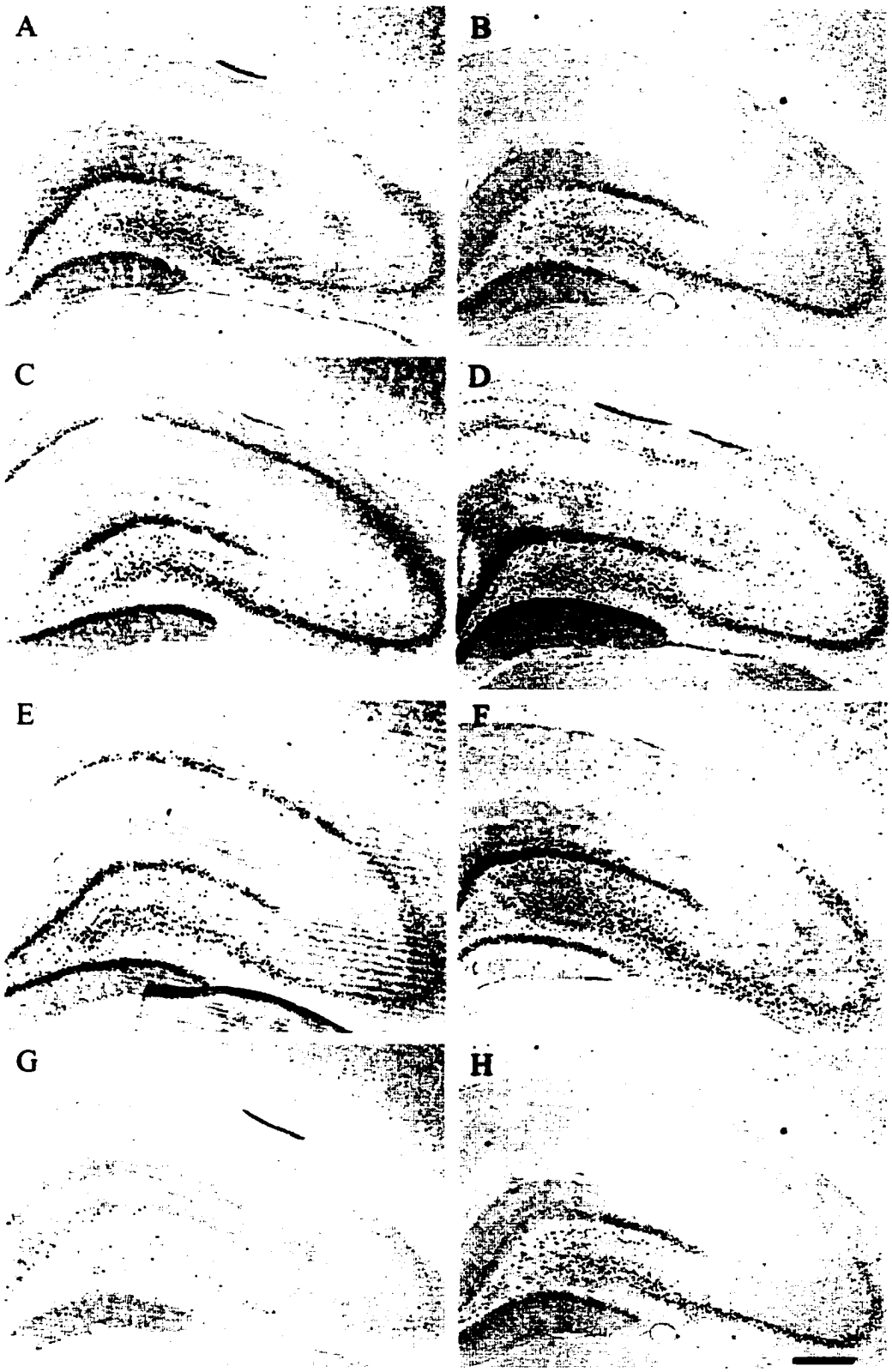

Figure 5-6

Figure 5-7

C Fos expression in the cortex of vehicle- and CMZ-injected H-I animals at varying post-hypoxic timepoints.

Photomicrographic representation of c Fos expression in the ipsilateral cortex of vehicle-injected (A, C, E, G) and CMZ-injected (B, D, F, H) H-I animals. Animals were sacrificed 2 (A, B), 3 (C, D), 6 (E, F) and 12 (G, H) hours post-injection. (Scale bar = 400 μm).

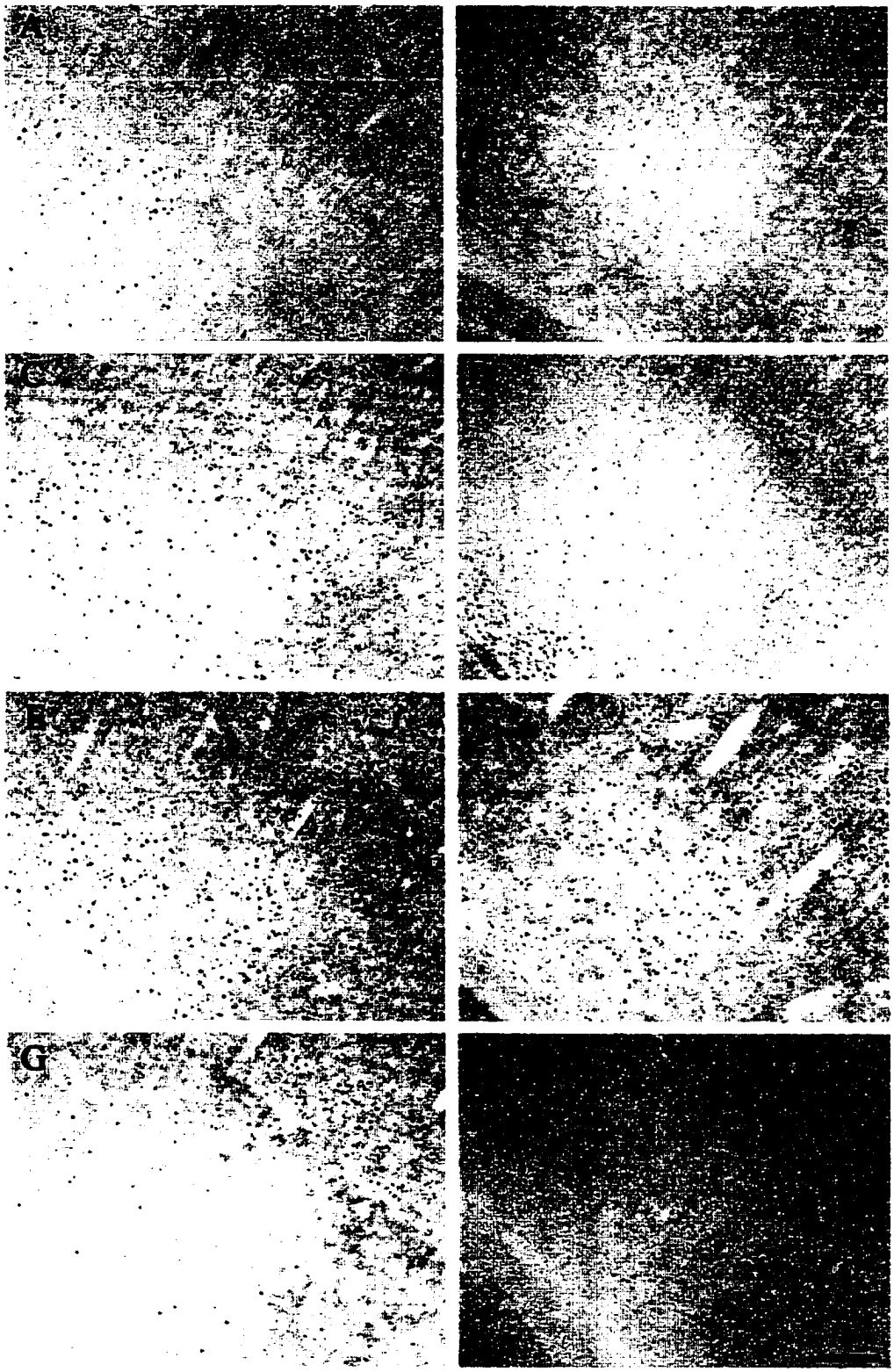

Figure 5-7

PCD-related Gene Expression

rAPO1 MPCR analysis does not permit quantitative assessment of the expression of PCD-related genes in cDNA populations. However, the presence of PCD-related genes can be examined in cDNA samples generated from total RNA. cDNA samples were produced from the ipsilateral and contralateral hippocampus of vehicle-injected and CMZ-injected H-I animals and from control animals. A 233 bp band, corresponding to the expected size of the PCR-amplified *bcl-2* product, was detected in the hippocampus of 6/8 CMZ-injected H-I animals sacrificed at 24 hours post-injection. However, a band of the same molecular weight was only detected in the ipsilateral hippocampus of 1/6 vehicle-injected H-I animals sacrificed at the same timepoint. It is important to note that the banding pattern for the putative *bcl-2* fragment was highly variable in CMZ- and vehicle-injected H-I animals sacrificed at 12 hours post-injection. No bands corresponding to the expected length of *P53* (203 bp) or *c-myc* (371 bp) were observed in any samples examined. Moreover, a band that corresponded to the expected length of *caspase-3* (658 bp) was evident in all samples examined including control animals. This experiment was conducted 3 separate times with varied cycling parameters and did not produce highly consistent results.

Discussion

The fact that an injection of CMZ (200 mg/kg) at 1 hour post-hypoxia was shown, in Chapter 1, to be less effective than the same dose injected at 3 hours post-hypoxia may indicate that CMZ interferes with a cellular mechanism that is not immediately active following H-I insult. Furthermore, the results of this experiment clearly demonstrate that CMZ administration, 3 hours following H-I, altered the normal pattern of expression for at least three genes currently believed to be involved in PCD-related events. These findings may suggest that PCD-mediated cellular events underlie H-I-induced delayed cell death and that CMZ administration interferes with the progression of these events in order to provide neuroprotection in the H-I model. Moreover, since recent research has suggested that PCD-induced cell death can be realized within hours, rather than days, after its initiation, it is conceivable that PCD even underlies the seemingly immediate (within 4 hours) cell death induced by severe models of ischemia. Therefore, the timepoint of administration for a putative neuroprotective agent, that interferes with the PCD process would be critical to its neuroprotective efficacy and would vary between animal models of ischemia. Based on the findings of this body of work and other studies that have investigated the neuroprotective effect of CMZ in animal models of ischemia, it would appear that CMZ does exhibit such a neuroprotective profile (Shuaib *et al.*, 1995; Sydserff *et al.*, 1995a).

c-fos and c-jun mRNA expression

Previous unpublished data produced using *in situ* hybridization and nothern blot analysis in our laboratory has shown an increased expression of *c-fos* mRNA at 1 and 3 hours post-hypoxia throughout the ipsilateral hippocampus and cortex. This increase was transient and levels of this transcript were at basal levels at 6, 12 and 24 hours post-hypoxia. A study conducted by Macaya *et al.* (1998) also demonstrated, using the Rice Vannucci model, that the induction of *c-fos* and *c-jun* mRNAs peaked 2 hours after H-I injury in both the ipsilateral hippocampus and cortex. A similar timeline has been reported for the expression of these transcripts following H-I in PND7 and PND23 rats (Aden *et al.*, 1994; Munell *et al.*, 1994). In all of these studies, the location of the

induction of these transcripts encompassed, but was not restricted to, those regions vulnerable to H-I injury. In this way, the mere expression of these transcripts was not predictive of ultimate cell fate. These studies also confirm that a high level of *c-fos* and *c-jun* mRNA was present in both the hippocampus and cortex of H-I animals before the 200 mg/kg dose of CMZ was administered in the present experiment (3 hours post-hypoxia).

Northern blot analysis revealed that mean transcript density for *c-fos* mRNA was significantly elevated, relative to control animals, in the ipsilateral cortices of CMZ-injected H-I animals sacrificed 12 hours post-injection. Based on these findings, it appears as though CMZ may cause either a biphasic or protracted elevation of *c-fos* mRNA expression that is specific to fully protected H-I tissue. Accordingly, prolonged expression of *c-fos* mRNA was reported in SOD-1 transgenic mice after mild focal cerebral ischemia when compared to wild-type mice (Kamii *et al.*, 1994). SOD-1 transgenic mice are bred to have an increased ability to scavenge and metabolize reactive oxygen species and have been shown to exhibit prolonged cellular survival following ischemia (Greenlund *et al.*, 1995). Thus, prolonged expression of *c-fos* mRNA may be correlated with neuronal protection following focal cerebral ischemia. In contrast, persistant *c-fos* mRNA expression has been assoicated with PCD-induced cell death (Dragunow *et al.*, 1993; Smeyne *et al.*, 1993; Chen *et al.*, 1995; Hafazi *et al.*, 1997). Such conflicting literature makes it difficult to determine the functional signficance of prolonged expression of *c-fos* mRNA following cellular injury.

It is also interesting that upon investigation into the localization of *c-fos* mRNA in CMZ-injected H-I animals sacrificed at 12 hours post-injection, a substantial increase in the expression of *c-fos* mRNA was observed the ipsilateral alveus of most CMZ-injected H-I animals. Unfortunately, the procedure used to extract brain regions for northern blot analysis (hippocampus and cortex) in this study can not ensure that all cells from the alveus were removed from either structure since the alveus is located within the interface of the ipsilateral hippocampus and cortex. Moreover, densitometric analysis of *c-fos* mRNA expression on an *in situ* hybridization autoradiogram did not detect a significant difference between any cell layers of the ipsilateral hippocampus or cortex in CMZ-injected relative to vehicle-injected H-I animals. Thus, it is conceivable that the increase

in *c-fos* mRNA observed using northern blot analysis is representative of a difference in *c-fos* mRNA expression within the ipsilateral alveus of these animal groups. The putative function of an increased expression of *c-fos* mRNA within the ipsilateral alveus of CMZ-injected H-I animals is currently unknown.

A study conducted by Kamme *et al.* (1995) investigated the effects of hypothermia-induced neuroprotection on the normal pattern of IEG expression following global ischemia. That study showed a delayed secondary peak expression of *c-jun* mRNA between 12-36 hours post-ischemia in normothermic animals but not in the protected hypothermic animals. A second, late induction of *c-fos* and *c-jun* mRNA has also been reported following H-I insult (Dragunow *et al.*, 1993). Accordingly, hippocampal protein binding to AP-1 has been shown to exhibit a biphasic enhancement at 3 and 72-120 hours post-ischemia (Domanska-Janik *et al.*, 1999). It has, therefore, been proposed that following ischemia there is an early, survival supporting, AP-1 response that is followed by a delayed phase of induction for these transcripts that is indicative of impending cell death (Domanska-Janik *et al.*, 1999). In the present study, the expression of *c-jun* mRNA was siginificantly lower in all susceptible cell layers of CMZ-injected H-I animals sacrificed at 12 hours post-injection than in vehicle-injected H-I animals sacrificed at the same timepoint. Thus, it appears as though the neuroprotective effects of CMZ may inhibit the second phase of *c-jun* induction in the H-I model.

It is interesting that the expression of *c-jun* mRNA was significantly higher in the DG than in any other hippocampal cell layer examined in vehicle-injected H-I animals despite the fact that the DG is the only surviving cell layer following H-I. A similar finding has been reported by Kamme *et al.* (1995) who demonstrated that the highest levels of IEG expression, both *c-fos* and *c-jun*, was observed in the DG (the most resistant region to ischemic insult) following 2-VO. These findings may indicate a rough correlation between the expression of IEGs and the survival of neurons. Information pertaining to the nature of target genes for the Fos/Jun-AP-1 complex is just beginning to emerge. Potential targets that contain binding sites for the AP-1 complex are proenkephalin, prodynorphin, GFAP and various growth factors such as NGF and BDNF (Sonnenberg *et al.*, 1989; Naranjo *et al.*, 1991). In light of these target sites, it is

conceivable that the Fos and Jun heterodimer is involved in the plasticity associated with cellular recovery from cellular injury (Gubits *et al.*, 1993). Nonetheless, no clear link between proto-oncogene induction and apoptotic or necrotic cell death has been established in models of cerebral H-I.

c-Fos and bcl-2

In this experiment, a prolonged expression of c-Fos protein was observed in the ipsilateral hippocampus and cortex of CMZ-injected H-I animals when compared to vehicle-injected H-I animals. Moreover, the prolonged expression of this protein in these animals appeared to be specific to cell layers that would normally die following H-I insult (CA1, CA3 and cortex). This finding is particularly interesting in light of recent research that has suggested that c-Fos may have anti-apoptotic properties. He *et al.* (1998) showed that c-Fos degradation was followed by caspase-3 activation in cells undergoing PCD. However, if the cells were transfected with a stable mutant form of c-Fos, that was not degraded by the proteosome, the cells did not undergo PCD. Also, in cells that overexpressed the anti-PCD protein, Bcl-2, c-Fos degradation was blocked and PCD was inhibited. The authors of that study concluded that prolonged c-Fos expression may have a neuroprotective action against PCD-mediated events, however, the neuroprotective effect can be eliminated by proteosome-mediated degradation of c-Fos, but preserved by Bcl-2 induction. Accordingly, the results of the present study demonstrated a prolonged expression of c-Fos in cell layers of CMZ-injected H-I animals that are known to die following H-I injury and may indicate an increased expression of *bcl-2* mRNA in CMZ-injected H-I animals sacrificed at 24 hours post-injection. These changes in expression were not evident in most vehicle-injected H-I animals sacrificed at the same timepoint. Additional data that is relevant to this finding was provided in a study conducted by Cheng *et al.* (1998) which demonstrated that the administration of caspase inhibitors at 3 hours post-hypoxia provided profound neuroprotection in the H-I model of ischemia-induced cell death. Clearly, these results can not confirm that CMZ-injection results the production of a mutant form of c-Fos, however, it seems reasonable to speculate that CMZ administration may ultimately cause a decrease in the activation of caspase-3 following H-I by prolonging c Fos and Bcl-2 expression.

The results of this experiment demonstrated a high level of *caspase-3* expression in all cDNA populations examined. Studies have shown that, despite the obvious role of caspases in PCD-mediated events, the expression of *caspase-3* mRNA is not specific to dying neuron populations. For instance, while transient global ischemia induced a prolonged (24-72 hours) expression of the *caspase-3* mRNA in rat hippocampal CA1 pyramidal neurons, elevation of the caspase transcript was also observed in cells that were not susceptible to the ischemic injury (Ni *et al.*, 1998). However, it is noteworthy that in contrast to the dying cell population, the expression of *caspase-3* mRNA was more transient in the non-susceptible cell layers lasting only 24 hours. Since the results obtained in the present study were generated using PCR-based methodology the level of expression of *caspase-3* across these animal groups could not be compared. Thus, futher work is required in order to determine whether the expression of *caspase-3* mRNA or protein, at timepoints beyond 24 hours post-injection, would be affected by CMZ administration in the H-I model.

Another study that may suggest an involvement for c-Fos in CMZ-induced neuroprotection against H-I and also illustrates differences between the effects of CMZ administration and administration of known $GABA_A$-agonists following excitotoxic injury was conducted by Zhang *et al.*, (1997). In that study, administration of muscimol (1 mg/kg) actually decreased c-Fos expression within the pyramidal cell layers of the hippocampus and cortex that is normally observed 6 hours following excitotoxic insult (Zhang *et al.*, 1997). Similarly, administration of diazepam has been shown to inhibit stress-induced c-Fos expression in the cerebral cortex and hippocampus (Bozas *et al.*, 1997). Differences in the effect of these GABA-potentiating compounds on the expression of c-Fos may be further evidence for a second mechanism of action for CMZ that could account for its increased neuroprotective ability relative to $GABA_A$-agonists.

In conclusion, the results of this study suggest that administration of a fully protective dose of CMZ following H-I altered the normal pattern of expression for PCD-related genes. The prolonged expression of c-Fos protein observed in cell layers that are susceptible to H-I injury may indicate that CMZ-induced neuroprotection is achieved by preventing the degradation of c-Fos by the proteosome. In addition, the evidence provided in this study that bcl-2 mRNA expression may be altered in CMZ-injected, but

not vehicle-injected, H-I animals at 12 hours post-hypoxia may suggest that CMZ prevents the induction of caspase-3 following H-I injury. However, the limitations of the techiniques used in this study do not warrant functional statements regarding the expression of these genes and their proteins. Furthermore, the inconsistency of the results produced by the rAPO1 kit warrant further research into the effect of CMZ-induced neuroprotection on bcl-2 mRNA and protein expression.

Part III

An Investigation into the Functional Integrity of Limbic Circuits Following CMZ-induced Neuroprotection in H-I Rats

Chapter 6: *Clomethiazole-Induced Neuroprotection in the H-I Model May Permanently Alter the Excitability of Hippocampal-Based Circuits.*

Summary

A post-hypoxic injection of 200 mg/kg CMZ, administered 3 hours following H-I, provided profound histological neuroprotection in PND25 male rats. While cells in susceptible brain regions appeared to be morphologically intact in CMZ-treated H-I animals, it can not be assumed that circuits driven through these cell layers were unaffected by the H-I event. To determine whether hippocampal-based circuits were functionally intact in H-I animals treated with CMZ (100 or 200 mg/kg), stimulating/ recording electrodes were implanted, bilaterally, in the hippocampii of rats approximately 60 days following H-I. Similarly, bilateral electrodes were implanted in animals that were used in several control groups including hypoxic controls, ligated controls, naïve controls and vehicle-injected H-I animals approximately 60 days following their respective treatments. Two weeks after surgical implantation of the electrodes, the after-discharge threshold (ADT) for both the right and left hippocampus was determined in each animal. Comparisons were made across all animal groups with respect to ADTs, AD durations and kindling rates in the ipsilateral and contralateral hippocampii of these animals. Mean ADT data indicated that H-I animals treated with 100 or 200 mg/kg CMZ at 3 hours post-hypoxia required a significantly higher stimulus intensity to elicit an ADT in the left (ipsilateral) hippocampus than did control or vehicle-injected H-I animals. However, the mean stimulus intensity required to elicit an ADT in the right (contralateral) hippocampus of CMZ-treated H-I animals was not significantly higher than in control animals. Vehicle-injected H-I animals exhibited a significantly longer pre-kindling AD duration in the ipsilateral hippocampus than any control animals or CMZ-injected H-I animals. Hypoxic control animals required a significantly lower number of stimulations to achieve stage 5 convulsions than did any other animal group examined which is indicative of a faster kindling rate for these animals. Results of this experiment suggest that a previous excitotoxic event, such as H-I or hypoxia alone, may facilitate seizure propagation and/or seizure susceptibility. Moreover, CMZ-induced neuroprotection following H-I may permanently decrease the local excitability of protected cell layers. It is unclear whether the increase in pre-kindling ADT observed in CMZ-injected H-I animals would be of any clinical advantage to stroke patients.

Introduction

The neuroprotective efficacy of CMZ has been measured in animal models of ischemia using a variety of histological procedures including cresyl violet nissl stain, silver impregnation and hematoxylin-eosin-safran (HES) stain (Cross *et al.*, 1991; Shuaib *et al.*, 1995; Sydserff *et al.*, 1995; Thaminy *et al.*, 1997). In addition, numerous studies have been conducted to establish whether the histological neuroprotection provided by CMZ administration also improves functional outcome measurements of susceptible neurons following ischemia. Baldwin *et al.* (1993) measured locomotor activity in gerbils following carotid artery occlusion and found a positive correlation between locomotor activity and severity of brain damage at post-ischemic intervals. However, an attenuation in ischemia-induced hyperexcitability was observed in gerbils that received an injection of CMZ following carotid artery occlusion. In that study, ischemic gerbils also exhibited decreased nest-building behavior relative to control animals at post-ischemic time-points, whereas nest-building behavior in gerbils that had received the protective dose of CMZ did not diminish relative to control animals. A study conducted by Liang *et al.* (1997) demonstrated that following ischemia there is an increase in cognitive (learning and memory) deficits in both rats and gerbils. This deficit manifested as an increase in working memory errors in ischemic animals relative to control animals when tested in the radial arm maze. However, treatment with CMZ (100 mg/kg or 200 mg/kg) prior to the ischemic event reduced working memory errors significantly when compared to non-drug treated ischemic animals. Moreover, functional neuroprotection resulting from post-ischemic CMZ administration has been observed in a primate model of ischemia. A loading dose of CMZ (40 mg/kg) administered at 5 minutes post-ischemia followed by prolonged minipump infusion reduced behavioral deficits in marmosets following MCAO. Specifically, evaluation of functional outcome measures using staircase tasks (hill and valley) and the 2 tube test revealed that CMZ-treated monkeys were better than non-drug treated monkeys in their use of the contralateral disabled arm and also showed a decrease in contralateral hemineglect relative to ischemic control animals (Marshall *et al.* 1999). Collectively, these studies indicate that reports of histological neuroprotection in CMZ-treated animals appear to coincide with reports of

heightened behavioral outcome when this compound is used in animal models of ischemia.

In chapter 1, we demonstrated that an injection of CMZ (200 mg/kg) at 3 hours post-hypoxia provided complete histological protection in all susceptible cell layers of the ipsilateral and parietal cortex. However, whether the apparent morphological neuroprotection observed in these animals actually translated into functional sparing of H-I neurons was not clear. Unfortunately, use of ischemia models that produce unilateral hippocampal damage, such as the Rice-Vannucci model of H-I, prevent the secondary use of traditional behavioral models to assess limbic system function because the contralateral structures remain intact and can, therefore, recover the function of the damaged hippocampus. In this way, the sensitivity of traditional behavioral models is not high enough to detect dysfunction in only one hippocampus. Nonetheless, functional improvement is a measure of great clinical significance, therefore, we used a well characterized behavioral animal model known as kindling to determine whether the synaptic circuitry driven through or originating from the ipsilateral hippocampus remained intact in CMZ-treated H-I animals.

Kindling

Kindling is the most commonly used animal model of human complex partial seizures and is characterized by a progressive and permanent increase in local and propagating seizure activity that is triggered through stimulation of discrete brain areas such as the amygdala, hippocampus and piriform cortex (Goddard *et al.*, 1969; Racine, 1972). A single kindling stimulus in any of these brain regions produces focal seizure activity, or an after-discharge (AD), which is essential for kindling to occur. One of the hallmark characteristics of kindling is that successive stimulation with a previously subconvulsive stimulus ultimately elicits seizure behavior which becomes progressively more prominent in spite of the fact that the stimulus intensity does not vary. This phenomenon relies on the fact that as the number of stimulations increase, the AD elicited progressively increases in amplitude, duration and frequency and subsequently propagates to other brain structures including those in the contralateral hemisphere. Associated with the increase in seizure discharges and the recruitment of distant brain

regions, is the reliable triggering of generalized motor convulsions (Kelly *et al.*, 1999). Since limbic structures themselves are unable to directly support motor seizure behavior, the local discharges triggered from these kindled sites must propagate to one or more intermediary structures that have direct access to spinal motor neurons (Kelly *et al.*, 1999). Numerous studies have shown that, once established, kindling-induced enhanced susceptibility to seizure activity is permanent (Goddard *et al.*, 1969; McNamara *et al.*, 1985; Kamphuis *et al.*, 1990). Since its discovery, the kindling phenomenon has been observed in various species and has been elicited from numerous brain structures. However, profound differences in kindling parameters have been reported across different species and brain regions (Losher *et al*, 1998). Both genetic and environmental influences are thought to be involved in this variability.

During the kindling protocol, measurement of various kindling parameters enables the detection of changes in synaptic circuitry within limbic regions. Such parameters include the after discharge threshold (ADT), AD duration and the kindling rate. After discharge is a term used to refer to the summary of all epileptiform activity at the site of stimulation and can be seen as a rhythmic pattern of spikes on an electroencephalographic (EEG) trace. The term ADT refers to the minimum stimulus intensity required to elicit an AD from a stimulated structure and provides information relevant to the local excitability of that structure. Measurement of the AD duration provides information pertaining to the propagation dynamics of the seizure circuit, or simply, the ability of cells within the stimulated brain region to recruit other structures into the seizure circuit. Generally, the AD duration is indicative of how long the seizure activity was maintained before it was terminated. Finally, the kindling rate is a term used to refer to the total number of stimulations required to elicit the first stage 5 convulsion and is also used as a measure of propagation dynamics in a kindling circuit.

Kindling as a Measure of the Functional Integrity of Limbic Structures

Kindling has been used as an animal model for temporal lobe epilepsy, learning and memory and neuronal plasticity (Stokes and McIntyre, 1985; McIntyre and Racine, 1986; Cain, 1989; Sato *et al.*, 1990). Kindling has also served as a very sensitive indicator of seizure susceptibility in the rat brain (Mosh9 *et al.*, 1983). In this study, we

proposed that the kindling model could also be used as a functional measure to evaluate the neuroprotective ability of various compounds in animal models of ischemia. Measurement and comparisons of kindling parameters such as kindling rate, ADT and AD duration may provide information pertaining to the functional state of susceptible cell layers in ischemic versus control animals. For instance, it has been suggested that seizure susceptibility in limbic structures, such as the hippocampus, may be positively correlated with the level of neurodegeneration in these regions (Meldrum *et al.*, 1997). Moreover, long term analysis of H-I animals has demonstrated that H-I injury leads to permanent impairment of the normal balance between binding sites of excitatory and inhibitory neurotransmitter receptors in numerous brain regions (Qu *et al.*, 1998). The kindling phenomenon is very sensitive to the balance between excitatory and inhibitory neurotransmission. Roberts (1986) defined the seizure evoked through the kindling procedure as a final common pathway taken by CNS tissue when excitatory activity exceeds the capacity of the tissue to modulate that activity. As such, amygdala kindling is generally retarded by local injections of GABA or the $GABA_A$-agonist, muscimol. Use of the kindling model in this way may indicate whether the morphologically intact cells observed in CMZ-injected H-I animals have retained all connectivity to other limbic structures and are, in fact, fully functional. Thus, this study may determine whether synaptic circuits within susceptible cell layers of CMZ-treated H-I animals exhibit fundamental differences in local excitability and propagation dynamics when compared to vehicle-injected H-I animals or control animals.

Methods

Animals

As in previous experiments, PND25 male rats were divided into 6 groups including naïve animals, ligated controls, hypoxic controls, vehicle-injected H-I animals and H-I animals that received 200 mg/kg or 100 mg/kg CMZ at 3 hours post-hypoxia. The H-I protocol used in this experiment was identical to the protocol outlined in Chapter 1. Following respective treatments all animals were returned to the Dalhousie Animal Care facility in groups of 6-10 animals. Approximately 2 weeks after returning to the facility, animals were separated and housed in groups of two. During the time spent in the facility all animals were handled daily to prepare for handling during the kindling protocol. In addition, all animals were continuously monitored for spontaneous seizure activity.

Kindling Surgery

Approximately 60 days following their respective treatments, all subjects were anesthetized using an injection of sodium pentobarbitol (65 mg/kg. ip.). If the subject did not respond completely, a supplemental injection (3.25 mg/kg) was administered. Once fully anesthetized, each animal was implanted with bilateral bipolar stimulating/recording electrodes using the co-ordinates 3.0 mm posterior to bregma, +/- 3.5 mm lateral to bregma and 3.0 mm below the surface of the skull. These coordinates were determined using bregma and lambda in flat skull measurements to ensure electrode tips were placed in the dorsal region (CA1) of both the ipsilateral and contralateral hippocampii. These coordinates were chosen in reference to the brain atlas of Paxinos and Watson (1986). The bipolar electrodes consisted of two twisted strands of 127 μm diameter Nichrome wire that were Diamel-insulated, with the exception of the tip, and attached to male Amphenol pins. The electrodes were cut to length, surgically implanted and secured to the skull with six jeweller's screws and a covering of dental acrylic. Once secure, the electrodes were fitted into a headplug conformation which was then secured to the skull with dental acrylic (Molino and McIntyre, 1972).

Kindling Procedure

Following surgery all animals were permitted to recover for 10 days before ADT determination. The ADT was defined as the minimum stimulus intensity required to provoke a clearly discriminable, high voltage, electrographic seizure event (an AD) that outlasted the stimulus by two or more seconds (Kelly *et al.*, 1999). To determine the ADT, a 2 second 60 Hz sine wave stimulus of progressively increasing intensity (beginning at 10 μA) was applied to the left (ipsilateral) hippocampus. If an AD was not produced the animal was successively stimulated in stepwise increments (10 μA) until an AD was evoked (450 μA peak-to-peak maximum). A one minute interval was allotted between stimulations. If an AD could not be evoked, even at the maximum stimulus intensity, the stimulation procedure was discontinued and the animal was allowed to rest for 24 hours before being re-tested. The ADT was first determined in the left (ipsilateral) hippocampus of each animal and 24 hours later the ADT was determined in the right (contralateral) hippocampus using the same protocol. In the event an AD could not be elicited from the hippocampus the animal was removed from the experiment.

Once the ADTs were determined, all animals were stimulated daily in the left (ipsilateral) hippocampus with a 2s, 60 Hz sine wave, at a stimulus intensity corresponding to the established ADT, until 6 consecutive stage 5 seizures were recorded or until an upper limit of 85 stimulations had been reached. Convulsive behavior was measured according to a modification of Racine's criteria which is as follows: Stage 0 = no response or immobility; Stage 1 = rhythmic mouth or facial movement; Stage 2 = rhythmic head nodding; Stage 3 = forelimb clonus; Stage 4 = rearing and bilateral forelimb clonus; Stage 5 = rearing and falling (Racine, 1972). Twenty-four hours following the last of 6 consecutive stage 5 seizures, the ADTs in both the left and right hippocampus were reassessed in each animal. Finally, 24 hours following ADT re-determination the left hippocampus was stimulated at the previous kindling intensity and the animals were perfused 2 hours later for histological assessment.

Perfusion and Tissue Fixation

Animals were sacrificed 2 hours following the final stimulation in the left hippocampus. Each rat was deeply anaesthetized with 65 mg/kg of sodium pentobarbitol and was then perfused through the ascending aorta with 0.9% saline (120 mls) followed by cold 100 mM phosphate buffer containing 4 % paraformaldehyde (120 mls). Brains were removed and post-fixed in 100 mM phosphate buffer containing 4% paraformaldehyde at 4°C for at least 24 hours. The brains were then processed for cresyl violet analysis according to the procedure outlined in Chapter 1.

Measurements of Interest

During the kindling protocol measurements of ADT, AD duration and kindling rate were recorded for each subject. Pre-kindling ADT was used to measure differences in relative local excitability in CA1 between CMZ- and vehicle-injected H-I animals and control groups. Pre-kindling AD duration was used as a measure of local seizure propagation dynamics in these animal groups. Finally, the kindling rate was measured in animals from each group and was used to reflect the relative excitability of the entire limbic seizure circuit.

Statistical Analysis

The parametric data was assessed using a one-way ANOVA followed by Tukey's post-hoc analysis. Differences were considered to be significant at $P<0.05$. The data are presented as means ± S.E.M.

Results

Histology

In 9 out of 45 animals that underwent kindling surgeries, the headplug assembly was dislodged during the kindling procedure. These animals were sacrificed immediately. Histological assessment of all kindled animals (N = 36) that were sacrificed 2 hours following the final stimulation to the ipsilateral hippocampus revealed that in 31 of 36 animals the stimulating/recording electrodes were located in or very near the CA1 pyramidal cell layer of both the ipsilateral and contralateral hippocampii. However, in 5 of 36 kindled animals one or both electrode tips were not correctly placed in CA1 and these animals were, therefore, eliminated from the study.

Measured Kindling Parameters

Kindling Rate

The number of stimulations required to elicit a fully generalized (Stage 5) seizure did not differ significantly between naïve animals (N = 6) and vehicle (5) or CMZ-injected animals (100 mg/kg N = 4; 200 mg/kg N = 5). However, a significantly faster kindling rate was observed in hypoxic control animals (N = 5) relative to naïve animals ($q=5.576$; $P<0.05$). In addition, the kindling rate of ligated control animals (N = 3) was significantly reduced when compared to hypoxic control animals ($q = 8.267$; $P<0.05$), vehicle-injected H-I animals ($q = 6.903$; $P<0.05$) or CMZ-injected H-I animals that received either 200 mg/kg ($q = 5.316$; $P<0.05$) or 100 mg/kg ($q = 6.755$; $P<0.05$) at 3 hours post-hypoxia. However, the kindling rate exhibited by the ligated control animals was not significantly different from naïve animals. See Figure 6-1.

Pre-Kindling ADT

Determination of the pre-kindling ADT in both the ipsilateral and contralateral hippocampii of each animal prior to kindling revealed that the ipsilateral hippocampus of CMZ (200 mg/kg)-injected H-I animals (N = 6) required a significantly higher stimulus intensity (ADT) to evoke an after discharge (AD) than did naïve (N = 6) control animals ($q = 10.153$; $P<0.05$). Moreover, the ADT established in the ipsilateral hippocampus of

Figure 6-1

Comparison of mean kindling rates in CMZ-injected versus vehicle-injected H-I animals.

Graphical illustration of the mean number of stimulations required to elicit a fully generalized (stage 5) seizure in the ipsilateral hippocampus across various animal groups. A P value of <0.05 was considered to be statistically significant (* = significantly different from naïve control animals; ■ = significantly different from ligated control animals).

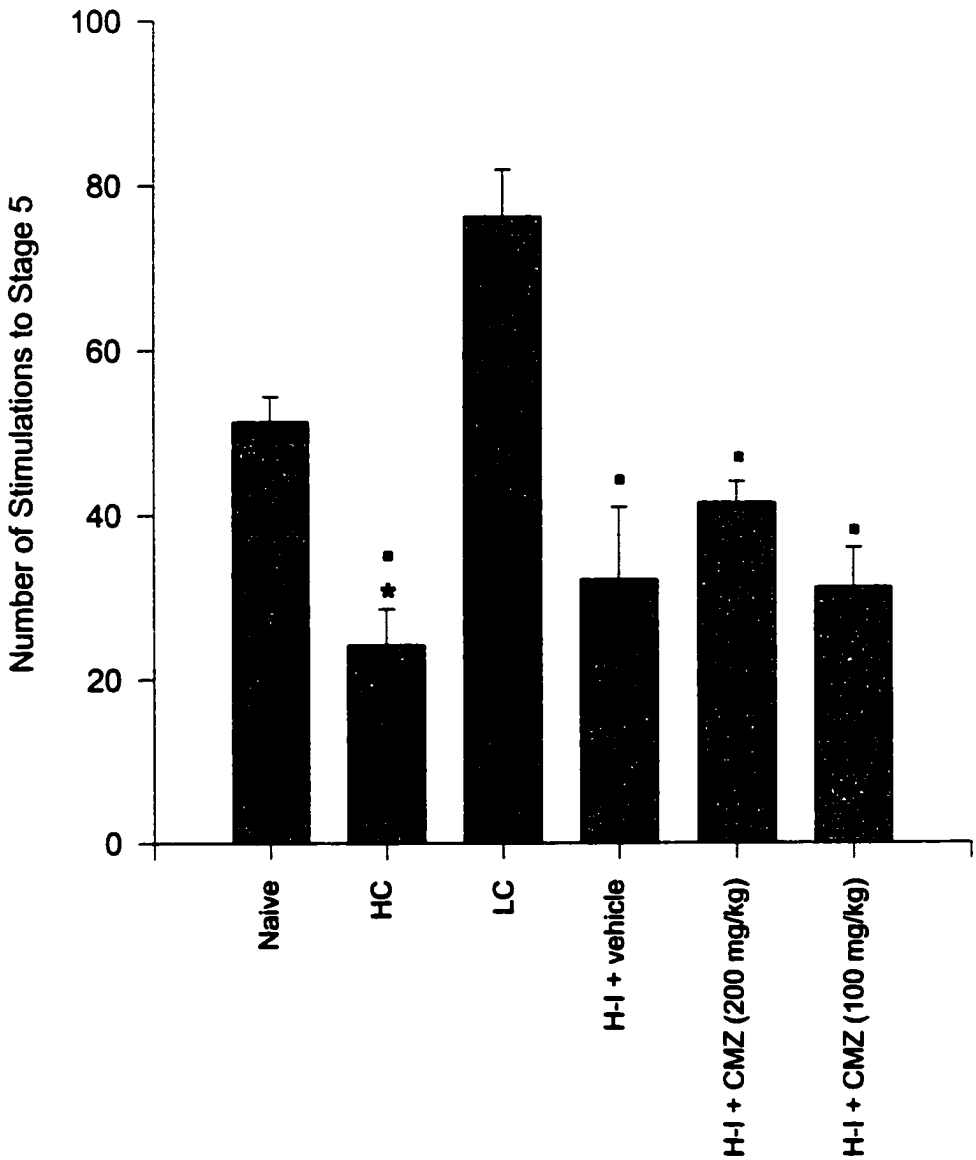
Number of Stimulations to Stage 5
100
80
60
40
20
0
Naive
HC
LC
H-I + vehicle
H-I + CMZ (200 mg/kg)
H-I + CMZ (100 mg/kg)

Figure 6-1

CMZ-injected H-I animals that received 200 mg/kg CMZ was significantly higher than in the ipsilateral hippocampus of hypoxic controls ($q = 9.552$; $P<0.05$; $N = 5$), ligated controls ($q = 8.18$; $P<0.05$; $N = 3$) and vehicle-injected H-I animals ($q = 9.135$; $P<0.05$; $N = 5$). The pre-kindling ADT was also significantly higher in the ipsilateral hippocampus of CMZ-injected H-I animals that received 100 mg/kg CMZ ($N = 4$) than it was in naïve controls ($q = 5.571$; $P<0.05$), hypoxic controls ($q = 5.244$; $P<0.05$) and vehicle-injected H-I animals ($q = 4.868$; $P<0.05$). No significant difference was noted in the ADTs elicited from the ipsilateral hippocampus of H-I animals that received 100 or 200 mg/kg CMZ. Significant differences in pre-kindling ADT were not evident in the ipsilateral or contralateral hippocampii of any other treatment/control groups examined. See Figure 6-2.

Pre-Kindling AD Duration

A significant increase in the pre-kindling AD duration was observed in the ipsilateral hippocampus of vehicle-injected H-I animals when compared to the ipsilateral and contralateral hippocampii of naïve control animals ($q = 5.98$; $q = 5.32$ respectively; $P<0.05$), hypoxic controls ($q = 5.383$; $q = 5.357$ respectively; $P<0.05$), ligated controls ($q = 5\ 362$; $q = 4.882$; $P<0.05$) and CMZ-injected H-I animals that received 200 mg/kg ($q = 5.335$; $q = 5.114$ respectively; $P<0.05$). However, while the pre-kindling AD duration in vehicle-injected animals was significantly different from the AD duration elicited from the contralateral hippocampus of H-I animals that received 100 mg/kg at 3 hours post-hypoxia ($q = 5.141$; $P<0.05$), no significant difference was observed relative to the ipsilateral hippocampus of these animals. See Figure 6-3.

Post-kindling Parameters

No significant differences were observed in post-kindling ADT in either the ipsilateral or contralateral hippocampus of any treatment group examined. Similarly, significant differences were not observed in the post-kindling AD duration in either the ipsilateral or contralateral hippocampus of any animal groups examined. See Figures 6-4 and 6-5 respectively.

Figure 6-2

Comparison of mean pre-kindling ADTs in CMZ-injected versus vehicle-injected H-I animals.

Graphical illustration of the mean pre-kindling ADTs elicited from the ipsilateral hippocampus across various animal groups. A P value of <0.05 was considered to be statistically significant (* = significantly different from all other animal groups except CMZ-injected H-I animals that received 100 mg/kg; ■ = significantly different from all other animals groups except CMZ-injected H-I animals that received 200 mg/kg).

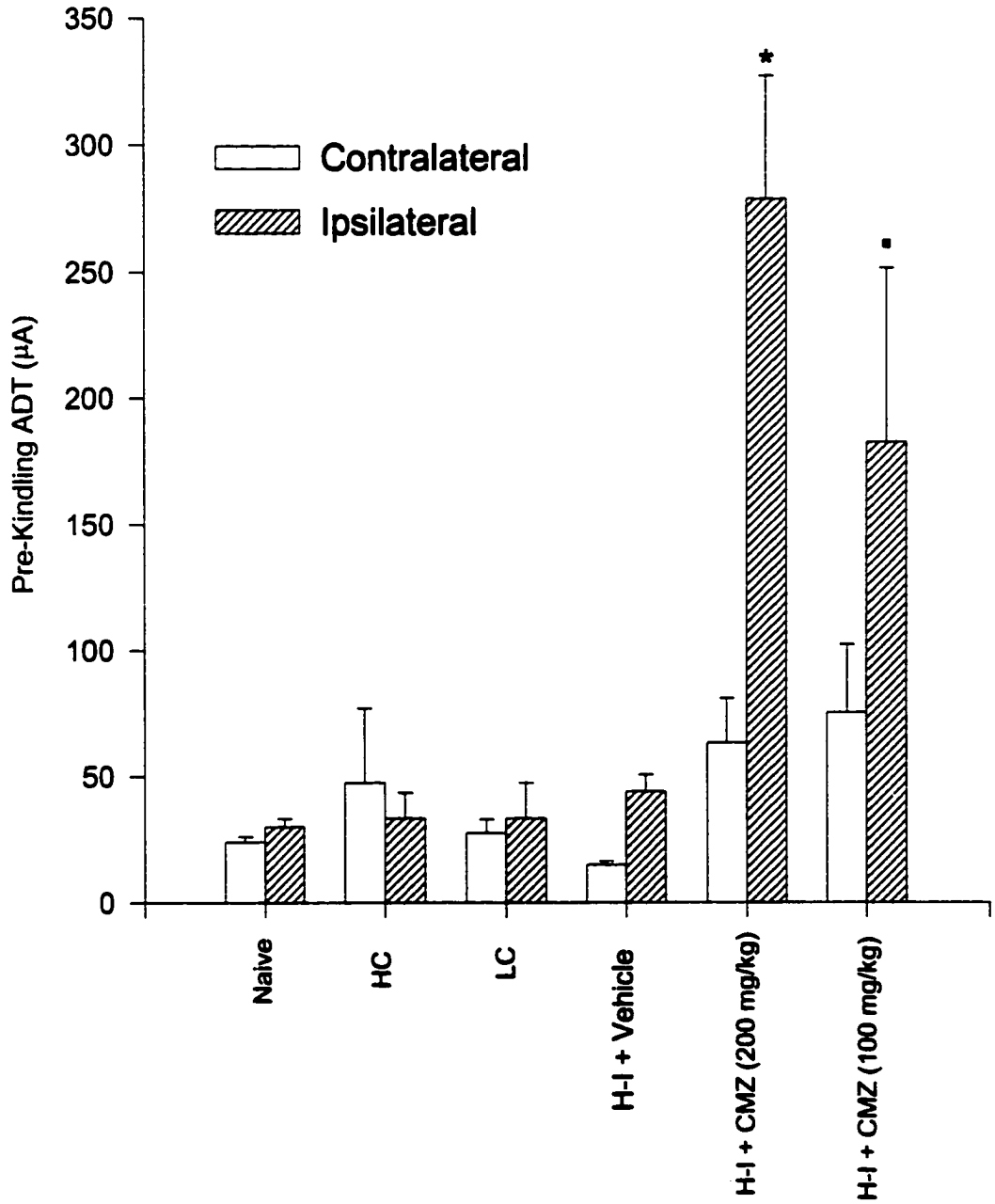
350
300
250
200
150
100
50
0
Pre-Kindling ADT (μA)
Contralateral
Ipsilateral
*
▪
Naive
HC
LC
H-I + Vehicle
H-I + CMZ (200 mg/kg)
H-I + CMZ (100 mg/kg)

Figure 6-2

Figure 6-3

Comparison of mean pre-kindling AD duration in CMZ-injected versus vehicle-injected H-I animals.

Graphical illustration of the mean duration of the AD elicited during the first ADT in the ipsilateral hippocampus across various animal groups. A P value of <0.05 was considered to be statistically significant (* = significantly different from all other animal groups).

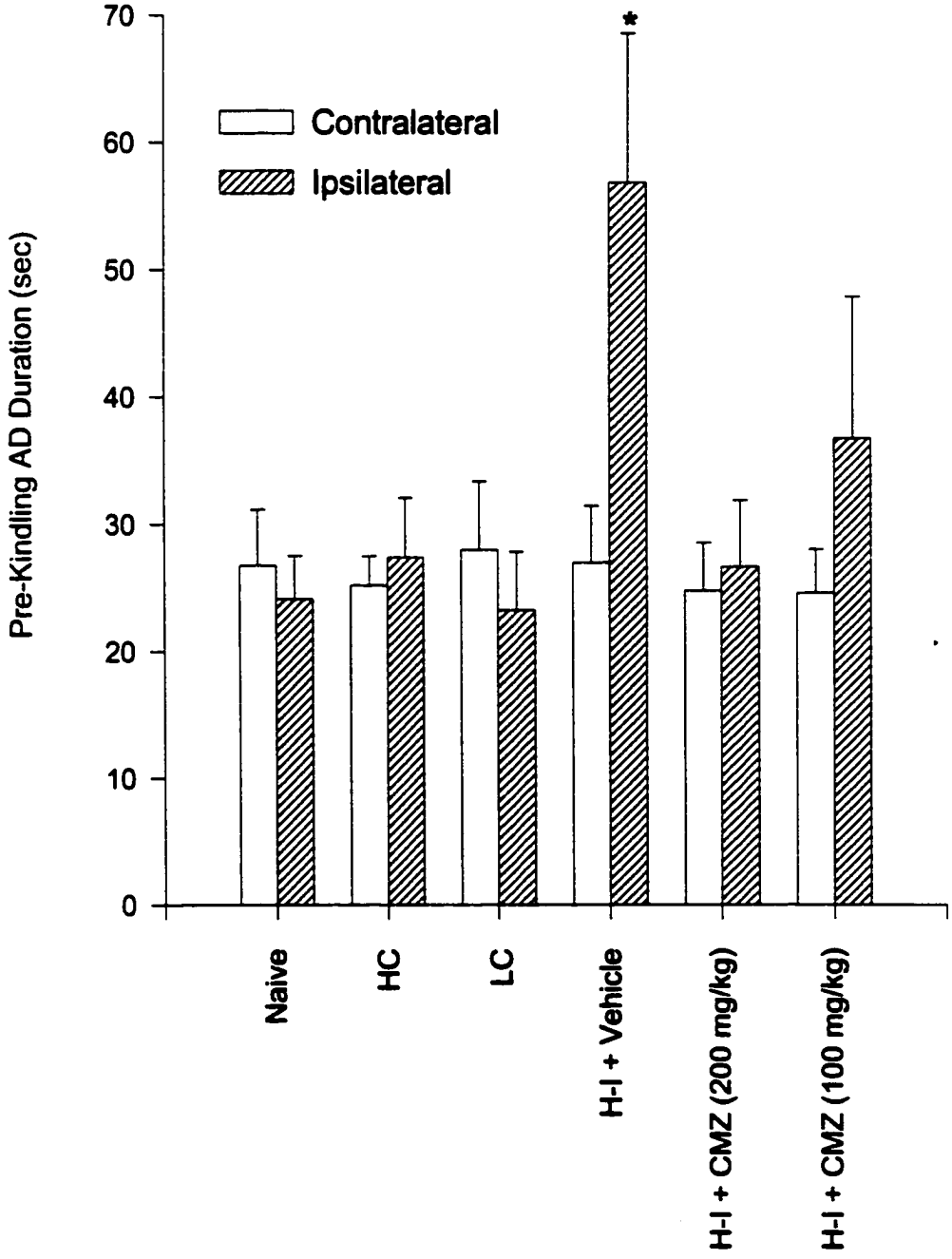
Pre-Kindling AD Duration (sec)
70
60
50
40
30
20
10
0
Contralateral
Ipsilateral
*
Naive
HC
LC
H-I + Vehicle
H-I + CMZ (200 mg/kg)
H-I + CMZ (100 mg/kg)

Figure 6-3

Figure 6-4

Comparison of mean post-kindling ADTs in CMZ-injected versus vehicle-injected H-I animals.

Graphical illustration of the mean post-kindling ADTs elicited from the ipsilateral hippocampus across various animal groups. A P value of <0.05 was considered to be statistically significant. Statistically significant differences were not observed between any two groups examined.

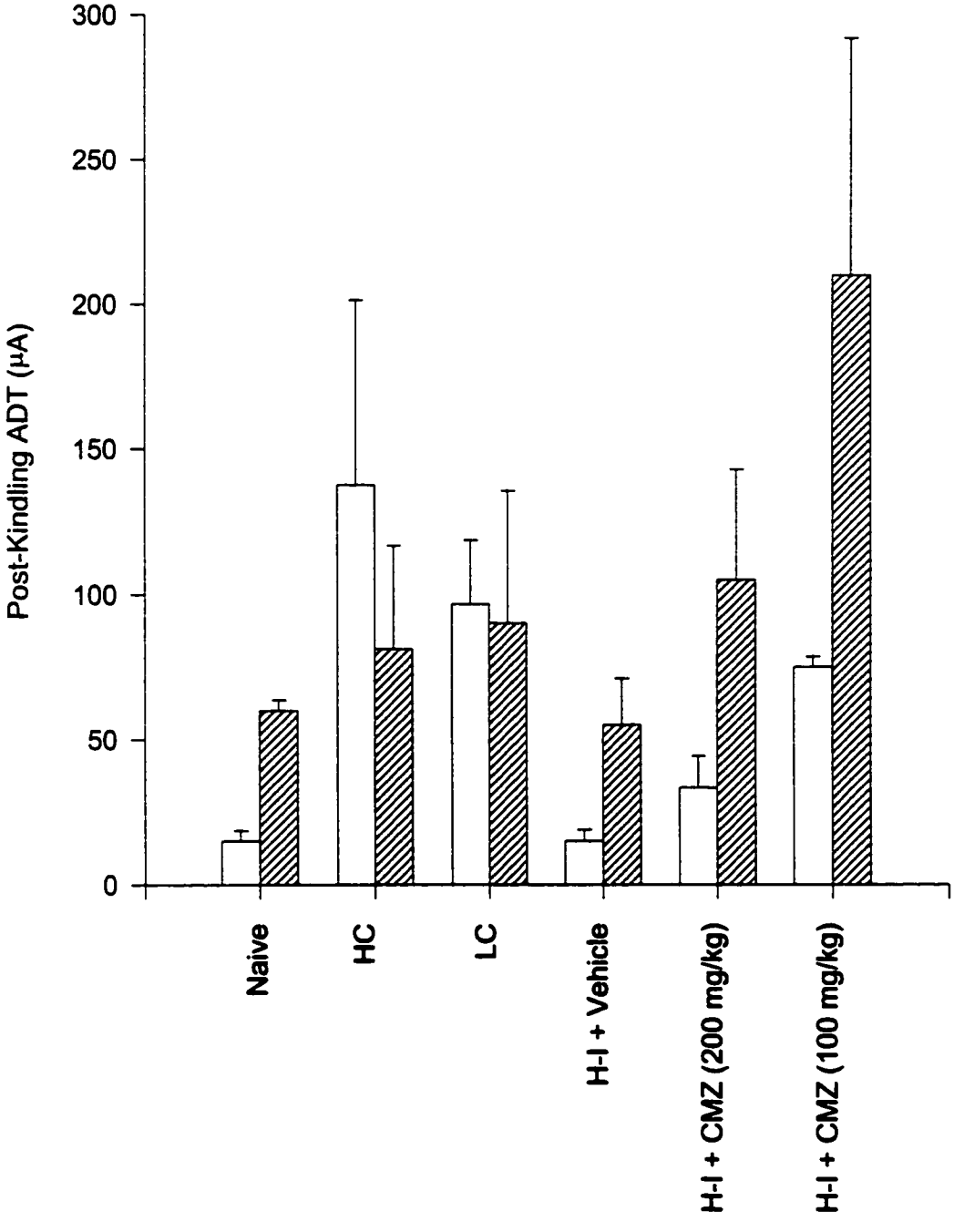
Post-Kindling ADT (μA)
300
250
200
150
100
50
0
Naive
HC
LC
H-I + Vehicle
H-I + CMZ (200 mg/kg)
H-I + CMZ (100 mg/kg)

Figure 6-4

Figure 6-5

Comparison of mean post-kindling AD duration in CMZ-injected versus vehicle-injected H-I animals.

Graphical illustration of the mean duration of the AD elicited in the ipsilateral hippocampus following the last stage 5 convulsion across various animal groups. A P value of <0.05 was considered to be statistically significant. A statistically significant difference was not observed between any of the animal groups examined.

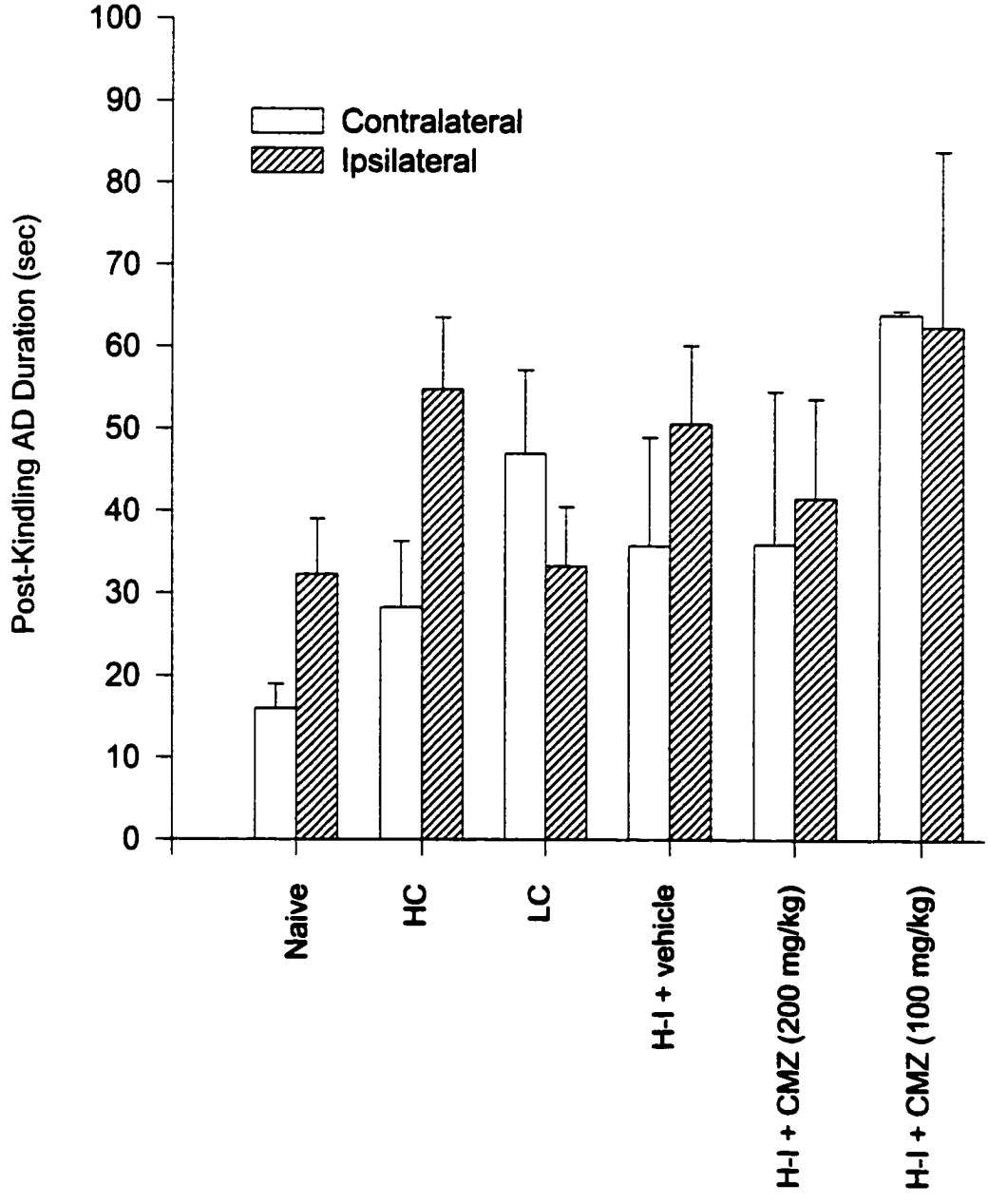
Post-Kindling AD Duration (sec)
100
90
80
70
60
50
40
30
20
10
0
Contralateral
Ipsilateral
Naive
HC
LC
H-I + vehicle
H-I + CMZ (200 mg/kg)
H-I + CMZ (100 mg/kg)

Figure 6-5

Discussion

Examination of kindling parameters such as kindling rate and pre-kindling AD duration indicated that H-I animals injected with the fully protective dose of CMZ (200 mg/kg) exhibited no differences in these parameters when compared to naïve animals. However, a significant increase in pre-kindled AD duration was observed in the ipsilateral hippocampus of vehicle-injected H-I animals relative to all other treatment groups that was not evident in CMZ-injected H-I animals. This finding may indicate that post-hypoxic CMZ (200 mg/kg) administration prevented ischemia-induced hyperexcitability in limbic brain structures.

Use of the H-I model has generally required the inclusion of hypoxic control and ligated control animals in the experimental design in order to account for the effect of the hypoxic event or ligation of a common carotid artery. While no neurodegeneration or differences in gene expression have been observed in hypoxic control or ligated control animals used in this model, the results of this study clearly indicate that long-term changes occur in the hippocampus of these control groups. Hypoxic control animals demonstrated a significant decrease in kindling rate relative to all other treatment or control groups. Similarly, Sato *et al.* (1994) demonstrated that PND10 rats exposed to a 2 hour hypoxic (3% oxygen) event exhibited a higher kindling rate (fewer stimulations to reach stage 5 seizure) and shorter cumulative AD duration to stage 5 convulsion than control animals. A facilitatory effect on primary site kindling was also observed in rats exposed to anoxia (0% oxygen) in the same experiment. Interestingly, the facilitation provided by previous exposure to hypoxia was significantly higher than previous exposure to anoxia in that study. Just as in our study, Sato *et al.* (1994) reported that the hypoxic event did not induce any morphological changes in the hippocampus that could be detected by microscopic inspection. Thus, permanent cellular changes may be induced by neurochemical factors, such as neurotransmitter systems, under hypoxic conditions that lead to subsequent vulnerability to hippocampal kindling. Interestingly, while the mean kindling rate was faster in hypoxic control animals used in the present study, the local excitability of the CA1 cell layer was not altered by the hypoxic event. This finding is supported by Applegate *et al.* (1996) who reported a similar effect using a

model of neonatal hypoxia.

A slight, but non-significant decrease in mean kindling rate was observed in ligated control animals relative to naïve animals. However, the decrease in mean kindling rate observed in these animals was significantly different relative to hypoxic controls, vehicle-injected H-I animals and CMZ-injected H-I animals (100 or 200 mg/kg). At no time has any morphological alteration been reported in the ipsilateral brain regions of ligated control animals, thus the reason for the increased kindling rate in these animals is unclear but may suggest that reduced blood flow inhibits the progression of the kindling phenomenon. A relevant study provided by Bortolotto *et al.* (1991) demonstrated that a moderate reduction in cerebral blood flow following bilateral clamping of the common carotid arteries, that is not associated with subsequent neuronal death, chronically increased the concentration of GABA in the hippocampus for at least 2 weeks. Bortolotto *et al*, (1991) also reported that the development of hippocampal kindling was difficult during that time.

Post-Ischemic Hyperexcitability in Vehicle-Injected H-I Animals

The pre-kindling AD duration was significantly longer in the ipsilateral hippocampus of vehicle-injected H-I animals than in any other treatment groups examined with the exception of H-I animals injected with 100 mg/kg CMZ. This finding is not surprising considering long term post-ischemic hyperexcitability is well documented (Cocito *et al.*, 1982; Kilpatrick *et al.*, 1990; Arboix *et al.*, 1997; Mittmann *et al.*, 1998). Simply, seizure susceptibility is dependent upon the interaction between excitatory and inhibitory neurotransmission (McCormick *et al.*, 1993). Cerebral ischemia is known to produce both short and long term changes in excitatory and inhibitory neurotransmitter systems by affecting extracellular transmitter levels and receptor binding characteristics (Erecinska *et al.*, 1984; Westerberg *et al.*, 1989; *Araki et al.*, 1993). Unfortunately, the long term effects of ischemia are far less frequently studied than short-term effects, in spite of the fact that long-term alterations may be more relevant to neurochemical and pathophysiological processes underlying neurological deficits or recovery in stroke patients. One study that examined long-term consequences of ischemic injury used MCAO in mice to quantitate *in vitro* receptor autoradiography of

ionotropic glutamate and GABA receptors one month following the insult (Qu *et al.*, 1998). Basically, Qu *et al.* (1998) demonstrated a pronounced hyperexcitability upon orthodromic synaptic stimulation in neurocortical slices, a strong concurrent activation of NMDA receptor-mediated excitatory post-synaptic potential and a reduction of GABA-mediated inhibition by 1 month post-ischemia. These findings were supported by receptor binding studies that revealed increased [^{3}H] MK 801 and decreased [^{3}H]-muscimol binding site densities bilaterally in the exofocal neocorticies by 4 weeks post-MCAO (Qu *et al.*, 1998). A relevant study in support of the hypothesis that enhanced excitatory neurotransmission persists for prolonged post-ischemic intervals has shown an increase in the synthesis of mRNA and protein for the key subunit of the NMDA receptor, NMDA-R1, following global ischemia (Heurteaux *et al.*, 1994). Moreover, it has been postulated that post-ischemic increases in NMDA receptor-mediated hyperexcitability may also be due to changes in phosphorylation of NMDA receptors (Raymond *et al.*, 1993; Hollmann and Heinemann, 1994). Conversely, a decrease in [^{3}H] muscimol binding has been observed 9 weeks after the induction of photothrombosis in the penumbral region of the infarcted cortex and a long term decrease in $GABA_A$ receptor mRNA expression has been reported in the hippocampus following global ischemia (Li *et al.*, 1991; Schiene *et al.*, 1996). Collectively these findings indicate a reduction in GABAergic neurotransmission at delayed post-ischemic time-points.

Alterations in the balance between excitatory and inhibitory neurotransmission following ischemia should be reflected in the relative seizure susceptibility of affected brain regions. One study that illustrates this relationship was conducted by Kim and Todd, (1999) and was designed to determine the impact of prior forebrain ischemia on seizure thresholds. Electrodes were implanted in the corticies of rats and each rat was then subjected to a 10 minute period of forebrain ischemia (2-VO). Six, 24 or 48 hours following the ischemic event, rats received intravenous infusions of various chemoconvulsants including PTZ, lidocaine, picrotoxin and NMDA in order to measure their susceptibility to seizures induced by these agents. Ultimately, 10 minutes of 2-VO caused drastically different and complex changes in the pattern of susceptibility to chemical convulsants. For instance, following ischemia the convulsive threshold for NMDA-induced seizures was reduced (greater sensitivity) at 6 hours post-ischemia, but

subsequently increased to values greater than observed in sham animals. In contrast, a marked decrease in the convulsive threshold to lidocaine was observed within the early post-ischemic periods of these animals (Kim and Todd, 1999).

Despite the significant increase in pre-kindling AD duration observed in vehicle-injected H-I animals compared to other animal groups, the pre-kindling ADT and kindling rate observed in these animals were not significantly different from control animals. A possible reason for this discrepancy may involve the increase in mean kindling rate that was observed in the ligated control animals used in this study such that permanent carotid artery ligation may independently slow the rate of kindling. This hypothesis would explain the faster kindling rate observed in hypoxic control animals than in H-I animals. Thus, permanent ligation of the carotid artery in vehicle-injected, and in CMZ-injected, H-I animals may have caused a reduction in the hyperexcitability that would normally be expected following an ischemic event. Moreover, Milward *et al.* (1999) investigated whether CA1 cell loss following global ischemic insult (4-VO) predisposed rats to intermittent, spontaneous, epileptic fits following an injection of tetanus toxin (a potent inhibitory neurotransmitter antagonist) into the hippocampus. The authors reported that no rats in the ischemia group exhibited reoccurring fits, instead the fits were delayed and reduced in number in ischemic relative to control animals. Thus, a CA1 lesion did not facilitate epileptogenesis in a rodent model of limbic epilepsy. Indeed, on its own, CA1 cell loss was more likely to restrict rather than promote spontaneous seizures. Finally, Romijn *et al.* (1994) demonstrated that damage to the cerebral cortex of Wistar rats following H-I in early post-natal life (PND13) did not lead to differences in the initial threshold for seizure susceptibility relative to control animals 2.5 months following the ischemic event. However, the ischemic rats did demonstrate a more rapid kindling rate than did control animals. These results are in complete disagreement with those observed in CMZ-injected H-I animals in the present study. An increased pre-kindling ADT relative to naïve animals was observed in CMZ-injected H-I animals used in this study, but these animals did not exhibit any difference in kindling rate or pre-kindling AD duration from naïve animals. It is also interesting that the AD duration observed in vehicle-injected H-I animals was not significantly different from CMZ-injected animals that received 100 mg/kg at 3 hours post-hypoxia. The similarity

in AD duration between these two treatment groups may reflect the incomplete histological neuroprotection in H-I animals that received 100 mg/kg CMZ. Indeed, incomplete neuroprotection in H-I animals injected with 100 mg/kg CMZ, 3 hours following H-I, was documented in Chapter 1.

Increased ADT in CMZ animals

One obvious difference between CMZ-injected (200 mg/kg) H-I animals and naïve control animals was the 5-fold increase in pre-kindling ADT in the ipsilateral hippocampus of CMZ-injected (200 mg/kg) H-I animals. Similarly, a 3-fold increase in the pre-kindling ADT was observed in the ipsilateral hippocampus of CMZ-injected H-I animals that received 100 mg/kg compared to naïve animals. This result suggests that CMZ-treated animals exhibit a much lower seizure susceptibility than vehicle-injected or control animals. Yet, once the seizure circuit was accessed through successive stimulation of CMZ-injected H-I animals, seizure propagation proceeded in a manner no different from naïve animals. The reason for the decrease in seizure sensitivity is unclear. Thus, CMZ treatment may permanently alter neuronal circuitry originating from or driving through the protected hippocampus such that it leaves neurons in a chronic hypoexcitable state. Whether these permanent alterations in circuitry would affect stroke victims is presently unknown. However, evidence has emerged suggesting that while treatment of ischemic injury with NMDA-antagonists and GABA-agonists does reduce infarct size it appears to have a harmful effect on relearning and neurologic recovery (Wahlgren and Martinsson, 1998).

In conclusion, CMZ-induced neuroprotection was evident upon functional analysis of seizure propagation circuits. However, it is unclear whether the increased pre-kindling ADT observed in these animals is indicative of dysfunctional neurons within the hippocampal cell layers. Furthermore, this study demonstrated, for the first time, that the kindling model may serve as an accurate way to assess function-related neuroprotective efficacy for an agent in animal models of ischemia. Of course, further characterization of the relationship between the various kindling parameters and their relevance to ischemia-induced deficits is required in order to maximize the potential of this model in such a capacity.

General Discussion

Given the heterogeneity of ischemic brain injury, many researchers have suggested that successful treatment of human stroke victims with a single compound is unlikely. However, this body of work has clearly demonstrated that a bolus dose of CMZ, administered within 3 hours of H-I in PND25 rats, provides near complete neuroprotection to all susceptible brain regions regardless of cell type, location or mode of cell death. While neuroprotective efficacy of a compound in ischemia models does not ensure a neuroprotective effect in human patients, recent clinical work has indicated that CMZ provided neuroprotection in stroke patients that exhibited symptoms of a large infarct volume (Wahlgren *et al.*, 1999). The fact that the H-I model produces a large infarct volume and that CMZ was particularly effective in this model may suggest that that the Rice-Vannucci model produces a pathophysiology similar to that of the subpopulation of patients that responded to CMZ administration in clinical trials.

Clinical studies have recently shown that one of the most unfavorable prognostic signs for human stroke patients is a low concentration of GABA in the cerebrospinal fluid during the first few days after an ischemic event (Skovortsova *et al.*, 1999). Thus, it is conceivable that CMZ produced its neuroprotective effect in human patients, and in animal models, by potentiating GABAergic neurotransmission. However, the results of the present study demonstrated that a wide dose range of known $GABA_A$-potientiating agents administered at 3 hours post-hypoxia did not produce an equivalent level of neuroprotection to that provided by CMZ in the H-I model. In fact, the highly potent GABA-agonist, muscimol, did not provide any neuroprotection against H-I injury. This finding strongly suggests that CMZ may act through a non-GABAergic mechanism in order to produce its neuroprotective effect. However, a unique interaction with the $GABA_A$ receptor may also underlie the neuroprotective effect of this compound.

In this study, a fully protective dose of CMZ produced dramatic alterations in the normal patterns of gene expression induced by H-I. As in any correlational study, it is difficult to draw functional significance from any one alteration in gene expression. However, collectively, the results of the molecular studies indicate that CMZ may interfere with the PCD process in order to achieve a neuroprotective effect. Specifically,

CMZ may prolong c-Fos expression in order to prevent caspase activation in this model. Support for this hypothesis can be derived from the fact that caspase-inhibitors provided a similar degree of neuroprotection to that provided by CMZ in the H-I model when administered at 3 hours post-hypoxia (Cheng *et al.*, 1998). Clearly, the functional relationship between gene expression and CMZ-induced neuroprotection needs to be addressed and the results of the present study have identified good candidate genes for such experiments. Further work towards uncovering the mechanism of action for CMZ would clearly influence future pharmacotherapy in stroke patients.

Functional analysis of CMZ-induced neuroprotection using the kindling model produced unexpected results. While administration of a fully protective dose of CMZ prevented the increased pre-kindling AD duration that was observed in vehicle-injected H-I animals, it also produced a decrease in the local seizure susceptibility in CA1. However, the fact that a decreased seizure susceptibility was not observed in the contralateral hippocampus of CMZ-injected H-I animals suggests that this result was not direct consequence of CMZ use in these animals. In fact, the effect may be reminiscent of the preconditioning phenomenon whereby a sublethal injury produces a certain degree of tolerance to a subsequent potentially lethal insult. Nonetheless, use of the kindling model in this study was shown to be a very sensitive way in which to assess the neuroprotective abilities of compounds in ischemia models.

Collectively, the results of these studies have provided some information regarding the mechanism responsible for CMZ-induced neuroprotection in the H-I model. However, further work should be conducting in order to pinpoint the site of action of this compound. These studies did not rule out the possibility that the GABA-potentiating properties of CMZ may play a role in its neuroprotective effect. However, it appears that an additional mechanism of action may be involved. Future work that may aid in the search for such a mechanism would include the cellular localization of the altered CaM and *c-fos* mRNA expression following CMZ administration in H-I animals. In addition, further research into the mechanism underlying the permanent hypoexcitability of cells in the CA1 region of CMZ-treated H-I animals may be important to the understanding of the mechanisms underlying plastic responses in the brain.

References

Addae, J.I. and Stone, T.W. (1988). Effects of anticonvulsants on responses to excitatory amino acids applied topically to rat cerebral cortex. *Gen. Pharmacol.* **19**, 455-462.

Aden, U., Bona, E., Hagberg, H. and Fredholm, B.B. (1994). Changes in *c-fos* mRNA in the neonatal rat brain following hypoxic ischemia. *Neurosci. Lett.* **180(2)**, 91-95.

Ahn, J.H., Ko, Y.G., Park, W.Y., Kang, Y.S., Chung, H.J. and Seo, J.S. (1999). Suppression of ceremide-mediated apoptosis by Hsp70. *Mol. Cells.* **9(2)**, 200-206.

Amaral, D.G. and M.P. Witter (1995). Hippocampal Formation. In: *The Rat Nervous System, Second Edition* (ed. G. Paxinos). pp. 443-486. Australia:Academic Press Inc.

Amin, V., Cumming, D.V. and Latchman, D.S. (1996). Over-expression of heat shock protein 70 protects neuronal cells against both thermal and ischemic stress but with different efficiencies. *Neurosci. Lett.* **206**, 45-48.

Ananthan, J., Goldberg, A.L. and Voellmy, R. (1986). Abnormal proteins serve as eukaryotic stress signals and trigger the activation of heat shock genes. *Science* **232**. 522-524.

Anderson, S.M.P., De Souza, R.J. and Cross, A.J. (1993). The human neuroblastoma cell line IMR-32 possesses a functional $GABA_A$ receptor lacking the benzodiazepine modulatory site. *Neuropharmacology* **32**, 455-460.

Applegate, C.D., Jensen, F. Burchfiel, J.L. and Lombroso, C. (1996). The effects of neonatal hypoxia on kindled seizure development and electroconvulsive shock profiles. *Epilepsia* **37**, 723-727.

Araki, T., Kato, H., Kogure, K. and Inoue, T. (1990). Regional neuroprotective effects of pentobarbital on ischemia-induced brain damage. *Brain Res. Bull.* **25**, 861-865.

Araki, T., Kanai, Y., Murakami, F., Kata, H. and Kogure, K. (1993). Post-ischemic changes in the binding of excitatory and inhibitory neurotransmitters in the gerbil brain. *Pharmacol. Biochem. Behav.* **45**, 945-949.

Arboix, A., Garcia-Eroles, L., Massons, J.B., Oliveres, M. and Comes, E. (1997). Predictive factors of early seizures after acute cerebrovascular disease. *Stroke* **28**, 1590-1594.

Armstrong, J.N., Plumier, J.C.L., Robertson, H.A. and Currie RW (1996). The inducible 70,000 molecular/weight heat shock protein is expressed in the degenerating dentate hilus and piriform cortex after systemic administration of kainic acid in the rat. *Neuroscience* **74**, 685-693.

Arrigo, A.P. and Landry, J. (1994). Expression and function of the low-molecular weight heat shock proteins. In: *The Biology of Heat Shock Proteins and Molecular Chaperones* (ed. R.I. Morimoto, A. Tissières and C. Georgopoulos). pp. 335-373. Cold Spring Harbor Laboratory Press, Cold Spring Harbor, NY.

Bagenholm, R., Andine, P. and Hagberg, H.(1996). Effects of the 21-amino steroid tirilazad mesylate (U-74006F) on brain damage and edema after perinatal hypoxia-ischemia in the rat. *Pediatr. Res.* **40**, 399-403.

Baldwin, H.A., Jones, J.A., Cross, A.J. and Green, A.R. (1993). Histological, biochemical and behavioral evidence for the neuroprotective action of chlormethiazole following prolonged carotid artery occlusion. *Neurodegeneration* **2**, 139-146.

Baldwin, H.A., Williams, J.L., Snares, M., Ferreira, T., Cross, A.J. and Green, A.R. (1994). Attenuation by chlormethiazole administration of the rise in extracellular amino acids following focal ischaemia in the cerebral cortex of the rat. *Br. J. Pharmacol.* **112**, 188-194.

Bates, S. and Vousden, K.H. (1996). *p53* in signalling checkpoint arrest or apoptosis. *Curr. Opin. Genet. Dev.* **6**, 12-19.

Beckmann, R.P., Lovett, M. and Welch, W.J. (1992). Examining the function and regulation of hsp70 in cells subjected to metabolic stress, *J. Cell Biol.* **117**, 1137-1150.

Beilharz, E.J., Williams, C.E., Dragunow, M., Sirimanne, E.S. and Gluckman, P.D. (1995). Mechanisms of delayed cell death following hypoxic-ischemic injury in the immature rat: evidence for apoptosis during selective neuronal loss. *Mol. Brain. Res.* **29**, 1-14.

Ben-Ari,Y., Cherubini, E., Corradetti, R. and Galarsa, J.L. (1989). Giant synaptic potentials in immature rat CA3 hippocampai neurones. *J. Physiol. (Lond.)* **416**, 303-325.

Beresewicz, A. (1989). Anti-ischemic and membrane stabilizing activity of calmodulin inhibitors. *Basic Res Cardiol.* **84**, 631-645.

Bertioll, D.J., Schlichter, U.H.A., Adams, M.J., Burrows, P.R., Steinbil B, H. and Antonlw, J.F. (1995). An analysis of differential display shows a strong bias towards high copy number mRNAs. *Nucl. Acids Res.* **23(21)**, 4520-4523.

Blumenfeld, K.S. and Welsh, F.A. *et al.* (1992). Regional Expression of c-fos and Heat Shock protein-70 mRNA following Hypoxia-Ischemia in Immature Rat Brain. *J. Cereb. Blood Flow and Metab.* **12**, 987-995.

Bona, E., Hagberg, H., Loberg, E.M., Bagenholm, R. and Thoresen, M. (1998). Protective effects of moderate hypothermia after neonatal hypoxia-ischemia: short and long-term outcome. *Pediatr. Res.* **43**, 738-745.

Bonfoco, E., Kraine, D., Ankarcrona, M., Nicotera, P. and Lipton, S.A. (1995). Apoptosis and necrosis: two distinct events induced, respectively, by mild and intense insults with N-methyl-D-aspartate or nitric oxide/superoxide in cortical cell cultures. *Proc. Natl. Acad. Sci. USA* **92**, 7162-7166.

Bortolotto, Z., Heim, C., Sieklucka, M., Block, F., Sontag, K. and Cavalheiro, E. (1991). Effects of bilateral clamping of carotid arteries on hippocampal kindling in rats. *Physiol. Behav.* **49(4)**, 667-671.

Bouvier, M., Szatkowski, M., Amato, A. and Attwell, D. (1992). The glial cell glutamate uptake carrier countertransports pH-changing anions. *Nature* **360**, 471-474.

Bowery, N.G. (1993). $GABA_B$ receptor pharmacology. *Ann. Rev. Pharmacol. Toxicol.* **33**, 109-117.

Bowery, N.G. and Brown, D.A. (1997). The cloning of GABA(B) receptors [news; comment]. *Nature* **386(6622)**, 223-4.

Bozas, E., Tritos, N., Phillipidis, H. and Stylianopoulou, F. (1997). At least three neurotransmitter systems mediate a stress-induced increase in *c-fos* mRNA in different rat brain areas. *Cell Mol. Neurobiol.* **17(2)**, 157-69.

Buchan, A. and Pulsinelli, W.A. (1990). Hypothermia but not the *N*-methyl-D-aspartate receptor antagonist, MK 801, attenuates neuronal damage in gerbils subjected to transient global ischaemia. *J. Neurosci.* **10**, 311-216.

Busto, R., Dietrich, W.D., Globus, M.Y., Valdos, A., Steinberg, P. and Ginsberg, W.D. (1987). Small differences in intro-ischemic brain temperature critically determine the extent of ischemic brain injury. *J. Cereb. Blood Flow Metab.* **7**, 729-738.

Buzzard, K.A., Giaccia, A.J., Killender, M. and Anderson, R.L. (1998). Heat shock protein 72 modulates pathways of stress-induced apoptosis. J. *Biol. Chem.* **273(27)**, 17147-53.

Cain, D.P. (1989). Long-Term potentiation and kindling: how similar are the mechanisms? *Trends Neurosci.* **12(1)**, 7-9.

Callard, D., Lescure, B. and Mazzolini, L.(1994). A method for the elimination of false positives generated by the mRNA differential display technique. *Biotechniques* **16(6)**, 1097-1103.

Cardell, M., Brosi-Mller, F. and Wieloch, T. (1991). Hypothermia prevents the ischemia-induced translocation and inhibition of protein kinase C in the rat striatum. *J. Neurochem.* **57**, 1814-1817.

Charonnat, R., Lechat, P. and Chareton, J. (1957). Sur les propiets pharmacoldynamiques d'un driv thiazole. *Therapie* **12**, 68-71.

Charriaut-Marlangue, C., Pollard, H., Kadri-Hassani, N., Khrest-Chatisky, M., Moeau, J., Dessi, F., Kang, K. and Ben-Ari, Y. (1992). Increase in specific proteins and mRNAs following transient anoxia-aglycaemia in rat CA1 hippocampal slices. *Eur. J. Neurosci.* **4**, 766-776.

Chen, S.C., Curran, T. and Morgan, J.I. (1995). Apoptosis in the nervous system: new revelations. *J. Clin. Pathol.* **48**, 7-12.

Chen, G., Trombley, P. and van den Pol, A.N. (1996a). Exitatory actions of GABA in developing rat hypothalamic neurones. *J. Physiol. (Lond.).* **494**, 451-464.

Chen, J., Graham, S.H., Zhu, R.L. and Simon, R.P. (1996b). Stress Proteins and Tolerance to Focal Cerebral Ischemia. *J. Cereb. Blood Flow Metab.* **16(4)**, 566-577.

Chen, J., Nagayama, T., Jin, K., Stetler, R.A., Zhu, R.L., Graham, S.H. and Simon, R.P. (1998). Induction of caspase-3-like protease may mediate delayed neuronal death in the hippocampus after transient cerebral ischemia. *J. Neurosci.* **18**, 4914-4928.

Chen, Y.C., Lin-Shiau, S.Y. and Lin, J.K. (1999). Involvement of heat-shock protein 70 and P53 proteins in attenuation of UVC-induced apoptosis by thermal stress in hepatocellular carcinoma cells [In process Citation].

Cheng, Y., Deshmukh, M., D'Costa, A., Demaro, J. A., Gidday, J.M., Shah, A., Sun, Y., Jacquin, M.F., Johnson, E.M. and Holtzman, D.M. (1998). Caspase inhibitor affords neuroprotection with delayed administration in a rat model of neonatal hypoxic-ischemic brain injury. *J. Clin. Invest.* **101**, 1992-1999.

Chesnut, T. and Swann, J., (1989). Disinhibitory actions of the $GABA_A$ agonist muscimol in immature hippocampus. *Brain Res.* **502**, 365-374.

Choi, D.W. (1990). Methods of antagonizing glutamate neurotoxicity. *Cerebrovascular Brain Metab. Rev.* **2**, 105-147.

Chopp M., Li Y, Dereski M.O., Levine, S.R., Yoshida, Y. and Garcia, J.H. (1991). Neuronal injury and expression of 72-kDA heat-shock protein after forebrain ischemia in the rat. *Acta Neuropathol (Berl).* **83**, 66-71.

Chopp, M. and Li, Y. (1996). Apoptosis in focal cerebral ischemia. *Acta Neurochir.* **66**, 21-26.

Churn, S.B., Taft, W.S., Billingsley, M.S., Blair, R.E. and Delorenzo, R.J. (1990). Temperature modulation of ischemic neuronal death and inhibition of calcium/calmodulin-dependent kinase II in the gerbil. *Stroke* **21**, 1715-1721.

Clark, R.S.B., Kochanek, P.M., Chen, M., Watkins, S.C., Marion, D.W., Chen, J., Hamilton, R.L., Loeffert, J.E. and Graham, S.H. (1999). Increases in Bcl-2 and cleavage of caspase-1 and caspase-3 in human brain after head injury. *FASEB* **13(8)**, 813-21.

Cocito, L., Favale, E. and Reni, L. (1982). Epileptic seizures in cerebral arterial occlusive disease. *Stroke* **13**, 189-195.

Colbourne, F. and Corbett, D. (1995). Delayed Post-ischemic hypothermia: a six month survival study using behavioural and histological assessments of neuroprotection. *J. Neurosci.* **15**, 7250-7260.

Colbourne, F., Auer, R.N. and Sutherland, G.R. (1998). Characterization of postischemic behavioral deficits in gerbils with and without hypothermic neuroprotection. *Brain Res.* **803**, 69-78.

Colbourne, F., Sutherland, G.R. and Auer, R.N. (1999). Electron microscopic evidence against apoptosis as the mechanism of neuronal death in global ischemia. *J. Neurosci.* **19**, 4200-4210.

Corbett, D., Evans, S., Thomas, L., Wang, D. and Jonas, R. (1990). MK 801 reduces cerebral ischaemic injury by inducing hypothermia. *Brain Res.* **514**, 300-304.

Cotman, C.W. and Anderson, A.J. (1995). A potential role for apoptosis in neurodegeneration and Alzheimer's disease. *Mol. Neurobiol.* **10(1)**, 19-45.

Cross, A.J., Stirling, J.M., Robinson, T.N., Bowen, D.M., Francis, P.T. and Green A.R. (1989). The modulation by chlormethiazole of the $GABA_A$ receptor complex in rat brain. *Br. J. Pharmacol.* **98**, 284-290.

Cross, A.J., Jones, J.A., Baldwin, H.A. and Green, A.R. (1991). Neuroprotective activity of chlormethiazole following transient forebrain ischaemia in the gerbil. *Br.J. Pharmacol.* **104**, 406-411.

Cross, A.J., Misra, A., Sandilands, A., Taylor, M.J. and Green, A.R. (1993a). Effect of chlormethiazole, dizocilpine and pentobarbital on harmaline-induced increase of cerebellar cyclic GMP and tremor. *Psychopharmacology* **111**, 96-98.

Cross, A.J., Snape, M.F. and Green, A.R. (1993b). Chlormethiazole antagonises seizures induced by N-methl-D-aspartate without interacting with the NMDA receptor complex. *Psychopharmacology* **112**, 403-406.

Cross, A.J., Jones, J.A., Snares, M., Jostell, K.G., Bredberg, U. and Green, A.R. (1995). The protective action of Chlormethiazole against ischaemia-induced neurodegeneration in gerbils when infused at doses having little sedative or anti-convulsant activity. *Br. J. Pharmacol.* **114**, 1625-1630.

Currie, R.W. and White, F.P. (1981). Trauma-induced protein in rat tissues: a physiological role for a "heat shock" protein? *Science* **214**, 72-73.

Davidson, D. (1983). Anticonvulsant drugs. *Br. Med. J.* **286**, 2043-5.

Defrance, J., Stanley, J., Marchand, J. and Enna, S.J. (1979). The effect of muscimol on hippocampal pyramidal cells. *Eur. J. Pharmacol.* **59(1-2)**, 155-8.

DeLorey, T.M., Kissin, I., Brown, P. and Brown, G.B. (1993). Barbiturate-benzodiazepine interactions at the gamma-aminobutyric $acid_A$ receptor in rat cerebral cortical synaptoneurosomes. *Anesth. Analg.* **77(3)**, 598-605.

Denovan-Wright, E.M., Gilby, K.L., Howlett, S. and Robertson, H.A. (2000). Cloning of differentially expressed brain cDNAs. In: PCR5 (Leslie, R and Robertson H.A., eds). Oxford University Press. *in press*.

Deshaies, R.J., Koch, B.D. and Schekman, R. (1988a). The role of stress proteins in membrane biogenesis. *Trends Biol. Sci.*, **13**, 384-388.

Deshaies, R.J., Koch, B.D., Werner-Washburne, M., Craig, E.A. and Schekman, R. (1988b). A subfamily of stress proteins facilitates translocation of secretory and mitochondrial precursor polipeptides. *Nature* **332**, 880-805.

Deshmukh, A. Wittert, W., Schnitzler, E. et al: (1986). Lorazepam in the treatment of refractory neonatal seizures. *Am. J. Dis. Child.* **140**, 1042.

Deshpande, J., Bergstedt, K., Linden, T., Kalimo, H. and Wieloch, T. (1992). Ultrastructural changes in the hippocampal CA1 region following transient cerebral ischemia: evidence against programmed cell death. *Exp. Brain Res.* **88(1)**, 91-105.

Dice, J.F., Agarraberes, F., Kirven-Brooks, M., Terlecky, L.J. and Terlecky, S.R. (1994). Heat shock 70-kD proteins and lysosomal proteolysis. In: *The Biology of Heat Shock Proteins and Molecular Chaperones* (ed. R.I. Morimoto, A., Tissieres and C. Georgopoulos), pp. 137-152. Cold Spring Harbor:Cold Spring Harbor Laboratory Press.

Dingledine, R. and Gjerstad, L. (1980). Reduced inhibition during epileptiform activity in the *in vitro* hippocampal slice. J. Physiol. Lond. **305**, 297-313.

Dix, D.J., Allen, J.W., Collins, B.W., Mori, C., Nakamura, N., Poormanallen, P., Goulding, E.H. and Eddy, E.M. (1996). Targeted gene disruption of hsp70-2 results in failed meiosis, germ cell apoptosis, and male infertility. *Proc. Natl. Acad. Sci. USA* **93**, 3264-3268.

Domaska-Janik, K., Bong, P., Bronisz-Kowalczyk, A., Zajc, H. and Zablocka, B. (1999). AP1 Transcriptional Factor Activation and Its Relation to Apoptosis of Hippocampal CA1 Pyramidal Neurons After Transient Ischemia in Gerbils. *J. Neurosci. Res.* **57**, 840-846.

Dragovich, T., Rudin, C.M. and Thompson, C.B. (1998). Signal transduction pathways that regulate cell survival and cell death. *Oncogene* **17**, 3207-3213.

Dragunow, M., Young, D., Hughes, P., MacGibbon, G., Lawlor, P., Singleton, K., Sirimanne, E., Beilharz, E. and Gluckman, P. (1993). Is c-Jun involved in nerve cell death following status epilepticus and hypoxic-ischaemic brain injury? *Mol. Brain Res.* **18**, 347-352.

Dragunow, M., Beilharz, E., Sirimanne, E., Lawlor, P., Williams, C., Bravo, R. and Gluckman, P. (1994). IEGP expression in neurons undergoing delayed death, but not necrosis, following hypoxic-ischemic injury to the young rat brain. *Mol. Brain Res.* **25**, 19-33.

Du, C., Hu, R., Csernansky, C.A., Hsu, C.Y. and Choi, D.W. (1996). Very delayed infarction after mild focal cerebral ischemia: a role for apoptosis? *J. Cereb. Blood Flow Metab.* **16**, 195-201.

Dubois, M.F., and O. Bensaude (1993). MAP kinase activation during heat shock in quiescent and exponetially growing mammalian cells. *FEBS lett.* **324**, 191-195.

Dulac, O., Bossi, L., Regnier, F., Poulain, D., Battin, J., Drossart, F., Dandelot, J.B. Bertsch, M. and Arthuis, M. (1985). Long-term open trial of progabide in epileptic children. In: *Epilepsy and GABA Receptor Agonists: Basic and Therapeutic Research*, (eds. Bartholini,G., Bossi L., Lloydm K.G. and Morseili, P.L.). pp. 389-398. New York: Raven.

Dwyer, B.E., Nishimura, R.N. and Brown, I.R. (1989) Synthesis of the major inducible heat shock protein in rat hippocampus after neonatal hypoxia-ischemia. *Exp. Neurol.* **104**, 28-31.

Eguchi, Y., Shimizu, S. and Tsujimoto, Y. (1997). Intracellular ATP levels determine cell death fate by apoptosis or necrosis. *Cancer Res.* **57**, 1835-1840.

Erecinska, M., Nelson, D., Wilson, D.F. and Silver, L.A. (1984). Neurotransmitter amino acids in the CNS: I. Regional changes in amino acid levels in rat brain during ischemia and reperfusion. *Brain Res.* **304**, 9-22.

Evan, G.I., Wyllie, A.H., Gilbert, C.S., Littlewood, T.D.L., Brooks, M., Waters, C.M., Penn, L.Z. and Hancock, D.C. (1992). Induction of apoptosis in fibroblasts by c-myc protein. *Cell* **69(1)**, 119-28.

Evan, G.I. and Littlewood, T. (1998). A matter of life and cell death. *Science* **281**, 1317-1321.

Evans, J.G., Feuerlein, W., Glatt, M.M., Kanowski, S. and Scott, D.B. (1986). Chlormethiazole 25 years: recent developments and historical perspectives. *Acta Psychiat. Scand.* **73**, Suppl 327, 198.

Fan, C.Y., Pan, J., Chu, R., Lee, D., Kluckman, K.D., Usuda, N., Singh, I., Yeldandi, A.V., Rao, M.S., Maeda, N. and Reddy, J.K. (1996). Targeted disruption of the peroxisomal fatty acyl-CoA oxidase gene: generation of a mouse model of pseudoneonatal adrenoleukodystrophy. *Ann. N.Y. Acad. Sci.* **804**, 530-41.

Feige, U. and Polla, B.S. (1994). Heat shock proteins: the *hsp70* family. *Experiencia.* **50**, 979-986.

Ferrer, I., Martin, F., Serrano, T., Reiriz, J., Prez-Navarro, E., Alberch, J., Macaya, A., Planas, A.M. (1995a). Both apoptosis and necrosis occur following intrastriatal administration of excitotoxins. *Acta. Neuropathol.* **90**, 504-510.

Ferrer, I., Soriano, M.A., Vidal, A. and Planas, AM (1995b). Survival of parvalbumin-immunoreactive neurons in the gerbil hippocampus following transient forebrain ischemia does not depend on HSP70 protein induction. *Brain Res.* **692(1-2)**, 41-6.

Ferriero, D.M. Soberano, H.Q., Simon, R.P. and Sharp, F.R. (1990). Hypoxia-ischemia induces heat shock protein-like (HSP72) immunoreactivity in neonatal rat brain. *Dev. Brain Res.* **53**, 145-150.

Filipkowski, R.K., Hetman, M., Kaminska, B., Kaczmarek, L. (1994). DNA fragmentation in rat brain after intraperitoneal adminsitration of kainate. *Neuroreport* **5**, 1538-1540.

Foutz, A.S., Pierrefiche, O. and Denavit-Saubie, M. (1994). Combined blockade of NMDA and non-NMDA receptors produces respiratory arrest in the adult cat. *Neuroreport.* **5(4)**, 481-4.

Frydman, J., Nimmesgern, E., Ohtsuka, K. and Hartl, F. U. (1994). Folding of nascent polypeptide chains in a high molecular mass assembly with molecular chaperones. *Nature* **370**, 111-7.

Fuhr, J.E., Overton, M. and Yang, T.J. (1976). Stimulatory effect of 3′, 5′-adenosine monophosphate on protein synthesis in heat-shocked murine leukemia lymphoblasts. *J. Natl. Cancer Inst.* **58**, 6189-6191.

Fuhr, J.E., Yang, T.J., Townes, T. and Overton, M. (1977). Effect of dibutyryl cyclic adenosine 5′-monophosphate on protein synthesis in L5178Y cells after hyperthermia. *J. Natl. Cancer Inst.* **59**, 1469-1473.

Gabaeur, I., Slezak, J., Styk, J. and Ziegelhoffer, A. (1991). Protective effect of calmodulin inhibitors on reperfusion injury. *Bratisl. Lek. Listy.* **92**, 184-194.

Gabai, V.L., Meriin, A.B., Mosser, D.D., Caron, A.W., Rits, S., Shifrin, V.I. and Sherman, M.Y. (1997). Hsp70 prevents activation of stress kinases. A novel pathway of cellular thermotolerance. *J. Biol. Chem.* **272(29)**, 18033-7.

Galvin, G. and Jelinek, G. (1987). Midazolam: An effective intravenous agent for seizure control. *Arch. Emerg. Med.* **4**, 169.

Gastaut, H., Naquet, R., Poire, R. et al: (1965). Treatment of *status epilepticus* with diazepam (Valium). *Epilepsia*, **6**, 167.

Gerner, E.W. and Schneider, M.J. (1975). Induced thermal resistance in HeLa cells. *Nature* **256(5517)**, 500-2.

Gidday, J.M., Fitzgibbons, J.C., Shah, A.R. and Park, T.S. (1994). Neuroprotection from ischemic brain injury by hypoxic preconditioning in the neonatal rat. *Neurosci. Lett.* **168**, 221-224.

Gilby, K.L., Armstrong, J.N., Currie, R.W. and Robertson, H.A. (1997). The effects of hypoxia-ischemia on expression of c-Fos, c-Jun and Hsp70 in the young rat hippocampus. *Mol. Brain. Res.* **48**, 87-96.

Gill, R., Foster, A.C. and Woodruff, G.N. (1988). MK-801 is neuroprotective in gerbils when administered during the post-ischaemic period. *Neuroscience* **25**, 847-855.

Gill, R. and Lodge, D. (1997). Pharmacology of AMPA antagonists and their role in neuroprotection. *Int. Rev. Neurobiol.* **40**, 197-232.

Gilland, E. and Hagberg, H. (1997). Is MK-801 neuroprotection mediated by systemic hypothermia in the immature rat? *Neuroreport* **8(7)**, 1603-1605.

Gillardon, F., Burle, J., Grsser-Cornhels, U. and Zimmermann, M. (1995). DNA fragmentation and activation of c-*jun* in the cerebellum of mutant mice [weaver Purkinje cell degeneration]. *Neuroreport* **6**, 1766-1768.

Gilliland, G., Perrin, S., Blanchard, K. and Bunn, H.F. (1990). Analysis of cytokine mRNA and DNA: detection and quantitation by competitive polymerase chain reaction. *Proc. Natl. Acad. Sci. U.S.A.* **87(7)**, 2725-9.

Globus, M.Y.-T., Busto, R., Lin, B., Schnippering, H. and Ginsberg, M.D. (1995). Detection of free radical formation during transient global ischemia and recirculation: effects of intraischemic brain temperature and modulation. *J. Neurochem.* **65**, 1250-1256.

Goddard, G. V., McIntyre, D. C. and Leech, C. K. (1969). A permanent change in brain function resulting from daily electrical stimulation. *Exp. Neurol.*, **25**, 295-330.

Golovko, A.I., Buriakova, L.V., Kutsenko, S.A. and Sviderskii, O.A. (1999). The molecular aspects of the functional heterogeneity of the GABA receptors. *Usp-Fiziol-Nauk.* **30(1)**, 29-38.

Gonzalez, M.F., Lowenstein, D., Fernyak, S. *et al* (1991). Induction of heat shock protein 72-like immunoreactivity in the hippocampal formation following transient global ischemia. *Brain Res. Bull.* **26**, 241-250.

Goto, K., Ishige, A., Sekiguchi, K., Iizuka, S., Sugimoto, A., Yuzurihara, M., Aburada, M., Hosoya, E. and Kogure, K. (1990). Effects of cycloheximide on delayed neuronal death in rat hippocampus. *Brain Res.* **534**, 299-302.

Gottron, F.J., Ying, H.S. and Choi, D.W. (1997). Caspase inhibition selectively reduces the apoptotic component of oxygen-glucose deprivation-induced cortical neuronal cell death. *Mol. Cell Neurosci.* **9**, 159-169.

Green, A.R. and Murray, T.K. (1989). A simple intravenous method in rodents for determining the potency of anticonvulsants acting through GABAergic mechanisms. *J. Pharm. Pharmacol.* **41**, 879-880.

Green, A., Cross, A.J., Snape, M.F. and De Souza, R.J. (1992a). The immediate consequence of middle cerebral artery occlusion on GABA synthesis in mouse cortex and cerebellum. *Neurosci. Lett.* **138**, 141-144.

Green, A.R. and Cross, A.J. (1994a). Attenuation by chlormethiazole of edema following focal ischemia in the cerebral cortex. *Neurosci. Lett.* **173**, 27-30.

Green, A.R. and Cross, A.J. (1994b). The neuroprotective actions of Chlormethiazole. *Prog. Neurobiol.* **44**, 463-484.

Green, A.R., Misra, A., Murray, T.K., Snape, M.F. and Cross, A.J. (1996). A behavioral and neurochemical study in rats of the pharmacology of loreclezole, a novel allosteric modulator of the $GABA_A$ receptor. *Neuropharmacology* **35**, 1243-1250.

Green, A.R., (1998a). Clomethiazole (Zendra®) in Acute Ischemic Stroke: Basic Pharmacology and Biochemistry and Clinical Efficacy. *Pharmacol. Ther.* **80(2)**, 123-147.

Green, A.R., Misra, A., Hewitt, K.E., Snape, M.F. and Cross, A.J. (1998b). An investigation of the possible interaction of clomethiazole with glutamate and ion channel sites as an explanation of its neuroprotective activity. *Pharmacol Toxicol.* **83(2)**, 90-4.

Green, A.R., Murray, T.K., Misra, A., Snape, M.F., Jones, J.A. and Cross, A.J. (2000). The metabolism of clomethiazole in gerbils and the neuroprotective and sedative activity of the metabolites. *Br. J. Pharmacol.* **129(1)**, 95-100.

Greenberg, M., Greene, L. and Ziff, E. (1985). Nerve growth factor and epidermal growth factor induce rapid transient changes in proto-oncogene transcription inbPC12 cells. *J. Biol. Chem.* **260**, 14101-14110.

Greenlund, L.J., Deckwerth, T.L. and Johnson, E.M. Jr. (1995). Superoxide dismutase delays neuronal apoptosis: a role for reactive oxygen species in programmed neuronal death. *Neuron* **14(2)**, 303-15.

Grondahl, T.O., Berg-Johnsen, J. and Langmoen, I.A. (1998). Chloride influx during cerebral energy deprivation. *Neurol. Res.* **20(2)**, 131-6.

Grotta, J., Clark,W., Coull, B., Pettigrew, L.C.; Mackay, B., Goldstein, L.B., Meissner, I., Murphy, D. and LaRue, L. (1995). Safety and tolerability of the glutamate antagonist CGS 19755 (Selfotel) in patients with acute ischemic stroke. Results of a phase II a randomized trial. *Stroke* **26(4)**, 602-5.

Grotta, J.C. and Hickenbottom, S. (1999). Neuroprotective therapy. *Rev. Neurol. Paris.* **155(9)**, 644-6.

Gubits, R., Burke, R., Casey-MacIntosh, G., Bandele, A. and Munell, F. (1993). Immediate early gene induction after neonatal hypoxia-ischemia. *Mol. Brain. Res.* **18**, 228-238.

Guido, M.E., Goguen, D., De Guido, L., Robertson, H.A. and B. Rusak (1999). Circadian and photic regulation of immediate-early gene expression in the hamster suprachiasmatic nucleus. *Neuroscience* **90**, 555-571.

Gulati, S., Ainol, L., Orak, J., Singh, A.K. and Singh, I. (1993). Alterations of peroxisomal function in ischemia-reperfusion injury of rat kidney. *Biochim. Biophys. Acta.* **182(3)**, 291-8.

Hafezi, F., Steinbach, J.P., Marti, A., Munz, K., Wang, Z.Q., Wagner, E.F., Aguzzi, A., and Reme, C.E. (1997). The absence of *c-fos* prevents light-induced apoptotic cell death of photoreceptors in retinal degeneration *in vivo*. *Nat. Med.* **3**, 346-349.

Hagberg, H., Lehmann, A., Sandberg, M., Nystrom, B., Jacobson, I. and Hamberger, A. (1985). Ischemia-induced shift of inhibitory and excitatory amino acids from intro to extracellular compartments. *J. Cereb. Blood Flow Metab.* **5**, 413-419.

Hagberg, H., Gilland, E., Diemer, N.H. and Andine, P. (1994). Hypoxia-ischemia in the neonatal rat brain: histopathology after post-treatment with NMDA and non-NMDA receptor antagonists. *Biol. Neonate.* **66**, 205-213.

Hagberg, H. and Bona E. et al. (1997). Hypoxia-ischaemia model in the 7-day-old rat: possibilities and shortcomings. *Acta Paediatrica Supplement.* **422**, 85-88.

Hajimohammadreza, I., Probert, A., Coughenour, L., Borosky, S., Marcoux, F., Boxer, P. and Wang, K. (1995). A specific inhibitor of calcium/calmodulin-dependent protein kinase-II provides neuroprotection against NMDA- and hypoxia/ hypoglycemia-induced cell death. *J. Neurosci.* **15**, 4093-4101.

Hales, T.G. and Lambert J.J.(1992) Modulation of $GABA_A$ and glycine receptors by chlormethiazole. *Eur. J. Pharmacol.* **210**, 239-246.

Hallmayer, J., Hossmann, K-A. and Mies, G. (1985). Low dose of barbiturates for prevention of hippocampus lesions after brief ischemic episodes. *Acta Neuropathol.* **68**, 27-31.

Hamada Y., Hayakawa T. and Hattori, H. (1994). Inhibitor of nitiric oxide synthase reduces hypoxic-ischemic brain damage in the neonatal rat. *Pediatr. Res.* **35**, 10-14.

Hansen, A.J. (1985). Effect of anoxia on ion distribution in the brain. *Physiol. Rev.* **65**, 101-148.

Hara, H., Fink, K., Endres, M., Friedlander, R.M., Gagliardini, V., Yuan, J. and Moskowitz, M.A. (1997). Attenuation of transient focal cerebral ischemic injury in transgenic mice expressing a mutant ICE inhibitory protein. *J. Cereb. Blood Flow Metab.* **7(4)**, 370-5.

Harrison, N.L. and Simmonds M.A. (1983). Two distinct interactions of barbiturates and chlormethiazole with the GABA receptor complex in rat cuneate nucleus *in vitro*. *Br. J. Pharmacol.* **80**, 87-394.

Hartl, F.U. (1996). Molecular chaperones in cellular protein folding. *Nature* **381**, 571-580.

He, H., Qi, X., Grossman, J. and Distelhorst C.W. (1998). c-Fos degradation by the proteasome. An early, Bcl-2-regulated step in apoptosis. *J. Biol. Chem.* **273(39)**, 25015-25019.

Hengartner, M.O. and Horvitz, H.R. (1994). *C. elegans* cell survival gene ced-9 encodes a functional homolog of the mammalian proto-oncogene *bcl-2*. *Cell* **76**, 665-676.

Herdegen, T., Kovary, K., Buhl, A., Bravo, R., Zimmermann, M., Gass, P. (1995). Basal expression of the inducible transcription factors c-Jun, JunB, JunD, C-FosB and Krox-24 in the adult brain. *J. Comp. Neurol.* **354**, 39-56.

Heron, A., Pollard, H., Dessi, F., Moreau, J., Lasbennes, F., Ben-Ari, Y., Charriault-Marlangue, C. (1993). Regional variability in DNA fragmentation after global ischemia evidenced by combined histological and gel electrophoresis observation in the rat brain. *J. Neurochem.* **61**, 1973-1976.

Herrera, D.G. and Robertson, H.A. (1996). Activation of *c-fos* in the brain. *Prog. Neurobiol.* **50**, 83-107.

Higashi, T., Takechi, H., Uemura, Y., Kikuchi, H. and Nagata, K. (1994). Differential induction of mRNA species encoding several classes of stress proteins following focal cerebral ischemia in rats. *Brain Res.* **650**, 239-248.

Hill, D.R. and Bowery N.G. (1981). [^{3}H]-baclofen and [^{3}H]-GABA bind to bicuculline-insensitive $GABA_B$ sites in the rat brain. *Nature (Lond).* **290**, 149-152.

Hisanaga, K., Sagar, S.M., Koistinaho, J., Hicks, K.J. and Sharp, F.R. (1993). VIP-induced stellation and immediate early gene expression in astrocytes: effects of dexamethasone. *Neurosci. Lett.* **156**, 57-60.

Hollmann, M. and Heinemann, S. (1994). Cloned glutamate receptors. *Ann. Rev. Neurosci.* **17**, 31-108.

Holtzman, D.M., Sheldon, R.A., Jaffe, W., Cheng, Y. and Ferriero, D.M. (1996). Nerve growth factor protects the neonatal brain against hypoxic-ischemic injury. *Ann. Neurol.* **39**, 114-122.

Hossmann, K.A. (1998). Experimental models for the investigation of brain ischemia. *Cardiovasc. Res.* **39(1)**, 106-20.

Hudome, S., Palmer C., Roberts, R.L., Mauger, D., Housman, C., and Towfighi, J. (1997). The role of neutrophils in the production of hypoxic-ischemic brain injury in the neonatal rat. *Pediatr. Res.* **41**, 1-10.

Hughes, P. Lawlor, P. and Dragunow, M. (1992). Basal expression of Fos, Fos-related, Jun, Krox 24 proteins in rat hippocampus. *Mol. Brain Res.* **13**, 355-357.

Hughes, P.E., Alexi, T., Yoshida, T., Schreiber, S.S. and Knusel, B. (1996). Excitotoxic lesion of rat brain with quinolinic acid induces expression of p53 messenger RNA and protein and p53-inducible genes Bax and Gadd-45 in brain areas showing DNA fragmentation. *Neuroscience* **74(4)**, 1143-60.

Hunter, A.J., Green, A.R. and Cross, A.J. (1995). Animal models of acute ischemic stroke: Can they predict clinically successful neuroprotective drugs? *Trends Pharmacol. Sci.* **16(4)**, 123-8.

Huot, J., Roy, G., Lambert, H., Chrétien, P. and Landry, J. (1991). Increased survival after treatments with anticancer agents of Chinese hamster cells expressing the human Mr 27,000 kDa heat shock protein. *Cancer Res.* **51**, 5245-5252.

Huot, J., Houle, F., Spitz, D.R. and Landry, J. (1996). HSP27 phosphorylation-mediated resistance against actin fragmentation and cell death induced by oxidative stress. *Cancer Res.* **56**, 273-279.

Ikonomidou, C., Mosinger, J.L., Salles, K.S., Labruyere, J. and Olney, J.W. (1989). Sensitivity of the developing rat brain to hypobaric/ischemic damage parallels sensitivity to N-methyl-D-aspartate neurotoxicity. *J. Neurosci.* **9**, 2809-2818.

Inglefield, J.R., Wilson, C.A. and Schwartz-Bloom, R.D. (1997). Effect of transient cerebral ischemia on gamma-aminobutyric $acid_A$ receptor alpha 1 subunit-immunoreactive interneurons in the gerbil CA1 hippocampus. *Hippocampus* **7(5)**, 511-523.

Ishikawa, Y., Yokoo, T. and Kitamura, M. (1997). c-Jun/AP-1, but not NF-kappa B, is a mediator for oxidant-initiated apoptosis in glomerular mesangial cells. *Biochem. Biophys. Res. Commun.* **240(2)**, 496-501.

Ishimaru, M.J., Ikonomidou, C., Tenkova, T.I., Der, T.C., Dikranian, K., Sesma, M.A., Olney, J.W. (1999). Distinguishing excitotoxic from apoptotic neurodegeneration in the developing rat brain. *J. Comp. Neurol.* **408(4)**, 461-76.

Ito, H., Watanabe, Y., Isshiki, A. and Uchino, H. (1999). Neuroprotective properties of propofol and midazolam, but not pentobarbital, on neuronal damage induced by forebrain ischemia, based on the $GABA_A$ receptors. *Acta Anaesthestologica Scandinavica.* **43**, 153-162.

Jacewicz, M., Kiessling, M. and Pulsinelli, W.A. (1986). Selective gene expression in focal cerebral ischemia. *J. Cereb. Blood. Flow. Metab.* **6(3)**, 263-72.

Jacob, U., Gaestel, M., Engel, K. and Buchner, J. (1993). Small heat shock proteins are molecular chaperones. *J. Biol. Chem.* **268**, 1517-1520.

Jaimovich, D., Shabino, C., Noorani, P., Bittle, B and Osborne, S. (1990). Intravenous midazolam suppression of pentylenetetrazol-induced epileptic activity in a porcine model. *Critical Care Medicine.* **18(3)**, 313-316.

James, P., Vorherr, T. and Carafoli, E. (1995). Calmodulin-binding domains: just two faced or multi-faceted? *Trends Biochem, Sci.* **20**, 38-42.

Jawad, S., Oxley, J., Wilson, J. and Richens, A. (1986). A pharmacodynamic evaluation of midazolam as an antiepileptic compound. *J. Neurol. Neurosurg. Psychiatry.* **49**, 1050.

Jenkins, R. and Hunt, S.P. (1991). Long-term increase in the levels of c-*jun* mRNA and Jun protein-like immunoreactivity in motor and sensory neurons following axon damage. *Neurosci. Lett.* **129**, 107-110.

Johansen, F.F., Christensen, T., Jensen, M.S., Valente, E., Jensen, C.V., Nathan, T., Lambert, J.D.C. and Diemer, N.H. (1991). Inhibition in postischaemic rat hippocampus: GABA receptors, GABA release, and inhibitory postsynaptic potentials. *Exp. Brain Res.* **84**, 529-537.

Kaina, B., Haas, S. and Kappes, H. (1997). A general role for c-fos in cellular protection against DNA-damaging carcinogens and cytostatic drugs. *Cancer Res.* **57**, 2721-31.

Kajstura, J., Liu, Y., Baldini, A., Li, B., Olivetti, G., Leri, A. and Anversa, P. (1998). *Am. J. Cardiol.* **82**, 30K-41K.

Kamme, F., Campbell, K. and Wieloch, T. (1995). Biphasic Expression of the Fos and Jun Families of Transcription Factors Following Transient Forebrain Ischaemia in the Rat. Effect of Hypothermia. *Eur. J. Neurosci.* **7**, 2007-2016.

Kamii, H., Kinouchi, H., Sharp, F.R., Epstein, C.J., Sagar, S.M. and Chan, P.H. (1994a). Expression of *c-fos* mRNA after a mild focal cerebral ischemia in SOD-1 transgenic mice. *Brain Res.* **662(1-2)**, 240-4.

Kamii, H., Kinouchi, H., Sharp, F.R., Koistinaho, J., Epstein, C.J. and Chan, P.H. (1994b). Prolonged expression of *hsp70* mRNA following transient focal cerebral ischemia in transgenic mice overexpressing CuZn-superoxide dismutase. *J. Cereb. Blood Flow Metab.* **14(3)**, 478-86.

Kamphuis, W. and Lopes da Silva, F. (1990). The kindling model of epilepsy: The role of GABAergic inhibition. *Neurosci. Res. Comm.* **6**, 1-10.

Kanai, Y., Araki, T., Kato, H. and Kogure, K. (1994). Effect of pentobarbital on postischemic MK-801, muscimol, and naloxone bindings in the gerbil brain. *Brain Res.* **657**, 51-58.

Kanthan, R., Shuaib, A., Griebel, R. and Miyashita, H. (1995). Intracerebral human microdialysis: in vivo study of an acute focal ischemic model of the human brain. *Stroke* **26**, 870-873.

Kapur, J. and MacDonald, R.L. (1998). Postnatal development of hippocampal dentate granule cell gamma- aminobutyric $acid_A$ receptor pharmacological properties. *Mol. Pharmacol.* **55**, 444-452.

Kato, H., Liu, Y., Kogure, K. and Kato K. (1994). Induction of 27-kDa heat shock protein following cerebral ischemia in a rat model of ischemic tolerance. *Brain Res.* **634(2)**, 235-44.

Kato, K. Hasegawa, K., Goto, S. and Inaguma, Y. (1994). Dissociation as a result of phosphorylation of an aggregated form of the small stress protein, hsp27. *J. Biol. Chem.* **269**, 11274-11278.

Kato, H., Araki, T., Itoyama, Y., Kogure, K. and Kato, K. (1995). An immunohistochemical study of heat shock protein-27 in the hippocampus in a gerbil model of cerebral ischemia and ischemic tolerance. *Neuroscience* **68(1)**, 65-71.

Kato, H., Kanellopoulos, G.K., Matsuo, S., Wu, Y.J., Jacquin, M.F., Hsu, C.Y., Kouchoukos, N.T. and Choi, D.W. (1997). *Exp. Neurol.* **148**, 464-474.

Kaushal, G.P., Singh, A.B. and Shah, S.V. (1998). Identification of gene family of caspases in rat kidney and altered expression in ischemia-reperfusion injury. *Am. J. Physiol.* **274**, F587-F595.

Kelly, M. E., Battye, R.A. and McIntyre, D.C. (1999). Cortical Spreading Depression Reversibly Disrupts Convulsive Motor Seizure Expression in Amygdala-Kindled Rats. *Neuroscience* **91(1)**, 305-313.

Kerr, J.F., Wyllie, A.H. and Currie, A.R. (1972). Apoptosis: a basic biological phenomenon with wide-ranging implications in tissue kinetics. *Br. J. Cancer.* **26(4)**, 239-57.

Khan, Z.U., Gutierrez, A., Mehta, A.K., Miralles, C.P. and De Blas, A.L. (1996a). The alpha 4 subunit of the $GABA_A$ receptors from rat brain and retina. *Neuropharmacology* **35(9-10)**, 1315-22.

Khan, Z.U., Gutierrez, A., Miralles, C.P. and De-Blas A.L. (1996b). The gamma subunits of the native $GABA_A$/benzodiazepine receptors. *Neurochem. Res.* **21(2)**, 147-59.

Kiang, J.G., Carr, F.E., Burns, M.R. and McClain, D.E. (1994). HSP-72 synthesis is promoted by increase in $[Ca^{2+}]_I$ or activation of G proteins but not pH_i or cAMP. *Am. J. Physiol. (Cell Physiol.)*. **265**, C104-C114.

Kiang, J.G. and Tsokos, G.C. (1998). Heat shock protein 70 kDa: molecular biology, biochemistry, and physiology. *Pharmacol. Ther.* **80(2)**, 183-201.

Kilpatrick, C., Davis, S., Tress, B., Rossiter, S., Hopper, J. and Vandendriesen, M. (1990). Epileptic seizures in acute stroke. *Arch. Neurol.* **47**, 157-160.

Kim, D.C. and Todd, M.M. (1999). Forebrain ischemia: effect on pharmacologically induced seizure thresholds in the rat. *Brain Res.* **831(1-2)**, 131-9.

Kimura, Y., Engelman, R., Rousou, J., Flack, J., Iyengar, J. and Das, D. (1992). Moderation of myocardial ischemia reperfusion injury by calcium channel and calmodulin receptor inhibition. *Heart Vessels.* **7**, 189-195.

King, G.A. (1979). Effects of systemically applied GABA agonists and antagonists on wave-spike EcoG activity in the rat. *Neuropharmacology* **18**, 47-55.

Kinouchi, H., Sharp, F.R., Koistinaho, J., Hicks, K., Kamii, H. and Chan, P.H. (1993). Induction of heat shock hsp70 mRNA and HSP70 kDa protein in neurons in the "penumbra" following focal cerebral ischemia in the rat. *Brain Res.* **619**, 334-338.

Kirino, T. and Sano, K. (1984). Fine structural nature of delayed neuronal death following ischemia in the gerbil hippocampus. *Acta. Neuropathol. Ber*l. **62(3)**, 209-18.

Kirino, T., Tsujita, Y. and Tamura, A. (1991). Induced tolerance to ischemia in gerbil hippocampal neurons, *J. Cereb. Blood Flow Metab.* **11**, 299-307.

Kitagawa, K., Matsumoto, M., Kuwabara, K., Tagaya, M., Ohtsuki, T., Hata, R., Ueda, H., Handa, N., Kimura, K. and Kamada, T., (1991). 'Ischemic tolerance' phenomenon detected in various brain regions. *Brain Res.* **561**, 203-211.

Knauf, U., Bielka, H. and Gaestel, M. (1992). Over-expression of the small heat-shock protein, hsp25, inhibits growth of Ehrlich ascites tumor cells. *FEBS Lett.* **309**, 297-302.

Kobayashi, S. and Welsh, F.A. (1995). Regional Alterations of ATP and Heat-Shock Protein-72 mRNA Following Hypoxia-Ischemia in Neonatal Rat Brain. *J. Cereb. Blood Flow Metab.* **15(6)**, 1047-1056.

Koroshetz, W.J. and Bonventre, J.V. (1994). Heat shock response in the central nervous system. *Experientia* **50**, 1085-1091.

Kristian, T. and Siesjo, B.K. (1996). Calcium-related damage in ischemia. *Life Sci.* **59**, 357-367.

Kure, S., Tominaga, T., Yoshimoto, T., Tada, K. and Narisawa, K. (1991). Glutamate triggers internucleosomal DNA cleavage in neuronal cells. *Biochem. Biophys. Res. Comm.* **179**, 39-45.

Kuroda, S., Nakai, A., Kristian, T. and Siesjo, B. (1997). The calmodulin antagonist trifluoperazine in transient focal brain ischemia in rats - anti-ischemic effect and therapeutic window. *American Heart Association, Inc.* **28**, 2539-2543.

Landry, J., Chrétien, P., Lambert, H., Hickey, E. and Weber, L.A. (1989). Heat shock resistance conferred by expression of the human HSP27 gene in rodent cells. *J. Cell Biol.* **109**, 7-15.

Lavoie, J.N., Gingras-Breton, G., Tanguay, R.M. and Landry, J. (1993). Induction of Chinese hamster HSP27 gene expression in mouse cells confers resistance to heat shock. HSP27 stabilization of the microfilament organization. *J. Biol. Chem.* **268**, 3420-3429.

Leah, J.D., Herdegen, T. and Bravo, R. (1991). Selective expression of Jun proteins following axotomy and axonal transport block in peripheral nerves in the rat: evidence for a role in regeneration process. *Brain Res.* **566**, 198-207.

Lechat, P. (1960). Pharmacodynamie de la thiamine et ses drivs. *Actual. Pharmacol.* **13**, 167-188.

Lechat, P. (1966). Toxicological and pharmacological properties of clomethiazole. *Acta Psychiatr. Scand.* **42 (Suppl. 192)**, 15-22.

Leeb-Lundberg, F., Snowman, A. and Olsen, R.W. (1981). Interaction of anticonvulsants with the barbiturate-benzodiazepine-GABA receptor complex. *Eur. J. Pharmacol.* **72**, 125-129.

Levine, S. (1960). Anoxic-ischemic encephalopathy in rats. *Am. J. Pathol.* **36**, 1-17.

Li, G.C., Li, L., Liu, R.Y., Rehman, M. and Lee, W.M.F. (1992). Heat shock protein hsp70 protects cells from thermal stress even after deletion of its ATP-binding domain. *Proc. Natl. Acad. Sci. USA*, **89**, 2036-2040.

Li, H., Siegel, R.E. and Schwartz, R.D. (1993). Rapid decline of $GABA_A$ receptor subunit mRNA expression in hippocampus following transient cerebral ischemia in the gerbil. *Hippocampus* **3**, 527-538.

Li, Y., Powers, C., Jiang, N. and Chopp, M. (1998). Intact, injured, necrotic and apoptotic cells after focal cerebral ischemia in the rat. *J. Neurol. Sci.* **156**, 119-132.

Liang, P. and Pardee A. (1992). Differential display of eukaryotic messenger RNA by means of the polymerase chain reaction. *Science* **257**, 967-971.

Liang, P. and Pardee A.B.(1995). Recent advances in differential display. *Curr. Opin. Immunol.* **7**, 274-280.

Liang, S., Kanthan, R., Shuiab, A. and Wishart, T. (1997). Effects of clomethiazole on radial-arm maze performance following global forebrain ischemia in gerbils. *Brain Res.* **751**, 189-195.

Lieberthal, W. and Levine, J.S. (1996). Mechanisms of apoptosis and its potential role in renal tubular epithelial cell injury. *Am. J. Physiol.* **271(3 Pt 2)**, F477-88.

Linquist, S. and Craig, E.A. (1988). The heat shock proteins. *Ann. Rev. Genet.* **22**, 631-677.

Lipton, S.A. (1993). Prospects for clinically tolerated NMDA antagonists: open-channel blockers and alternative redox states of nitric oxide. *Trends Neurosci.* **16(12)**, 527-32.

Liu, X.H., Eun B.L., Silverstein, F.S. and Barks, J.D.E. (1996). The platelet-activating factor antagonist BN 52021 attenuates hypoxic-ishemic brain injury in the immature rat. *Pediatr. Res.* **40**, 797-803.

Loddick, S.A., MacKenzie, A. and Rothwell, N.J. (1996). An ICE inhibitor, z-VAD-DCB attenuates ischaemic brain damage in the rat. *Neuroreport* **7(9)**, 1465-8.

Loscher, W., Cramer, S. and Ebert, U. (1998). Differences in kindling development in seven outbred and inbred rat strains. *Exp. Neurol.* **154(2)**, 551-559.

LoTurco, J.J., Owens, D.F. Heath, M.J.S., Davis, M.B.E. and Kriegstein, A.R. (1995). GABA and glutamate depolarize cortical progenitor cells and inhibit DNA synthesis. *Neuron* **15**, 1287-1298.

Lowenstein, D.H., Chan, P.H. and Miles, M.F. (1991). The stress protein response in cultured neurons: characterization and evidence for a protective role in excitotoxicity. *Neuron.* **7**, 1053-1060.

Lyden, P.D. and Lonzo, L. (1994). Combination therapy protects ischemic brain in rats. A glutamate antagonist plus a gamma-aminobutyric acid agonist. *Stroke* **25**, 189-196.

Lyden, P. (1997). GABA and neuroprotection. *Int. Rev. Neurobiol.* **49**, 233-258.

Macaya, A., Munell, F., Ferrer, I., deTorres, C. and Revents, J. (1998). Cell death and associated c-*jun* induction in perinatal hypoxia-ischemia. Effect of the neuroprotective drug dexamethasone. *Mol. Brain Res.* **56**, 29-37.

MacGregor, D.G., Graham, D.I. and Stone, T.W. (1997). The attenuation of kainate-induced neurotoxicity by chlormethiazole and its enhancement by dizocipine, muscimol, and adenosine receptor agonists. *Experimental Neurology* **148(1)**, 110-123.

Mailhos, C., Howard, M.K. and Latchman, D.S. (1994). Heat shock proteins *hsp90* and *hsp70* protect neuronal cells from thermal stress but not from programmed cell death. *J. Neurochem.* **63**, 1787-1795.

Mainprize, T., Shuaib, A., Ijaz, S., Kanthan, R., Miyashita, H. and Kalra, J. (1995). GABA concentrations in the striatum following repetitive cerebral ischemia. *Neurochem. Res.* **20**, 957-961.

Marber, M.S., Mestril, R., Chi, S.H., Sayen, M.R., Yellon, D.M. and Dillmann, W.H. (1995). Overexpression of the rat inducible 70-kD heat stress protein in a transgenic mouse increases the resistance of the heart to ischemic injury. *J. Clin. Invest.* **95**, 1446-1456.

Marie, C., Mossiat, C. and Bralet, J., (1994). Neurologic and Cytologic Outcome Following Repeated Ischemia. Effect of Pentobarbital. *Brain Res. Bull.* **35(2)**, 161-166.

Marshall, J.W., Cross, A.J. and Ridley, R.M. (1999). Functional benefit from clomethiazole treatment after focal cerebral ischemia in a nonhuman primate species. *Exp. Neurol.* **156**, 121-129.

Martin, L.J., Al-Abdulla, N.A., Brambrink, A.M., Kirsch, J.R., Sieber, F.E. and Portera-Cailliau, C. (1998). Neurodegeneration in excitotoxicity, global cerebral ischemia, and target deprivation: A perspective on the contribution of apoptosis and necrosis. *Brain Res. Bull.* **46(4)**, 281-309.

Mathieu-Daude, F., Welsh, J., Vogt, T. and McClelland, M. (1996). DNA rehybridization during PCR: the 'Cot effect' and its consequences. *Nucleic Acids Res.* **24(11)**, 2080-6.

McBurney, R.N. (1997). Development of the NMDA ion-channel blocker, aptiganel hydrochloride, as a neuroprotective agent for active CNS injury. *Int. Rev. Neurobiol.* **46**, 299-317.

McCormick, D.A., Wang, Z., Huguenard, J. (1993). Neurotransmitter control of neocortical neuronal activity and excitability. *Cereb. Cortex* **3**,387-398.

McIntyre, D.C. and Racine, R.J. (1986). Kindling mechanisms: current progress on an experimental epilepsy model. *Prog. Neurobiol*, **27(1)**, 1-12.

McNamara, J., Bonhaus, D., Shin, C., Crain, B., Gellman, R. and Giacchino, J. (1985). The kindling model of epilepsy: A critical review. *CRC Critical Rev. Clin. Neurobiol.* **1**, 341-391.

Mehlen, P., Preville, X., Chareyron, P., Briolay, J., Klemenz, R. and Arrigo, A.P. (1995). Constitutive expression of human hsp27, Drosophila hsp27, or human alpha B-crystallin confers resistance to TNF – and oxidative stress-induced cytotoxicity in stably transfected murine L929 fibroblasts. *J. Immunol.* **154**, 363-374.

Mehlen, P., Schulzeosthoff, K. and Arrigo, A.P. (1996). Small stress proteins as novel regulators of apoptosis-heatshock protein 27 blocks Fas/APO-1-and staurosporine-induced cell death. *J. Biol. Chem.* **271**, 16510-16514.

Meldrum, B. (1990a). Protection against ischaemic neuronal damage by drugs acting on excitatory neurotransmission. *Cerebrovasc. Brain Metab. Rev.* **2**, 27-57.

Meldrum, B., and Garthwaite, J. (1990b). Excitatory amino acid neurotoxicity and neurodegenerative disease. *Trends Pharmacol. Sci.* **11**, 379-387.

Meldrum, B. (1992). Excitatory amino acids and neuroprotection. In: Emerging strategies in neuroprotection. (eds. Marangos, P.J. and Lal, H.). pp. 106-128.

Meldrum, B. (1997). Epileptic brain damage: A consequence and a cause of seizures. (Review). *Neuropathol. Appl. Neurobiol.* **23**, 185-202.

Meriin, A.B., Yaglom, J.A., Gabai, V.L., Mosser, D.D., Zon, L. and Sherman M.Y. (1999). Protein damaging stresses activate c-jun N-terminal kinase via inhibition of its dephosphorylation: a novel pathway controlled by HSP72. *Mol. Cell Biol.* **19(4)**, 2547-2555.

Miron, T., Vancompernolle, K., Vandekerckhove, J., Wilchek, M. and Geiger, B. (1991). A 25kD inhibitor of actin polymerization is a low molecular mass heat shock protein. *J. Cell Biol.* **114**, 255-261.

Mittmann, T., Luhmann, H.J., Qü, M. and Zilles, K. (1998). Long-term cellular dysfunction after focal cerebral ischemia: *in vitro* analyses. *Neuroscience* **85**, 15-27.

Mizzen, L.A. and Welch, W.J. (1988). Characterization of the thermotolerant cell. I. Effects on protein synthesis activity and the regulation of heat-shock protein 70 expression. *J. Cell Biol.* **106(4)**, 1105-16.

Mok, S.C., Wong, K.K.; Chan, R.K.; Lau, C.C.; Tsao, S.W.; Knapp, R.C., Berkowitz, R.S. (1994). Molecular cloning of differentially expressed genes in human epithelial ovarian cancer. *Gynecol-Oncol.* **52(2)**, 247-52.

Monaghan, D.T., Holets, V.R., Toy, D.W. and Cotman, C.W. (1983). Anatomical distributions of four pharmacologically distinct [^{3}H]-L-glutamate binding sites. *Nature* **306**, 176-179.

Moody, E.J. and Skolnick, P. (1989). Chlormethiazole: neurochemical actions at the gamma-aminobutyric acid receptor complex. *Eur. J. Pharmacol.* **164**, 153-158.

Morgan, J.I. and Curran, T. (1991). Stimulus-transcription coupling in the nervous system: involvement of the inducible proto-oncogenes fos and jun. *Ann. Rev. Neurosci.* **14**, 421-451.

Morimoto, R.I., Tissières, A. and Georgopoulos, C. (1990). The stress response, function of the proteins, and perspectives. In: *The Stress Proteins in Biology and Medicine* (R.I. Morimoto, A. Tissières and Georgopoulos C.eds.). pp 1-36, Cold Spring Harbor Laboratory Press, Cold Spring Harbor, NY.

Morimoto RI, Jurivich DA, Kroeger PE, et al. (1994). Regulation of heat shock gene transcription by a family of heat shock factors. In: *The Biology of Heat Shock Proteins and Molecular Chaperones* (Morimoto RI, Tissières A, Georgopoulos C. eds), pp 417-455, Cold Spring Harbor, NY, Cold Spring Harbor Laboratory Press.

Moshé, S.L., Albala, B.J., Ackermann, R.F. and Engel, J. Jr. (1983). Increased seizure susceptibility of the immature brain. *Dev. Brain Res.* **7**, 81-85.

Mosser, D.D., Caron, A.W., Bourget, L., Denis-Larose, D. and Massie, B. (1997). Role of the Human Heat Shock Protein hsp70 in Protection against Stress-Induced Apoptosis. *Mol. Cell. Biol.* **17(9)**, 5317-5327.

Munell, F., Bruke, R.E., Bandele, A. and Gubits, R.M. (1994). Localization of *c-fos*, and hsp70 mRNA expression after neonatal hypoxia-ischemia. *Dev. Brain. Res.* **77**, 111-121.

Nagata, K., Hirayoshi, K., Obara, M., Saga, S. and Yamada, K.M., (1988). Biosynthesis of a novel transformation-sensitive heat-shock protein that binds to collagen. *J. Biol. Chem.* **263**, 8344-8349.

Nagata, K., Nakai, A., Hosokawa, N., Kudo, M., Takechi, H., Sato, M. and Hirayoshi, K. (1991). Interaction of HSP47 with newly synthesized procollagen, and regulation of HSP expression. In: *Heat Shock* (eds. B. Maresca and S. Lindquist). pp. 105-110, Springer, New York.

Nakai, A. Satoh, M., Hirayoshi, K. and Nagata, K., (1992). Involvement of the stress protein HSP47 in procollagen processing in the endoplasmic reticulum. *J. Cell. Biol.* **117**, 903-914.

Naranjo, J.R., Mellstrom, B., Achaval, M. and Sassone-Corsi, P. (1991). Molecular pathways of pain: Fos/Jun-mediated activation of a noncanonical AP-1 site in the prodynorphin gene. *Neuron* **6**, 607-617.

Ni, B., Wu, X., Su, Y., Stephenson, D., Smalstig, E.B., Clemens, J. and Paul, S.M. (1998). Transient global forebrain ischemia induces a prolonged expression of the *caspase-3* mRNA in rat hippocampal CA1 pyramidal neurons. *J. Cereb. Blood Flow Metab.* **18(3)**, 248-56.

Nishio, Y., Aiello, L.P., King. G.L. (1994). Glucose induced genes in bovine aortic smooth muscle cells identified by mRNA differential display. *FASEB* **8(1)**, 103-6.

Nitatori, T., Sato, N., Waguri, S., Karasawa, Y., Araki, H., Shibanai, K., Kominami, E. and Uchiyama, Y. (1995). Delayed neuronal death in the CA1 pyramidal cell layer of the gerbil hippocampus following transient ischemia is apoptosis. *J. Neurosci.* **15(2)**, 1001-11.

Nitsch, C., Goping, G. and Klatzo, I. (1991). Preservation of GABAergic perikarya and boutons after transient ischemia in the gerbil hippocampal CA1 field. *Brain Res.* **495**, 243-252.

Noda, T., Iwakiri, R., Fujimoto, K., Matsuo, S. and Aw, T.Y. (1998). *Am. J. Physiol.* **274**, G270-G276.

Nowak, T.S. (1985). Synthesis of a stress protein following transient ischemia in the gerbil. *J. Neurochem.* **45**, 1635-1641.

Nowak, T.S., Ikeda, J. and Nakajima, T. (1990). 70-kDa heat-shock protein and c-*fos* gene expression after transient ischemia. *Stroke* **21 (Suppl. 11)**, 107-111.

Nunez, G., Benedict, M.A., Hu, Y. and Inohara, N. (1998). Caspases: the proteases of the apoptotic pathway. *Oncogene* **17**, 3237-3245.

Nurse, S. and Corbett, D. (1996). Neuroprotection after several days of mild drug-induced hypothermia. *J. Cereb. Blood Flow Metab.* **16**, 474-480.

Obrietan, K. and van de Pol, A.N. (1995). GABA neurotransmission in the hypothalamus: developmental reversal from Ca^{2+} elevating to depressing. *J. Neurosci.* **15**, 5065-5077.

Ogren, S.O. (1986). Chlormethiazole - mode of action. *Acta Psychiatr. Scand. Suppl.* **329**, 13-27.

Olney, J.W. (1971). Glutamate-induced neuronal necrosis in the infant mouse hypothalamus. An electron microscopic study. *J. Neuropathol. Exp. Neurol.* **30(1)**, 75-90.

Olney, J.W., Rhee, V. and Ho, O.L. (1974). Kainic acid: a powerful neurotoxic analogue of glutamate. *Brain Res.* **77(3)**, 507-12.

O'Regan, M.H., Smith-Barbour, M., Perkins, L.M. and Phillis, J.W. (1995). A possible role for phospholipases in the release of neurotransmitter amino acids from ischemic rat cerebral cortex. *Neurosci. Lett.* **185(3)**, 191-4.

Otani, H., Engelman, R., Rousou, J., Breyer, R., Clement, R., Prasad, R., Klar, J. and Das, D. (1992). Improvement of myocardial function by trifluoperazine, a calmodulin antagonist, after acute coronary artery occlusion and coronary revascularization. *J. Thorac. Cardiovasc. Surg.* **97**, 264-274.

Palleros, D.R., Welch, W.J. and Fink, A.L. (1991). Interaction of hsp70 with unfolded proteins: effects of temperature and nucleotides on the kineties of binding. *Proc. Natl. Acad. Sci. USA.* **88**, 5719-5723.

Palmer, C., Towfighi, J., Roberts, R.L. and Heitjan, D.E. (1993). Allopurinol administered after inducing hypoxia-ischemia reduces brain injury in 7-day-old rats. *Pediatr. Res.* **33**, 405-411.

Papadopoulos, M.C., Sun, X.Y., Cao J., Mivechi, N.F. and Giffard, R.G. (1996). Over-expression of HSP-70 protects against combined oxygen-glucose deprivation. *Neuroreport* **7**, 429-432.

Paxinos, G. and Watson, C. (1986). The rat brain in stereotaxic coordinates. *Academic Press, London.*

Pearson, H.A., Campbell, V., Berrow, A., Menon-Johansson and Dolphin, A.C. (1994). Modulation of voltage-dependent calcium channels in cultured neurons. *Ann. NY Acad. Sci.* **747**, 325.

Pedley, T.A., Horton, R.W. and Meldrum, B.S. (1979). Electroencephalographic and behavioral effects of a GABA agonist muscimol on photosensitive epilepsy in the baboon. *Papio papio, Epilepsia.* **20**, 409-416.

Peeling, J., Wong, D. and Sutherland, G.R. (1989). Nuclear magnetic resonance study of regional metabolism after forebrain ischemia in rats. *Stroke* **20**, 633-640.

Pentikinen, P.J., Neuvonen, P.J. and Jostell, K.G. (1980). Pharmacokinetics of chlormethiazole in healthy volunteers and patients with cirrhosis of the liver. *Eur. J. Pharmacol.* **17**, 275-284.

Petito, C.K., Torres-Munoz, J., Roberts, B., Olarte, J.P., Nowak, T.S. Jr. and Pulsinelli, W.A. (1997). DNA fragmentation follows delayed neuronal death in CA1 neurons exposed to transient global ischemia in the rat. *J. Cereb. Blood Flow Metab.* **17(9)**, 967-76.

Picone, C., Grotta, J., Earls, R., Strong, R. and Dedman, J. (1989). Immunohistochemical determination of calcium-calmodulin binding predicts neuronal damage after global ischemia. *J. Cereb. Blood Flow Metab.* **9**, 805-811.

Plumier, J.C., Krueger, A.M., Currie, R.W., Kontoyiannis, D., Kollias, G. and Pagoulatos, G.N. (1997). Transgenic mice expressing the human inducible Hsp70 have hippocampal neurons resistant to ischemic injury. *Cell Stress Chaperones* **2**, 162-167.

Plumier J.C., Ross B.M., Currie R.W., *et al* (1995). Transgenic mice expressing the human heat shock protein 70 have improved post-ischemic myocardial recovery. *J. Clin. Invest.* **95**, 1854-1860.

Plumier, J.C.L., J.N. Armstrong, J. Landry, J.M. Babity, H.A. Robertson and R.W. Currie (1996). Expression of the 27,000 Mol. WT heat shock protein following kainic acid-induced status epilepticus in the rat. *Neuroscience* **75**, 849-856.

Pulera, M.R., Adams, L.M., Liu, H., Santos, D.G., Nishimura, R.N., Yang, F., Cole, G.M. and Wasterlain, C.G. (1998). Apoptosis in a neonatal rat model of ceberal hypoxia-ischemia. *Stroke* **29**, 2622-2630.

Qü, M., Mittmann, T., Luhmann, H.J., Schleicher, A. and Zilles, K. (1998). Long-term changes of ionotropic glutamate and GABA receptors after unilateral permanent focal cerebral ischemia in the mouse brain. *Neuroscience* **85(1)**, 29-43.

Racine, R.J. (1972). Modification of seizure activity by electrical stimulation. II. Motor seizures. *Electroencephalogr. Clin. Neurophysiol.* **32**, 281-294.

Radford, N.B., Fina, M., Benjamin, I.J., *et al* (1996). Cardioprotective effects of 70-kDa heat shock protein in transgenic mice. *Proc. Natl. Acad. Sci. USA.* **93**, 2339-2342.

Reed, J.C. (1998). Bcl-2 family proteins. *Oncogene* **17**, 3225-3236.

Rohrbough, J. and Spitzer, N.C. (1996). Regulation of intracellular Cl^- levels by Na^+ dependent Cl^- co-transport distinguishes depolarizing from hyperpolarizing GABA, receptor-mediated responses in spinal neurons. *J. Neurosci.* **16**, 82-91.

Romijn, H.J., Janszen, A.W.J.W. and van Marle, J. (1994). Quantitative immunofluorescence data suggest a permanently enhanced GAD_{67}/GAD_{65} ratio in nerve endings in rat cerebral cortex damaged by early postnatal hypoxia-ischemia: a comparison between two computer-assisted procedures for quantification of confocal laser scanning microscopic immunofluorescence images. *Brain Res.* **657**, 245-257.

Rumpel, H. and Buchli, R., Gehrmann, J., Aguzzi, A., Illi, O. and Martin, E. (1995). Magnetic Resonance Imaging of Brain Edema in the Neonatal Rat: A Comparison of Short and Long Term Hypoxia-Ischemia. *Pediatr. Res.* **38(1)**, 113-118.

Saeed, D., Goetzman, B.W. and Gospe, S.N. (1993). Brain injury and protective effects of hypothermia using triphenyltetrazolium chloride in neonatal rat. *Pediatr. Neurol.* **9**, 263-267.

Saikumar, P, Dong, Z., Weinberg, J.M. and Venkatachalum, M.A. (1998). Mechanisms of cell death in hypoxia/reoxygenation injury. *Oncogene* **17**, 3341-3349.

Saikumar, P., Dong, Z., Patel, Y., Hall, K., Hopfer, U., Weinberg, J.M. and Venkatachalam, M.A. (1998). Mechanisms of cell death in hypoxic/reoxygenation injury. *Oncogene* **17(25)**, 3341-9.

Saji, M. and Reis, D. (1987). Delayed Transneuronal Death of Substantia Nigra Neurons prevented by y-Aminobutyric Acid Agonist. *Science* **235**, 66-68.

Sakamuro, D., Eviner, V., Elliott, K.J., Showe, L., White, E. and Prendergast, G.C. (1995). c-Myc induces apoptosis in epithelial cells by both p53-dependent and p53-independent mechanisms. *Oncogene* **11(11)**, 2411-8.

Samali, A., Cai, J., Zhivotovsky, B., Jones, D.P. and Orrenius, S. (1999). Presence of a pre-apoptotic complex of pro-caspase-3, Hsp60 and Hsp10 in the mitochondrial fraction of jurkat cells. *EMBO J.* **18(8)**, 2040-8.

Sargent, C., Sleph, P., Dzwonczyk, S., Smith, M. and Grover, G. (1992). Effect of calmodulin and protein kinase C inhibitors on globally ischemic rat hearts. *J. Cardiovasc. Pharmacol.* **20**, 251-260.

Sato, M., Racine, R.J. and McIntyre, D.C. (1990). Kindling: basic mechanisms and clinical validity. *Electroencephalogr. Clin. Neurophysiol.* **76(5)**, 459-72.

Sato, K., Morimoto, K., Ujike, H., Yamada, T., Yamada, N., Kuroda, S. and Hayabara, T. (1994). The Effects of Perinatal Anoxia or Hypoxia on Hippocampal Kindling Development in Rats. *Brain Res.* **35(2)**, 167-170.

Sato, K., Saito, H. and Matsuki, N. (1996). HSP70 is essential to the neuroprotective effect of heat-shock. *Brain Res.* **740**, 117-123.

Sato, T., Morishima, Y., Sugimura, M., Uchida, T. and Shirasaki, Y. (1999). DY-9760e, a novel calmodulin antagonist, reduces brain damage induced by transient focal cerebral ischemia. *Eur. J. Pharmacol.* **370(2)**, 117-23.

Schaden, H., Strmer, C.A.O. and Bhr, M. (1994). GAP-43 immunoreactivity and axon regeneration in retinal ganglion cells of the rat. *J. Neurobiol.* **25**, 1570-1578.

Schett, G., Steiner, C.W., Groger, M., Winkler, S., Graninger, W., Smolen, J., Xu, Q. and Seiner, G. (1999). Activation of Fas inhibits heat-induced activation of HSF1 and up-regulation of hsp70. *FASEB J.* **13(8)**, 833-42.

Schielke, G.P., Yang, G.Y., Shivers, B.D. and Betz, A.L. (1997). Reduced ischemic brain injury in interleukin-1 converting enzyme-deficient mice. *J. Cereb. Blood Flow Metab.* **17**, 1143-1151.

Schiene, K., Bruehl, C., Zilles, K., Qü, M., Hagemann, G., Kraemer, M. and Witte, O.W. (1996). Neuronal hyperexcitability and reduction of $GABA_A$-receptor expression in the surround of cerbral photothrombosis. *J. Cerebr. Blood Flow Metab.* **16**, 906-914.

Schwartz, R.D. and Yu, X. (1992a). Inhibition of GABA-gated chloride channel function by arachidonic acid. *Brain Res.* **585(1-2)**, 405-10.

Schwartz, R.D., Yu, X., Wanger, J., Ehrmann, M., and Mileson, B.E. (1992b). Cellular regulation of the benzodiazepine/GABA receptor; arachidonic acid, calcium, and cerebral ischemia. *Neuropsychophamacology* **6**, 119-125.

Schwartz-Bloom, R.D., McDonough, K.J., Chase, P.J., Chadwick, L.E., Inglefield, J.R. and Levin, E.D. (1998). Long-term neuroprotection by benzodiazepine full versus partial agonists after transient cerebral ischemia in the gerbil. *J. Cereb. Blood Flow Metab.* **8(5)**, 548-58.

Scott, D.B., Beamish, D., Hudson, I.N. and Jostell, K.G. (1980). Prolonged infusion of chlormethiazole in intensive care. *Br. J. Anaesth.* **52**, 541-545.

Scott, R. and Neville, B. (1999). Pharmacological management of convulsive status epilepticus in children. *Developmental Medicine and Child Neurology* **41**, 207-210.

Scotti de Carolis, A. and Massotti, M. (1978). Electroencephalographic and behavioural investigations on GABAergic drugs: muscimol, baclofen and sodium-hydroxybutyrate: implications on human epileptic studies. *Prog Neuro Psychopharmacol.* **2**, 431-443.

Sei, Y., Von Lubitz, D.K.J.E., Basile, A.S., Borner, M.M., Lin, R.C.S., Skolnick, P. and Fossom, L.H. (1994). Internucleosomal DNA fragmentation in gerbil hippocampus following forebrain ischemia. *Neurosci. Lett.* **171**, 179-82.

Serafini, R., Valeyev, A.Y., Barker, J.L. and Poulter, M.O. (1995). Depolarizing GABA-Activated Cl-channels in embryonic rat spinal and olfactory bulb cells. *J. Physiol. (Lond.).* **488**, 371-386.

Sharp, F.R., Lowenstein, D., Simon, R. and Hisanaga, K. (1991). Heat shock protein hsp72 induction in cortical and striatal astrocytes and neurons following infarction. *J. Cereb. Blood Flow Metab.* **11(4)**, 621-7.

Sheardown, M.J., Nielsen, E.O., Hansen, A.J., Jacobsen, P. and Honore, T. (1990). 2,3-Dihydroxy-6-nitro-7-sulfamoyl-benzo(F) quinoxaline: A neuroprotectant for cerebral ischemia. *Science* **247**, 571-574.

Sheng, M. and Greenberg, M.E. (1990). The regulation and function of c-fos and other immediate early genes in the nervous system. *Neuron* **4**, 477-485.

Shi, Y., Shi, Y., Glynn, J.M., Guilbert, L.J., Cotter, T.G., Bissonnette, R.P. and Green, D.R. (1992). Role for c-myc in activation-induced apoptotic cell death in T cell hybridomas. *Science* **257**, 212-14.

Shima, S., Kitagawa, Y, Kitamura, T., Fujinawa, A. and Watanabe, Y. (1994). Post-stroke depression. *Gen. Hosp. Psychiatry.* **16**, 286-289.

Shimizu, S., Eguchi, Y., Kamiike, W., Waguri, S., Uchiyama, Y., Matsuda, H. and Tsujimoto, Y. (1996). Retardation of chemical hypoxia-induced necrotic cell death by Bcl-2 and ICE inhibitors: possible involvement of common mediators in apoptotic and necrotic signal transductions. *Oncogene* **12(10)**, 2045-50.

Shuaib, A., Ijaz, S., Husan, S. and Kalra, J. (1992). Gamma-vinyl GABA prevents hippocampal and substantia nigra reticulata damage in repetitive transient forebrain ischaemia. *Brain Res.* **590**, 13-17.

Shuaib, A., Mazagri, R. and Ijaz, S. (1993). GABA agonist "muscimol" is neuroprotective in repetitive transient forebrain ischemia in gerbils. *Exp. Neurol.* **123(2)**, 284-8.

Shuaib, A., Ijaz, S. and Kanthan, R. (1995). Clomethiazole protects the brain in transient forebrain ischemia when used up to 4 h after the insult. *Neurosci. Lett.* **197**, 109-112.

Shuaib, A., Marabit, M.A., Kanthan, R., Howlett, W. and Wishart, T. (1996). The neuroprotective effects of gamma-vinyl GABA in transient global ischemia: a morphological study with early and delayed evaluations. *Neurosci. Lett.* **204**, 1-4.

Sieghart, W. (1992). $GABA_A$ receptors: ligand-gated chloride ion channels modulated by multiple drug-binding sites. *Trends Pharmacol. Sci.* **13**, 446.

Siesjö, B.K. (1992a). Pathophysiology and treatment of focal cerebral ischemia. Part I: Pathophysiology. *J. Neurosurg.* **77**, 169-184.

Siesjö, B.K. (1992b). Pathophysiology and treatment of focal cerebral ischemia. Part II: Mechanisms of damage and treatment. *J. Neurosurg.* **77**, 337-354

Siesjö, B.K. and Siesjö, P. (1996). Mechanisms of secondary brain injury. *Eur. J. Anesthes.* **13(3)**, 247-268.

Silverstein, F.S. and Johnston, M.V. (1984). Effects of hypoxia-ischemia on monoamine metabolism in the immature brain. *Ann. Neurol.* **15**, 342-347.

Silverstein, F.S., Buchanan, K., Hudson, C. and Johnston, M.V. (1986). Flunarizine limits hypoxia-ischemia induced morphologic injury in immature rat brain. *Stroke* **17**, 477-482.

Simon, R.P., Cho, H., Gwinn, R. and Lowenstein, D.H. (1991). The temporal profile of 72-kDa heat shock protein expression following global ischemia. *J. Neurosci.* **11**, 881-889.

Small, D.L. and Buchan, A.J. (1997). NMDA antagonists: their role in neuroprotection. *Int. Rev. Neurobiol.* **40**, 137-171.

Smeyne, R.J., Vendrell, M., Hayward, M., Baker, S.J., Miao, G.G., Schilling, K., Robertson, L.M., Curran, T. and Morgan, J.I. (1993). Continuous c-*fos* expression precedes programmed cell death *in vivo*. *Nature* **363**, 166-169.

Smith, B.J. and Yaffe, M.P. (1991). Uncoupling thermotolerance from the induction of heat shock proteins. *Proc. Natl. Acad. Sci. USA.* **88**, 11091-11094.

Snape, M.F., Baldwin, H.A., Cross, A.J. and Green, A.R. (1993). The effect of chlormethiazole and nimodipine on cortical infarct area after focal cerebral ischemia in the rat. *Neuroscience* **53**, 837-844.

Sommer, C., Gass, P. and Kiessling, M. (1995). Selective c-Jun expression in CA1 neurons of the gerbil hippocampus during and after acquisition of an ischemia-tolerant state. *Brain Path.* **5**, 135-144.

Sonnenberg, J.L., Macgregor-Leon, P.F., Curran, T., Morgan, J.I. (1989a). Dynamic alterations occur in the levels and composition of transcription factor AP-1 complexes after seizure. *Neuron* **3**, 359-365.

Sternau, L.L., Lust, W.D., Ricci, A.J. and Ratcheson, R. (1989). Role for y-aminobutyric acid in selective vulnerability in gerbils. *Stroke* **20**, 281-287.

Stokes, K. and McIntyre, D. C. (1985). Lateralized state-dependent learning produced by hippocampal kindled convulsions: effect of split-brain. *Physiol. Behav.* **34(2)**, 217-224.

Stokoe, D., K. Engel, D.G. Campbell, P. Cohen, and M. Gaestel (1992). Indentification of MAPKAP kinase 2 as a major enzyme responsible for the phosphorylation of the small mammalian heat shock proteins. *FEBS Lett.* **313**, 307-313.

Study, R.E. and Barker, J.L. (1981). Diazepam and pentobarbital: Fluctuation analysis reveals different mechanisms for potentiation of y-aminobutyric acid responses in cultured central neurones. *Proc. Natl. Acad. Sci. USA.* **78**, 7180.

Sugito, K., Yamane, M., Hattori, H., Hayashi, Y., Tohnai, I., Ueda, M., Tsuchida, N. and Ohtsuka, K. (1995). Interaction between hsp70 and hsp40, eukaryotic homologues of DnaK and DnaJ, in human cells expressing mutant-type p53. *FEBS-Lett.* **358(2)**, 161-4.

Sun, X., Shin, C. and Windebank, A. (1997). Calmodulin in ischemic neurotoxicity of rat hippocampus in vitro. *NeuroReport.* **8**, 415-418.

Sutcliffe, J.G., Milner, R.J. and Bloom, F.E. (1983). Cellular localization and function of the proteins encoded by brain-specific mRNAs. *Cold Spring Harb. Quant. Biol.* **48**, 477-484.

Swain, J.A., McDonald, T.J. Jr.; Griffith, P.K., Balaban, R.S., Clark, R.E. and Ceckler, T. (1991). Low-flow hypothermic cardiopulmonary bypass protects the brain. *J. Thorac. Cardiovasc. Surg.* **102(1)**, 76-84.

Swann, J.W. and Brady, R.J. (1989). Postnatal Development of GABA-mediated Synaptic Inhibition in Rat Hippocampus. *Neuroscience* **28(3)**, 551-561.

Sydserff, S. G., Cross, A.J., West, K.J. and Green, A.R. (1995a). The effect of chlormethiazole on neuronal damage in a model of transient forebrain ischaemia. *Br. J. Pharmacol.* **114**, 1631-1635.

Sydserff, S.G., Cross, A.J., and Green, A.R. (1995b). The neuroprotective effect of chlormethiazole on ischemic neuronal damage following permanent middle cerebral artery ischaemia in the rat. *Neurodegeneration* **4**, 323-328.

Tecoma, E.S. and Choi, D.W. (1989). GABAergic neocortical neurones are resistant to NMDA receptor-mediated injury. *Neurology* **39**, 676-682.

Thaminy, S., Revmann, J.M., Heresbach, N., Allain, H., Lechat, P. and Bentin-Ferrer, D. (1997). Is clomethiazole neuroprotective in experimental global cerebral ischaemia? A microdialysis and behavioural study. *Pharmacol. Biochem. Behav.* **56**, 737-745.

Thordstein, M., Bagenholm, R., Thiringer, K. and Kjellmer, I. (1993). Scavengers of free oxygen radicals in combination with magnesium ameliorate perinatal hypoxic-ischemic brain damage in the rat. *Pediatr. Res.* **34**, 23-26.

Thoren, P. and Sjolander, J. (1993). Chlormethiazole attenuates the derangement of sensory evoked potential (SEP) induced by i.v. administration of NMDA. *Psychopharmacology* **111**, 256-258.

Thoresen, M., Bågenholm R., Løberg, E.M., Apricena, F. and Kjellmer, I. (1996). Posthymic cooling of neonatal rats provides protection against brain injury. *Arch Dis Child.* **74**, F3-F9.

Thoresen, M., Satas, S., Puka-Sundvall, M., Whitelaw, A., Hallstrom, A., Loberg, E.M., Ungerstedt, U., Steen, P.A. and Hagberg, H. (1997). Post-hypoxic hypothermia reduces cerebrocortical release of NO and excitotoxins. *Neuroreport* **8**, 3359-3362.

Tomimoto, H., Yamamoto, K., Homburger, H.A. and Yanagihara, T. (1993). Immunoelectron microscopic investigation of creatine kinase BB-isoenzyme after cerebral ischemia in gerbils. *Acta Neuropathol. (Berl)* **86**, 447-455.

Tominaga, T., Kure, S., Narisawa, K. and Yoshimoto, T. (1993). Endonuclease activation following focal ischemic injury in the rat brain. *Brain Res.* **608**, 21-26.

Toshiyuki, A., Yoshiyuki, M., Sugimura, M., Uchida, T. and Shirasaki, Y. (1999). DY-9760e, a novel calmodulin antagonist, reduces brain damage induced by transient focal cerebral ischmia. *Eur. J. Pharmacol.* **370**, 117-123.

Towfighi J., Yager, J.Y., Housman C. and Vanucci, R.C. (1991). Neuropathology of remote hypoxic-ischemic damage in the immature rat. *Acta Neuropathol.* **81**, 578-587.

Trescher, W. H., Ishiwa, S. and Johnston, M.V. (1997). Brief post-hypoxic ischemic hypothermia markedly delays neonatal brain injury. *Brain Dev.* **19**, 326-338.

Trifiletti, R.R. (1992). Neuroprotective effect of N^G-nitro-L-arginine in focal stroke in the 7-day old rat. *Eur. J. Pharmacol.* **218**, 197-198.

Twyman, R.E., Rogers, C.J., and Macdonald, R.L. (1989). Pentobarbital and picrotoxinin have reciprocal actions on single $GABA_A$ receptor channels. *Neurosci. Lett.* **96**, 89.

Utans, U., Liang, P., Wyner, L., Karnovsky, M. and Russell, M. (1994). Chronic cardiac rejection: identification of five upregulated genes in transplanted hearts by differential mRNA display. *Proc. Natl. Acad. Sci. USA.* **91**, 6463-6467.

Vannucci, R. C. and Mujsce D. J. (1992). The effect of glucose on perinatal hypoxic-ischemic brain damage. *Biol. Neonate.* **62**, 215-224.

Vannucci, R.C., Towfighi, J., Heitjan, D.F. and Brucklacher, R.M. (1995). Carbon dioxide protects the perinatal brain from hypoxic-ischemic damage. An experimental study in the immature rat. *Pediatrics* **95**, 868-874.

Vannucci, R.C., and Vannucci, S.J. (1999a). Perinatal brain damage. *J. Neurochem.* **71(3)**, 1215-20.

Vannucci, R.C., Connor, J.R., Mauger, D.T., Palmer, C., Smith, M.B., Towfighi, J., and Vannucci, S.J. (1999). Rat model of perinatal hypoxic-ischemic brain damage. *J. Neurosci. Res.* **55**, 158-163.

Vergnes, M., Marescaux, C., Micheletti, G., Depaulis, A., Rumbach, L. and Warter J.M. (1984). Enhancement of spike and wave discharges by GABAmimetic drugs in rats with spontaneous petit-mal like epilepsy. *Neuroscience Lett.* **44**, 91-94.

Verheij, M., Bose, R., Lin, X.H., Yao, B., Jarvis, W.D., Grant, S., Birrer, M.J., Szabo, E., Zon, L.I., Kyriakis, J.M., Haimovitz-Friedman, A., Fuks, Z. and Kolesnick, R.N. Requirement for ceramide-initiated SAPK/JNK signalling in stress-induced apoptosis. *Nature* **380(6569)**, 75-9.

Viani, R. and Romeo, A. (1984). Effect of progabide on seizures and behavior in therapy-resistant epileptic children. In: Epilepsy and GABA Receptor Agonists: Basic and Therapeutic Research (eds. G. Bartholini, L. Bossi, K.G. Lloyd and P.L. Morseili), pp 369-375, Raven, New York.

Vicini, S. (1991). Pharmacologic-significance of the structural heterogeneity of he $GABA_A$ receptor-chloride ion channel complex. *Neuropsychopharmacology* **4**, 9.

Vincens, M., Enjalabert, A., Lloyd, K.G., Paillard, J.J., Thuret, F., Kordon, C. and Lechat, P. (1989). Evidence that chlormethiazole interacts with the macromolecular $GABA_A$-receptor complex in the central nervous system and in the anterior pituitary gland. *Naunyn Schmiedenbergs Arch. Pharmacol.* **339**, 397-402.

Volloch V, Mosser DD, Massie B. and Sherman MY (1998). Reduced thermotolerance in aged cells results from a loss of an hsp72-mediated control of JNK signaling pathway. *Cell Stress Chaperones* **3(4)**, 265-71.

Volpe, J.J. (1995). Hypoxic-ischemic encephalopathy: clinical aspects. In: Neurology of the newborn (eds. J.J. Volpe, W.B.Saunders), pp. 314-369, Philadelphia, PA.

Voorhies, T. M., Rawlinson, D. and Vannucci, R. C. (1986). Glucose and perinatal hypoxic-ischemic brain damage in the rat. *Neurology* **36**, 1115-1118.

Vrbaski, S.R. (1998). Gamma aminobutyric acid – its function, disorders and their sequelae. *Med. Pregl.* **51(7-8)**, 319-24.

Wagstaff, M.J.D., Collao-Moraes, Y., Aspey, B.S., Coffin, R.S., Harrison, M.J.G., Latchman, D.S. and de Belleroche, J.S. (1996). Focal cerebral ischaemia increases the levels of several classes of heat shock proteins and their corresponding mRNAs. *Mol. Brain Res.* **42**, 236-244.

Wahlgren, N.G. and Martinsson, L. (1998). New concepts for drug therapy after stroke. Can we enhance recovery? *Cerebrovasc. Dis.* **8 (Suppl 5)**, 33-8.

Wahlgren, N.G., Ranasinha, K.W., Rosolacci, T., Franke, C.L., vanErven, P.M.M., Ashwood, T. and Claesson, L., for the CLASS Study Group (1999). Clomethiazole Acute Stroke Study (CLASS). *Stroke* **30**, 21-28.

Wang, X., Ruffolo, R. and Feuerstein, G. (1996). mRNA Differential display: application in the discovery of novel pharmacological targets. *Trends in Pharmacol. Sci.* **17**, 276-279.

Wang, Y., Knowlton, A.A. (1999). Prior heat stress inhibits apoptosis in adenosine triphosphate-depleted renal tubular cells. *Kidney Int.* **55(6)**, 2224-35.

Wei, Y., Zhao, Q., Kariya, X. Y., Teshigawara, K. and Uchida, A. (1995). Inhibition of proliferation and induction of apoptosis by abrogation of heat-shock protein (HSP) 70 expression in tumor cells. *Cancer Immunol. Immunother.* **40**, 73-78.

Welsh, F.A., Vannucci R.C. and Brierley, J.B. (1982). Columnar alterations of NADH flourescence during hypoxia-ischemia in immature rat brain. *J. Cereb. Blood Flow Metabol.* **2**, 221-228.

Welsh, F.A., Moyer, D.J. and Harris, V.A. (1992). Regional expression of heat shock protein-70 mRNA and c-fos mRNA following focal ischemia in rat brain. *J. Cereb. Blood Flow Metab.* **12**, 204-212.

Welsh, W.J. (1993). Heat shock proteins functioning as molecular chaperones: their roles in normal and stressed cells. *Philos. Trans. R. Soc. Lond. B Biol. Sci.* **339**, 327-333.

Westerberg, E., Monaghan, D.T., Kalimo, H., Cotman, C.W., Wielock, T.W. (1989). Dynamic changes of excitatory amino acid receptors in the rat hippocampus following transient cerebral ischemia. *J. Neurosci.* **9**, 798-805.

WHO MONICA Project (1988). The World Health Organization Monica Project (monitoring trends and determinants in cardiovascular disease): a major international collaboration. *J. Clin. Epidemiol.* **41**, 105-114.

Widmann, R., Miyazawa, T. and Hossmann, K.A. (1993). Protective effect of hypothermia on hippocampal injury after 30 minutes of forebrain ischemia in rats is mediated by post ischemic recovery of protein synthesis. *J. Neurochem.* **61**, 200-209.

Williams, C.E., Mallard, C., Tan, W. and P.D. Gluckman (1993). Pathophysiology of perinatal asphyxia. *Clin Perinatol.* **20**, 305-325.

Williams, G.D., Dardzinski, B.J., Buckalew, A. R. and Smith, M.B. (1997). Modest hypothermia preserves cerebral energy metabolism during hypoxia-ischemia and correlates with brain damage a ^{31}P nuclear magnetic resonance study in unanesthetized neonatal rats. *Pediatr. Res.* **42**, 700-708.

Witts, D.J., Arnold, K. and Exton-Smith, A.N. (1983). The plasma levels of chlormethiazole and two of its metabolites in elderly subjects after single and multiple dosing. *J. Pharm. Biomed. Anal.* **1**, 311-320.

Wyllie, A.H., Kerr, J.F.R. and Currie, A.R. (1980). Cell death: the significance of apoptosis. *Int. Rev. Cytol.* **68**, 251-307.

Xue, D., Huang, Z.G., Barnes, K., Lesiuk, H.J., Smith, K.E. and Buchan, A.M. (1994). Delayed treatment with AMPA, but not NMDA antagonists reduces neocortical infarction. *J. Cereb. Blood Flow Metab.* **14**, 251-26.

Yager, J.Y., Heitjan, D.F., Towtight, J. and Vannucci, R.C. (1992). Effect of insulin induced and fasting hypoglycemia on perinatal hypoxic-ischemic brain damage. *Pediatr. Res.* **31**, 138-142.

Yager, J.Y., Towfighi, J. and Vannucci, R.C. (1993). Influence of mild hypothermia on hypoxic-ischemic brain damage in the immature rat. *Pediatr. Res.* **34**, 525-529.

Yager, J.Y. and Asselin, J. (1996). Effect of mild hypothermia on cerebral energy metabolism during the evolution of hypoxic-ischemic brain damage in the immature rat. *Stroke*. **27**, 919-926.

Yamamoto, K., Hayakawa, T., Mogami, H., Akai, F. and Yanagihara, T. (1990). Ultrastructural investigation of the CA1 region of the hippocampus after transient cerebral ischemia in gerbils. *Acta Neuropathol. (Berl)* **80**, 487-492.

Yamane, M., Hattori, H., Sugito, K., Hayashi, Y., Tohnai, I., Ueda, M., Nishizawa, K. and Ohtsuka, K. (1995). Cotranslocation and colocalization of hsp40 (DnaJ) with hsp70 (DnaK) in mammalian cells. *Cell Struct. Funct.* **20(2)**, 157-66.

Yang, F., Sun, X., Beech, W., Teter, B., Wu, S., Sigel, J., Vinters, H.V., Frautschy, S.A., Cole, G.M. (1998). Antibody to caspase-cleaved actin detects apoptosis in differentiated neuroblastoma and plaque-associated neurons and microglia in Alzheimer's disease. *Am. J. Pathol.* **152**, 379-389.

Yaoita, H., Ogawa, K., Maehara, K. and Maruyama, Y. (1998). Attenuation of ischemia/reperfusion injury in rats by a caspase inhibitor [see comments]. *Circulation*, **97**, 276-281.

Yenari, M., Fink, S.L., Sun, G.H., Patel, M., Kunis, D., Onley, D., Sapolsky, R.M. and Steinberg, G.K. (1998). Gene therapy with HSP72 is neuroprotective in rat models of stroke and epilepsy. *Ann. Neurol.* **44**, 584-591.

Yoneda, Y., Azuma, Y., Inoue, K., Ogita, K., Mitani, A., Zhang, L., Masuda, S., Higashihara, M. and Kataoka, K. (1997). Positive correlation between prolonged potentiation of binding of double-stranded oligonucleotide probe for the transcription factor AP1 and resistance to transient forebrain ischemia in gerbil hippocampus. *Neuroscience* **79**, 1023-1037.

Yost, H.J. and Lindquist, S., (1986). RNA splicing is interrupted by heat shock and is rescued by heat shock protein. *Cell* **45**, 185-193.

Young, R.S.K., Olenginski, T.P., Yagell, S.K. and Towfighi, J. (1983). The effect of graded hypothermia on hypoxic-ischemic brain damage: a neuropathologic study in the neonatal rat. *Stroke* **14**, 929-934.

Yuan, J., Shaham, S., Ledoux, S, Ellis, H.M. and Horvitz, H.R. (1993). The C. elegans cell death gene ced-3 encodes a protein similar to mammalian interleukin-1 beta-converting enzyme. *Cell* **75**, 641-652.

Yuglom, J.A., Gabai, V.L., Merlin, A.B., Mosser, D.D., and Sherman, M.Y. (1999). The function of HSP72 in suppression of c-Jun N-terminal kinase activation can be dissociated from its role in prevention of protein damage. *J. Biol. Chem.* **274(29)**, 20223-8.

Zamzami, N., Hirsch, T., Dallaporta, B., Petit, P.X. and Kroemer, G. (1997). Mitochondrial implication in accidental and programmed cell death: apoptosis and necrosis. *J. Bioenerg. Biomembr.* **29(2)**, 185-93.

Zhang, H., Rosenberg, H.C. and Tietz, E.I. (1989). Injection of benzodiazepines but not GABA or muscimol into pars reticulata substantia nigra suppresses pentylenetetrazol seizures. *Brain Res.* **488(1-2)**, 73-79.

Zhang, X., Boulton, A.A. and Yu, P.H. (1996). Expression of heat shock protein-70 and limbic seizure-induced neuronal death in the rat brain. *Eur. J. Neurosci.* **8**, 1432-1440.

Zhang, X., Le-Gal-La-Salle, G., Ridoux, V., Yu, P.H. and Ju, G. (1997). Prevention of kainic acid-induced limbic seizures and Fos expression by the $GABA_A$ receptor agonist muscimol. *Eur. J. Neurosci.* **9(1)**, 29-40.

Zhong, Y. and Simmonds, M.A. (1997). Interactions between loreclezole, chlormethiazole and pentobarbitone at $GABA_A$ receptors: functional and binding studies. *Br. J. Pharmacol.* **121**, 1392-1396.

Zhou, L., Moyer, J., Muth, E., Clark, B., Palkovits, M. and Weiss, B. (1985). Regional distribution of calmodulin activity in rat brain. *J. Neurochem.* **44**, 1657-1662.

Zimmerman, J.L., Petri, W.L. and Meselson, M. (1983). Accumulation of a specific subset of D. melanogaster heat shock mRNAs in normal development without heat shock. *Cell* **32**, 1161-1170.